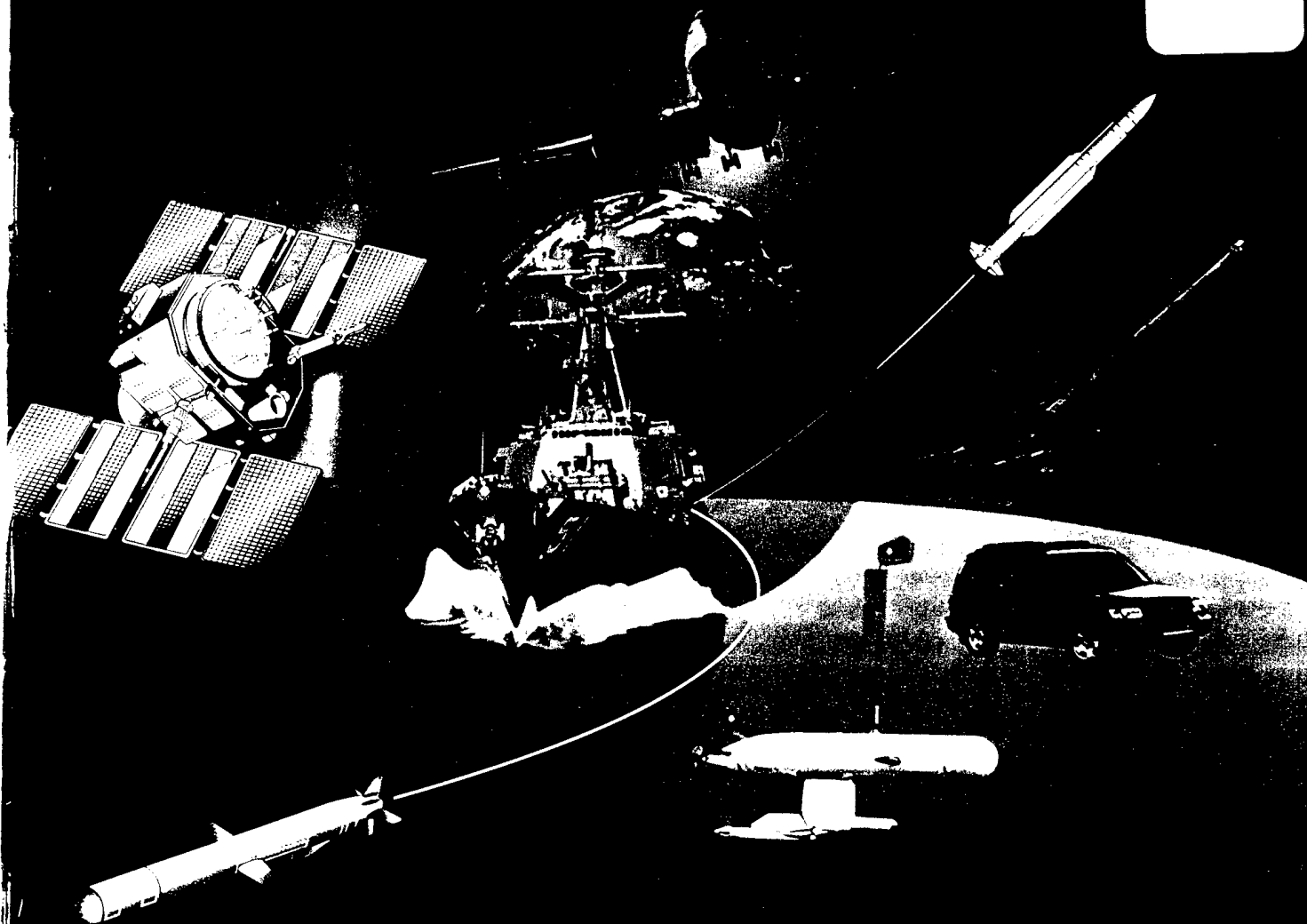


Naval Surface Warfare Center
Dahlgren Division

Technical Digest

1998 Issue

19981207 033



**Technology Transition and
Dual-Use Technology**

NAVY SYSTEMS MANAGEMENT A

Approved for public release
Distribution Unlimited

Technical Advisory Board

Dr. Frank G. Moore, Chairman
Dr. Kenneth C. Baile
Dr. Francis E. Baker, Jr.
Mr. Sidney H. Hankerson, Jr.
Mr. Raymond H. Hughey, Jr.
Mr. Michael J. Kuchinski
Mr. Edward C. Linsenmeyer
Dr. Lisle H. Russell
Dr. Jon J. Yagla

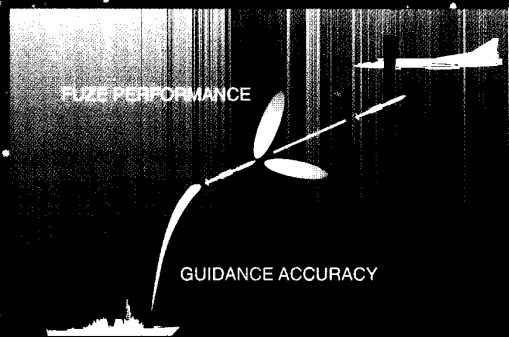
Editorial Staff

Mrs. M. Patrice Waits, Managing Editor
Mr. David M. Bozicevich, Associate Editor
Mr. Clement Bryant, Graphic Designer

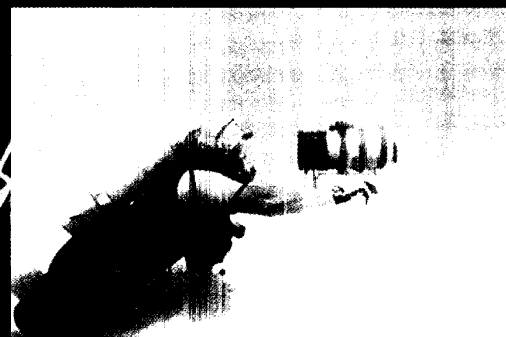
The Naval Surface Warfare Center, Dahlgren Division Technical Digest presents unclassified articles, contributed primarily by Division scientists and engineers, on selected research and development programs. The Dahlgren Division, under the leadership of the Naval Surface Warfare Center, provides research, development, test and evaluation, engineering, and fleet support for surface warfare systems, surface ship combat systems, ordnance, mines, amphibious warfare systems, mine countermeasures, special warfare systems, Marine Corps weaponry systems, and strategic systems. Please address any correspondence concerning the NSWCDD Technical Digest to: Dahlgren Division, Naval Surface Warfare Center, Technical Digest (Code B60), 17320 Dahlgren Road, Dahlgren, VA 22448-5100. Telephone (540) 653-3200 (DSN 249-3200).

About the cover: Shown clockwise from directly above the earth are a commercial airliner, a Standard Missile, a howitzer, a sport utility vehicle, a Remote Minehunting System, a Tomahawk Missile, USS *Arleigh Burke* (DDG 51) guided-missile destroyer, and a Global Positioning System (GPS) satellite. What does this apparently incongruous group have in common? They all have a connection to GPS technology for some of their current or future capability. Satellites within a GPS operational constellation transmit precise, specially coded signals to a GPS receiver, which computes position, velocity, and time. The last article of this issue discusses the many technology contributions NSWCDD has made to the GPS system.

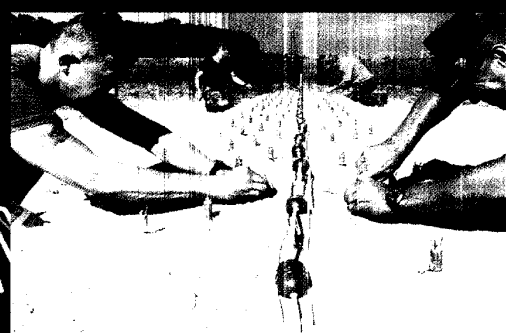
NSWCDD/MP-98/98
Approved for public release;
distribution is unlimited.



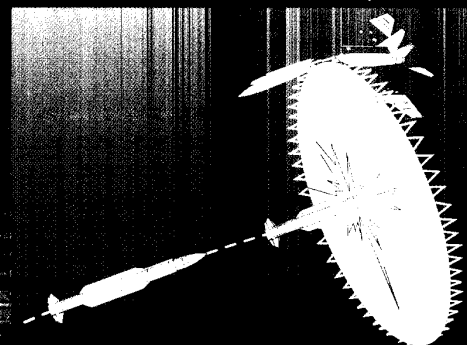
FATEPEN Target Interaction Model



Diver Portable Sonar



Breaching Operations and Expeditionary Warfare



Evolution of Air Target Warheads

*Naval Surface Warfare Center
Dahlgren Division*

Technical Digest

1998 Issue

Farewell Note	T. A. Clare	3
Guest Editors' Introduction	R. R. Staton E. C. Linsenmeyer R. D. Johnson	4
VLSTRACK	T. J. Bauer	10
Mine Countermeasures Simulator AN/SSQ-94(V) Advanced Technology for MIW Training	J. R. Denton	22
The Aeroprediction Code: Past, Present, and Future	F. G. Moore	28
FATEPEN—A Model to Evaluate Behavior of Warhead Fragments and Penetrators, and Their Damaging Effects on Military Targets	D. L. Dickinson T. L. Wasmund J. D. Yatteau R. H. Zernow G. W. Recht	44
Remote Detection of Chemical Warfare Agents: Advanced Research to Full-Scale Production of the AN/KAS-1	S. R. Horman	62
The Development and Application of the Shipboard Collective Protection System (CPS)	D. W. Sisson, Jr.	74
Magic Lantern Deployment Contingency	J. M. Lloyd, Jr.	86

1998 Issue (Continued)

Remote Minehunting System (RMS) AN/WLD-1	G. A. Santora	94
Upgrading the Fleet AN/PQS-2A Diver-Portable Sonar	J. L. Lopes	108
The Evolution of Air Target Warheads	S. S. Waggener	118
The APOBS MK7 Mod 1 Moves Assault Breaching Operations and Expeditionary Warfare into the 21st Century!	R. C. Woodall, Jr. F. A. García	128
Radio Frequency Coupling Characteristics of Avionics Measured on a Passenger Aircraft and in a Reverberation Chamber	D. M. Johnson M. O. Hatfield	140
Contributions to the NAVSTAR Global Positioning System (GPS) by the Naval Surface Warfare Center, Dahlgren Division	B. L. Miller B. R. Hermann E. R. Swift R. W. Hill A. G. Evans J. P. Cunningham J. N. Blanton	152

FAREWELL NOTE

The *Naval Surface Warfare Center, Dahlgren Division Technical Digest* has provided our scientists and engineers the opportunity to communicate the excellence of their work in a manner that has added great value to our Navy. When we publish in journals, we are typically contributing to the state of knowledge in that field, usually a discipline or academic topic. This is certainly a good thing and one we should continue to pursue. It is equally important that the Naval and Department of Defense (DoD) community understand the relevance of the technical topics to Naval, DoD, and National Missions. We exist to understand the technical dimensions of military problems, know where to go to get solutions, and know when a competent solution has been provided. The *Technical Digest* helps us achieve these purposes.

I am grateful for the opportunity to have contributed to the *Technical Digest*. I am also extremely grateful to the people who have served on the Technical Advisory Board and Editorial Staff and, most especially, to the guest editors and authors of the excellent articles that have graced the last eight issues. They have all been superb. I know that this particular area will be a highlight in my memories of serving as Executive Director of the Naval Surface Warfare Center, Dahlgren Division.



THOMAS A. CLARE

GUEST EDITORS' INTRODUCTION

Mr. Robin R. Staton, Mr. Edward C. Linsenmeyer, and Mr. Ramsey D. Johnson

What, exactly, IS *technology* and what is meant by "Technology Transition"? *Webster's Seventh New Collegiate Dictionary* defines *technology* as "a technical method of achieving a practical purpose." *Webster's Third International Dictionary* defines *technology* as "the application of scientific knowledge to practical purposes in a particular field." A sixth-grade social studies textbook defines *technology* as "the tools and skills used to build things." All three definitions (and many others that could be quoted) suggest that *technology* is more than components or "hardware." This view of technology is possibly best captured by the definitions of *science* and *technology* provided by Richard Feynman in *The Meaning of it All*:

"SCIENCE MEANS, SOMETIMES, A SPECIAL METHOD OF FINDING THINGS OUT. SOMETIMES IT MEANS THE BODY OF KNOWLEDGE ARISING FROM THE THINGS FOUND OUT. IT MAY ALSO MEAN THE NEW THINGS YOU CAN DO WHEN YOU HAVE FOUND SOMETHING OUT, OR THE ACTUAL DOING OF NEW THINGS. THIS LAST FIELD IS USUALLY CALLED TECHNOLOGY."

Technology, therefore, is more than new devices or industrial tools or processes used to fabricate hardware. Technology also incorporates scientific knowledge of how/why things work and, by extension, an ability to predict how something works based on scientific principles. This last concept—the ability to predict—can easily be considered to fall within the "skills" part of the social studies textbook definition. It also encompasses scientific or engineering models and tools used in the acquisition process, and decision algorithms used in radar signal processors or combat direction systems.

A *Naval Surface Warfare Center, Dahlgren Division (NSWCDD) Technical Digest* issue devoted to "Technology Transition" should therefore incorporate technology in its broadest sense. The articles selected for this issue have been chosen to illustrate the fullest possible range of technology transition. The main discriminate used in the selection process was that the product must have transitioned to the operational Navy, or the technology product (such as aeroprediction models or lethality models) must have clearly impacted items transitioned to the fleet. Major acquisition decisions are made based on lethality predictions. Major tactical and operational decisions are made based on weapon effectiveness data published in tactical manuals such as the Joint Munitions Effectiveness Manual. The fact that new weapons with new kill mechanisms (or new targets) often require new lethality evaluation technologies to

evaluate or predict effectiveness is not widely understood. Not every case can be tested in live-fire exercises. Hopefully, the articles in this issue will help to broaden the understanding that technology is not just components. It is also knowing how to achieve some desired result.

As the mismatch between Navy needs and funding resources continues to grow, there will be increasing pressure on funding for government technology development. A secondary discriminate for selecting articles for this issue was therefore the desire to show a significant military benefit from long-term investment in basic research, applied research, and technology development/demonstration within the Navy and the Department of Defense (DoD). While no one seriously expects government research to compete with Silicon Valley in chip design and manufacture, many militarily significant technologies have (and continue to) come from DoD laboratories. This issue of the *NSWCDD Technical Digest* will provide examples that support that claim.

So, what is "technology" and what is "technology transition"? For the Navy Science and Technology community, technology is generally focused on developing hardware components, algorithms (computer programs), methods, techniques, or combinations to do something that we currently do not know how to do. This process typically involves a high risk of failure, but the potential benefit of success is judged to be worth the dollar investment risk. The desired "output" of this process is usually "evidence" (scientific grounds for belief) that the desired goal is achievable—given additional engineering and testing. An acceptable output is evidence that a particular approach is NOT promising, and should not be pursued further. Technology transition (for this issue) occurs when basic or applied research has been taken through the entire process of concept formulation, analytical and experimental proof-of-concept, component or breadboard laboratory validation, demonstration in a relevant environment, engineered system prototype demonstration, qualification for operational use, and ultimate use or deployment. Each article in this issue describes a technology transition.

The technology transitions presented in this publication are representative successes from diverse elements of NSWCDD's technology continuum. We will share examples of mission-specific products as well as dual-use technologies having both military and civilian applications. The underlying technology that originated these successful transitions supports our principal Research, Development, Test, and Evaluation (RDT&E) activities in the areas of surface warfare systems, surface ship combat systems, ordnance, amphibious warfare systems, diving, mine countermeasures (MCM), special warfare systems, and strategic systems.

There are a number of ways that articles in this issue could have been grouped. For a naval technical journal, one of the first methods that comes to mind is to group the articles by naval mission area or warfare area: chemical and biological defense, mine warfare, antiair warfare, expeditionary warfare, etc. The method chosen, however, was to group the articles into three broad categories that more accurately reflect the product of the technology or the nature of the technology transition. The three broad categories are:

- ◆ Engineering models, simulations, or analysis tools that provide needed capabilities to the technical, acquisitional, or operational communities within Navy, DoD, or industry/academia.
- ◆ Hardware components, devices, or systems transitioned to the operational Navy.
- ◆ Applications of DoD-developed technologies to both military and commercial needs.

Within these three broad categories, the articles are grouped by naval mission area.

In the first article, "VLSTRACK," Mr. Timothy Bauer describes the development and application of the U.S. Navy's vapor, liquid, and solid tracking computer model to research and operational purposes. The model addresses a key capability needed for chemical, biological, and radiological defense throughout DoD and other federal agencies.

Training is a necessary component of enhancing the capabilities of our fleet in conducting their mission. Based on a broad range of technical knowledge in computer software engineering, and modeling and simulation technology, a team of engineers developed the MCM Simulator (AN/SQQ-94). Mr. John Denton describes how laboratory-based technology was transformed into a fleet trainer for the combat information center on board the Navy's new MCM and Minehunter Coastal (MHC) class ships.

In the third article, Dr. Frank Moore describes the 26+ year history of the Aeroprediction Code. Fast, accurate, user-friendly aerodynamic prediction capabilities have been a continuing need for over 30 years. Not only has the need for increasing accuracy with lower setup and execution time continued to evolve, but the spectrum of missiles, projectiles, submunitions, and nonsymmetric aerodynamic shapes that must be addressed has continued to expand.

Mr. David Dickinson and others then chronicle Fast Air Target Encounter Penetration (FATEPEN). This article, like the Aeroprediction and VLSTRACK articles, describes a technology with broad application within the Navy science and technology, acquisition, and operational communities, as well as to other components of DoD. As previously stated, decisions based on predictions of lethality have far-reaching consequences.

In the article on the AN/KAS-1, Mr. Roger Horman describes the difficult, often convoluted process of actually transitioning a concept from applied research to a widely deployed operational asset.

The article on the shipboard collective protection system by Mr. Dale Sisson, Jr., describes a key capability in chemical and biological protection. The system, originally developed for ships, has found wide application in land-based sites around the world.

Airborne electro-optic minehunting systems are a new capability for the MCM community. Teaming

between Kaman Aerospace Corporation and scientists and engineers from NSWCDD Coastal Systems Station (CSS) has resulted in the Magic Lantern imaging lidar system. Dr. Jack Lloyd reports on the history of this project as the basic research efforts in NSWCDD/CSS's modeling and simulation of an electro-optics system have enabled this concept to provide a truly unique capability to the fleet.

In order to implement the maritime warfare strategy articulated in *Forward...From The Sea*, the U.S. Navy must be able to conduct operational maneuvers in coastal waters. One of the most effective defensive weapons of Third World nations is sea mines. In the article on the Remote Minehunting System, Mr. Guy Santora describes a new organic MCM system for providing self defense to surface ships from mines.

Dr. Joe Lopes reports on his efforts and success in upgrading the capability of the military divers' portable sonar—the AN/PQS-2A. Spectral processing techniques developed in the core 6.2 sonar technology program at NSWCDD/CSS were incorporated to provide a combined audio and visual detection capability. The success of this effort has resulted in technology transition to the Navy's special warfare community.

In "The Evolution of Air Target Warheads," Mr. Sam Waggener traces the evolving threat characteristics and warhead design responses over a 30-year period and identifies key technologies that have allowed warheads to adapt as the threat changes.

Antipersonnel mines are a realistic and deadly threat to our land combatants. Breaching these fields is a time-consuming and dangerous mission of the amphibious assault team, who are often in direct fire while trying to accomplish their objectives. Mr. Robert Woodall and Mr. Felipe García describe the development of new insensitive munitions in the rocket-deployed Antipersonnel Obstacle Breaching System (APOBS MK7 Mod 1). Transition of the APOBS to the U.S. Marines is one aspect in establishing U.S. Marine Corps (USMC) leadership in the 21st century.

THE GUEST EDITORS

MR. ROBIN R. STATON



Mr. Robin R. Staton is currently the NSWCDD Senior Program Manager for Surface Weapons Technology. He received a B.S. degree in physics from North Carolina State University in 1969 and did graduate study in electrical engineering from Virginia Polytechnic Institute and State University (1970-1972). He joined the Naval Weapons Laboratory at Dahlgren in 1969 and was initially assigned to conduct analysis of circuit fault detection programs for the Poseidon MK88 Digital Control Computer. During 1972-1973 he did test planning, data collection, and analysis of shipboard electromagnetic compatibility issues for the SH-52 LAMPS MK III helicopter. Since 1973 he has worked almost exclusively in technology development, beginning with an exploratory development project to minimize the electromagnetic signature vulnerability of U.S. Navy ships to the Soviet Ocean Surveillance System. He was the senior engineer and later program manager of the Navy's exploratory development program in antiradiation missile countermeasures (1975-1986). From 1978 to 1986 he was the principal Navy representative to the OSD Tri-Service ARM Countermeasures Joint Working Group and a member of the Joint Directors of Laboratories Technical Panel for Electronic Warfare. He was the technical principal for the Surface Launched Weaponry Search and Track project investigating shipboard surveillance and fire control radar and EO/IR sensor technology, 1986-1991. He was also the NSWCDD Deputy NATO AAW Program Manager (Sensors) from 1986-1989. Mr. Staton has authored or co-authored 22 technical reports or papers in DoD technical symposia. He is a member of the Phi Kappa Phi national honorary society, the Sigma Pi Sigma physics society, and the IEEE.

Mr. EDWARD C. LINSENMEYER



Mr. Edward C. Linsenmeyer has earned a B.S. degree in physics from the Illinois Institute of Technology and an M.S. degree in physics from the University of Florida's Quantum Theory Project, where he was the Professor John C. Slater Graduate Research Fellow. After teaching in the Florida Community College System, Mr. Linsenmeyer came to CSS in 1981. In his first years at CSS, he was the project engineer for the first Amphibious Warfare Master Plan for OP954. He next worked as project engineer for the Marine Corps 6.2 Magnetic Land Mine Detection Tasks. Mr. Linsenmeyer then worked as Assistant Block Manager for the Air/Sea Mine Countermeasures Program working also as a project engineer in Buried Mine Detection. Collaterally he became the Manager for the Coastal Systems Station's Small Business Innovation Research Program. In 1987/88 Mr. Linsenmeyer served as Deputy for Mine Warfare Programs under Dr. Wally Ching at the Office of Naval Technology. Returning to CSS, Mr. Linsenmeyer served as Block Manager for Sea Mine Countermeasures. Since 1994, Mr. Linsenmeyer has been the Manager of the CSS Office of Research and Technology Transfer, and in that capacity, has served actively on the Executive Board of the Federal Laboratory Consortium. Mr. Linsenmeyer has received the Technical Cooperation Panel GTP-13 Meritorious Award for work in Mine Burial Prediction and the Federal Laboratory Consortium Southeast Regional Laboratory Representative of the Year Award (August 1995). He is also the Federal Laboratory Consortium National Award Winner for Laboratory Representative of the Year Award (November 1995).

Mr. RAMSEY D. JOHNSON



Mr. Ramsey D. Johnson is the Dahlgren site's technology transfer manager, the industry Independent Research and Development (IR&D) program coordinator, and has other technical management responsibilities in the Systems Research and Technology Department. His Navy career began at NSWCDD (then the Naval Weapons Laboratory) in 1960, initially as an analyst with the Polaris Missile Program and then as a field test engineer investigating electromagnetic radiation effects on ordnance components in the Terrier and Talos missiles. After transferring to the White Oak site (then the Naval Ordnance Laboratory) he managed the test and evaluation of a variety of weapons systems in support of the Small Craft Armament (SCRAM) program for the "brown water" Navy in South Vietnam. As a volunteer in-country Vietnam Laboratory Assistance Program (VLAP) representative he trained and assisted South Vietnamese Navy troops with the deployment of prototype detection and surveillance equipment for 8 months in 1971-72. His tour as Navy Science Assistance Program (NSAP) representative in 1974 with the Marine Corps Development and Education Command at Quantico, Virginia, was followed with a 3-year contracting officer technical representative (COTR) assignment supporting the development and testing of a high-energy chemical laser system in California. He was a combat systems engineering support manager for the CGN-38 and DDG-993 combat system upgrade programs prior to joining the Division Planning Staff, where he emphasized the expanding role of NSWCDD in technology transfer. In 1988 he was selected for the Navy Science and Technology Exchange Program and served in the Navy Technology Transfer Program Office at the Office of Naval Research. He earned A.B. and M.S. degrees in physics from Miami University (Oxford, Ohio) and the University of Illinois (Urbana, IL) in 1960 and 1966, respectively. He's a member of Phi Beta Kappa National Honor Society and Sigma Pi Sigma Physics Honor Society.

VLSTRACK

Mr. Timothy J. Bauer

The U.S. Navy's Vapor, Liquid, and Solid Tracking (VLSTRACK) computer model is a user-friendly, chemical and biological warfare (CBW), downwind hazard assessment model that provides approximate hazard predictions for a wide range of chemical and biological (CB) agents and munitions of military interest. VLSTRACK was originally developed and distributed during Operations Desert Shield and Storm and has been continuously extended and improved since. The model has been used for operational and research and development purposes by the Army, Navy, Air Force, Marine Corps, intelligence agencies, Department of Energy laboratories, and federally funded research and development centers. VLSTRACK coding is very portable between computer systems, and graphical user interfaces (GUIs) have been developed for Microsoft Windows, X-Window, MS-DOS, OS/2, and Tektronix operation. An ASCII character graphics version is also available for other computer systems. VLSTRACK has been designated by the Department of Defense (DoD) as the interim standard model for predicting CBW hazards resulting from enemy use of CB weapons.

INTRODUCTION

CBW refers to enemy forces' intentional use of a highly toxic chemical compound or biological organism or toxin, with the intent to kill or incapacitate friendly forces. The U.S. Navy's CB Agent VLSTRACK Computer Model provides approximate downwind hazard predictions for many currently known or suspected CB agents, as well as a wide variety of munitions capable of disseminating chemical or biological agents.

GENERAL OPERATION

The range of capabilities included in VLSTRACK allows the model to be used for operational hazard assessment or for research and development studies, with operation being "user-friendly." The model is also suitable for training applications.

GUIs have been developed for a variety of computer systems:

- ◆ A 386/486/Pentium or equivalent microprocessor-based Personal Computer (PC) running Microsoft Windows 3.1, Windows 95, or Windows NT
- ◆ The same microprocessor-based PC running MS-DOS
- ◆ A PC running OS/2
- ◆ A UNIX workstation running X-Window

Also, a character graphics version of VLSTRACK 3.0 is available that will run on just about any computer system for which a FORTRAN compiler is available. In addition, Tektronix color graphics output can be made available for systems run from a Tektronix monitor.

VLSTRACK features smart input windows that check input parameter combinations to ensure that a reasonable attack is being defined, and simple and informative output graphics that display the hazard "footprint" for agent deposition, dosage, or concentration. Selection sets are used for entering and changing parameters with minimal keystrokes. Output can be obtained either as a cumulative hazard from the time of the attack or as a periodic hazard for each time period. The model can accommodate meteorology that varies with time, height, and geographic location, allowing for the attack to be interfaced with a meteorology forecast. This feature is very important for computations involving biological agent transport and diffusion, and evaporation of chemical agent liquid from a surface. Time-variable meteorology is necessary for hazards that exist for more than an hour. Vertical wind profile measurements or forecasts are important for high-altitude releases. Spatially variable meteorology is needed to obtain the best hazard prediction for releases that cover large distances over complex terrain.

Some CBW situations normally require large amounts of computations, which can take quite some time, to compute the hazard. For quick estimates, the model features a rapid approximations option for each such situation, which can be used for preliminary hazard evaluation. The rigorous computations can then be done if a more accurate hazard estimate is required, and time permits.

THE PROPERTIES OF CHEMICAL AND BIOLOGICAL AGENTS

Chemical agents can be divided into several categories. The most well-known chemical agents are nerve agents—such as sarin and soman—and

blister agents such as mustard gas. These agents can be dispersed explosively from one or more munitions or from an aircraft spray tank. The agent is released as a combination of vapor and droplets. Vapor is an inhalation hazard and possibly a percutaneous hazard to unprotected personnel, and droplets form a contact hazard, both in the air and on the ground. The droplets evaporate as they fall to the ground. After impacting the ground, the droplets evaporate from the surface. If the surface is porous or organic, the droplets absorb into the surface and, subsequently, desorb from the surface. The vapor produced from droplet evaporation, surface evaporation, and desorption is also an inhalation hazard to unprotected personnel. Depending on the agent volatility and meteorological conditions, the combined inhalation and contact hazard from nerve and blister agents can last from several hours to several days.

A second category of chemical agents includes compounds such as hydrogen cyanide, phosgene, chlorine, and other highly volatile toxic chemicals. These agents also form an inhalation hazard to unprotected personnel and are stored under pressure as liquids. When they are released into the atmosphere via explosion or spray, the liquid vaporizes. In the process, the cloud mass cools, leading to a dense vapor mass. Since the toxic cloud is denser than the surrounding air, it settles to the ground. These chemical agents can persist at toxic levels for many minutes in depressions on the ground, well after the main cloud mass has moved on with the wind.

A third category of chemical agents has been produced by loading nerve or blister-agent liquid onto micron-sized, porous particles such as silica gel. When dispersed into the air, the particles travel with the wind and form an inhalation hazard. In addition, the particles are small enough to penetrate clothing and deposit on the skin, where the liquid is transferred and absorbed.

The category of biological agents includes the different types of single-celled organisms, organisms in their spore form, and toxins produced by the organisms. Any organism that leads to sickness or

disease is a candidate for a biological warfare agent. The sickness or disease does not have to lead to death to be an effective biological warfare agent, as long as the infected persons cannot perform their military duties. Such a list of potential organisms may include more than 100 entries; however, biological organisms tend to die quickly due to atmospheric exposure, sunlight, and humidity, so most of the entries would not make suitable biological warfare agents.

Biological agents can be dispersed from munitions or a variety of sprayers in either a dry powder form or a slurry form. The dry form is already milled into respirable particles. The slurry form, which is usually water-based, is dispersed as a fine mist of droplets that evaporate quickly to form respirable particles. Whereas chemical agents will travel only up to several kilometers at toxic levels, biological agent toxicities are several orders of magnitude higher. Biological agents can remain at toxic airborne concentrations for 100 kilometers or more.

VLSTRACK MODEL ORIGINATION

Prior to the invasion of Kuwait by Iraqi forces in the fall of 1990, few computer models existed that could compute the unique processes which occur to toxic chemical compounds or biological organisms or toxins released into the atmosphere and provide an estimate of the resulting size, location, and level of hazard. The threat had been considered to come from the countries that made up the former Soviet Union and its allies and primarily involved chemical warfare. Biological warfare was less of a concern since it would most likely affect both sides if used in a warfare situation. So, biological warfare expertise mostly disappeared. Assumptions about CBW changed dramatically with the invasion of Kuwait and the threat of potential terrorist actions by Third-World countries.

The Chemical Systems Branch (now the CB Systems Analysis Branch) had been using an Army model called the Nonuniform Simple Surface Evaporation (NUSSE) model, which computed all

relevant physical processes involved with the intentional release of nerve and blister agents. Additional methodology was added to the NUSSE model to address the other types of chemical agents for analyzing them as threats to Navy and Marine Corps forces. The major shortcoming of the NUSSE model and other models having some CBW modeling capabilities was that it was a research and development model that required the user to know and enter detailed characteristics of the release.

When Iraq invaded Kuwait it was already known that Iraq possessed chemical weapons and was willing to use them, as they had already used them in their war against Iran. The Navy had an existing requirement for a chemical warfare hazard prediction model that could be operated aboard ship on a 286 PC. The Chemical Systems Branch acted on this requirement and developed the VLSTRACK computer model, Version 1.0 over a 3-month period during Operation Desert Shield. VLSTRACK 1.0 was sent to approximately 50 ship and shore facilities in the Persian Gulf region in November 1990. VLSTRACK 1.0 comprised the NUSSE model, with additions made at the Naval Surface Warfare Center, Dahlgren Division (NSWCDD), plus a user-friendly interface for defining the chemical attack via menu input and an ASCII-character graphics hazard representation. A brief source-code verification and validation effort was done by the Naval Postgraduate School (NPS) to meet Navy requirements for using VLSTRACK operationally.

Subsequent to the development of VLSTRACK 1.0, it became apparent that Iraq had been manufacturing biological warfare agents and was prepared to use them against Israel and allied forces in the Gulf. The Chemical Systems Branch researched the processes involved with a biological warfare attack. Modifications were made to VLSTRACK to address appropriate source characterization, particle physics, agent demise (decay), and time-variable meteorological conditions. NSWCDD worked closely with the Defense Nuclear Agency (DNA) (now the Defense Special Weapons Agency (DSWA)) during Operation Desert Storm to run this biological warfare model several times a day to predict possible hazards for a variety of releases using meteorological forecasts coming from U.S. forces in the Gulf region.

THE ORIGINAL VLSTRACK, VERSION 1.0

The user interface of VLSTRACK 1.0 was simple but functional. The input menu is shown in Figure 1, and an example hazard representation is shown in Figure 2.

The author and two other Chemical Systems Branch employees, Roger Gibbs and Paul Kirk, were awarded the Technology to Sea Excellence Award for FY91 for developing and fielding VLSTRACK 1.0.

FOLLOW-ON DEVELOPMENT

NSWCDD was tasked in FY91 by the Office of Naval Technology (ONT) (now the Office of Naval

Research (ONR)) to further develop the VLSTRACK 1.0 chemical warfare hazard assessment model as a CBW hazard assessment model; the result was Version 1.2. VLSTRACK 1.2 was distributed to the CBW modeling community and used primarily for various research and development projects. Because of its user-friendly interface, color-graphics hazard display (new for Version 1.2), and range of capabilities, VLSTRACK 1.2 gained quite wide distribution outside of the Navy. Based on user feedback, Version 1.3 was then developed and distributed in FY92.

In response to evolving requirements from the Space and Naval Warfare Systems Command (SPAWAR), U.S. Marine Corps, U.S. Army Space and Strategic Defense Command (USASSDC),

```

MS-DOS Prompt - EDIT
File Edit Search View Options Help
C:\up51\hauer\fig1.out

VLSTRACK program. Version 1.0
November 19, 1990
Naval Surface Warfare Center, Dahlgren, Virginia

0 - RUN PROGRAM
1 - munition= Munition 6
2 - chemical agent= HD
3 - height of burst= 50.0 (m)
4 - wind speed= 10.0 (knots)
5 - air temperature= 80.0 (F)
6 - time of day= day
7 - ground surface type= water
8 - droplet size distribution= equal lognormal size spacing
9 - munition wind angle= 180.0 (deg)
13 - number of munitions= 8
14 - random number generator seed= 874585
15 - munition range= 250.0 (m)
16 - true munition bearing= 0.0 (deg)
17 - true ship bearing= 0.0 (deg)
18 - true wind bearing= 135.0 (deg)
19 - PRINT OUTPUT FILE
20 - END PROGRAM

enter number
  
```

Figure 1—VLSTRACK 1.0 Menu Interface

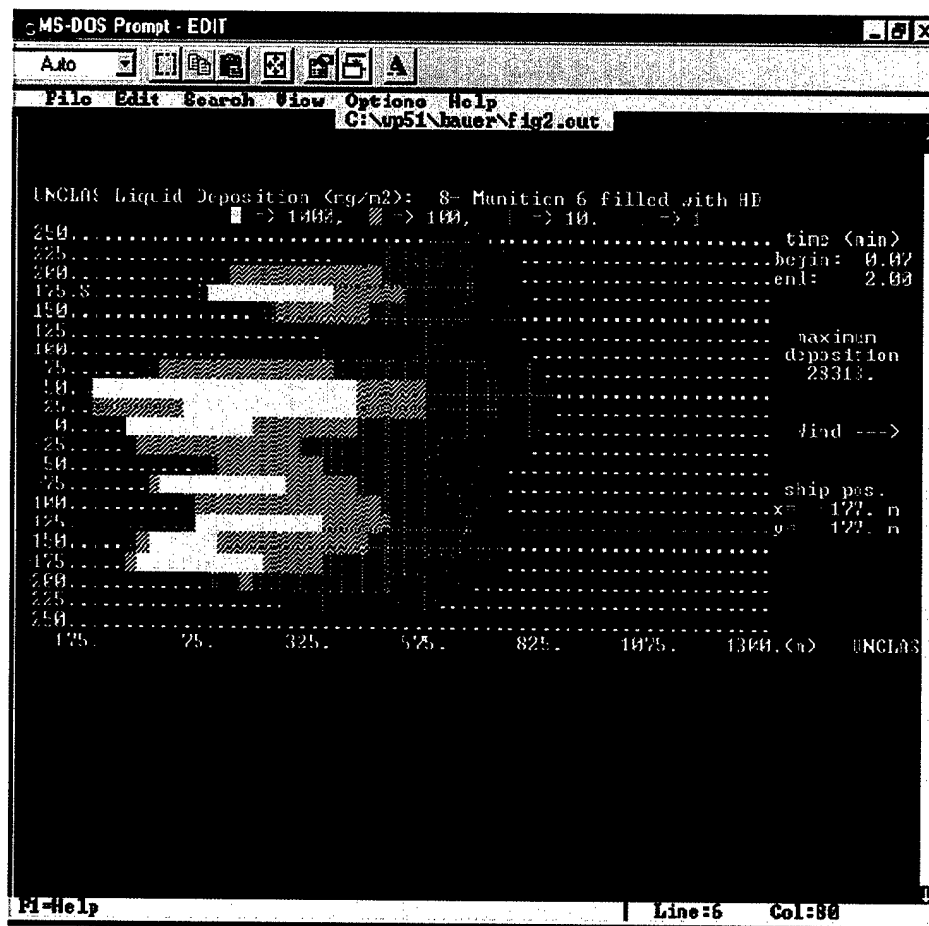


Figure 2—VLSTRACK 1.0 Hazard Representation

U.S. Army Nuclear and Chemical Agency (USANCA), and DNA, a major revision and enhancement to Version 1.3 was undertaken. VLSTRACK 1.5, which was distributed in FY93, included all of the features of previous versions and added the capability to address many of the situations resulting from high-altitude intercepts of chemical or biological warheads. VLSTRACK 1.5 was also designed to exchange information with the U.S. Army's Automated Nuclear, Biological, and Chemical Information System (ANBACIS) ATP-45 model. VLSTRACK 1.5.1 was distributed in FY94 as an intermediate release. VLSTRACK 2.0 was developed for SPAWAR in parallel with VLSTRACK 1.3 through 1.5.1 and added the capability to utilize two- and three-dimensional, time-variable meteorological conditions. Specialized versions were also developed for use of VLSTRACK as part of larger software systems; these systems included:

- ◆ JANUS combat simulation model
- ◆ Postengagement Ground Effects Model (PEGEM)
- ◆ Distributed Interactive Simulation (DIS) compliant Chemical, Biological, and Radiological (CBR) Simulator
- ◆ CBD-IMPACT regional hazard assessment model
- ◆ Tactical Environmental Support System (TESS)
- ◆ Oceanographic and Atmospheric Master Library (OAML)
- ◆ HAZWARN remote detection and warning system

Special capabilities were also added for use with the Battle Area Dense Gas Effects (BADGE) model, CRYSTAL-MIST high-altitude diffusion trial analysis, and user-defined surface characterization.

VLSTRACK 1.6 was developed during FY95 to correct theoretical errors identified in an Independent Technical Review (ITR) performed by the National Oceanic and Atmospheric Administration (NOAA) under funding by USANCA. During development of VLSTRACK 1.6, the opportunity was taken to integrate many features from the specialized versions. A multidimensional meteorology version, VLSTRACK 2.1, was also developed to replace VLSTRACK 2.0. VLSTRACK 1.6 and 2.1 were designed to share a common set of subroutines except those relating to the additional meteorology capability and the GUIs. Minor revisions were made for follow-on versions 1.6.1/2.1.1 and 1.6.2/2.1.2. These intermediate version releases were made in FY96 and FY 97, respectively. As before, the difference between the 1.6.x versions and the 2.1.x versions is due to the added capability in the 2.1.x versions to use spatially variable meteorology

forecasts and terrain. VLSTRACK is currently being integrated into the Navy's Multiwarfare Assessment Research System (MARS) and into the Joint Warning and Reporting Network (JWARN).

The currently distributed versions of VLSTRACK are Versions 1.6.3/2.1.3 (distributed in early FY98). The main methodology addition for these versions is the incorporation of the Global Reference Atmospheric Model, 1995 (GRAM-95) to provide atmospheric properties to VLSTRACK at very high altitudes, allowing VLSTRACK to simulate agent behavior at altitudes relevant to future tactical ballistic missile interception systems.

THE CURRENT VLSTRACK— VERSIONS 1.6.3 AND 2.1.3

GUIs have been developed for Microsoft Windows, X-Window, MS-DOS, OS/2, and Tektronix systems. Figures 3 and 4 show the Main Attack Window and a representative hazard display from the Microsoft Windows GUI for VLSTRACK 1.6.3.

Munition <input type="text" value="100kg Bomb"/>	Trajectory Angle (DTN) (0.0-359.9): <input type="text" value="45.0"/>	Output File Prefix <input type="text" value="VLSEXAMP"/>
Chemical/Biological Agent <input type="text" value="GD (Soman)"/>	Ground Surface Type <input type="radio"/> Water <input type="radio"/> Sand <input type="radio"/> Barren <input checked="" type="radio"/> Grass <input type="radio"/> Brush <input type="radio"/> Forest <input type="radio"/> User-Defined	Map Scale <input checked="" type="radio"/> Fill Screen <input type="radio"/> 10,000:1 <input type="radio"/> 50,000:1 <input type="radio"/> 100,000:1 <input type="radio"/> 500,000:1 <input type="radio"/> 1,000,000:1
Date (DDMMYY) Date: <input type="text" value="02Jun97"/>	Local Attack Time (HHMM) Time: <input type="text" value="1900"/> (0100Z) Day	Output Type <input checked="" type="radio"/> Deposition <input type="radio"/> Dosage <input type="radio"/> Concentration
Attack Location <input checked="" type="radio"/> Deg Lat/Long <input type="radio"/> DDDMMSS <input type="radio"/> DDDMM.M <input type="radio"/> UTM Cord. Latitude: <input type="text" value="39.0000 N"/> Longitude: <input type="text" value="78.0000 W"/>	Output Mode <input checked="" type="radio"/> Cumulative <input type="radio"/> Periodic <input type="radio"/> Periodic with size bins	

Figure 3—Main Attack Window for Microsoft Windows VLSTRACK 1.6.3

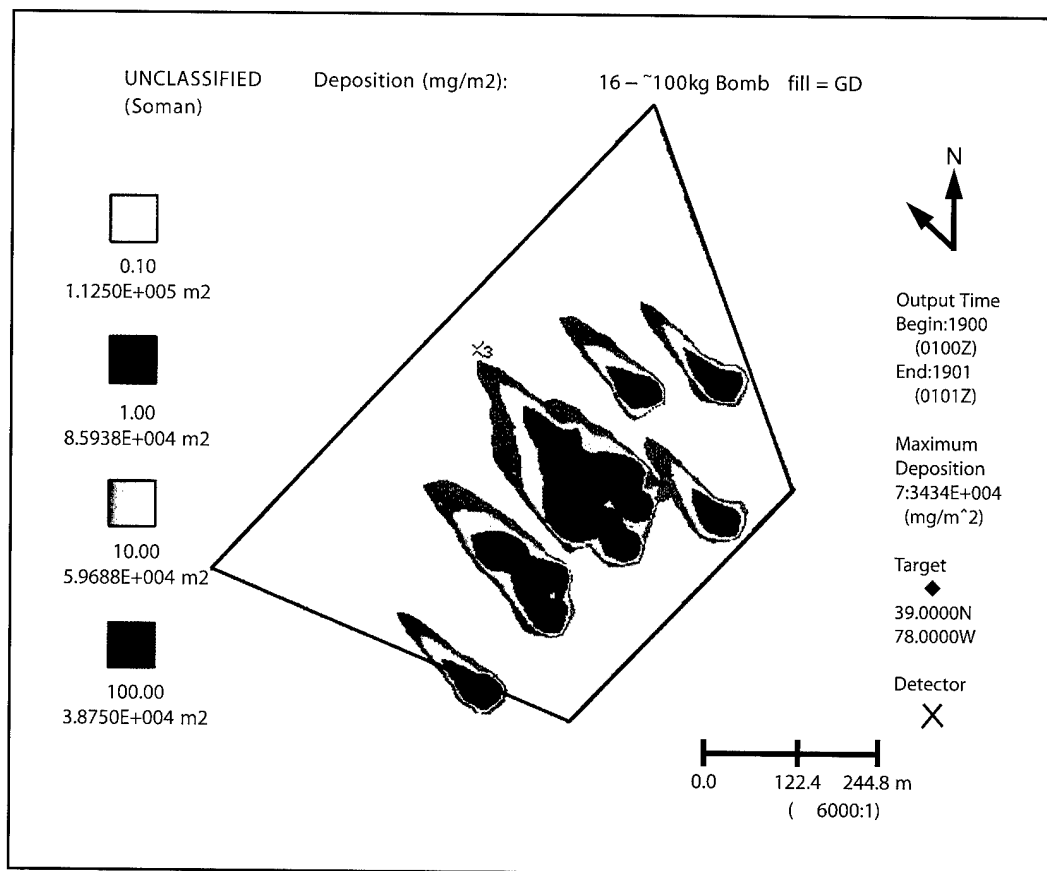


Figure 4—Microsoft Windows VLSTRACK 1.6.3 Hazard Display

A character graphics version has been maintained for other operating systems. A different Microsoft Windows GUI was also developed for the Mobile Oceanographic Support System (MOSS).

In early FY97, VLSTRACK was recognized by the offices of the Assistant to the Secretary of Defense (Nuclear, Chemical, & Biological) (CB Matters) and the Deputy Under Secretary of the Army for Operations Research as the DoD interim standard model for predicting hazards resulting from CB weapon attacks. VLSTRACK 1.6.1 was also approved by SPAWAR for distribution to the fleet. The author and other Chemical and Biological Systems Analysis Branch members Roger Gibbs, Matthew Wolski, Paul Kirk, and Michael Armistead were recognized by NSWCCD with an Award of Merit for Group Achievement for these accomplishments.

VERIFICATION, VALIDATION, AND DOCUMENTATION

Because of the emergency situation involved in getting the original VLSTRACK 1.0 out to the fleet, only a source-code verification effort was performed at NPS. The validation done for the NUSSE model was considered sufficient for the situation. Documentation involved a user's manual¹ and the NPS verification effort summary.² With the development of VLSTRACK 1.2, a full verification, validation, and documentation effort was undertaken. A large sensitivity study was performed at the Fleet Numerical Oceanography Center (FNOC) (now the Fleet Numerical Meteorology and Oceanography Center (FNMOC)), and VLSTRACK 1.2 was validated against field trial data from a dozen reports. These

efforts were documented with NSWCDD technical reports (TRs).^{3,4} VLSTRACK was also documented to meet MIL-STD-2167A requirements for operational computer models, as interpreted by the Naval Oceanographic Office (NAVOO). These documents included:

- ◆ An Operational Concept Document (OCD)
- ◆ A Software Requirements Specification (SRS)
- ◆ A Software User's Manual (SUM)
- ◆ A Software Design Document (SDD)
- ◆ A Software Test Description (STD)

When VLSTRACK 1.5/2.0 was developed, the same process was repeated. The verification and validation efforts were performed and documented in TRs by an independent contractor.^{5,6} The validation effort was also expanded to include several additional field trial reports. The five MIL-STD-2167A documents were also updated. The report from the NOAA ITR⁷ documents their evaluation of the source code.

No verification effort has been performed for VLSTRACK 1.6.x/2.1.x. However, the validation effort has been expanded to include 60 field trial reports summarizing over 400 field trials, with results summarized in a classified TR. The five MIL-STD-2167A documents were also updated, and a Software Test Report (STR) was added. The SUM has recently been converted to meet the newer MIL-STD-498 documentation requirements. VLSTRACK is the most extensively verified, validated, and documented computer model applicable to CBW hazard prediction.

NSWCDD CBW ANALYSIS EFFORTS

VLSTRACK has been used by the Chemical and Biological Systems Analysis Branch in support of various studies, wargames, and analysis efforts.

VLSTRACK has been used to provide hazard predictions for several wargames:

- ◆ The Prairie Warrior '95 wargames
- ◆ The Global '95, Global '96, and Global '97 wargames
- ◆ The Army After Next Winter and Summer wargames of 1997
- ◆ The Army After Next Spring wargames of 1998

Figure 5 shows a VLSTRACK hazard simulation for a biological release during the Global '95 wargames.

VLSTRACK has been used to model the expected sensitivity of different biological detector arrangements around air bases and ports as part of the biological port protection Advanced Concept Technology Demonstration (ACTD) (now called Portal Shield) and to predict particle concentration profiles for the biological detection Advanced Technology Demonstration (ATD). VLSTRACK was also used to support the Navy's Cost and Operational Effectiveness Analysis (COEA) for Theater Ballistic Missile Defense (TBMD). Analysis has been done for incoming missiles bulk-filled with chemical agent liquid and includes hazard area prediction on the ground, keep-out altitude determination, and high altitude droplet breakup simulation. VLSTRACK is also being used to support the Office of the Special Assistant for Gulf War Illness (OSAGWI) in analyzing the potential hazards to U.S. troops in the vicinity of bunkers containing chemical munitions that were destroyed by Allied forces. NSWCDD is working closely with the naval research laboratories in Monterey, California and Washington, D.C. (NRL-MRY and NRL-DC) to analyze these releases by coupling VLSTRACK with output from the Navy's Coupled Ocean/Atmosphere Mesoscale Prediction System (COAMPS) meteorology forecasting model. Figure 6 shows a hazard prediction for a release at one of these munition storage locations.

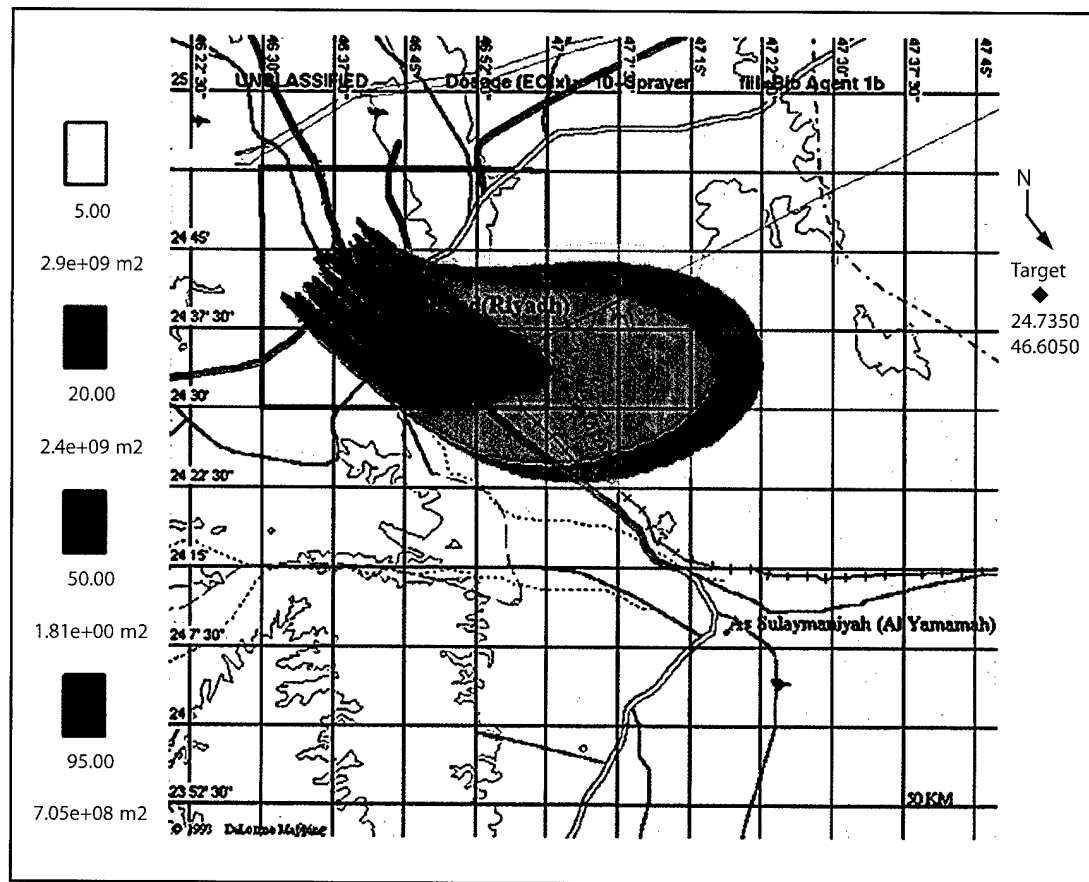


Figure 5—Biological Agent Release During Global '95

CURRENT AND FUTURE DEVELOPMENT

A fully functional VLSTRACK, Version 3.0 has already been developed that further expands many of the existing model capabilities. VLSTRACK 3.0 also provides either probabilistic or simultaneous deposition, dosage, and concentration hazard estimation. The new version also provides a greater range of meteorological capabilities. This version is currently being validated and documented in the form of its predecessors and will replace both VLSTRACK 1.6.3 and VLSTRACK 2.1.3. Future versions of VLSTRACK will continue the tradition of adapting to ever-changing customer needs and listening to user feedback.

CONCLUSIONS

VLSTRACK has been developed as an operational CBW hazard assessment model that can also be used for research and development purposes. VLSTRACK can run on almost any computer system and has been extensively verified, validated, and documented to meet operational requirements. VLSTRACK has been distributed to approximately 300 offices, about half of which are outside of the Navy. Also, VLSTRACK has been incorporated into several larger software systems and has been used in support of a variety of studies and wargames. VLSTRACK has been and continues to be an important asset to the Navy with the persistent threat of CBW.

REFERENCES

1. Bauer, T. and Kirk, P., *Operator's Instruction Manual for VLSTRACK Version 1.0*, Draft, Naval Surface Warfare Center, Dahlgren, VA, Nov 1990.
2. Kamada, R., Skupniewicz, C. and Drake, S., *Preliminary Evaluation and Upgrade of the Airborne Toxic Dispersion Model, VLSTRACK*,
3. Bauer, T. and Macke, G., *Model Verification of VLSTRACK 1.2*, NSWCDD/TR-94/29, NSWCDD, VA, Sep 1994.
4. Bauer, T. and Wolski, M., *Initial Validation of VLSTRACK Version 1.2*, NSWCDD/TR-92/647, NSWCDD, Dahlgren, VA, Sep 1993.

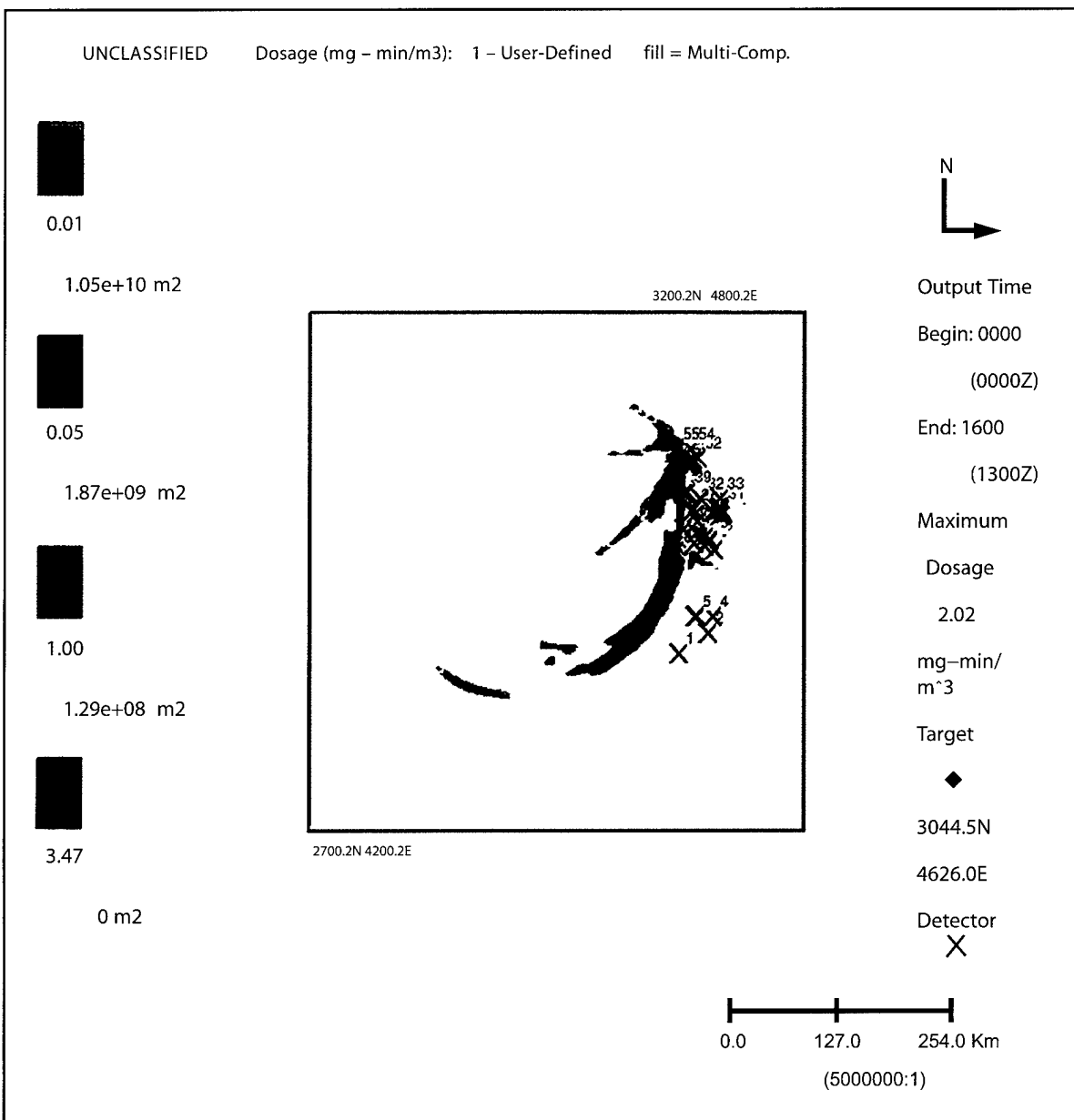


Figure 6—VLSTRACK Hazard Prediction for the Khamisiyah Release

5. Sterle, T. et. al., *Verification of VLSTRACK Version 1.5 and Version 2.0*, AL/CF-TR-1995-0067, Air Force Materiel Command, Wright-Patterson Air Force Base, OH, Oct 1994.
6. Sterle, T., et. al., *Initial Validation of VLSTRACK Version 1.5 and Version 2.0*, AL/CF-TR-1994-0055, Air Force Materiel Command, Wright-Patterson Air Force Base, OH, Dec 1993.
7. Nappo, C., et. al., *Technical Review of the VLSTRACK Dispersion Model*, Draft Report, National Oceanic and Atmospheric Administration, Oak Ridge, TN, Sep 1994.

THE AUTHOR

MR. TIMOTHY J. BAUER



Mr. Timothy J. Bauer is a member of the Chemical and Biological Systems Analysis Branch where he has worked as a chemical engineer since 1988. Tim earned a B.S. degree in chemical engineering at the University of Delaware in 1985 and an M.S. degree in chemical engineering at North Carolina State University in 1987. Tim's job at NSWC has always involved mathematical modeling of various processes occurring with the intentional release of chemical or biological warfare agents into the atmosphere. Tim is also a member of the Allied Technical Publication Number 45 (ATP-45) Custodian Group, which consists of representatives from various NATO countries who are responsible for maintaining and updating the NATO standard procedures for warning and reporting Nuclear, Biological, and Chemical (NBC) incidents.

MINE COUNTERMEASURES SIMULATOR AN/SSQ-94(V) ADVANCED TECHNOLOGY FOR MIW TRAINING

Mr. John R. Denton

The AN/SSQ-94 Mine Countermeasures Simulator (MCS) provides training for the combat information center (CIC) crew on board Mine Countermeasures (MCM) and Minehunter Coastal (MHC) class ships. This article describes MCS and its use of technological advancements in computer, software engineering, and modeling and simulation technology. The phased approach used to develop the system is described and, for each phase, the technology transitioned from the “lab” to the fleet is identified. The technologies include advanced tactical computers, modeling, and simulation algorithms implemented in digital signal processors and computer graphics. The program’s very successful use of the ADA programming language is described, as is the software development methodology.

Minehunting is certainly not one of the most glamorous jobs in the Navy, but it is an important one. Since World War II, more U.S. Navy ships have been sunk or damaged by mines than by any other weapon (see Figure 1). Mines are cheap, yet extremely effective, weapons. Hunting mines requires patience and a wide range of skills. Minehunting is conducted by MCM and MHC class ships. A typical minehunting mission involves steering the ship down a set of parallel tracks while searching for mines using the AN/SQQ-32 Minehunting Sonar Set (MSS) high-resolution sonar. When a mine-like object is detected, an unmanned underwater vehicle called the Mine Neutralization Vehicle (MNV) is guided to the mine. If the mine is moored to the bottom, the MNV will cut the mooring cable, allowing the mine to float to the surface where it will be destroyed by the ship’s 50-caliber machine gun. If the mine is lying on the ocean floor, the MNV will drop a bomblet near the mine. After the MNV has been recovered, the bomblet is detonated to destroy the mine. When the mine has been neutralized, the ship continues down the tracks searching for the next mine.

MCM and MHC ships have a similar suite of combat systems (see Figures 2 and 3). Both ships have the AN/SQQ-32 MSS and the AN/SLQ-48 Mine Neutralization System (MNS). MCM ships use the AN/SSN-2(V) Precise Integrated Navigation System (PINS) for navigation and tactical display functions. MHC class ships use the AN/SYQ-13(V) Navigation Command and Control (NAVC²) system to perform similar functions. Historically, the only effective means of training the CIC crew of MCM and MHC ships has involved having the entire ship and crew hunt mines in a “dummy” minefield—a very costly and time-consuming procedure.

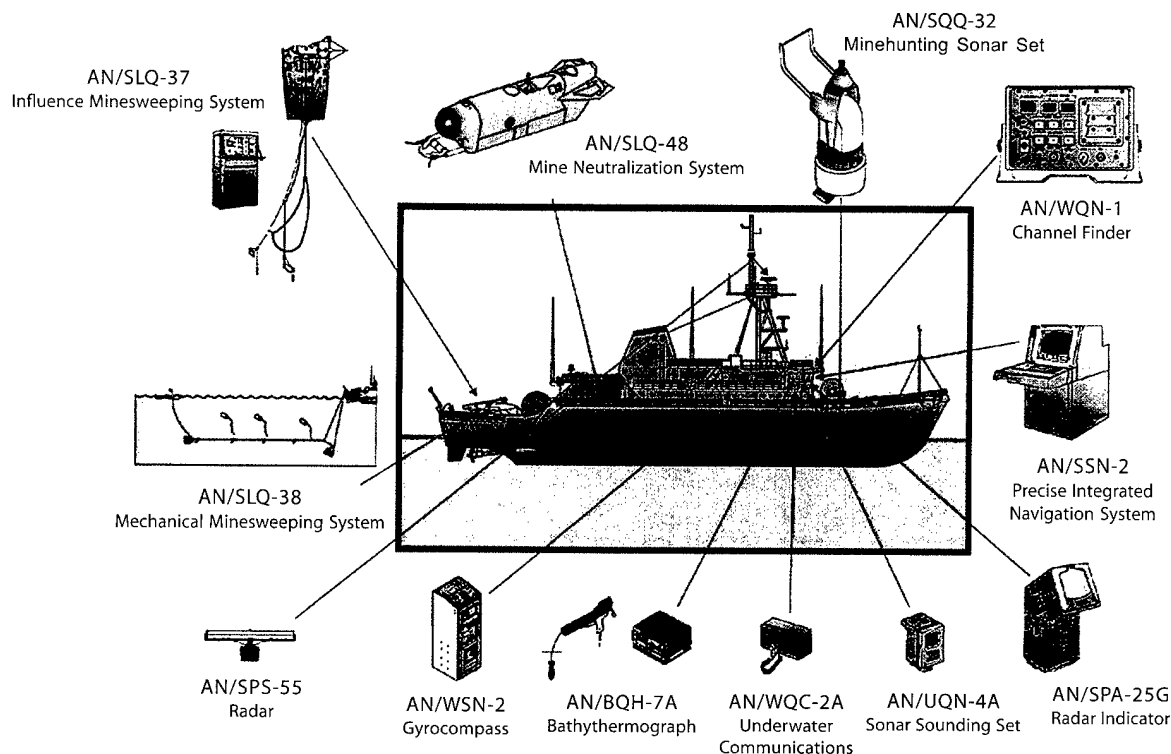


Figure 2—MCM Combat Systems

chosen. The Training Coordinator may also edit a canned scenario, or create a new one from scratch. Only the Training Coordinator knows the layout of the gameboard before the training scenario begins.

After a training scenario has been selected, a hardware setup page is displayed, which indicates the proper initial configuration for each combat system prior to starting the training scenario. At this point, each combat system is placed in "training mode" and the controls are set to their proper starting position. If an MCS team training scenario has been selected, the Training Coordinator will give a mission brief to the CIC team in which he describes the anticipated threat, such as potential mine types and mine density, along with known environmental parameters, such as water current and bottom type. Combat system operators will then return to their consoles, and the Training Coordinator will begin the training mission.

Typical team training missions last five or six hours, but may be extended to more than 24 hours. The Training Coordinator may pause or end a training mission at any time. During the training mission, the CIC team has complete freedom to prosecute the minefield in any manner they choose. However, MCS will record all operator actions, and will provide a mission summary and overall grade at the end of the training mission based on official minehunting tactics, as described in NWP27.

System requirements for MCS were developed based on the training requirements of each combat system and on minehunting tactics described in NWP27. From these requirements, a set of testable software requirements was developed. The software architecture of MCS was based on the Object Connection Update (OCU) model developed by the Software Engineering Institute at Carnegie Mellon University. The OCU model was developed specifi-

cally for trainers. The OCU model was in the concept phase when it was first introduced to the MCS project. The MCS design team took this concept and molded it into a working model. The OCU model provides a logical framework for partitioning the software into a set of design elements and a communication mechanism for these design elements. Each design element is supported by a form for capturing information about individual instances of each design element. These forms were used to develop the design documentation for MCS. A tool was written to analyze the completed design document and generate a set of software code templates. Simulation models were added to these templates to complete the code. This process ensured a consistent software structure and close correlation between the design documentation and code.

Software development was divided into three phases. In the first phase, software requirements, design, and code for the MNV Simulator and Scenario Controller (SC) were developed. The SC provides an Operator Machine Interface (OMI) to the MCS operator and overall control of training missions. The MNV Simulator inputs operator thruster commands and uses an MNV hydrodynamic model to realistically model MNV motion. The MNV Simulator also includes MNV sensor simulations, two-camera simulations and a sonar simulation. Software development processes and documentation formats were also developed during the first phase of development. In the second phase the PINS Simulator was added. The PINS Simulator uses ship position calculated by an MCM hydrodynamic model to provide simulated navigation sensor inputs to PINS. The third development phase

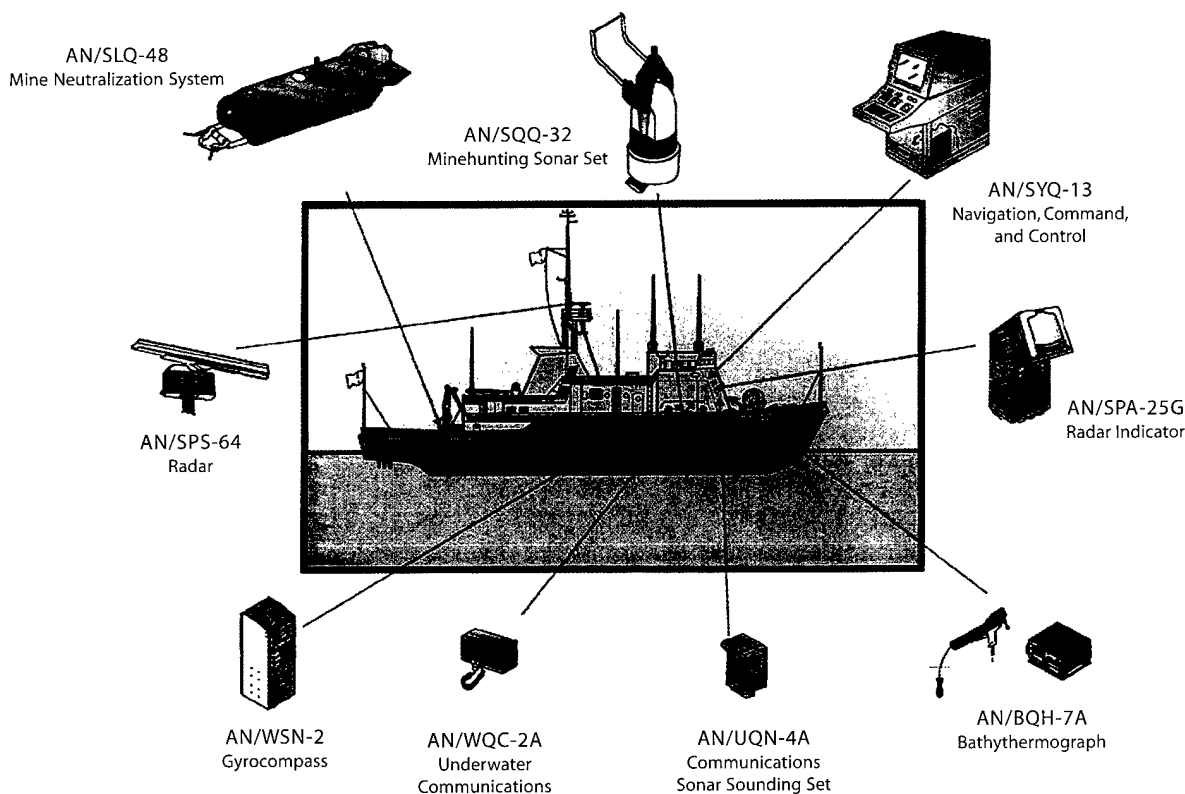


Figure 3—MHC Combat Systems

included the addition of the MSS simulation, subteam training, and team training. MSS uses a variable depth towed sonar array, or Towed Body (TB) to detect and classify mines. The MSS Simulator simulates all TB sonar image and sensor data and provides this data to the MSS consoles. The winch used to raise and lower the TB, and the motions of the TB are also simulated. During each phase, the combat system being simulated was modified to include a "training mode," which would accept simulated data from MCS in place of real sensor data. This phased development approach allowed process improvements and lessons learned from one development phase to be applied to successive development phases.

The ADA software language was used in all phases of development. The advanced software concepts embedded in the ADA language significantly reduced the number of run-time errors normally associated with more primitive software languages. Approximately 95 percent of MCS is written in ADA, with the remaining five percent written in "C." The bulk of the "C" code resides in the MSS sonar simulation algorithms, which were reused from a previous simulation project.

MCS is composed primarily of commercial off-the-shelf (COTS) hardware. The computer platform chosen for the first phase of MCS development was the Silicon Graphics 440VGX computer. The 440VGX contains four R4000 RISC processors and has a powerful graphics engine for three-dimensional rendering. The 440VGX was chosen because it was the lowest cost computer at the time that could handle the processing load required to simulate the MNV cameras and sonar. During the second phase of development, MCS was ported from the 440VGX to the more logistically supportable Navy standard TAC-4 Computer. The TAC-4 used by MCS has two Hewlett-Packard (HP) PA 120 MHz RISC processors. An HP Visualize-48 graphics engine was added for the MNV camera simulation. The TAC-4 was bridged to a 21-slot VME cage containing interface boards for the MNS and PINS. The addition of the MSS Simulator during the third phase of development required considerably more processing power. A Force Computer Systems SPARC-20VT RISC processor board, and 24 Mercury Computer Systems

I860 Array processors were added to the VME cage to provide the 1.5 Giga-FLOPS of processing power needed to generate the simulated sonar images. MCS is housed in a standard 19-inch rack. See Figure 4. MCS meets Electromagnetic Interference standard MIL-STD-461D and shock standard MIL-S-9001D grade B.

During MCS development, several MCM and MHC crews were invited to use and evaluate MCS. All participating crew members felt that MCS was an effective and user-friendly trainer. Integration testing of MCS was successfully completed in November 1997. MCS installation on board MCM ships began in June 1998. The MHC version of MCS is currently under development, with installations scheduled to begin September 1999. Future upgrade plans include integrating MCS into the Battle Force Tactical Trainer (BFTT). BFTT links various Navy shipboard trainers together for coordinated training using Distributed Interactive Simulation protocols. Integrating MCS into BFTT will allow MCM class ships to participate in force-level exercises using the simulated theater of war provided by BFTT.

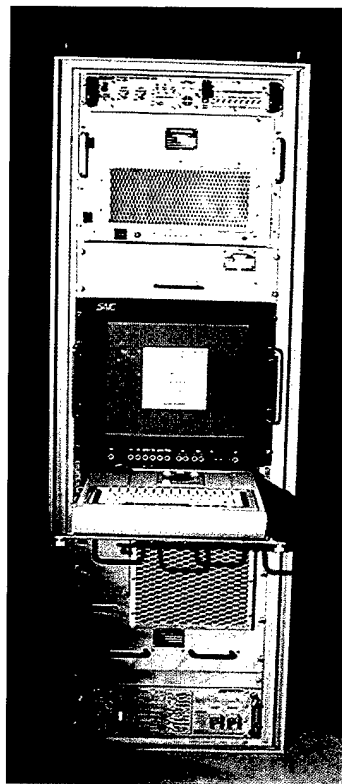
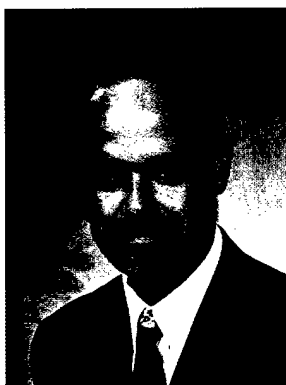


Figure 4—MCS Hardware

THE AUTHOR

MR. JOHN R. DENTON



Mr. John R. Denton received his B.S. degree in electrical engineering from Auburn University in June 1983. He started at CSS in Panama City, Florida, and worked on the Precise Integrated Navigation System (PINS) Program. In 1990, he returned to school and earned his M.S. in computer engineering at the University of Central Florida. He returned to work at CSS in 1991 as a task leader for the AN/SSQ-94 MCS Program. In 1998 he became the project engineer for the AN/SSQ-94 Program.

THE AEROPREDICTION CODE: PAST, PRESENT, AND FUTURE

Dr. Frank G. Moore

This article discusses the evolution of the Aeroprediction Code (APC) from its first version in 1972 to the latest version being released to the public in 1998 (AP98). Current theoretical methodology used in the AP98 is shown, and past references are given where the new methods were developed. Typical application examples of the code are given. These include conceptual design, trim aerodynamics, structural loads, and aeroheating. Future opportunities for the APC are also discussed.

INTRODUCTION

In the late 1960s and early 1970s, the Naval Surface Warfare Center, Dahlgren Division (NSWCDD) was highly involved in projectile designs for improved range and accuracy. These designs were primarily associated with ballistic or unguided ammunition, but many were associated with the idea of a guided projectile (which at that time was just a concept). Being a fairly young engineer, with a Ph.D. degree in aerospace engineering with an emphasis in computational fluid dynamics (CFD), I was called upon to estimate the static aerodynamics of these projectile concepts and to offer suggestions on how to improve the designs to meet desired goals. Naturally, I was eager to spend several months to modify a code¹ that had been developed using the three-dimensional method of characteristics and small crossflow approximation to compute both the inviscid and viscous aerodynamics of these projectiles. However, I was informed by the sponsors of these projectile designs that they wanted answers “yesterday” rather than 6 months to a year later.

As a result of this desire for fast turnaround with reasonable accuracy, I began to look around for approximate aerodynamic prediction codes for calculating static aerodynamics of projectiles. Finding no accurate codes available for total force and moment prediction, I resorted to the use of handbooks, wind tunnel data bases, and simple theoretical prediction methods that could yield answers in a very short manner. After performing numerous hand calculations, I was able to look at a design and estimate the zero-lift drag reasonably accurately based on my “mental data base.” If this could be done with the brain as a computer, why couldn’t this process be automated and made more predictable in terms of bounds of accuracy? This idea was suggested to a sponsor in the Naval Sea Systems Command (Mr. Lionel Pasiuk), and he provided financial support for the first version of the NSWCDD APC. The words “aerodynamic prediction” were joined together in 1972 as aeroprediction and shortened even further in 1993 as AP72, AP74, etc., to denote the particular version and year the APC was developed.

The original objective of the first version of the APC, the AP72,² was to "predict aerodynamics with reasonable accuracy and cost effectively over the flight envelope of interest to weapons designers." This original objective is still true today. However, as will be discussed in more detail later, in order to meet this objective, many new technologies have been developed along the way. These new technologies have been well documented²⁻¹⁸ and have been used not only by the APC series, but transitioned to other codes as well (see Reference 19 for example).

The reason for the new technology needs was the changing requirements of the tactical weapons community. The first version² of the code was limited to unguided projectiles. This meant body-alone configurations, which had nose shapes that could be sharp, blunt, or truncated, Mach numbers 0 to 3, and small angles of attack (AOA). Fins were added to the configurations allowed so that guided projectiles, missiles, and rockets could be considered in 1974.³ Dynamic aerodynamic derivative computational methods were added in 1977.⁵ The desire for higher Mach numbers was partially addressed by the AP81²⁰ and more completely in 1993.²¹ Also, nonlin-

ear aerodynamics were considered for AOA to 30 deg in 1993 and to 90 deg in 1995.²² Also, the AP95 was made much easier to use by creating pre- and post-processing software packages and making it interactive on a personal computer.²³ As of the writing of this article, 139 copies of the AP95 had been transitioned. This included 83 copies to

industry, 38 to government agencies, 14 to universities and 4 to foreign countries. The APC has become one of a few mainline tools in the aerospace industry for weapon aerodynamics.

The AP98²⁴ is the latest version of the APC series, and it is in the process of being released outside NSWCDD. The AP98 improves upon the AP95 in several respects. First of all, it gives much better axial force predictions at higher AOA due to new technology developed.¹⁷

Secondly, it distributes all loads over the body and lifting surfaces to make the code more useful to structural engineers.¹⁶ Thirdly, it extended the AP95 to include nonaxisymmetric body cross sections through significant new technology developed just recently.¹⁸ Fourth, it provides all aerodynamics and loads in the roll stable position $\Phi = 45$ deg (fins in

NOMENCLATURE

C_A	Axial force coefficient
C_{AF}	Forebody axial force coefficient (excludes the base pressure component)
C_{ℓ_P}	Roll damping moment coefficient
C_M	Pitching moment coefficient
$C_{M_q} + C_{M_{\dot{\alpha}}}$	Pitch damping moment coefficient
C_N	Normal force coefficient
$C_{n_{p\alpha}}$	Magnus moment coefficient derivative
d	Diameter
ℓ_n	Nose length
M_∞	Freestream Mach number
P_∞	Freestream pressure (lb/ft ²)
\dot{q}	Heat transfer rate (BTU/(ft ² sec))
R_N	Reynolds number
r/s	Ratio of body radius to body radius plus wing semispan
r_n, r_B	Radius of nose and base respectively
T_∞, T_w	Freestream and wall temperature respectively (degrees Rankine)
X_{CP}	Center of pressure measured from some reference point
α	Angle of attack (degrees)
α_{TRIM}	Angle of attack where pitching moment is zero
δ	Control deflection (degrees) with positive being leading edge up
Φ	Roll angle with $\Phi = 0$ being windward plane and signifying fins in plus fin orientation

"x" or cross roll position) in addition to the $\Phi = 0$ deg roll stable position (fins in "+" or plus roll position).¹⁴ Finally, it provides an improved pre- and post-processing software package with significant added graphics options.²⁵

Table 1 shows the objective, application uses and overall flight requirements of today's tactical weapons. Table 2 shows the evolution of the APC as it attempted to meet these evolving requirements.

This article will briefly summarize the theoretical methods used in the APC, will give some examples of the types of uses for the code, and finally, will discuss future versions of the code. References will be given for some of the theoretical methods used so the interested reader can refer to them for more details. For a brief summary of the theoretical methodology up through 1998, the reader is referred to Reference 24.

THEORETICAL METHODOLOGY

The APC seeks to give average accuracy levels of ± 10 percent on axial and normal force coefficient prediction, and ± 4 percent of body length on center of pressure estimation. Here, average accuracy is used to indicate that enough Mach numbers and AOA are considered to give a good statistical sample versus a single data point, where accuracy can (on occasion) exceed the average accuracy goals. Center of pressure accuracy—versus pitching moment accuracy—is used because it is independent of where the reference point is taken, whereas pitching moment accuracy in percent is dependent on where the reference point is taken. These accuracy levels

have proven to be quite acceptable to meet the objective and application uses shown in Table 1.

To meet the objective of cost effectiveness in Table 1, a semiempirical, component-buildup, aerodynamic prediction approach is utilized. This is in contrast to a numerical solution for the entire flowfield that encompasses the configuration. A component buildup approach was utilized first in the APC by the AP74,³ where the body, wing, tail,

and mutual interference effects were estimated independently and then added together to get the total forces and moments. Most of the aerodynamics were estimated analytically by linearized theories, second-order theories, and slender-body theory. However, there were some aerodynamic terms that could only be estimated based on use of experimental data. These included base drag and the separation drag that occurs in the vicinity of a vehicle with a large cone angle at subsonic Mach numbers. Other terms were estimated analytically, but the amount of computations were too long for rapid computation, so these computations were made off-line and included in a table

look-up format. An example of this was transonic wave drag. As a result of the combination of theoretical, empirical, and table look-up methods, the APC is a semiempirical code.

The various theoretical aerodynamic prediction methods used for the AP98 are shown in Tables 3 through 5. Table 3 gives the body-alone methods; Table 4, the wing-alone and interference methods; and Table 5, the dynamic derivative methods. Also, the references upon which the methods are based

Table 1—Objective and Requirements for APC

OBJECTIVE	
PREDICT AERODYNAMICS COST EFFECTIVELY AND WITH REASONABLE ACCURACY OVER THE FLIGHT ENVELOPE OF INTEREST TO WEAPONS DESIGNERS.	
APPLICATION REQUIREMENTS OF APC	
◆	AERODYNAMIC DESIGN (PRELIMINARY)
◆	INPUTS TO 3-DOF/TRIM PERFORMANCE MODELS
◆	PRELIMINARY STRUCTURAL LOADINGS
◆	CONVECTIVE HEAT TRANSFER INPUTS
OVERALL FLIGHT REQUIREMENTS	
MACH NUMBER:	0-15
ANGLE-OF-ATTACK:	0-90°
CONTROL DEFLECTION:	$\pm 30^\circ$
ROLL ORIENTATION:	0°, 45°
SETS OF FINS:	0, 1, 2 REQUIRED; 3 DESIRED
BODY GEOMETRY:	AXISYMMETRIC REQUIRED; NONAXISYMMETRIC TREATMENT DESIRED

Table 2—Evolution of Aeroprediction Code

VERSION	WEAPONS	FLIGHT CONDITIONS				
		AERODYNAMICS	MACH NUMBER	AOA RANGE	ROLL	COMPUTERS
1972	UNGUIDED PROJECTILES	$C_{A'} C_{N'} X_{CP}$	0 - 3	0 - 15°	$\Phi = 0^\circ$	CDC
1974	MISSILES PROJECTILES ROCKETS	$C_{A'} C_{N'} X_{CP}$	0 - 3	SAME	SAME	CDC
1977	MISSILES PROJECTILES ROCKETS	$C_{A'} C_{N'} X_{CP}$ $C_{l_p}, C_{m_q} + C_{m_{\dot{\alpha}}}$ $C_{n_p \alpha}$	0 - 3	SAME	SAME	CDC, IBM
1981	MISSILES PROJECTILES ROCKETS	SAME	0 - 8	0 - 15° (LIMITED CONF. AT HIGHER α)	SAME	CDC, IBM, VAX
1993	MISSILES PROJECTILES ROCKETS	SAME	0 - 20	0 - 30°	SAME	CDC, IBM, VAX, SILICON GRAPHICS
1995	MISSILES PROJECTILES ROCKETS	SAME	SAME	0 - 90°	SAME	INTERACTIVE PC
1998	SAME (ASYMMETRIC BODY TREATMENT)	SAME	SAME	SAME	$\Phi = 0^\circ, 45^\circ$	INTERACTIVE PC

are indicated in the figures. These references are the summary documents, and additional references and details can be found in these summary documents. There are over 35 different methods shown in Tables 3 through 5. These amount to about 23,000 lines of computer code and over 120 subroutines. However, a single case (one Mach number, one AOA, one configuration, and one roll angle) executes on the personal computer in less than a second (INTEL 200-MHz chip). Moreover, with the new interactive software,²⁵ one can obtain a set of aerodynamics on a configuration (including configuration setup and aerodynamics plots) in about 15 minutes. This is in contrast to typically a half day on the AP93, where coordinates of body points had to be computed off-line and then input to the APC.

As already mentioned, references are given in Tables 3 through 5 for the various theoretical methods, so no discussion of any of the theories is planned. Suffice it to say, however, that—in general—linearized theories, slender-body theory, or second-order theories are used for low AOA aerodynamic estimation. Several large wind tunnel data bases²⁶⁻³⁰ are then used to estimate the nonlinear aerodynamic terms as functions of the key geometric and freestream parameters. These nonlinear aerodynamics are then integrated into the later versions of the APC (AP93 and later versions) through either simplified analytical formulations, table look-up, or both. The code then adds the linear and nonlinear terms together to obtain the total forces and moments.

Table 3—AP98 Methods for Body-Alone Aerodynamics

COMPONENT/MACH NUMBER REGION	SUBSONIC $M_\infty < 0.8$	TRANSONIC $0.8 \leq M_\infty \leq 1.2$	LOW SUPERSONIC $1.2 \leq M_\infty \leq 1.8$	MOD/HIGH SUPERSONIC $1.8 \leq M_\infty \leq 6.0$	HYPERSONIC $M_\infty > 6.0$
NOSE WAVE DRAG	EMPIRICAL (Ref. 2)	SEMIEMPIRICAL BASED ON EULER SOLUTIONS (Ref. 2,7)	SECOND-ORDER VAN DYKE PLUS MNT (Ref. 2)	SOSET PLUS IMNT (Ref. 6)	SOSET PLUS IMNT MODIFIED FOR REAL GASES (Ref. 8)
BOATTAIL OR FLARE WAVE DRAG	---	WU AND AOYOMA (Ref. 2)	SECOND-ORDER VAN DYKE (Ref. 2)	SOSET (Ref. 6)	SOSET FOR REAL GASES (Ref. 8)
SKIN FRICTION DRAG	VAN DRIEST II (Ref. 2)				
BASE DRAG	IMPROVED EMPIRICAL METHOD (Ref. 11)				
AEROHEATING INFORMATION	---			SOSET PLUS IMNT FOR REAL GASES (Ref. 10)	
INVISCID LIFT AND PITCHING MOMENT	EMPIRICAL (Ref. 2)	SEMIEMPIRICAL BASED ON EULER SOLUTIONS (Ref. 20)	TSIEN FIRST- ORDER CROSSFLOW (Ref. 20)	SOSET (Ref. 6)	SOSET FOR REAL GASES (Ref. 8)
VISCOUS LIFT AND PITCHING MOMENT	IMPROVED ALLEN AND PERKINS CROSSFLOW (Ref. 22, 24)				
NONAXISYMMETRIC BODY AERO ($\Phi = 0.45^\circ$)	MODIFIED JORGENSEN FOR AP98 (Ref. 24)				
NONLINEAR ST. LOADS AVAIL. ($\Phi = 0.45^\circ$)	NO		YES FOR AP98 (Ref. 16)		

APPLICATIONS

This portion of the article will illustrate some of the application uses of the APC as defined in Table 1. The first of these is for estimating aerodynamics of a conceptual design, either to perform flight dynamics analysis, or to perform conceptual design tradeoffs. During this process, the user is interested in obtaining possibly zero-lift drag for a number of designs as a function of some design parameter(s). These could be total length, nose length and shape, boattail length and shape, or nose bluntness, etc. Another parameter of interest is trim aerodynamics for use in three degree-of-freedom (3-DOF) trajectory models. Each of the above applications can require hundreds of data points (one data point is one configuration, one M_∞ , one α , and one δ). This is the reason for the requirements of ease of use, reasonable accuracy and fast computational and turnaround time.

The first design application shown is for estimating the effect on zero-lift drag of various levels of nose bluntness and nose length. Here, a set of forebody axial force data³¹ is available for tangent-ogive-cylinder configurations. The data was obtained without a boundary layer trip for Reynolds number varying from $1.8 \times 10^6/\text{ft}$ to $5.3 \times 10^6/\text{ft}$, at Mach numbers from 0.6 to 4.0 and AOA from -6 to 14 deg. Figure 1 shows the configuration being tested. Figure 2 gives the forebody axial force results (no base drag included) compared to the experimental data. As seen in the comparison to data, results are well within the ± 10 percent average accuracy goal. Moreover, if one wanted to look at other geometric or freestream variations for drag reduction, this level of accuracy and consistency gives one confidence that the predictions (exclusive of other data) will be reasonable.

Another design application could be to investigate the improvements in the lift-to-drag ratio

afforded by noncircular cross-section bodies for potential range improvement. Figure 3 presents a series of 10-caliber, body-alone configurations tested³² at various Mach numbers and AOA. Figure 4 gives the AP98 results (solid lines) compared to experimental data for the elliptical, square or diamond, and triangular or inverted triangular cross-section shapes, all with a constant cross-sectional area. Note that the theory gives reasonable

agreement with the experiment in all cases. Also worthy of note is the improvement in lift-to-drag ratio afforded by the various noncircular cross-section shapes.

The second application mentioned is to generate trim aerodynamics over the flight envelope over which a weapon flies. This means generation of normal force, pitching moment, and axial force as a

Table 4—AP98 Methods for Wing-Alone and Interference Aerodynamics

COMPONENT/MACH NUMBER REGION	SUBSONIC $M_\infty < 0.8$	TRANSONIC $0.8 \leq M_\infty \leq 1.2$	LOW SUPERSONIC $1.2 \leq M_\infty \leq 1.8$	MOD/HIGH SUPERSONIC $1.8 \leq M_\infty \leq 6.0$	HYPERSONIC $M_\infty > 6.0$
WAVE DRAG		EMPIRICAL (Ref. 3)	LINEAR THEORY PLUS MNT (Ref. 3)	SHOCK EXPANSION (SE) PLUS MNT ALONG STRIPS (Ref. 6, 20)	SE PLUS MNT FOR REAL GASES ALONG STRIPS (Ref. 8)
SKIN FRICTION DRAG	VAN DRIEST II (Ref. 3)				
TRAILING EDGE SEPARATION DRAG	EMPIRICAL (Ref. 3)				
BODY BASE PRESSURE CAUSED BY TAIL FINS	IMPROVED EMPIRICAL (Ref. 11)				
INVISCID LIFT AND PITCHING MOMENT • LINEAR	• LIFTING SURFACE THEORY (Ref. 3)	• EMPIRICAL (Ref. 3)	• 3DTWT (Ref. 3)	• 3DTWT OR SE (Ref. 3)	• 3DTWT OR SE (Ref. 3)
• NONLINEAR	• EMPIRICAL (Ref. 12)				
WING-BODY, BODY-WING INTERFERENCE ($\Phi = 0, 45^\circ$) • LINEAR	• SLENDER-BODY THEORY OR LINEAR THEORY MODIFIED FOR SHORT AFTERBODIES (Ref. 3, 35)				
• NONLINEAR	• EMPIRICAL (Ref. 22,14)				
WING-BODY, INTERFERENCE DUE TO δ ($\Phi = 0, 45^\circ$) • LINEAR	• SLENDER-BODY THEORY (Ref. 3)				
• NONLINEAR	• EMPIRICAL (Ref. 22,14)				
WINGTAIL INTERFERENCE ($\Phi = 0, 45^\circ$)	LINE VORTEX THEORY WITH MODIFICATIONS FOR $K_{W(B)}$ TERM AND NONLINEARITIES				
AEROHEATING	NONE PRESENT			SE PLUS MNT (Ref. 10)	SE PLUS MNT REAL GASES (Ref. 10)
NONAXISYMMETRIC BODY AERO ($\Phi = 0, 45^\circ$)	IMPROVED NELSON ESTIMATE FOR AP98 (Ref. 24)				
NONLINEAR ST. LOADS AVAIL. ($\Phi = 0, 45^\circ$)	NO		YES FOR AP98 (Ref. 16)		

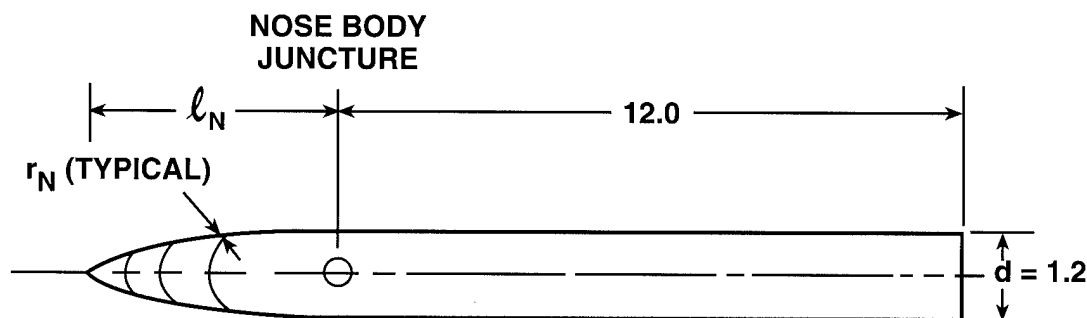
Table 5—AP98 Methods for Dynamic Derivatives (Reference 5)

COMPONENT/MACH NUMBER REGION	SUBSONIC $M_\infty < 0.8$	TRANSONIC $0.8 \leq M_\infty \leq 1.2$	LOW SUPERSONIC $1.2 \leq M_\infty \leq 1.8$	MOD/HIGH SUPERSONIC $1.8 \leq M_\infty \leq 6.0$	HYPERSONIC $M_\infty > 6.0$
BODY ALONE	EMPIRICAL (Ref. 38)				
WING AND INTERFERENCE ROLL DAMPING MOMENT	LIFTING SURFACE THEORY	EMPIRICAL	LINEAR THIN- WING THEORY	LINEAR THIN-WING OR STRIP THEORY	
WING MAGNUS MOMENT	ASSUMED ZERO				
WING AND INTERFERENCE PITCH DAMPING MOMENT	LIFTING SURFACE THEORY	EMPIRICAL	LINEAR THIN- WING THEORY	LINEAR THIN-WING OR STRIP THEORY	

function of AOA, control deflection, Mach number, and altitude. Typically, these data are stored in the form of tables in a 3-DOF trim performance model and accessed as a function of flight time based on a current set of flight conditions (i.e., altitude, Mach number, and weight). The AOA and control deflection, to allow equilibrium flight, are then calculated based on the set of conditions α , δ , where pitching moment is zero, and all forces and moments are in equilibrium. Another alternative that is sometimes used by flight dynamicists is to derive nonlinear equations (based on the known aerodynamics) that can be used in the performance model to generate the aerodynamics for a given set of conditions. This is faster computationally but requires the derivation of the nonlinear equations.

An important part of the trim performance model is a reasonable estimate of the set of α 's and δ 's that allow trim conditions to occur (i.e., pitching moment is zero). Figure 5 considers a wing-body-

tail configuration tested³³ over a fairly broad range of flight conditions. These include Mach numbers 1.5 to 4.6; control deflections of 10 to 20 deg, and AOA to 40 deg at $\Phi = 0$ and 45 deg. The model was tested at a R_N /ft of 2.5×10^6 and had boundary layer trips present. Figure 6 shows a couple of examples for pitching moment as a function of AOA for Mach numbers of 2.35 and 4.6 at a control deflection of 20 deg and for $\Phi = 0$ deg. These cases were chosen because data were available from Reference 33 for comparison purposes. In general, good agreement between the theory and data is obtained up to AOA of 25 to 30 deg. Above that AOA, apparently internal shock interactions between the bow and wing shocks acting on the tail surfaces decrease stability. This is not accounted for in the predictions. However, even at the worst condition of $M = 4.6$ and $\alpha = 44$ deg, the center-of-pressure error is 0.65 cal or 3.6 percent of the body length, which is still within the goal of the ± 4 percent of body length for the center of pressure.

Figure 1—Butler, Sears, and Pallas³¹ Wind Tunnel Model Tested (Dimensions in Inches)

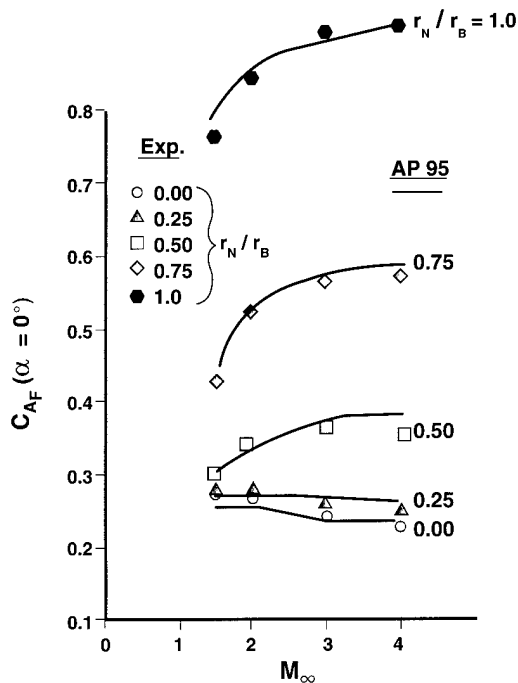


Figure 2—Variation of Forebody Axial Force Coefficient with Mach Number for Various Noses on 10-cal Afterbody ($R_N/\text{ft} = 1.8 \times 10^6$, $\ell_N = 2$ cal)

Figure 7 presents values of α_{TRIM} versus δ for Mach numbers of 1.5 and 4.6. The only data available from Reference 33 was for $M = 1.5$ and $\delta = 10$ deg, and $M = 4.6$ and $\delta = 20$ deg. These points are indicated on the figure. Both data points are slightly lower than those for the theory. This is not unusual because, for gentle sloping pitching moment curves, a slight error in the slope can cause a 2- to 4-deg error in the α_{TRIM} value. It is also interesting to note the shape of the two curves in Figure 7. For higher Mach numbers, the controls gain effectiveness due to compressibility effects as control deflection increases. However, as Mach number decreases, the controls lose effectiveness with increasing control deflection. This is caused by wing stall and blow-by effects. Figure 7 also illustrates that the AP98 can be used outside an available data base or, in many cases, in lieu of data for conceptual and preliminary design. As one refines the design, more accurate numerical code and wind tunnel results will be desired.

The third application also utilizes the Figure 5 configuration, but this time, for structural loads. In the preliminary design of weapons, the structural engineer may use a beam analysis approach (or two-dimensional) versus a full finite element (or three-dimensional) analysis. For this type of analysis, local loads along the body and wings or tails is needed at conditions where the loads are the highest. Figures 8 through 10 therefore give the body, wing, and tail load; shear; and bending moment, respectively, for $\alpha = 40$ deg, and Mach numbers of 4.6, 2.87, and 1.5 at sea-level conditions. The lines are the APC results, and the solid symbols are thin-layer Navier-Stokes code results.¹⁶ Note that in Figure 8, even though the APC-predicted load does not agree with the CFD results as well as desired for the body alone at $M = 4.6$, when these loads are integrated to get shear and then bending moment, excellent agreement with the CFD results is obtained. The CFD results were compared to the total force and moment experimental data³³ before they were used to compare to the APC local loads. Excellent agreement between the CFD and experimental results was obtained.¹⁶

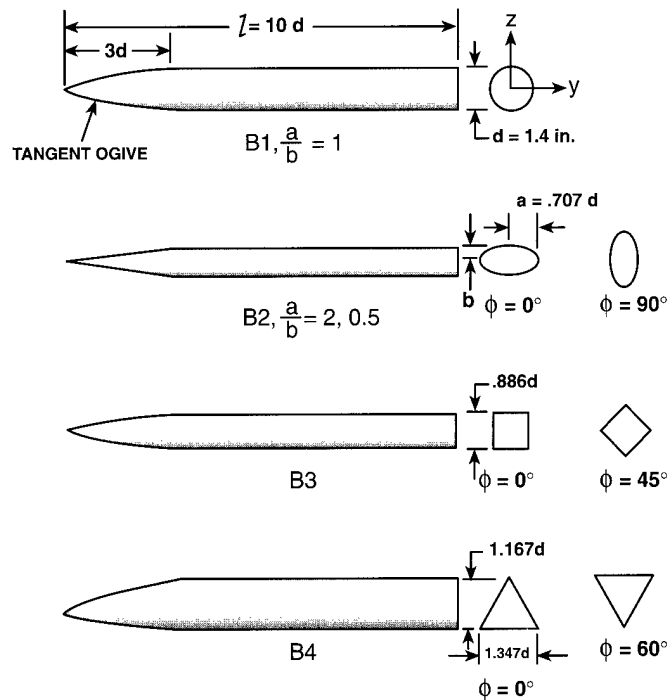


Figure 3—Body Alone Configurations³² with Elliptical, Square, Diamond, Triangular, and Inverted Triangular Shapes

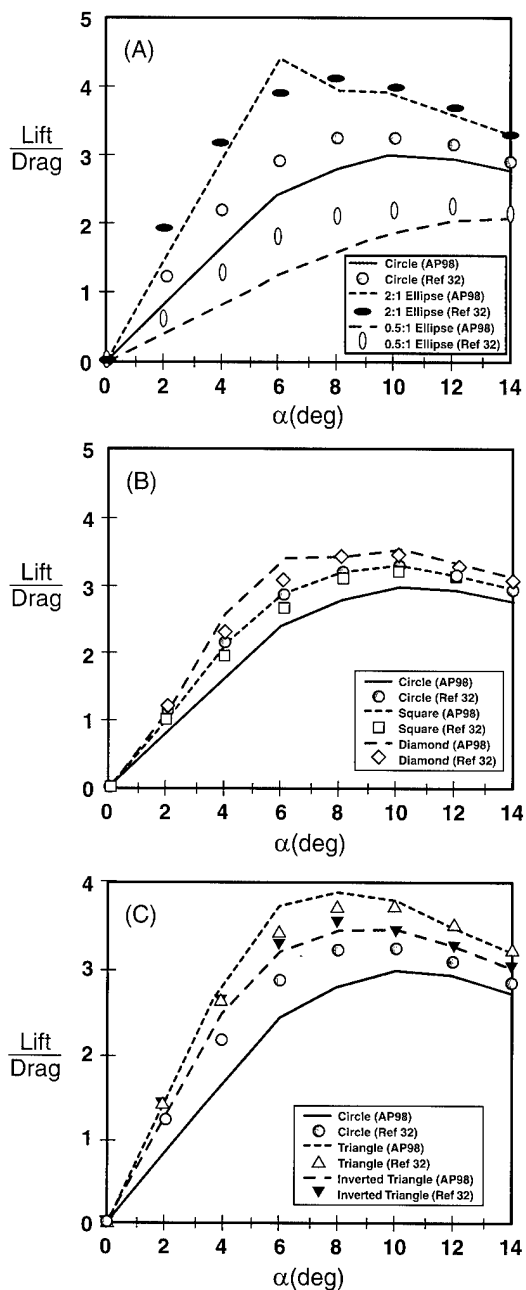


Figure 4—Lift to Drag Ratio of Figure 3 Noncircular Bodies Compared to Circular at $M_\infty = 3.88$: (A) Ellipse, (B) Square, (C) Triangle

Figures 9 and 10 give the wing and tail local loads, shear, and bending moment, again for the Figure 5 configuration. Very good agreement with the CFD results is obtained for all conditions. The results of Figures 8 through 10 were incorporated into the AP98. The AP95 does not have all the nonlinear aerodynamic loads distributed along the body and lifting surfaces, only the linear loads.

The last application referred to in Table 1 was for computing the convective heat transfer for use in conducting heat transfer analysis. In order to perform heat transfer analysis, one must know the type of material the configuration is made of, as well as the material characteristics. This allows the convective heat transfer input to be conducted into or out of the vehicle, depending on the internal and external temperatures. Up through the AP81, no emphasis was placed on calculating the convective heat transfer. However, as Mach numbers at which many weapons fly increased more and more, this term became of increasing interest. Moreover, the inviscid surface temperature—that is, the temperature at the outer edge of the boundary layer—could no longer be calculated based on a perfect gas; so new technology was developed to extend second-order-shock expansion theory to include a real gas.⁸ These real-gas inviscid properties at the outer edge of the boundary layer were then taken through the boundary layer to the surface of the configuration through state-of-the-art engineering formulations.¹⁰

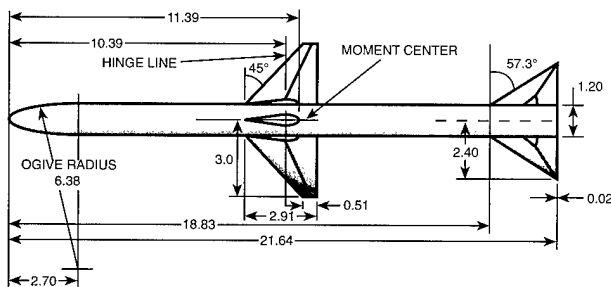


Figure 5—Wing-Body-Tail Used in Validation³³

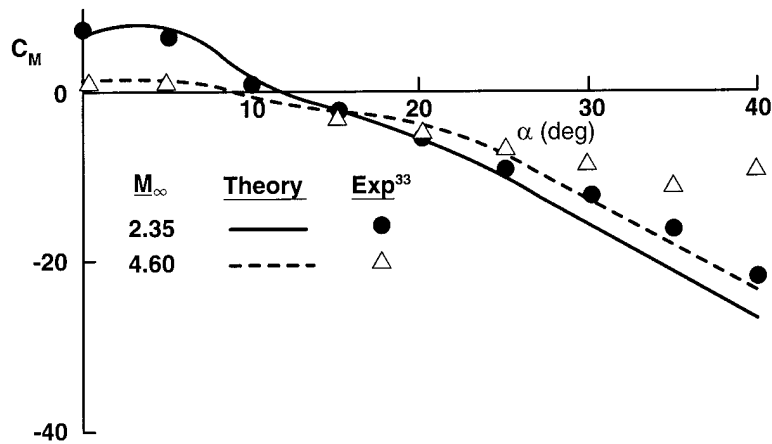


Figure 6— C_M Versus α for Configuration of Figure 5
($\delta = 20$ deg, $\Phi = 0$ deg)

In carrying out these analyses, the importance of real-gas effects at high Mach number on the surface temperature and convective heat-transfer terms cannot be underestimated. To assume perfect gas at Mach 15, for example, can give temperatures in the vicinity of a blunt nose too high by a factor of 2; and on the surface behind the blunt nose, by almost a factor of 2. Hence, if one were to assume perfect- as opposed to real-gas properties, the configuration structural design would be quite different due to external insulations and material requirements. Also, it should be reiterated that, at present, the AP98 gives only the convective term of heat transfer as a function of α , Φ , M_∞ , as well as other freestream and geometry inputs. These properties are available on the body and lifting surfaces up to AOA of 30 deg. Above that AOA, the nonlinear aerodynamic loads have not been incorporated into the heat transfer term, even though they have been incorporated into the structural loading. This means that to perform heat transfer analysis, the AP98 convective heat transfer is used as inputs to a complete heat transfer code that contains the conduction and radiation heat transfer terms as well.

To illustrate the convective heat transfer methodology, a case is selected

from Reference 10. The case selected is a 15-deg, half-angle blunt cone at $\alpha = 10$ deg, with a freestream Mach number of 10.6. This case is selected because it has experimental data³⁴ and other analysis^{35,36} codes available for comparison. Figure 11 gives the heat transfer rate in the windward plane ($\Phi = 0$ deg) as a function of distance along the body. In addition to the aeroprediction and experimental results, results from two codes that use small crossflow, boundary-layer approximations—along with numerical inviscid results³⁵—are shown, as well as the engineering results from MINIVER.³⁶ The APC and MINIVER are similar in the windward plane, except that the APC includes entropy-layer swallowing, whereas the MINIVER does not. The numerical codes agree quite closely with the data. For engineering purposes, all results are quite good and acceptable.

Figure 12 gives the heat transfer rate at a position down the body ($x/r_n = 4.86$) as a function of roll,

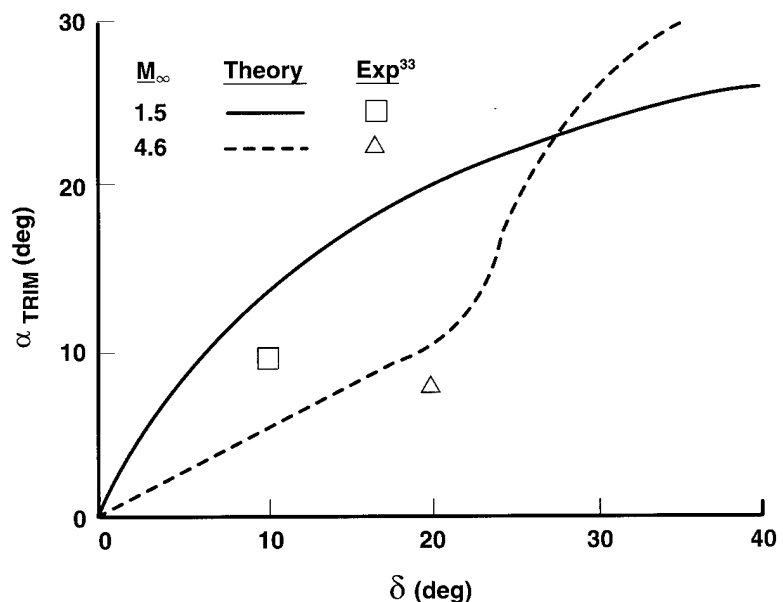


Figure 7—AOA for Zero Pitching Moment Versus Control Deflection
($\Phi = 0$ deg)

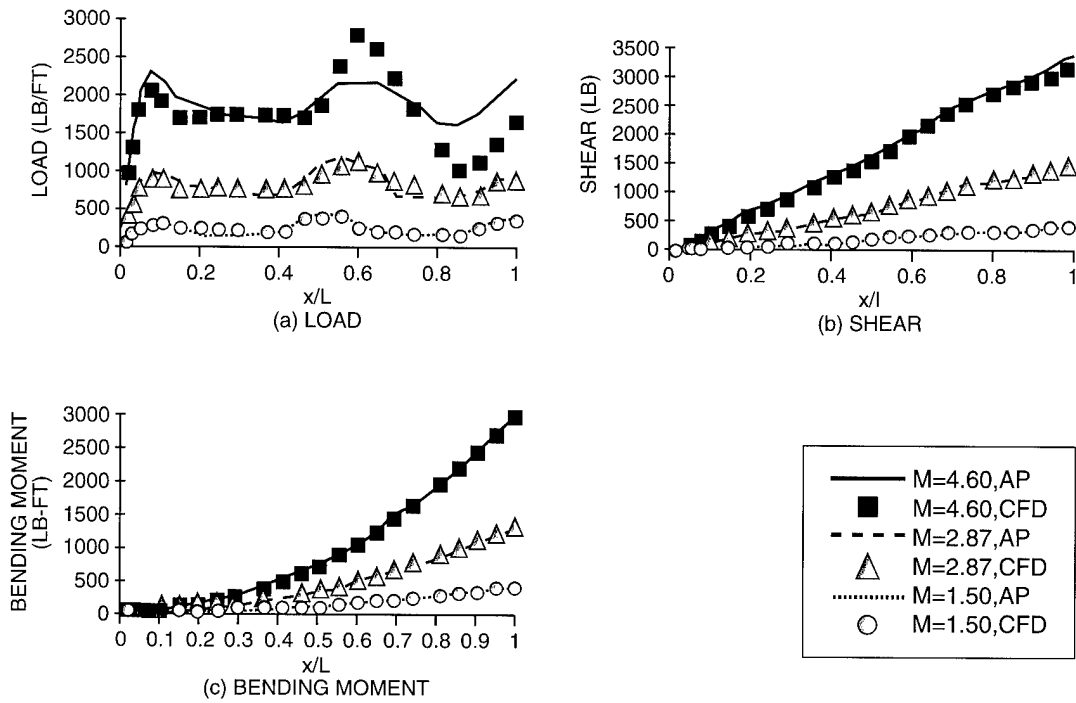


Figure 8—Body Load, Shear, and Bending Moment for Figure 5 Configuration ($\Phi = 0^\circ$, $\alpha = 40^\circ$)

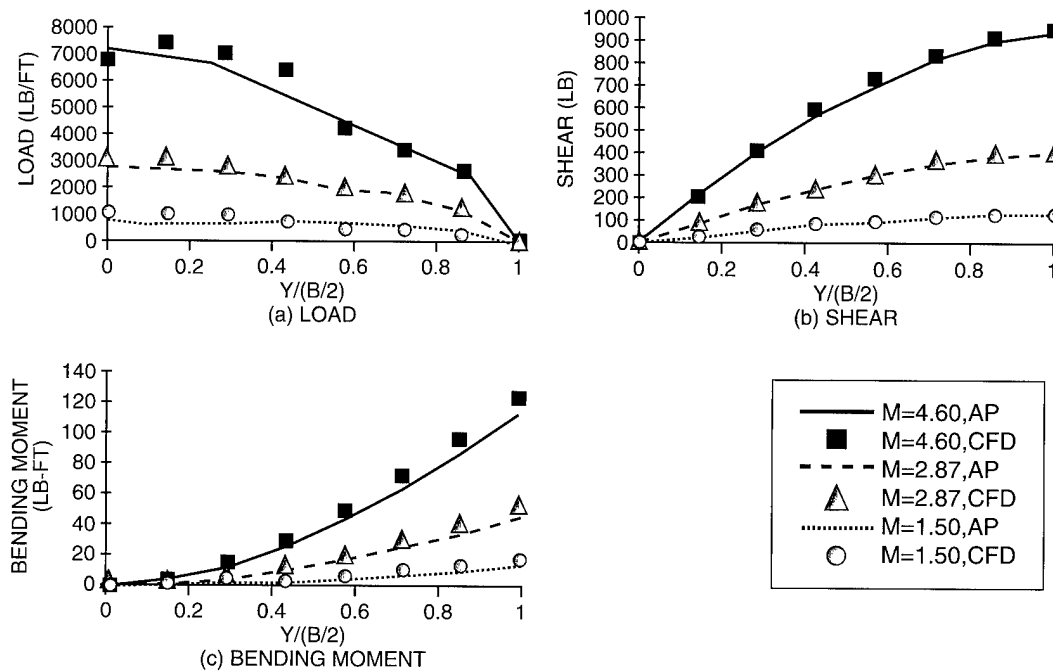


Figure 9—Wing Load, Shear, and Bending Moment for Figure 5 Configuration ($\Phi = 0^\circ$, $\alpha = 40^\circ$)

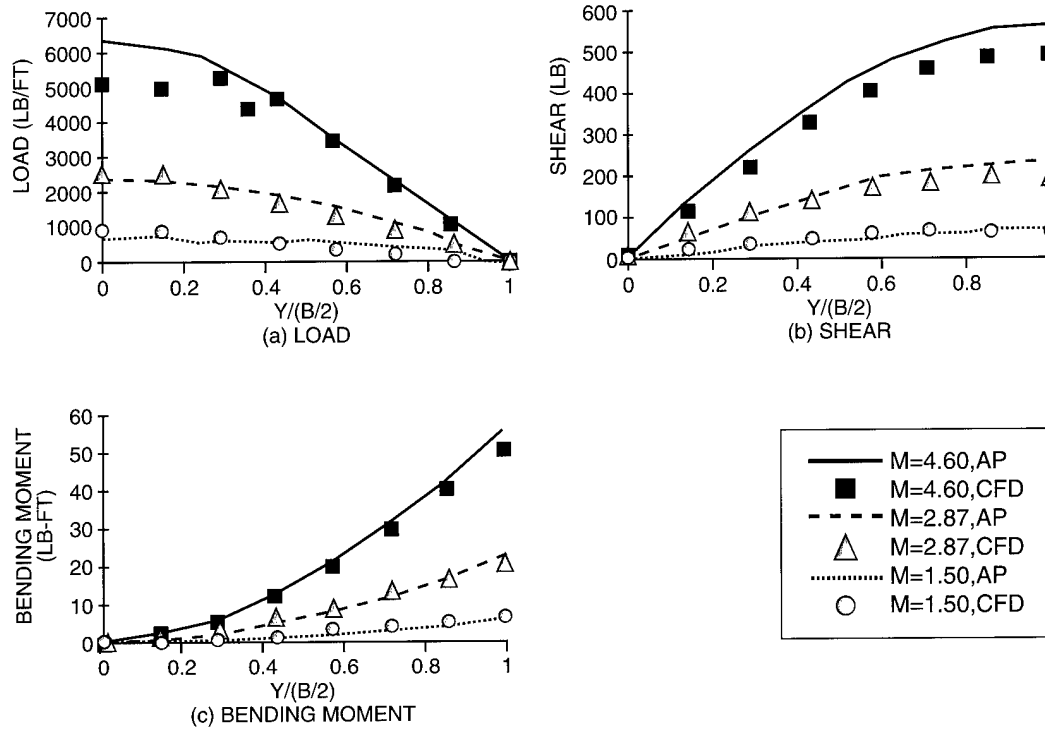


Figure 10—Tail Load, Shear, and Bending Moment for Figure 5 Configuration ($\Phi = 0$ deg, $\alpha = 40$ deg)

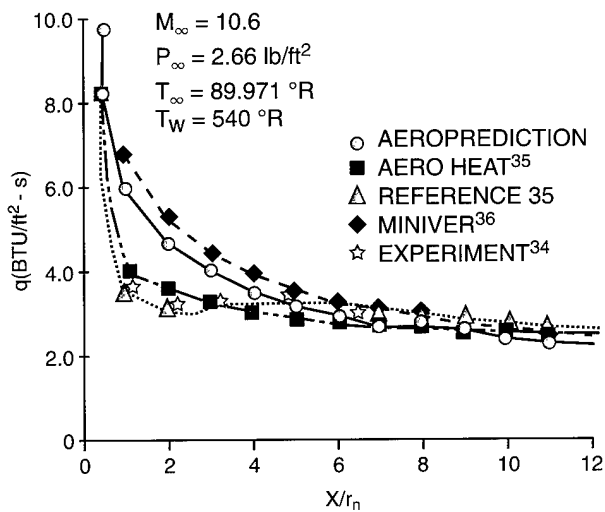


Figure 11—Heat Transfer Rates for 1.1-in. Nose Radius, 15-deg Half-Angle Cone at $\alpha = 10$ deg

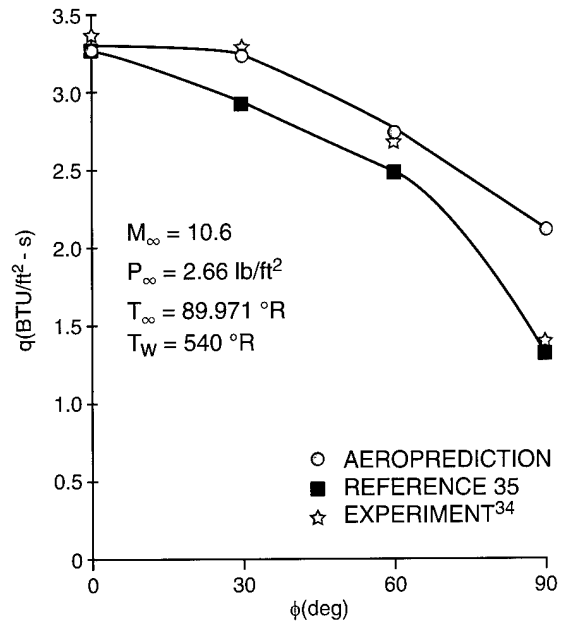


Figure 12—Circumferential Variation of Heating Rates on 1.1-in. Nose Radius, 15-deg Half-Angle Cone at $\alpha = 10$ deg, $x/r_n = 4.86$

where $\Phi = 0$ is the windward plane, and $\Phi = 180$ deg is the leeward plane. Results are shown only from $\Phi = 0$ to 90 deg. MINIVER results are not shown, as the MINIVER apparently computes only heat transfer in a single plane along the body. Reasonable agreement is obtained between the APC results, and the more accurate numerical code and experimental data in Figure 12.

FUTURE PLANS

The AP98 will be transitioned to requesting users in 1998 and beyond. As already mentioned, 139 copies of the AP95 have been transitioned, and it is expected at least that many copies of the AP98 will eventually be transitioned. Approved foreign countries can get a copy of the AP98 by going through the International Programs Office and paying a transition fee. The Navy sponsors pay the transition fees for companies within the United States.

Looking past the AP98, several possibilities exist. Two areas that would be highly desirable would be to refine the nonlinear empirical aerodynamics based on the more recent data,³⁷ which varies the body radius to wing semispan ratio, in contrast to the Reference 26 data base, which used a constant value of 0.5. Another area would be to include the effects of side jets (used for control) on the aerodynamics. This would require a generic wind tunnel data base for open literature usage, which is not available. Both of the above efforts will require sponsor support, of course. Many other minor improvements are also being considered.

SUMMARY

This article has discussed the evolution of the APC from its roots in 1971 to the present. Six versions of the code have been developed and transitioned (AP72, AP74, AP77, AP81, AP93, and AP95) to users. A seventh version, the AP98, is in the process of starting transition to users outside NSWCDD. These versions have each improved upon former versions by adding additional capability and

developing new technology that allows more applications to a broader class of weapon concepts. Typical application uses now include conceptual design, zero-lift and trim aerodynamics, structural loads, and aeroheating inputs. The latest version of the code (AP98) applies to AOA 90 deg, for Mach numbers 0 to 20, for general shaped bodies with up to two sets of lifting surfaces, and at the $\Phi = 0$ or 45-deg roll positions.

ACKNOWLEDGMENTS

Numerous investigators have assisted the author in the aeroprediction work at NSWCDD over the past 27 years. Many of them are listed in the references. These individuals include, at NSWCDD, R. McInville, T. Hymer, S. Rowles, M. Armistead, J. Sun, L. Mason, L. Devan, R. Swanson, Gil Graff, and W. McKerley. Also, contributions have been made by F. DeJarnette at North Carolina State, Frank Baltakis of Advanced Technologies Associates, Nielsen Engineering and Research, and Lockheed Missiles and Spacecraft. Appreciation is expressed to each of these individuals and organizations for their roles.

Those who had the foresight to sponsor the work are not referenced and are also acknowledged. W. Pasiuk of the Naval Sea Systems Command was the first individual to sponsor the work. He was joined by the Naval Air Systems Command, B. Volz and D. Hutchins in 1977. A small amount of support was also given by the U.S. Army Missile Command, R. Deep and D. Washington; and the Air Force Armament Lab, Dr. D. Daniel. Currently, the work is being supported by the Office of Naval Research (Mr. Dave Siegel) by the following programs: the Air-Launched Weapons Program managed at the Naval Air Warfare Center, China Lake, California, by Mr. Tom Loftus and Dr. Craig Porter, and the Surface Weapons Systems Technology Program managed at NSWCDD by Mr. Robin Staton and Mr. Gil Graff. Also, some support is provided by the Marine Corps Weaponry Technology Program managed at NSWCDD by Mr. Bob Stiegler. The author expresses appreciation for support received in this work.

REFERENCES

1. Moore, F.G., *Calculation of Inviscid and Viscid Flow Fields Past Pointed Bodies at Angles of Attack in Supersonic Nonuniform Freestreams*, Dissertation at VPI&SU, Blacksburg, VA, Mar 1971.
2. Moore, F.G., *Body Alone Aerodynamics of Guided and Unguided Projectiles at Subsonic, Transonic, and Supersonic Mach Numbers*, [AP72] NWL TR-3796, Nov 1972.
3. Moore, F.G. and McKerley, C.W., *Aerodynamics of Guided and Unguided Weapons: Part I - Theory and Application*, [AP74] NWL TR-3018, Dec 1973.
4. Graff, G. and Moore, F.G., "Empirical Method for Predicting the Magnus Characteristics of Spinning Shells," *AIAA Journal*, Vol. 15, No. 10, pp. 1379-1380, Oct 1977.
5. Moore, F.G. and Swanson, C., *Aerodynamics of Tactical Weapons to Mach Number 3 and Angle of Attack 15 Degrees: Part I - Theory and Application*, [AP77] NSWC DL TR-3584, Feb 1977.
6. DeJarnette, F.R.; Ford, C.P. and Young, D.E., "Calculation of Pressures on Bodies at Low Angles of Attack in Supersonic Flow," AIAA Article No. 79-1552r, *Journal of Spacecraft and Rockets*, Vol. 17, No. 6, pp. 529-536, Nov-Dec 1980.
7. Chaussee, D.S., *Improved Transonic Nose Drag Estimates for the NSWC Missile Aerodynamic Computer Program*, Nielsen Engineering Contractor Report Prepared for NSWC as NSWC/DL TR-3830, Apr 1978.
8. Moore, F.G.; Armistead, M.; Rowles, S. and DeJarnette, F.R., *Second-Order Shock Expansion Theory Extended to Include Real Gas Effects*, NAVSWC TR 90-683, Feb 1992.
9. Moore, F.G.; Hymer, T. and Devan, L., *New Methods for Predicting Nonlinear Lift, Center of Pressure, and Pitching Moment on Missile Configurations*, NSWCDD/TR-92/217, Jul 1992.
10. McInville, R.M. and Moore, F.G., *Incorporation of Boundary Layer Heating Predictive Methodology into the NAVSWC Aeroprediction Code*, NSWCDD TR-93/29, Apr 1993.
11. Moore, F.G.; Wilcox, F. and Hymer, T., *Improved Empirical Model for Base Drag Prediction on Missile Configurations Based on New Wind Tunnel Data*, NSWCDD TR-92-509, Oct 1992.
12. Moore, F.G. and McInville, R.M., *A New Method for Calculating Wing Alone Aerodynamics to Angle of Attack 180 Degrees*, NSWCDD/TR-94/3, Mar 1994.
13. Moore, F.G.; McInville, R.M. and Hymer, T.C., "An Aeroprediction Code for Angles of Attack Above Thirty Degrees," *Journal of Spacecraft and Rockets*, Vol. 33, No. 3, May-Jun 1996.
14. Moore, F.G. and McInville, R.M., *Extension of the NSWCDD Aeroprediction Code to the Roll Position of 45 Degrees*, NSWCDD/TR-95/160, Dec 1995.
15. Moore, F.G. and McInville, R.M., "A New Semiempirical Model for Wing-Tail Interference," AIAA Paper 96-3393, AFM Conference, San Diego, CA, 29-31 Jul 1996.
16. McInville, R.M.; Moore, F.G. and Housh, C., *Nonlinear Structural Load Distribution Methodology for the Aeroprediction Code*, NSWCDD/TR-96/133, Sep 1996.
17. Moore, F.G. and Hymer, T.C., *An Improved Method for Predicting Axial Force at High Angle of Attack*, NSWCDD/TR-96/240, Feb 1997.
18. Moore, F.G. and McInville, R.M., *An Improved Semiempirical Method for Calculating Aerodynamics of Missiles with Noncircular Bodies*, NSWCDD/TR-97/20, Sep 1997.
19. Vukelich, S.R. and Jenkins, J.E., "Missile DATCOM: Aerodynamic Prediction on Conventional Missiles using Component Build-up Techniques," AIAA Paper 84-0388, 1984, Reno, NV.

20. Devan, L., *Aerodynamics of Tactical Weapons to Mach Number 8 and Angle of Attack 180°: Part I, Theory and Application*, [AP81] NSW TR 80-346, Oct 1980.
21. Moore, F.G.; Hymer, J. and McInville, R., *Improved Aeroprediction Code: Part I - Summary of New Methods and Comparison with Experiment*, [AP93] NSWCDD TR-93/91, May 1993.
22. Moore, F.G.; McInville, R.M. and Hymer, T.C., *The 1995 Version of the NSWC Aeroprediction Code: Part I - Summary of New Theoretical Methodology*, [AP95] NSWCDD/TR-94/379, Feb 1995.
23. Hymer, T.C.; Downs, C. and Moore, F.G., *A Interactive, User-Friendly, Personal Computer Version of the Aeroprediction Code*, NSWCDD/TR-94/107, Jun 1994.
24. Moore, F.G.; McInville, R.M. and Hymer, T.C., *The 1998 Version of the NSWC Aeroprediction Code: Part I—Summary of New Theoretical Methodology*, [AP98] NSWCDD/TR-98/1, Mar 1998.
25. Hymer, T.C.; Cornell, Downs and Moore, F.G., *User's Guide for the Interactive Personal Computer Interface for the 1998 Aeroprediction Code*, NSWCDD/TR-98/1, May 1998.
26. NASA Langley Research Center Tri-Service Missile Data Base, Transmitted from NASA/LRC Jerry M. Allen to NSWCDD, 5 Nov 1991 (formal documentation of data base in process).
27. Stallings, R.L., Jr., and Lamb, M., "Wing-Alone Aerodynamic Characteristics for High Angles of Attack at Supersonic Speeds," NASA Technical Paper 1989, Jul 1981.
28. Baker, W.B., Jr., *Static Aerodynamic Characteristics of a Series of Generalized Slender Bodies With and Without Fins at Mach Numbers from 0.6 to 3.0 and Angles of Attack from 0 to 180°*, AEDC TR-75-124, Vols. I and II, Tullahoma, TN, May 1976.
29. Meyer, J., "Effects of the Roll Angle on Cruciform Wing-Body Configurations at High Incidences," *Journal of Spacecraft and Rockets*, Vol. 31, No. 1, pp. 113-122, Jan-Feb 1994.
30. Nielsen, J.N.; Hemsch, M.J. and Smith, C.A., *A Preliminary Method for Calculating the Aerodynamic Characteristics of Cruciform Missiles to High Angles of Attack Including Effects of Roll Angle and Control Deflections*, Office of Naval Research Report CR215-226-4F, Arlington, VA, Nov 1977.
31. Butler, C.B.; Sears, E.S. and Pallas, S.G., *Aerodynamic Characteristics of 2-, 3- and 4-Caliber Tangent-Ogive Cylinders with Nose Bluntness Ratios of 0.00, 0.25, 0.50 and 0.75 at Mach Numbers from 0.6 to 4.0*, AFATL-TR-77-8, Eglin Air Force Base, FL, Jan 1977.
32. Jorgensen, L.H., "Inclined Bodies of Various Cross Sections at Supersonic Speeds," NASA Memo 10-3-58A, 1958.
33. Monta, W.J., *Supersonic Aerodynamic Characteristics of a Sparrow III Type Missile Model with Wing Controls and Comparison with Existing Tail-Control Results*, NASA TP 1078, Nov 1977.
34. Cleary, J.W., *Effects of Angle of Attack and Bluntness on Laminar Heating Rate Distribution of a 15° Cone at a Mach Number of 10.6*, NASA TN D-5450, 1969.
35. Riley, C.J. and DeJarnette, F.R., "Engineering Aerodynamic Heating Method for Hypersonic Flow," *Journal of Spacecraft and Rockets*, Vol. 29, No. 3, May-Jun 1992.
36. Hender, D.R., *A Miniature Version of the JA70 Aerodynamic Heating Computer Program, H800(MINIVER)*, McDonnell-Douglas Astronautics, Co., Report MDC G0462, Jun 1970.
37. NASA Langley Research Center Fin-Body Interference Data Base, Transmitted from NASA LRC Jerry M. Allen Electronically on 29 Aug 1996 (formal documentation in process).

THE AUTHOR

DR. FRANK G. MOORE



Dr. Frank G. Moore was employed at NSWCDD in 1963 as a cooperative engineering student. He completed his B.S., M.S., and Ph.D. degrees in aerospace engineering from Virginia Polytechnic Institute in 1967, 1968, and 1971, respectively. He has had a wide variety of experience at NSWCDD including researcher, project manager, line manager of several different branches, program manager and, more recently, staff scientist. In his current role, Dr. Moore's primary responsibilities include Senior Aerodynamicist, chairman of the Technical Advisory Board of the *NSWCDD Technical Digest*, and chairman of the G Department Technical Advisory Committee. He has published extensively in the open literature and given many invited lectures and talks both in the United States and internationally.

FATEPEN—A MODEL TO EVALUATE BEHAVIOR OF WARHEAD FRAGMENTS AND PENETRATORS, AND THEIR DAMAGING EFFECTS ON MILITARY TARGETS

Mr. David L. Dickinson, Mr. Thomas L. Wasmund, Dr. Jerome D. Yatteau,

Mr. Richard H. Zernow, and Mr. Gunnar W. Recht

This article describes the development, status, and current usage of the Fast Air-Target Encounter Penetration (FATEPEN) model in the design, development, and evaluation of new antiair weapon systems. The mission of an antiair missile warhead is to defeat a threat target by inflicting a predetermined level of damage on the target so that it can be declared "killed." Simulation of this process involves modeling the intercept kinematics of the missile and target, the fuzing and detonation of the missile warhead, and finally the critical and complex interaction of the warhead fragment damage effects on the target and its components. FATEPEN, the model described here, is a set of fast-running algorithms that simulate the penetration of, and damage to, spaced target structures by compact and noncompact warhead fragments, and long rods at speeds of up to 5 km/s. The model predicts penetrator mass loss, velocity loss, trajectory change, and tumbling throughout a target. The mass loss model includes a robust impact fracture model that transforms an incident-intact warhead fragment into an expanding, multiparticle debris cloud, which FATEPEN then tracks through the remaining target structure. FATEPEN also predicts multiparticle loading and damage to plate structures. FATEPEN has been transitioned to use by all three services and is used as a submodel in a number of simulations.

INTRODUCTION

Antiair warfare is a critical component of U.S. national defense and a thrust area for NSWCDD. In this area, simulation plays an ever-increasing role in the design, development, test, and evaluation of new weapon systems. The use of simulations in weapon technology and system development processes:

- ◆ Allows evaluation of a large number of initial concepts or variants
- ◆ Allows the final optimization of a specific design
- ◆ Allows evaluation in system operating regimes that cannot be tested
- ◆ Reduces the number of developmental and operational tests required to evaluate system performance

The overall result is significant cost savings and increased battlefield performance. These gains are realized, however, only if the simulations are sufficiently accurate representations of the real world. A large technology effort is generally required in the development of complex models of weapon system performance. This article discusses the development of one such model: FATEPEN.

FATEPEN models the penetration of warhead fragments through a target and the consequent damage to target elements. The model was initially developed under the Air and Surface Weaponry Technology Program sponsored by the Office of

Naval Research. The FATEPEN model is used in the design, development, and evaluation of anti-air missile systems at NSWCDD. It is also in use by the Army and Air Force.

ANTIAIR MISSILE SIMULATION AND WARHEAD DESIGN

Figure 1 depicts the major elements in a simulation used to determine and quantify the performance of an anti-air missile system in its role of damaging and defeating a threat target:

- ◆ Missile flight and guidance accuracy
- ◆ Warhead fuze performance
- ◆ Warhead performance
- ◆ Warhead interaction with the target

The outcome of this type of simulation is a determination of whether a predetermined sufficient level of damage has been inflicted on the target so that it can be declared "killed."

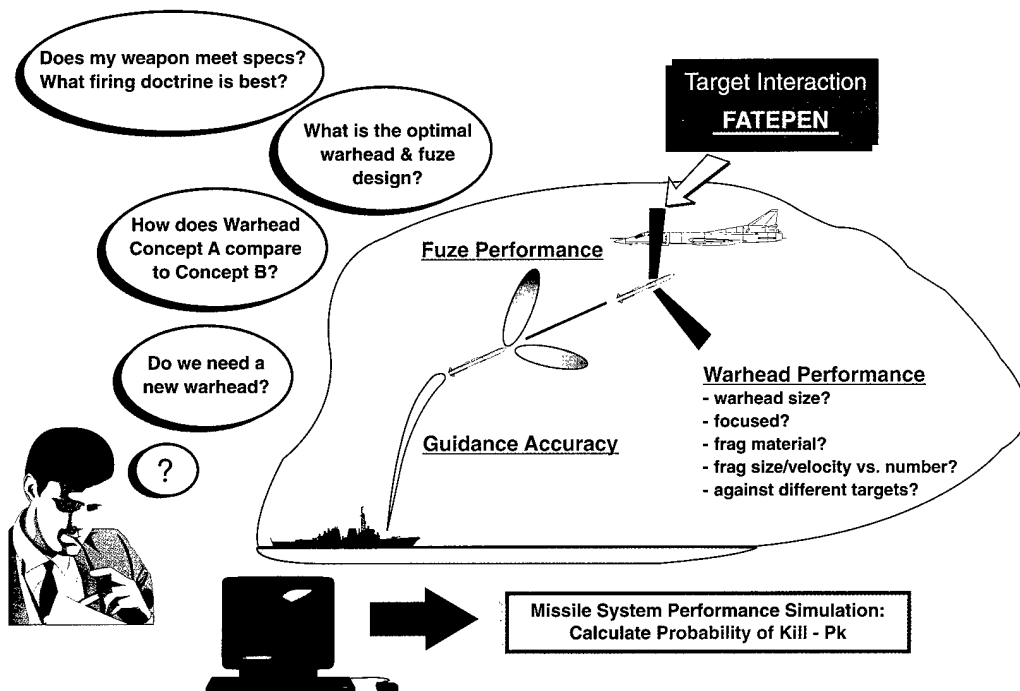


Figure 1—Elements and Example Usage of a Missile System Performance Simulation

If the simulation is performed parametrically—repeating it a statistically sufficient number of times while varying a number of parameters, such as miss distance—the final outcome becomes a probability of killing the target (Pk) given the range of conditions sampled. For example, the major variables that generally drive the outcome are the distance of the warhead from the target when it detonates and the kinematics of the intercept; i.e., the approach directions and velocities of the missile and target. An antiair missile must engage a wide variety of target types over a broad range of altitudes and kinematic conditions. Because of limits in missile guidance and maneuver capabilities, this can result in significant miss distances and a large range of relative orientations of the missile and target. It becomes the job of the warhead and its target detection device, or fuze, to compensate for these variations in targets and intercept conditions, and maximize the probability of doing sufficient damage to the target. In the simplest terms, these then are the design objectives for the warhead and fuze.

The missile warhead and its fuze constitute the major elements of the missile ordnance system. The designs of these two elements are optimized together. We will focus on warhead design parameters and on the warhead fragment-target interaction model required to optimize the warhead design.

The major basic design parameters for conventional types of missile warheads, given a constraint of total weight, are:

- ◆ Fragment size, shape, and number
- ◆ Material (steel, tungsten, etc.)
- ◆ Initial velocity after warhead detonation
- ◆ Fragment dispersion angles

Each of these parameters is affected by specific selections of the others. If one were to analyze all possible combinations, the number of possible designs would be enormous. However, design experience and the results of prior analyses reduce this to a tractable number.

An initial warhead concept down-select process consists of running the missile-target intercept simulation parametrically, varying all parameters over the ranges of interest. That is, each warhead concept is evaluated for its capability to defeat each target over a large range of intercept conditions. The concepts that achieve the highest average probability of defeating all targets are selected for the next iterative level of design, test and evaluation. A critical part of the simulation is to calculate damage and defeat of the target by the warhead fragments. The model that calculates this damage must be of sufficient accuracy and fidelity to be sensitive to changes in warhead design parameters.

FATEPEN TARGET INTERACTION MODEL

FATEPEN was originally developed to simulate compact fragment penetration of thin to moderately thick, spaced plates at impact velocities up to about 5 km/s.¹⁻⁶ Recent model developments have extended FATEPEN applications to long rod penetrators and thick plates.^{7,8} Over the intervening years, improvement and extension of FATEPEN has been the unifying focus of many otherwise independent experimental and analytical efforts to investigate high-velocity and hypervelocity penetration characteristics for a wide variety of penetrator and target materials and structures.⁹⁻¹⁷ The primary application of the code has been weapons effectiveness assessments involving air targets and lightly armored surface targets.

TARGET DESCRIPTIONS AND REPRESENTATIONS

Warhead terminal effects simulations utilize detailed target models comprising thousands of geometric elements, as illustrated in Figure 2. The target models mathematically describe the spatial distribution of target materials and structures. The target descriptions are probed by shotline models to determine which target structures will be intercepted along specific fragment trajectories. For penetration calculations, the target structures are represented by flat plates or fluid-filled volumes, with properties defined by the target description at the intersection points. Figure 3 is a cartoon that illustrates the shotlining process for a target.

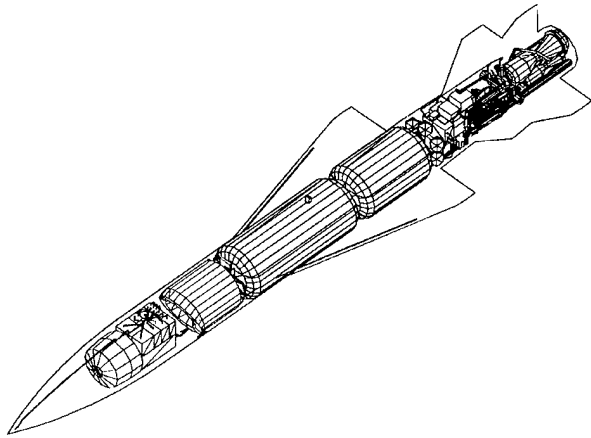


Figure 2—Cruise Missile Geometric Model

APPROACH TO MODEL DEVELOPMENT

FATEPEN has been developed to predict the sequential transformations in a penetrator (changes in mass, velocity, orientation, etc.) and corresponding target damage as the penetrator passes through the series of spaced plates and/or fluid volumes. Considering the large number of shotlines in a typical simulation, the number of target

intersections along each shotline, and the wide variety of penetrator threats and target materials, terminal interaction models must be fast-running and also quite general in their application. FATEPEN meets these dual requirements through a collection of analytical/empirical, terminal interaction models.

FATEPEN incorporates “engineering” terminal-ballistic penetration models in contrast to “first-principle” finite-element/finite-difference codes. The core penetration models have been developed, as much as possible, by applying the laws of mechanics to the dominant terminal-ballistic loading and response mechanisms, as revealed by penetration experiments and first-principle code calculations. Some of these models pertain to ideal impact geometries such as unyawed cylinders impacting plates at normal obliquity. The ideal models are extended to nonideal impact geometries by employing supplemental relationships to approximate the effects of impact geometry on the dominant penetrator, and target inertial and strength factors. Additional relationships are included to provide for rational and smooth transitions between ideal models as functions of the

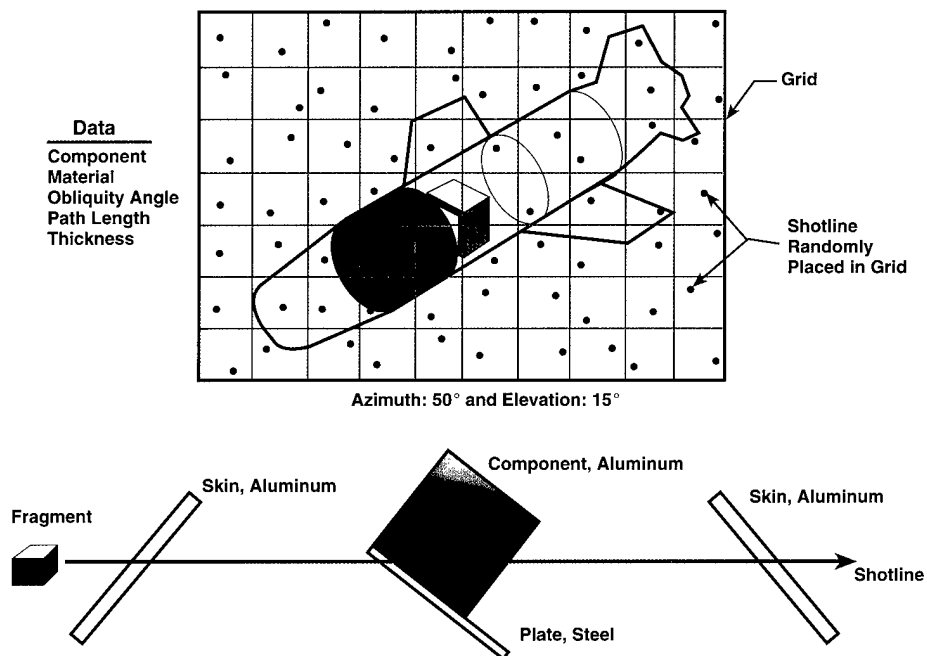


Figure 3—Target Shotline Analysis

appropriate encounter variables. For example, a function of penetrator-normalized length (L/D) is used to transition between penetration predictions from the compact fragment model and those from the long-rod penetration model.

Finally, empirical model parameters are incorporated as needed to account for loading and response effects that could not be modeled either because of their complexity or because of time and funding constraints. The empirical parameter values in FATEPEN are collectively one of the greatest assets of the code. Evaluation of these parameters, either through testing or first-principle code calculations, furnishes a straightforward means for extending the code to new penetrator and target materials and structures. The empirical parameter values also provide a very useful legacy for the many penetration experiments used in developing and validating the models and computer code.

HIGH-VELOCITY PENETRATION CHARACTERISTICS

At low speeds, fragments perforate thin plates without deformation or mass loss. As impact velocity increases, impact pressures become more intense, and fragments begin to “mushroom.” Against harder and/or heavier plates, penetrator material extruded beyond a certain radius will be sheared from the fragment as it passes through the plate (see Figure 4). At higher impact speeds, the relative velocity between the penetrator and the moving impact interface will exceed the speed at which plastic deformation can propagate into the penetrator. When this occurs, a shock wave forms in the penetrator just upstream of the impact interface, and penetrator material passing through it will be ejected radially outward (see Figure 5).¹⁸ Later in the perforation, when the relative velocity falls below the plastic wave speed, the relative motion can be accommodated by plastic deformation in the penetrator, and shock erosion gives way to extrusion-shear mass loss. Above a material-dependent critical impact speed, fragments will also fracture or shatter upon impact (see Figure 6),¹ and the fractured pieces will disperse radially behind the plate.

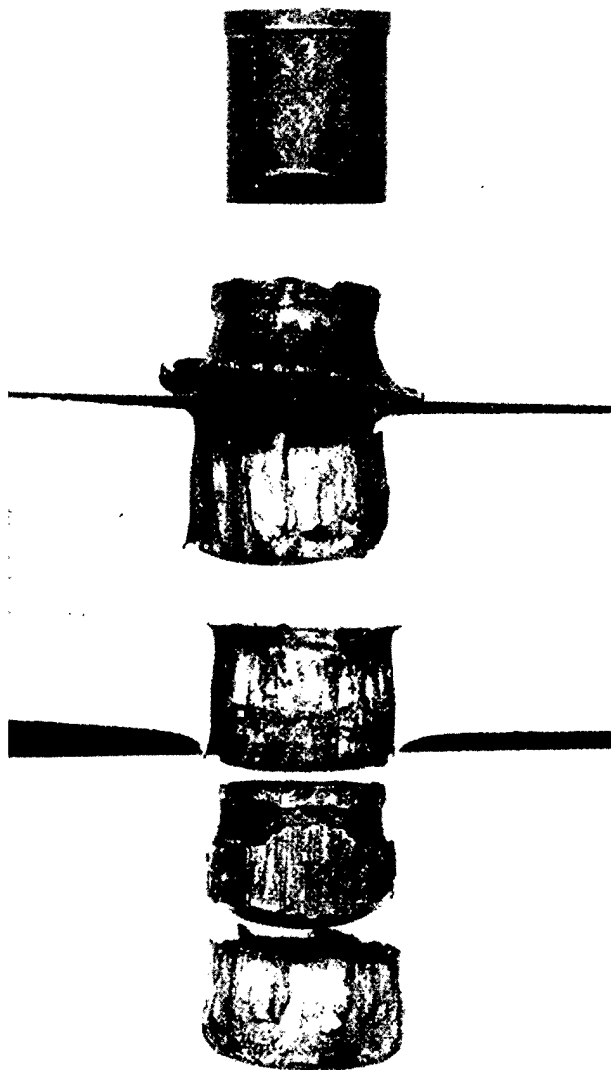


Figure 4—Illustration of Extrusion-Shear Mass Loss for a Steel Fragment Simulating Projectile (FSP) Perforating a Mild Steel Plate

Threshold fracture speeds are sensitive to fragment shape and impact orientation. Fragments with flat surfaces impacting flat produce the highest impact pressure and thus the lowest threshold fracture speed for a given fragment material. Steel cylinders (Rc 30) impacting mild steel plates begin to deform when impact velocity exceeds about 450 m/s. The onset of extrusion-shear mass loss occurs at a velocity near 600 m/s, and shock-erosion mass loss will occur at speeds above about 750 m/s.¹⁸ Flat-impacting, mild steel cubes begin to fracture at speeds near 730 m/s when impacting steel plates and

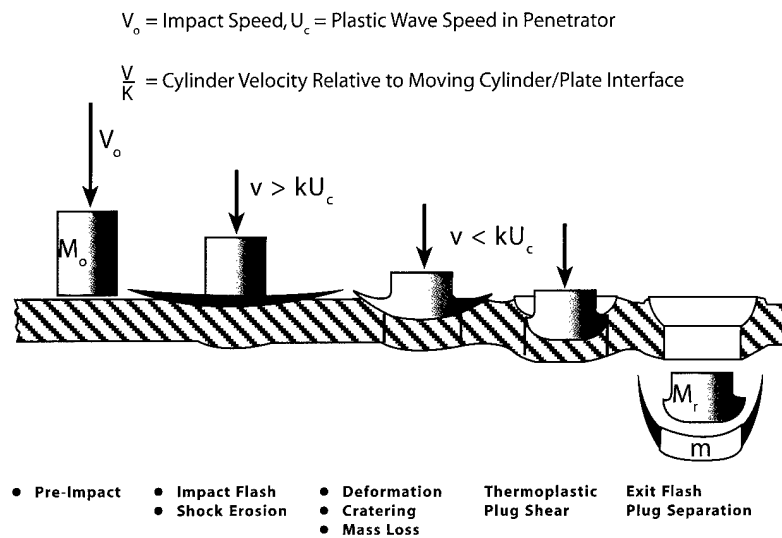


Figure 5—FATEPEN Compact Fragment Penetration Model (see Reference 18)

at speeds near 900 m/s on impact with aluminum plates.⁵ The severity of fracture and the number of debris particles increase with increasing impact speed above the fracture threshold (see Figure 7).¹⁴

Typical high-velocity, multiple-plate penetration damage is illustrated in Figure 8 for the steel cube in Figure 6.¹ The double-exposure flash radiograph in Figure 6 shows dispersion of the fractured cube behind the first plate in Figure 8. The cross-shaped hole pattern in the second plate is typical for a

fractured cube and reflects separation along diagonal planes. Hole patterns in subsequent plates are consistent with a progressive stripping away of the outer debris particles. Figure 9 reveals the effect of increasing impact speed on cube fracture and damage to the subsequent plate. Note the increased number of particles and the larger dispersion angle compared to the cube in Figure 6. The synergistic effect of central hole enlargement due to the high density of small particles impacting near the center of the pattern can also be seen in Figure 9.



Figure 6—Double-Exposure Radiograph of a 240-Grain Steel Cube After Perforating a 1.6-mm Aluminum Plate at 2.05 km/s (see Reference 1)

The radiographs in Figure 10 show the effects of increasing impact obliquity on steel-cube penetration and mass loss.¹⁵ At impact obliquities below about 60°, penetration characteristics are similar to those for normal plates but with a longer line-of-sight path length through the target (see Figure 10a). At higher obliquities, large shear stresses are developed lengthwise through the fragment, which may split the fragment, leaving a remnant on the impact side of the plate (see Figure 10b). Ballistic-limit velocities (i.e., minimum perforation velocities) increase rapidly with increasing impact obliquities above 60° due to trajectory deflections while cutting through the plate, which causes increased mass loss. It is possible to breach a plate without actually penetrating it at very high impact obliquities (see Figure 10c). Also, after ricocheting from

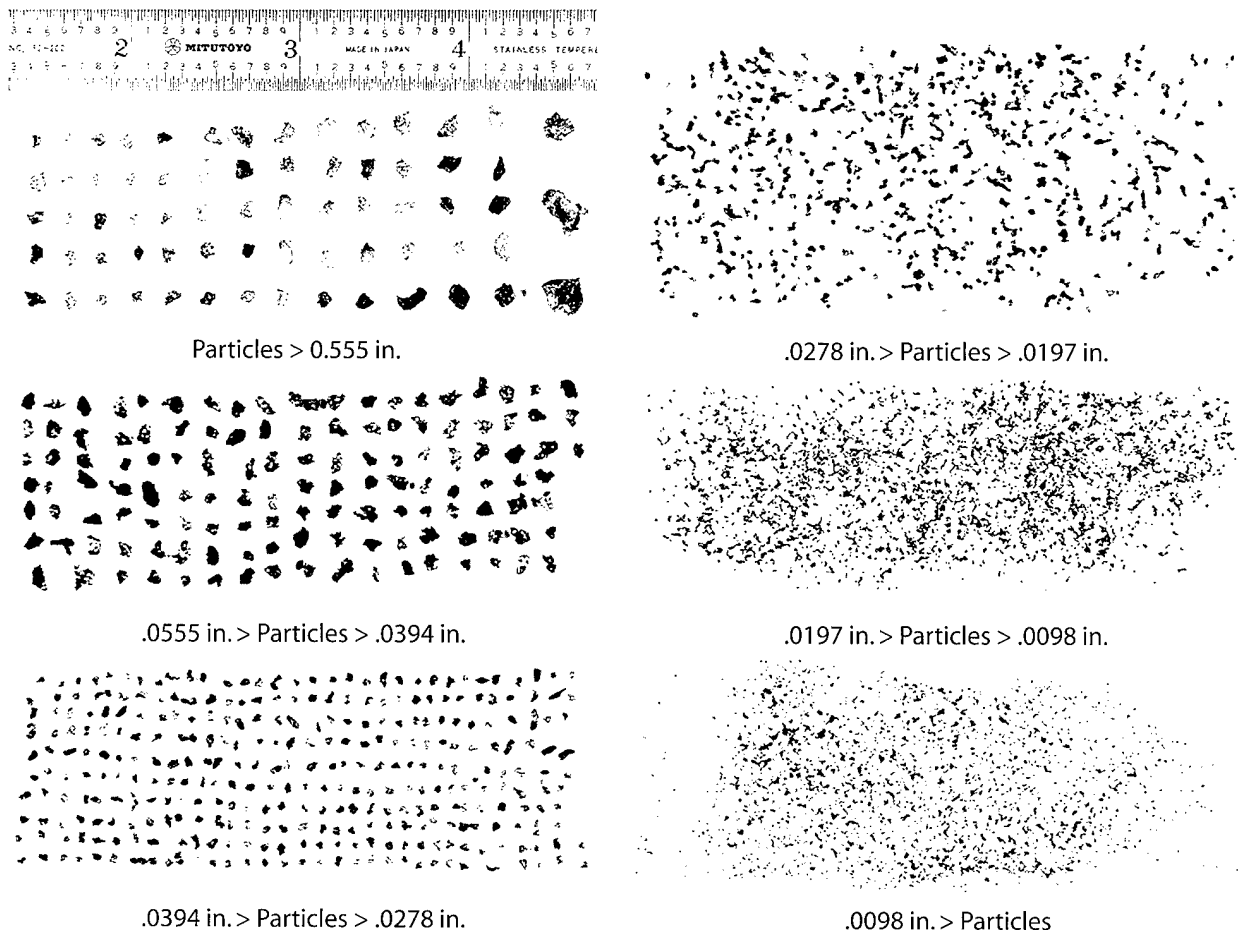


Figure 7—Penetrator Impact Fracture Debris Particles, Steel Sphere vs. Copper Plate, $V = 3.8 \text{ Km/s}$ (see Reference 14)

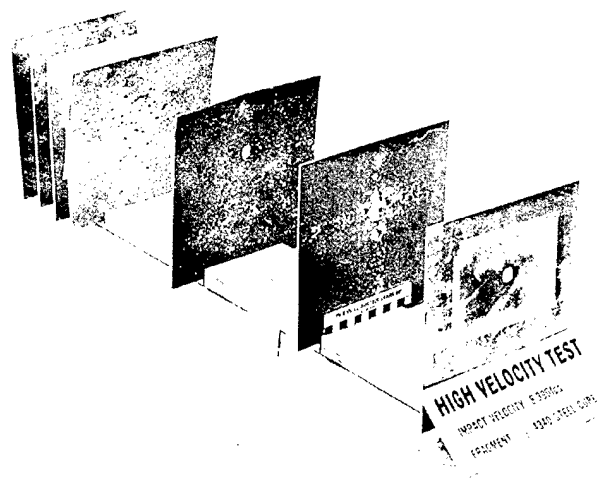
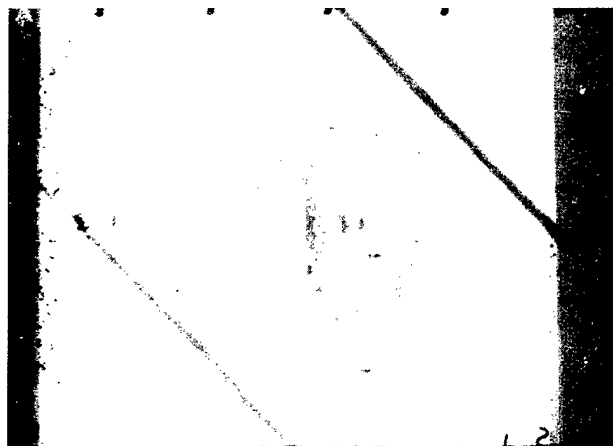


Figure 8—High-Velocity, Multiple-Plate Penetration Damage Caused by Steel Cube shown in Figure 6 (see Reference 1)

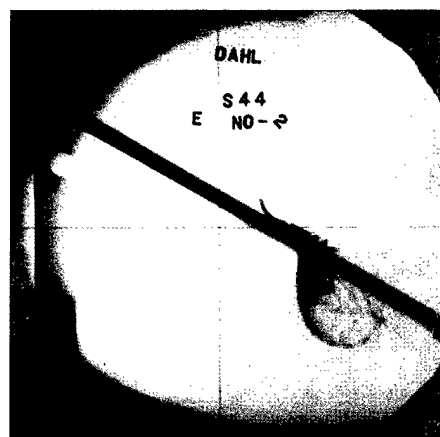


Double-Exposure Radiograph of the Fragment Cloud Behind the First Plate (1/16 in. 2024-T3 A1)

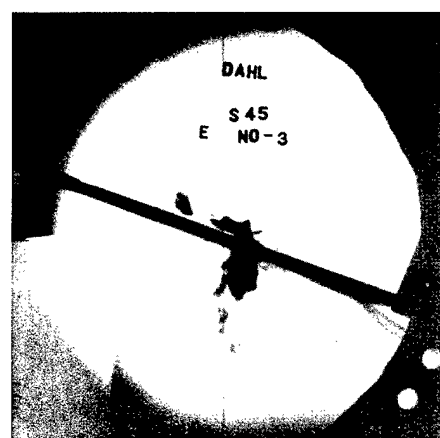


Second Plate Damage (1/8 in. 2024-T3 A1)

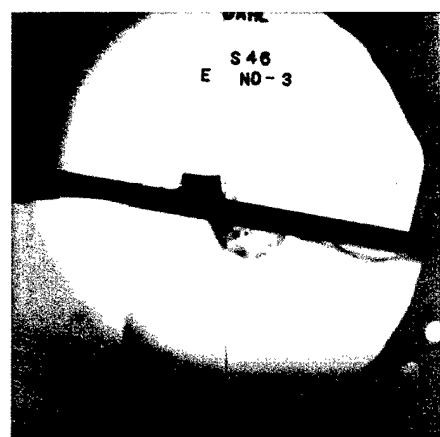
Figure 9—Debris Cloud at Witness Plate Damage for a 30-Grain Steel Cube after Impacting a 1.6-mm Aluminum Plate at 4700 m/s (see Reference 1)



a) 60° Obliquity, $V = 1750$ m/s



b) 70° Obliquity, $V = 1650$ m/s



c) 80° Obliquity, $V = 2150$ m/s

Figure 10—Effects of Increased Impact Obliquity on Fragment Mass Loss, 248-Grain Mild Steel Cube vs. 3.18-mm 2024 Aluminum Plate; Impact is from Right to Left (see Reference 15)

high-obliquity plates, fragments and impact debris may be lethal to target structures further down the shotline, which is not the case for ricochet from low-obliquity impacts.

The multiple-exposure radiographs in Figure 11 were obtained from recent experiments to investigate and model the penetration characteristics of long rods involved in nonideal impacts (combinations of impact yaw and obliquity).⁸ For the same impact conditions against a normal plate, the rod would lose about 10 percent of its length to erosion and extrusion-shear mass loss. The rod in Figure 11 lost about 40 percent of its length in penetrating the oblique plate, was severely bent in the process, and can be seen to be rotating behind the plate. Most impacts in real targets involve nonideal impact geometries, which often result in significant transverse loading, and deformation and fracture in long-rod penetrators. These effects severely limit the subsequent penetration effectiveness of the rods and must be modeled for accurate lethality assessment for warheads utilizing this kind of penetrator.



Figure 11—Tungsten Rod (L/D = 20) vs. Steel Plate (T/D = 2) at 75° Obliquity, $V = 1833$ m/s (see Reference 8)

Allowable plate materials include:

- ◆ steel
- ◆ aluminum
- ◆ titanium
- ◆ doron
- ◆ magnesium
- ◆ phenolic
- ◆ pine
- ◆ oak
- ◆ cast iron
- ◆ copper
- ◆ lead
- ◆ tuballoy
- ◆ lexan
- ◆ cast plexiglas
- ◆ stretched plexiglas
- ◆ unbonded nylon
- ◆ bonded nylon
- ◆ bullet-resistant glass
- ◆ face-hardened steel
- ◆ graphite epoxy fiber-reinforced composites

FATEPEN PENETRATION MODEL OVERVIEW

Figure 12 contains a flowchart mapping the penetration computational loop in FATEPEN. A typical run begins by specifying the initial penetrator (primary fragment) characteristics, the plate-array characteristics, and the encounter conditions (impact velocity, penetrator orientation, and spin rate). Penetrator shapes and target structures currently recognized in FATEPEN are shown in Figure 13. The PC version of FATEPEN is an interactive program, and the user may select preprogrammed penetrator characteristics from a default catalog and define new fragments by editing the catalog entries or by reading previously saved penetrator files. Likewise, plate-array characteristics can be changed by editing the default plate array or by reading and editing previously saved FATEPEN plate-array descriptions.

Possible penetrator materials include:

- ◆ steel
- ◆ aluminum
- ◆ tungsten alloy
- ◆ tantalum
- ◆ titanium
- ◆ depleted uranium

Fluids are specified by their specific gravity.

After the primary fragment, plate array, and encounter conditions are specified, FATEPEN searches the input plate array for laminated plates (i.e., occurrences of zero spacing between plates) and replaces them with equivalent single plates for the penetration calculations. (The original plate array is returned after the penetration calculations for input/output and further editing.) Following this, FATEPEN assigns values to parameters, describing characteristics of the secondary particles in the debris cloud incident on the first plate. The parameters are currently all set to zero so that only the primary fragment impacts the first plate. However, any set of initial debris cloud parameters, which conform to the general FATEPEN debris cloud model, could be substituted for the current null specification. In general, the debris cloud may include the primary penetrator particle (as described above), two sizes of secondary penetrator particles, and one average size for plate particles. A fourth penetrator debris category is reserved for broken long-rod penetrator pieces.

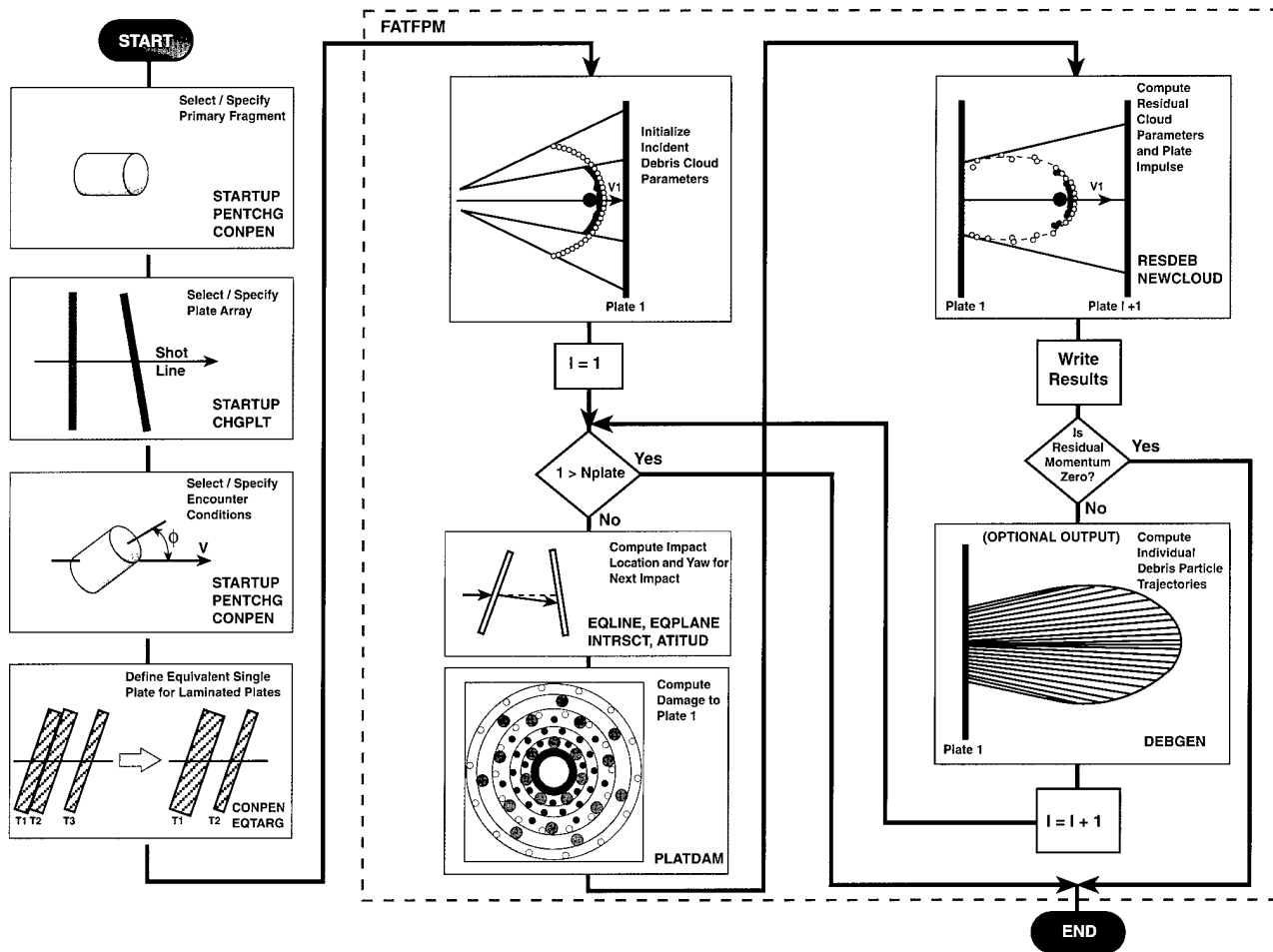


Figure 12—FATEPEN Penetration Model Flowchart

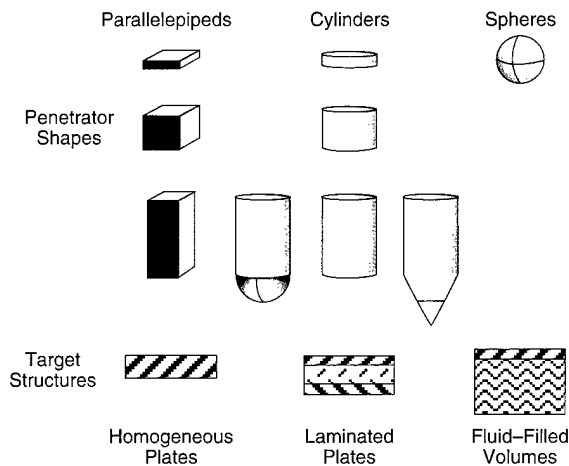


Figure 13—FATEPEN Penetrator Shapes and Target Structures

The primary fragment is presumed to be situated at the leading edge of the debris cloud. The secondary penetrator and plate particle trajectories are bounded by the cone half-angles, which are computed from the impact conditions. The secondary particles are presumed to emanate from the plate where impact fracture first occurred and reside on the surface of an expanding ellipsoidal cloud. The spatial distribution of the secondary particle trajectories is governed by an experimentally determined distribution function, which presumes that the areal density of particle trajectories is inversely proportional to the radius from the shotline. The velocity distribution of the debris particles derives from the shape of the cloud.

Following definition of the initial debris characteristics, the main computational loop is entered. The primary fragment velocity and angular momentum vectors are first used to compute the impact location, obliquity, and orientation at the next plate. Plate damage caused by the incident primary fragment and debris cloud is computed next as shown in Figure 12. Possible plate damage includes holes and/or craters made by individual particles and a central hole-out region caused by the particles acting in unison.

The residual debris characteristics are determined after the plate damage calculations. In general, some of the incident debris particles will penetrate, and some will be stopped. Those particles that penetrate will generally lose mass and velocity, and drive additional new plate particles into the residual debris cloud. The primary penetrator particle is monitored separately. It may fracture on any impact in addition to losing mass to the other mechanisms listed above. The primary penetrator may also generate single or multiple-plate particles. When the primary penetrator particle and/or its plate-plug fractures, it produces a new debris cloud. The primary fragment residual velocity and angular-momentum vectors are computed for use in determining the encounter conditions for the next impact. Lateral loading and response are computed for rod penetrators ($L/D > 2$), including the bend angle, and if the rod fractures, the sizes of each piece are assigned to the fourth penetrator debris category.

Thus, behind any particular plate, it is possible to find:

- ◆ A residual primary penetrator fragment
- ◆ New secondary penetrator particles resulting from impact fracture of the primary particle at the current plate
- ◆ Secondary plate particles driven from the current plate by the primary particle
- ◆ Residual secondary penetrator particles, which were generated at a previous impact
- ◆ Secondary plate particles produced by these residual penetrator particles

The sizes, velocities, and dispersion angles of each type of secondary particle are compared, and an averaging process is used to recast the residual debris particles into the standard debris cloud comprising the primary particle, two sizes of secondary penetrator particles, and one size of plate particles. Once the standard residual debris cloud particle sizes and velocities have been selected, the associated numbers of each particle are adjusted so that the individual particle momenta and the total residual cloud momentum are consistent with the values determined by the individual particle penetration calculations. Next, the impulse delivered to the current plate is computed as the difference between debris cloud momenta in front of and behind the plate. At this point, an optional debris trajectory routine can be called to generate and store individual debris particle trajectory descriptors that may be used outside FATEPEN to produce graphical displays of impact patterns and debris cloud profiles. Finally, the computation returns to the beginning of the main loop to compute the impact location and damage to the next plate. As shown in Figure 12, the main computational loop is repeated until the plate array is completely penetrated or all particles are stopped.

Typical FATEPEN model predictions are compared with test results in Figures 14 and 15.¹⁴ The graphical depictions of the debris cloud and plate damage were generated from the predicted secondary particle velocity and trajectory distributions behind the first plate and the plate damage maps derived from the hole-size calculations and trajectory distributions behind the first and second plates. The plate array consisted of a 2.4-mm copper plate followed by three 3.3-mm aluminum witness plates. Note that the steel-sphere debris particles in Figure 7 were collected behind the same copper plate after an impact at 3800 m/s.

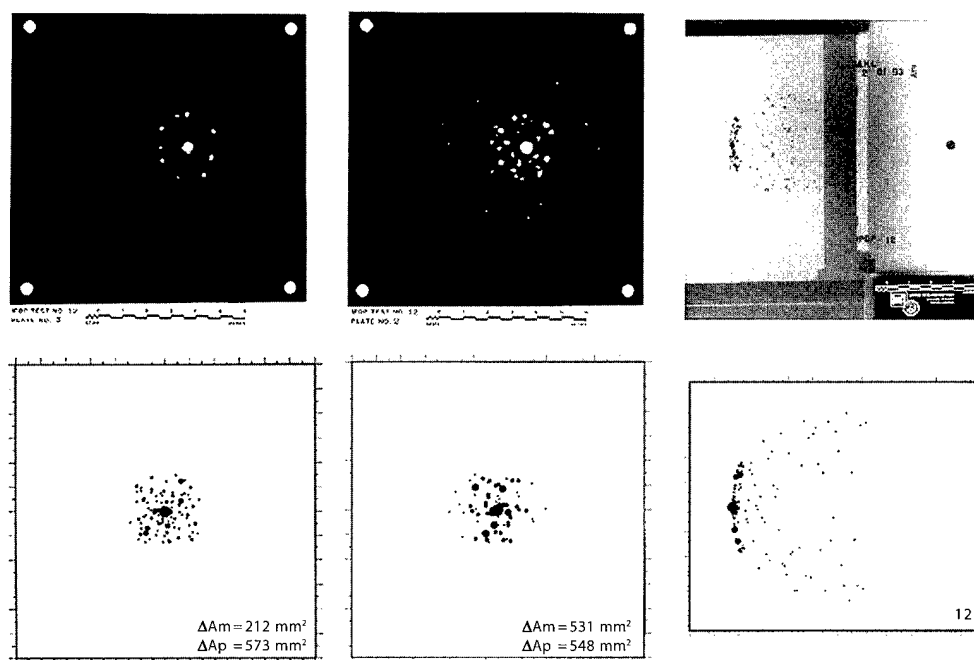


Figure 14—Debris Cloud and Plate Damage, Steel Sphere vs. Copper Shatter Plate and Aluminum Witness Plater, $V = 2.4$ Km/s, Test Results (Top), FATEPEN Predictions (Bottom) (see Reference 14)

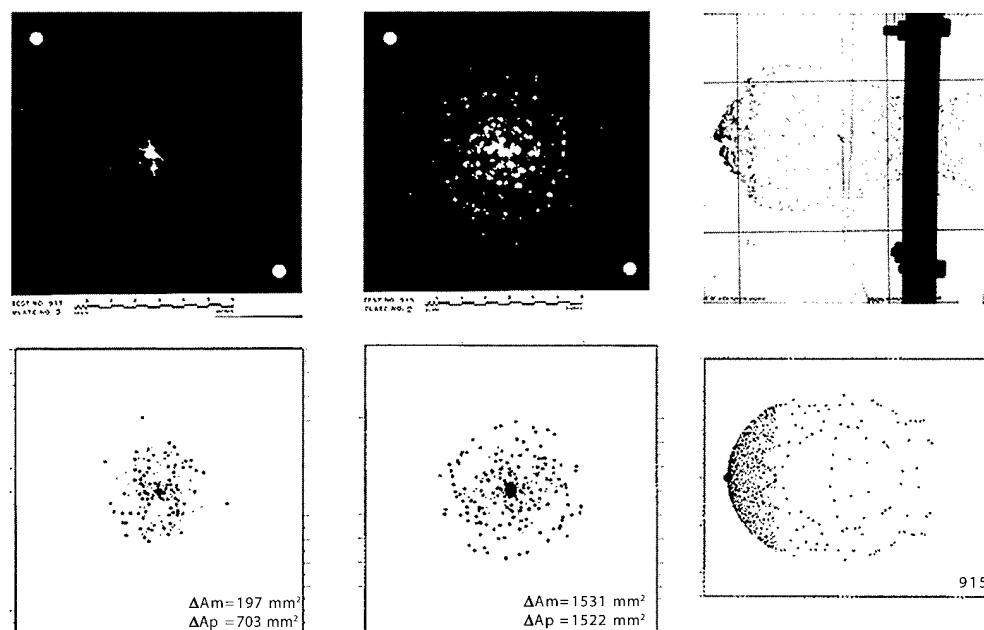


Figure 15—Debris Cloud and Plate Damage, Steel Sphere vs. Copper Shatter Plate and Aluminum Witness Plater, $V = 4.0$ Km/s, Test Results (Top), FATEPEN Predictions (Bottom) (see Reference 14)

SUMMARY OF FATEPEN PENETRATION MODELS

The fragment penetration models required for accurate weapons-effectiveness simulations are listed in Table 1, and the primary penetration models installed in FATEPEN are listed in Table 2. In general, preliminary penetration experiments are used to reveal the primary penetration loading and response mechanisms. Preliminary analytical models are then developed, and first-principle code calculations are used to confirm or reveal loading and response details that cannot be observed experimentally. More extensive experiments are then conducted to verify and/or modify the models, as needed, and to evaluate any required empirical parameter values.

government agencies and by industry, both as a stand-alone model and as a submodel in higher-level models and simulations. It has been accepted by both the Joint Technical Coordinating Group for Munitions Effectiveness (JTTCG/ME) and by the Joint Technical Coordinating Group on Aircraft Survivability (JTTCG/AS) as the standard model for predicting warhead fragment effects in aircraft. The JTTCG/ME is in the process of accrediting the model for their use in producing Joint Munitions Effectiveness Manuals for antiair weapon systems; these manuals are required for all weapon systems when they achieve initial operational capability.

FATEPEN has been incorporated as a submodel in other higher-level models that evaluate the overall vulnerability of a platform or the lethality of fragments against specific targets. These higher-level

Table 1—Penetration Model Requirements for Weapons Effectiveness Simulation

- ◆ Primary Fragment Residual Mass and Debris Cloud Constituents
- ◆ Primary Fragment Residual Velocity and Debris Cloud Velocity Distribution
- ◆ Rod Penetrator Deformation and Fracture
- ◆ Trajectory Deflections
- ◆ Primary Fragment Tumbling or Gyration
- ◆ Plate Damage

Development of the models and comparison with test results are described in detail in the references cited at the end of this article. The FATEPEN methodology documentation is scheduled for an extensive update in 1998. The updated documents will include a complete methodology volume, a validation document, and a user guide.

FATEPEN TRANSITION AND USAGE—A SUCCESS STORY

The FATEPEN model is being successfully used to evaluate weapon effects by a number of

models include Computation of Vulnerable Areas and Repair Times (COVART), which is the standard model currently accepted by JTTCG/ME and JTTCG/AS. It is used by all three services to calculate the vulnerability of both air targets and nonarmored, mobile ground targets. The Advanced Joint Effectiveness Model (AJEM) is a new model developed by the JTTCG/ME and JTTCG/AS to evaluate the effectiveness of both warheads and small-caliber projectiles against air targets; it uses FATEPEN for penetration and damage calculations. The Army has incorporated FATEPEN in the Modular Unix-Based Vulnerability Estimation Suite (MUVES), which evaluates the effects of a variety of weapons against

Table 2—FATEPEN Primary Penetration Models

SUBROUTINE NAME	COMPUTATION	PENETRATOR
CLOSED-FORM ANALYTICAL/EMPIRICAL MODELS		
IMPED/RESMAS	Erosion/Extrusion-Shear Mass Loss	Compact Fragments
MHYDRO + IMPED/RESMAS	Erosion/Extrusion-Shear Mass Loss	Rod Penetrators
LATERO	Lateral Erosion Mass Loss	Compact and Rods
SHATR	Impact Fracture and Debris Particles	Compact and Rods
VRPLATE	Plate Perforation Residual Velocity	Compact and Rods
VRFLUID	Fluid Penetration Velocity Decay	Compact and Rods
RODCON + RODSHEAR	Lateral Loading and Response	Rod Penetrators
RAM	Residual Angular Momentum	Compact and Rods
ATTITUDE	Penetrator Orientation Changes	Compact and Rods
HOLE	Individual Particle Hole Size	Compact and Rods
PUNCH	Multi-Particle Hole Enlargement	Compact and Rods
TIME-RESOLVED PENETRATION MODEL		
TPPM	Erosion/Extrusion-Shear Mass Loss	Compact and Rods

ground mobile targets, including armored targets. The Air Force uses Modular Effectiveness/Vulnerability Assessment (MEVA) to evaluate air-to-surface weapons against underground targets and buildings, and this model also uses FATEPEN.

The Technical Cooperation Program (TTCP)—involving Australia, Canada, the United Kingdom, and the United States—established FATEPEN as an accepted comprehensive penetration methodology following a 2½-year collaborative test and evaluation effort under their conventional weapons terminal effects technology panel.

A number of weapon acquisition programs are using FATEPEN as a part of comprehensive lethality or vulnerability test and analysis programs, including:

- ◆ Sidewinder (AIM-9X)
- ◆ Evolved Sea-Sparrow Missile (ESSM)
- ◆ Standard Missile (SM-2 Blk IVA)
- ◆ AMRAAM P31 (AIM-120)
- ◆ F-22
- ◆ F-18E/F
- ◆ Joint Strike Fighter (JSF)

**OVER 1900 IMPACT EXPERIMENTS HAVE BEEN CONDUCTED
IN SUPPORT OF FATEPEN MODEL DEVELOPMENT SINCE THE
ORIGINAL TEST PROGRAM IN 1978.**

FATEPEN improvement and development has been continuing under various Navy research, development, and acquisition programs in order to provide increased capability to evaluate the performance of new penetrator shapes and materials against new target materials, such as those found in ballistic missile targets.

SUMMARY

As acquisition programs continue to rely more and more on modeling and simulation to optimize their weapons to be more effective or more survivable for the warfighter, physical models of the interaction of weapon effects with targets must be made more accurate and of higher fidelity. Because of the generally long development period required for complex models, especially with limited funding, they must be developed initially under technology programs rather than under acquisition programs, which generally have a shorter development cycle. The FATEPEN model—developed over many years under the Navy Air and Surface Weaponry Technology Program and now accepted and in use throughout government and industry—is a proven technology success.

ACKNOWLEDGMENTS

The authors welcome this opportunity to acknowledge their indebtedness to Rodney F. Recht for his major contributions to the development of FATEPEN and, more generally, for showing us the way to combine experiment and analysis in developing realistic analytical/empirical engineering models for complex terminal-ballistic interactions. Rod, formerly of the Denver Research Institute and Applied Research Associates, Inc. and now retired, has been our mentor. The fragment erosion/extrusion-shear mass loss and residual velocity models in FATEPEN were developed by Rod as part of the Fragment Penetration and Impact Initiation Model (FPIIM) code, which he developed under Navy and Raytheon sponsorship. Rod also developed the original version of the high-obliquity, lateral-erosion, mass-loss model in FATEPEN. Rod's numerous contributions advancing the science of

terminal ballistics extend well beyond his contributions to FATEPEN and are well known around the world.

The authors also gratefully acknowledge the contributions to development of the FATEPEN code by James Dunn, Steven Lightsey, Steven Ford, and Dave Mann of the Denver Research Institute, and Mr. Andy Williams of the Naval Research Laboratory for their innovative and resourceful accomplishment of the many impact experiments used in developing and verifying the penetration models.

REFERENCES

1. Dickinson, D.L., *Investigations of High Velocity Fragments Impacting Plate Arrays*, NWSC TR-79-66, Naval Surface Weapons Center, Dahlgren, VA, Mar 1979.
2. Yatteau, J.D., *High Velocity Multiple Plate Penetration Model*, Denver Research Institute, Denver, CO, NSWC-TR-82-123, Naval Surface Weapons Center, Dahlgren, VA, Feb 1982.
3. Recht, R.F. and Finnegan, S.A., *Penetration Equations for Tungsten Fragments*, Denver Research Institute, Denver, CO, NWC TP 6768, Naval Weapons Center, China Lake, CA, May 1986.
4. Recht, R.F., *High Obliquity Ballistic Perforation Models (Program FPIIM)*, Denver Research Institute, Denver, CO, Final Report, Contract N60921-86-D-A070, Task B009, Naval Surface Warfare Center, Dahlgren, VA, Mar 1988.
5. Yatteau, J.D.; Dunn, J.A. and Dickinson, D.L., *Terminal Ballistic Impact Fracture of Steel Cubes*, Applied Research Associates, Inc., Littleton, CO, for Naval Surface Warfare Center, Dahlgren, VA, NSWC TR 91-397, Mar 1994.
6. Yatteau, J.D.; Zernow, R.H. and Recht, R.F., *Compact Fragment Multiple Plate Penetration Model (FATEPEN 2), Volume I - Model*

- Description, Volume II - User's Manual*, NAVSWC TR-91-399, Naval Surface Warfare Center, Dahlgren, VA, Jan 1991.
7. Recht, G.W., *An Analytical Residual Mass and Velocity Model for Long Rod Penetrators - FATEPEN Subroutine MHYDRO*, Applied Research Associates, Inc., Littleton, CO, Naval Surface Warfare Center, Dahlgren, VA, Dec 1996.
 8. Yatteau, J.D.; Recht, G.W. and Zernow, R.H., *FATEPEN Rod Penetration Model - Part I*, Applied Research Associates, Inc., Littleton, CO, Naval Surface Warfare Center, Dahlgren, VA, Feb 1998.
 9. Yatteau, J.D., and Dunn, J.A., *Penetration Methodology for Bar Fragments*, Applied Research Associates, Inc., Lakewood, CO, Air Force Armament Laboratory, Eglin Air Force Base, FL, AFATL-TR-90-100, Feb 1991.
 10. Yatteau, J.D., *Effects of Fragment Shape on Impact Fracture*, Applied Research Associates, Inc., Lakewood, CO, Naval Surface Warfare Center, Dahlgren, VA, ARA Letter Report 5591-52, Apr 1991.
 11. Yatteau, J.D. and Dickinson, D.L., "An Engineering Model to Predict Damage to Plates Impacted by High Velocity Debris Clouds," *Proceedings, 1992 Hypervelocity Impact Symposium, Int. J. Impact Engng.*, Vol. 14, 1993.
 12. Yatteau, J.D.; Zernow, R.H.; Dzwilewski, P.T.; Patel, G.A. and Recht, R.F., *Analytical Support for the Patriot Program*, Final Report, Raytheon/ARA Subcontract 71-613-CD-0072, Applied Research Associates, Inc., Littleton, CO, Apr 1994.
 13. Yatteau, J.D.; Zernow, R.H. and Dunn, J.A., *Fragment Penetration Fluid-Backed Plates*, Denver Research Institute, University of Denver, Denver, CO, Air Force Armament Test Laboratory, AFATL-TR-89-59, Sep 1989.
 14. Yatteau, J.D.; Zernow, R.H.; Ford, S.R. and Dickinson, D.L., "Debris Cloud Constituents and Plate Damage Throughout a Spaced Plate Array Impacted at Speeds Between 1.5-4.0 km/s," *15th International Symposium on Ballistics*, Jerusalem, Israel, 21 May 1995.
 15. Recht, G.W.; Yatteau, J.D. and Dickinson, D.L., "An Engineering Model for Residual Mass and Velocity of Kinetic Energy Penetrators Impacting Highly Oblique Plates," *16th International Ballistics Symposium and Exhibition*, San Francisco, CA, Sep 1996.
 16. Yatteau, J.D., *Penetration Characteristics and FATEPEN Model Parameters for Tungsten Fragments and Laminated Plates*, Applied Research Associates, Inc., Littleton, CO, ARA Report No. 5242 (NSWC Technical Report Pending), Naval Surface Warfare Center, Dahlgren, VA, Apr 1997.
 17. Zernow, R.H.; Recht, G.W.; Yatteau, J.D. and Dzwilewski, P.T., *Missile Battery Damage Prediction Methodology, Vol. II, FATEPEN/CVAT (Component Vulnerability analysis Tool) User's Guide*, Applied Research Associates, Inc., Littleton, CO, Aug 1997.
 18. Recht, R.F., "Taylor Ballistic Impact Modeling Applied to Deformation and Mass Loss Determinations," *Int. J. Engng. Sci.*, Vol. 16, pp. 809-827, 1978.

THE AUTHORS

MR. DAVID L. DICKINSON



Mr. David L. Dickinson is an engineer in the Lethality and Weapons Effectiveness Branch of the Weapons Systems Department. He is currently the manager for the STANDARD Missile 3 Lethality Program. He is responsible for overseeing the evaluation of lethality for this nontraditional warhead. The program includes warhead lethality testing and effectiveness. His prior experience includes developing new penetration and vulnerability methodologies to evaluate warhead effects on air targets. He was instrumental in the penetration methodology development and warhead vulnerability analyses that supported development of new warheads for the Standard Missile. Prior to joining the Naval Surface Warfare Center, Dahlgren Division (NSWCDD) full-time, Mr. Dickinson was a co-op student at NSWCDD. He received a B.S. in mechanical engineering at Virginia Tech in 1978. Mr. Dickinson's awards include the NSWCDD Technology-to-Sea Excellence Award and the Technical Cooperation Program Achievement Award.

MR. THOMAS L. WASMUND



Mr. Thomas L. Wasmund is a senior scientist in the Lethality and Weapons Effectiveness Branch of the Weapons Systems Department. For over 20 years, Mr. Wasmund has been the Technology Principal for anti-air lethality and vulnerability under the (now) Air and Surface Weaponry Technology Program sponsored by the Office of Naval Research. He is responsible for developing new methodologies to evaluate warhead effects on air targets and for integrating these methodologies—as well as those stemming from other service programs—into vulnerability analysis efforts for Navy missile engineering development programs. Mr. Wasmund is on a number of triservice committees that are coordinating joint development of new lethality and vulnerability methodologies. He was instrumental in the methodology development and threat vulnerability analyses that supported development of new warheads for the SEASPARROW, PHOENIX, and Standard missiles. Prior to joining NSWCDD in 1971, Mr. Wasmund was a pilot in the U.S. Navy. He received a B.S. in electrical engineering from the University of Washington in 1959, and B.S. and M.S. degrees in aerospace engineering from the Naval Postgraduate School in 1966, and 1967, respectively. Mr. Wasmund's awards include the Department of the Navy Meritorious Civilian Service Award, the NSWCDD Technology-to-Sea Excellence Award, and the Technical Cooperation Program Achievement Award.

DR. JEROME D. YATTEAU



Dr. Jerome D. Yatteau received a B.S. in engineering mechanics from Virginia Polytechnic Institute and an M.S. and Ph.D. in applied mechanics from Stanford University. From 1971 to 1975 he was a dynamicist at Martin Marietta Aerospace, where he developed mathematical models and computer programs for the loading and response of spacecraft structures. Dr. Yatteau joined the Denver Research Institute (DRI) of the University of Denver in 1975, where he began his work in terminal ballistics under the mentorship of Rodney F. Recht. At DRI until 1987, he conducted several analytical and experimental studies dealing with terminal ballistic response and dynamic material behavior, and developed the original versions of the MPPM and FATE multiple-plate penetration models and computer codes. Since 1987, Dr. Yatteau has headed the Penetration Mechanics Group at Applied Research Associates' (ARA) Rocky Mountain Division in Littleton, Colorado. His work at ARA has included continued development of the FATEPEN, MPPM, and TCAM penetration computer codes and the design of end plates for a deformable warhead; survivable, reactive armor module attachment hardware for armored vehicles; and optimum penetrators for defeat of missile submunition payloads.

MR. RICHARD H. ZERNOW



Mr. Richard H. Zernow graduated from San Diego State University in 1975 with a degree in geophysics. He worked in the oil and gas industry from 1975 to 1986 as an analyst performing 2-D and 3-D seismic signal processing. He spent 5 years working in South America as a computer center manager, answering directly to the Brazilian national oil company. His combination of field experience and computer experience allowed him to transition into the field of ballistics when he began working with the Denver Research Institute in 1986. At this time, Mr. Zernow began his association with the FATEPEN model and code by converting the program from a mainframe to a PC. Mr. Zernow began working with Applied Research Associates, Inc., in 1987, continuing his work with the FATEPEN code. He adapted the code to 3-D geometry tracking, helped modularize the code, and developed the current Graphical User Interface.

MR. GUNNAR W. RECHT



Mr. Gunnar W. Recht is a chemical engineering graduate of the Colorado School of Mines. He began his career at the UNOCAL Science and Technology Center in Brea, California, designing and building research and chemical pilot plant apparatus, where he was awarded a patent and a creativity award for innovative design. Moving back to Colorado, he began work for a local contract engineering firm providing process engineering and project management, primarily to upgrade existing refinery units to meet the requirements of the Clean Air Act. Mr. Recht currently works at Applied Research Associates in the area of terminal ballistic modeling. His contributions to FATEPEN include improved models for characterizing the effects of highly oblique targets and long-rod penetration. His chemical engineering background has helped in producing a reactive fragment terminal-effects code that predicts the terminal ballistics, pressure rise within a target void, and target failure due to internal pressure.

REMOTE DETECTION OF CHEMICAL WARFARE AGENTS: ADVANCED RESEARCH TO FULL-SCALE PRODUCTION OF THE AN/KAS-1

Mr. S. Roger Horman

The role of naval technology programs is to identify options for solving known or envisioned challenges and to transfer these technologies into products for the fleet. An ideal program might be one that progresses seamlessly from Advanced Research (6.2), which had been inspired by products from the Basic Research (6.1) community, to Exploratory Research (6.3) and then Engineering and Manufacturing Development (E&MD) (6.4). At the conclusion of each phase, the acquisition community, in conjunction with the Office of Naval Research, would conclude that further development was needed and merited, and out-year plans and funding would be modified to reflect their consensus. This progression from basic science to developing a system suitable for full-scale production is conceptually appealing but differs markedly from the processes that typify technology transfer. Political, financial, and regulatory forces frequently place severe constraints on the evolution of an idea into a system that is successfully tested, produced, widely deployed and logistically supported. The research and development leading to the full-scale production of the AN/KAS-1 Chemical Warfare Directional Detector (CWDD) provides insight into the processes—technical and political—that were required to transition a promising technology into the fleet.

INTRODUCTION

The AN/KAS-1 CWDD is a thermal imaging system modified to remotely detect and identify clouds of deadly nerve agents. The AN/KAS-1 entered into full-scale production in 1983 and was eventually produced in numbers sufficient to outfit every ship in the fleet with two units, along with spares for integrated logistics support. The system has been used for a wide variety of applications beyond the detection of chemical warfare (CW) agents, including:

- ◆ General night vision
- ◆ Collision avoidance
- ◆ Man-overboard detection
- ◆ Pilotage navigation
- ◆ Detection and identification of small surface craft
- ◆ Fire control adjunct sensor for special operations vessels

It was the first thermal imager to enter full-scale production for surface ships and remains in use throughout the fleet today.

GROWTH OF THE CONCEPT

The evolution of ideas leading to the AN/KAS-1 can be traced back to August 1971. USS *Marvin Shields* (DE 1066) was evaluating a prototype electro-optical fire control sensor package for support of shore bombardment. This sensor suite used an early-generation long-wave infrared (LWIR) band thermal imager for detection and angle track. Tape-recorded imagery of a shore bombardment exercise showed that a huge cloud of dust was created by shell detonations, which completely obscured its background and persisted for minutes. Posttest analysis of this phenomenon by scientists and engineers at the Naval Weapons Laboratory (later to be the Naval Surface Warfare Center, Dahlgren Division (NSWCDD)) showed that the dust cloud was composed of silica (SiO_2), which has a strong absorption band in the LWIR.

The LWIR extends over a region of the electromagnetic spectrum where the atmosphere is relatively transparent and covers the nominal range of wavelengths from roughly 7.5 to 14 mm.¹ Fortunately, this spectral band also corresponds to the peak of blackbody emission at room temperature, making possible thermal imaging sensors that are both passive and which provide performance that is essentially the same any time of the day.

The same people who analyzed the *Marvin Shields* tapes were also responsible for evaluation of an embryonic U.S. Army device, the long-path infrared (LOPAIR) sensor, designed to remotely detect CW agent clouds. Those investigators therefore knew that all nerve agents have strong spectral absorption peaks centered at about 9.7 mm. Figure 1 shows the contrast versus wavelength of a cloud of the nerve agent sarin, GB. This group hypothesized that a nerve agent cloud would be detectable by the B-52 Bomber's AN/AAS-28A LWIR thermal imagers that were evaluated in the *Marvin Shields* test for shipboard fire control applications (Figure 2.) To test

this theory, remote releases of Freon 12 were observed by USS *Tattnall* (DLG-19) in February 1972. These releases of Freon 12, which has two strong absorption peaks in the LWIR band, were remotely detected and tracked for over a minute. This result prompted further investigation as a formal portion of the advanced research investigation of LOPAIR.² Subsequent releases of ethyl alcohol and talc, which have strong absorption in the LWIR, were also successfully observed. By inference, it was then believed that nerve agents could be detected with an LWIR thermal imager.

At this point, the investigation was incorporated into the CW/biological radiological (BR) Countermeasures Project.³ The focus changed from the feasibility of *detecting* a nerve agent to that of *identifying* a cloud to be a nerve agent versus an interferent. An interferent was defined to be any of the many innocuous clouds of dust or other chemicals that would commonly be seen during a littoral battle. It was decided that an ability to perform coarse spectral discrimination needed to be added to a thermal imager in order to perform this function. This function was to be provided by the introduction of a spectral filter wheel (SFW) just before the detector array.

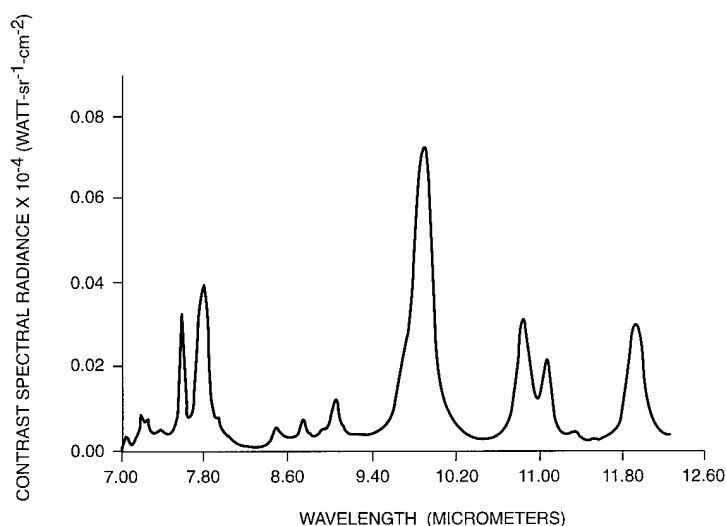


Figure 1—Spectral Contrast Radiance of GB

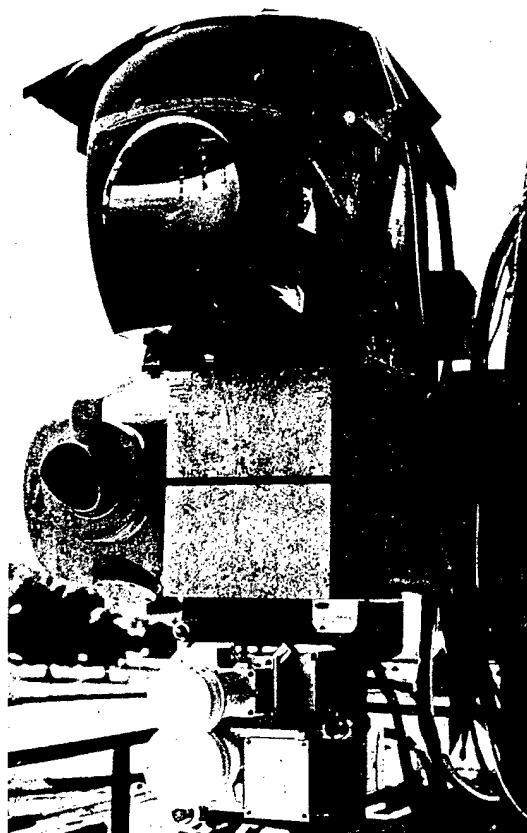


Figure 2—AN/AAS-28A Thermal Imager on MK 68 Gun Fire-Control System Director

The concept of operation was as follows. The filter wheel would contain one antireflection-coated blank filter, one bandpass filter that bracketed the band between 10 and 10.6 μm , where nerve agents have low emission, and two filters that bracket the adjacent bands where the agents have their greatest absorption and emission. The process is shown on Figure 3.

The thermal imager would normally be operated with the antireflection-coated blank filter in the optical path, thereby retaining its sensitivity. If an operator saw an event that looked threatening, such as the rapid evolution of a cloud from an exploding missile or from an aircraft, he or she would push a switch, which would rapidly turn the filter wheel first to the

band of low emission. In this band, the nerve agent cloud would have low contrast with respect to its background. The operator would then push the switch twice more, rotating in turn to the next two filters. In the case of an agent cloud, the operator would see the cloud lose and then regain contrast with respect to its background. Another effect would be that an agent cloud would first shrink when viewed through the first filter, then expand in the next two. In the case of an interferent cloud, which would have a different spectral structure, the sequence of cloud contrast and apparent size would differ. For example, in the case of a water cloud, the cloud would show greater apparent contrast with the filter wheel in the first filter position than in the following two.

In order to carry this concept into development of a feasibility demonstration prototype, the investigators had to develop analytical tools that would allow calculation of diverse LWIR-cloud contrast signatures from first principles, calculation of the effect of the atmosphere and differing backgrounds on those signatures, and modeling of the response of sensors and operators to essentially subjective stimuli.⁴ It was found that a rapid

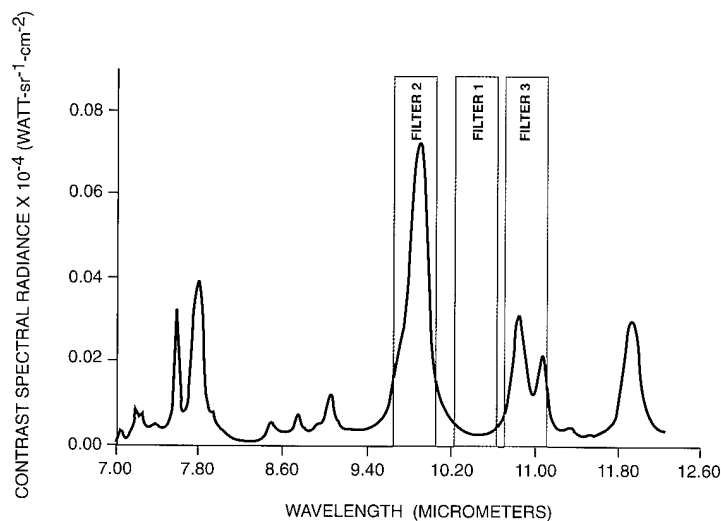


Figure 3—Bandpass Filters

transition from one filter to the next was critical to perform the identification function. With short transition delays between filter positions, the operator's eyes performed the contrast comparison using "retinal processing." Delays longer than about 250 msec forced the operator to "remember" the cloud contrast and to compare it to the display. Such processing had to take place in the brain and was much less accurate and effective.

The first prototype SFW was made for the Electro-Optical Sensor System (EOSS) thermal imager. They are shown, respectively, on Figures 4 and 5. The EOSS consisted of a thermal imager and a Laser Rangefinder/Designator (LRF/D) in

engineering development to support the digital MK-68 gun fire control system. The SFW was evaluated against a variety of agent simulants and interferents, which were released from helicopters, jet aircraft, and artillery shells, as well as dust and sand clouds.^{5,6} Figure 6 shows the appearance of a chemical agent simulant cloud when viewed with the SFW in each filter position. False alarms were rare, and the technique reliably identified agent simulants at long range. By 1978, feasibility had been demonstrated with a prototype installed in a system that was needed by the fleet. However, it was another four years before the technology was approved for service use and then, in a significantly different system, after a quick-reaction development. To understand why, this technology program needs to be viewed against contemporary events that were driven by nontechnical factors.

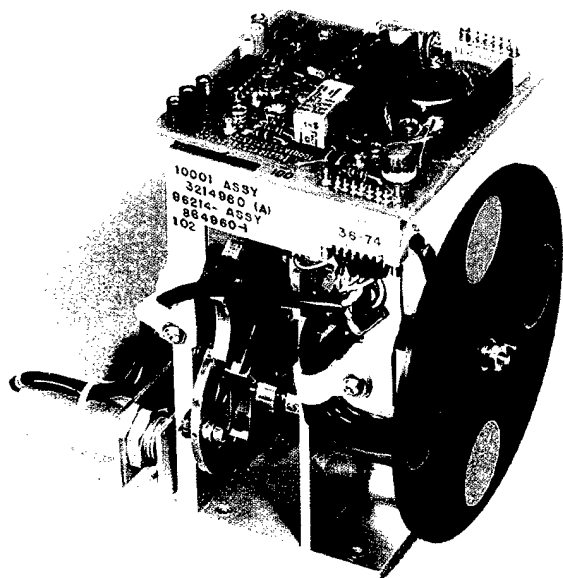


Figure 4—Spectral Filter Wheel

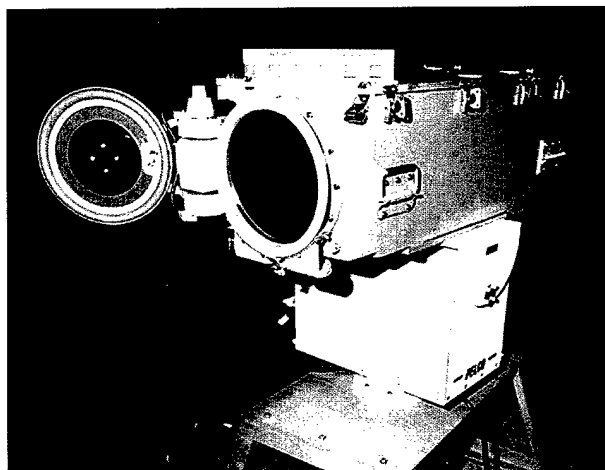


Figure 5—EOSS Thermal Imager

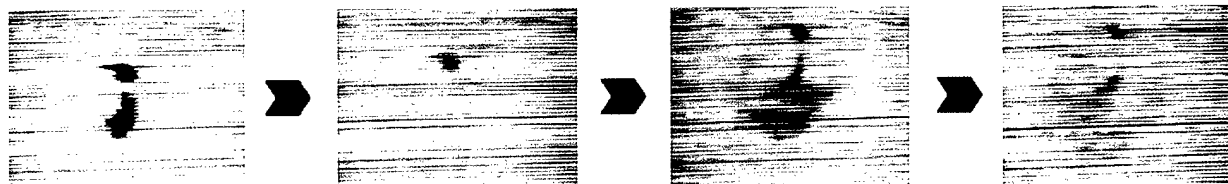


Figure 6—Operation of the SFW Against a Chemical Agent Simulant

THE RDT&E ENVIRONMENT

The Research, Development, Test and Evaluation (RDT&E) of the SFW technique began at a time that the Office of the Secretary of Defense (OSD) was formulating a new policy, which was aimed at designating each of the services to be the lead agent for selected technology areas. The U.S. Army was viewed as the service with the greatest probable exposure to chemical agent attack. It also had the largest annual investment into technologies to counter this threat. OSD, therefore, reasonably named the Army as the lead agent for CW agent defense. A direct result of this decision was that any other service that had a requirement for a technology investigation or a development program related to CW defense had to task and fund the Army to execute the work. In the event that the Army decided not to perform the work, they could choose to permit the requesting service to execute the work through other means. The LOPAIR system, briefly mentioned above, had been under development for more than 15 years. LOPAIR was designed to detect massive clouds of a highly dilute chemical agent drifting with the wind. These clouds would be the result of attacks on other locations. The agent clouds would dissipate and drift downwind. Although the clouds would be dilute, they would also be very large, and could constitute a significant threat if breathed for protracted periods. This was called the "downwind hazard."

The LOPAIR system concept was to detect these clouds by measuring the spectral signature of the cloud combined with that of the background. Performance of the system was limited by the infrared technology of the time, and the program was in danger of being terminated by OSD and/or Congress. The SFW concept was to detect CW agent clouds shortly after release, while they were still dense and had relatively well defined edges. The thermal imagers of that time responded only to the contrast of objects in the scene relative to their background. No thermal imager of the time would have ever detected the downwind hazard, much less identified it as a threat. However, the SFW technique was inexpensive and had the potential (later to be demonstrated) to detect agent releases at significant

ranges. Therefore, in a cost-conscious environment, the embryonic Navy technology project placed the venerable Army program at risk of termination, since both sensors were designed to remotely detect chemical agents.

Thus, when the Army was tasked to develop the SFW technique, the response was to discredit it. The Army's LOPAIR scientists and engineers showed how a thermal imager with an SFW would perform poorly against the downwind hazard, and would be subject to false alarms and failures to detect under many battlefield conditions due to its fundamental design and coarse spectral resolution. In addition, its ability to detect chemical agent releases was considered to be of dubious or negative value. The rationale was that the thermal imager detected such clouds at such long ranges that the clouds would not endanger the sensor site but would create concern and premature transition to a chemical defensive posture. This would significantly reduce the combat capability of the soldiers in the vicinity of the sensor. Therefore, the Army refused to develop the technology. The scientists and engineers at NSWCDD defended the approach by showing how it would provide critical advance warning for amphibious forces in time for them to don protective clothing and equipment. The Army provided permission to the Navy to pursue the investigation and development. However, the dissent over approach had been heard at OSD and by Congress.

The debate between the two services became acrimonious. Project engineers and managers found themselves defending their approach on a frequent basis to the Director of Defense, Research and Development (DDR&E.) Eventually, Congress directed that the Army perform a comparative, side-by-side test of LOPAIR and Army thermal imagers modified to use SFWs with filters provided by the Navy. Both services were directed to defer their developments and direct their efforts towards preparation and support of this test.

LOPAIR engineers wrote the test plan, since they worked for the lead service. Each service was required to predict what performance was expected from their system against a wide variety of

simulants and interferents in diverse tactical situations. The test was directed and executed by the LOPAIR engineers, with Navy personnel being allowed to observe the process but not comment or participate. The test was executed in a fully professional manner, and the findings supported most of the Navy predictions. The differences were primarily that the SFW technique worked under a few conditions where it was expected to fail. On the other hand, the tests showed a number of weaknesses in the design of LOPAIR, prompting recommendations for a new development program. This required a sensor that was more sensitive, with higher spectral resolution, and a shorter response time. In time this led to the Army XM-21 Program.

This process, and a subsequent General Accounting Office (GAO) investigation, effectively stopped work on the spectrally filtered thermal imager for more than a year and a half. The Army was given the opportunity for a fresh start on a system to detect the downwind hazard, and the Navy was free to complete development of the SFW technique. Letters of commendation were sent by the Secretary of the Army, DDR&E of OSD, and the Chief of Naval Operations (CNO) to the Navy team for their contributions. However, the remainder of the RDT&E environment had not remained static. The EOSS adjunct to the digital MK-68 Gun Fire Control System (GFCS) had provided substantial improvements in tracking accuracy and resultant gunfire accuracy. The LRF/D had successfully supported the 5-in., Semiactive, Laser-Guided Projectile (SALGP), providing precision gunfire, with long-range miss distances measured in inches.

This was an exciting time to be working in the field of electro-optics (EO) for the Surface Navy. EO, a relatively new realm of technology, promised to provide astounding capabilities at modest cost. The EOSS was highly effective but was dependent upon the MK-68 director for stabilization and pointing. The director was heavy and was being phased out. It was not used at all on ships using the MK-86 GFCS, which was widespread in the fleet. A decision was made to develop a new system that provided its own stabilization and pointing. This system would be compatible with a wide range of ship classes, incorporating lessons learned from the EOSS, the

digital MK-68 GFCS, and SALGP testing. After the approval of an operational requirement, the engineering development effort became known as SEAFIRE.

The SFW specifications were incorporated into those of SEAFIRE. Proposals from industry were evaluated, and a contract was awarded for development of the system. Now that the technology had transitioned into engineering development, there was little left to be done except to make certain that the salient features of the SFW were properly executed by the SEAFIRE contractor and to wait for system delivery. Then disaster struck. Projected SEAFIRE development costs started to climb. They eventually reached a threshold where a decision had to be made to restructure or terminate the program. The high projected development costs also caused a reevaluation of the expected benefits of the SEAFIRE system. SEAFIRE was fundamentally limited to line-of-sight operation, and many warfighters desired to engage targets while they were beyond the visible horizon. Other sources of laser illumination for SALGP were available on aircraft and from man-portable systems. After a painful process of restructuring, the program was terminated.

When the SEAFIRE program began to show signs of distress, the supporters of the SFW technique in OPNAV became concerned that the Surface Navy might never get an advance warning capability against CW agents. In 1979, NSWCCD was challenged to demonstrate a feasibility prototype in about one year that could perform the CW advance warning function as a stand-alone sensor. The constraints were that it had to be inexpensive, could be operated by sailors with minimal training, and would use a thermal imager constructed with common modules. Common modules were basic infrared imaging sensor "building blocks" developed to support the needs of all the services. Experience during the comparative testing of LOPAIR and man-portable Army thermal imagers fitted with the SFW had shown that these small devices could perform the mission required. Human-factors concerns made the AN/TAS-6 Night Observation Device, Long Range (NODLR) the baseline sensor of choice. However, the low availability and high

demand for the NODLR made rapid procurement of one for modification impossible within the timeframe mandated by the office of the CNO (OPNAV). To meet the schedule goals of the project, NSWCDD selected the AN/TAS-4 night sight. The AN/TAS-6 and AN/TAS-4 are shown in Figures 7 and 8. An AN/TAS-4 was purchased through the Army, and the Army's Night Vision Laboratory was tasked to build and install an SFW into the sensor using specifications and filters provided by NSWCDD.

It was decided to test the resultant sensor at the U.S. Army Dugway Proving Ground, Utah, using enlisted U.S. Marine Corps (USMC) operators who knew nothing about the theory of operation of the SFW, and who had not had previous training with infrared devices. They were instructed in the use of the sensor and its use in the field just prior to the test using videotapes, lectures, and several days of "hands-on" training. A USMC officer was allowed to observe, but not coach, the operators. Air releases of nerve agent simulants and interferents were made using an aircraft-mounted, USMC CW weapon—the AERO 14-B spray tank. Other tests were performed with 155-mm artillery shells filled with CW agent simulants, 155-mm high-explosive (HE) rounds, and against the dust clouds raised by explosions. Because the cost of such

tests is high, it was hoped that attention to detail, combined with the use of nonscientist operators, would result in a data set that would be considered technically significant by the Navy's independent operational test agent, the Commander, Operational Test and Evaluation Force (COMOPTEVFOR). The testing was completed with an operator error rate that was extremely

low, even when compared with that obtained by the scientists and engineers who developed the sensor. Independently written statements from the operators and their commissioned observer were obtained. Their assessments of the sensor's utility, ease of use, maintenance, reliability and the value of the training received were high.

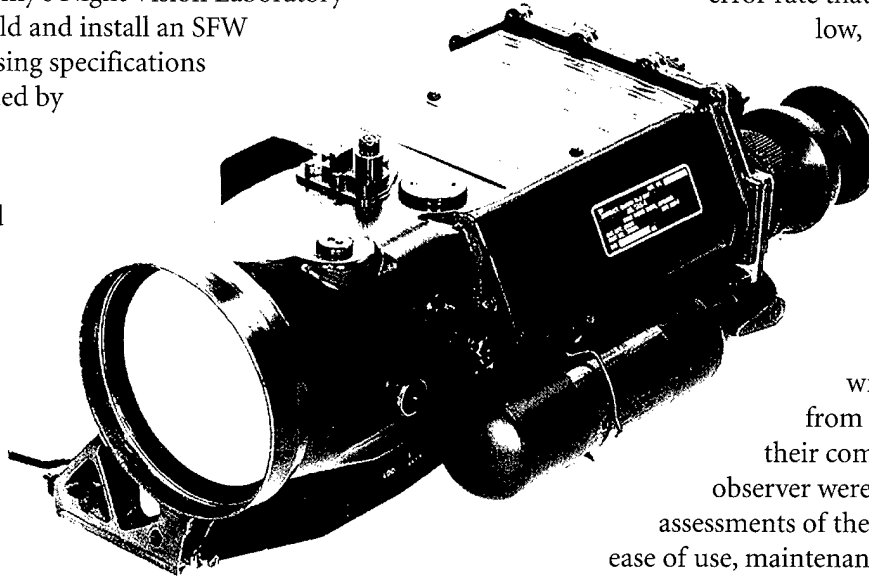


Figure 7—AN/TAS-4

When the OPNAV sponsor was briefed of the test results, he directed that engineering development begin the next fiscal year, with a quick-reaction development to be completed within one year. In one year, specifications had to be

developed, a contract awarded, the sensor developed, and the system tested to exacting military standards for ship-board use. Several waivers were granted to expedite the process, most notable being relaxation from the requirement to withstand heavy shock and continue to operate. Since the AN/TAS-6 was not designed to withstand the shock environment, this waiver was critical to a rapid development.

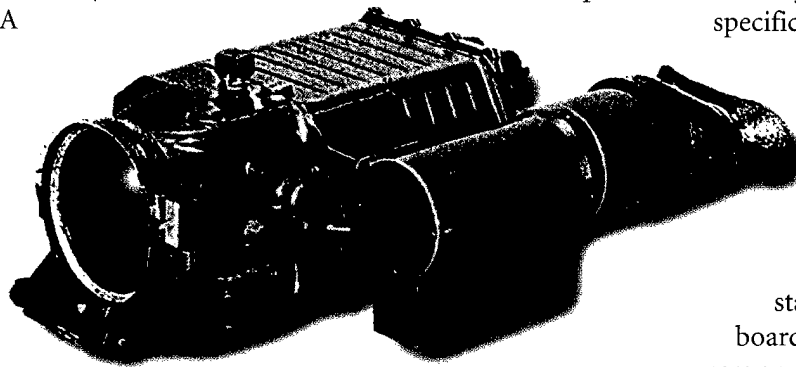


Figure 8—AN/TAS-6

QUICK-REACTION ENGINEERING DEVELOPMENT

Engineering Development (now known as E&MD) was a process to take the lessons learned from a successful prototype and develop both a design and manufacturing tools that allowed the system to be economically purchased, operated, maintained, and logistically supported. The process culminated with a certification that the system met its performance specifications, and that its documentation, plans, and approved funding met naval requirements. Some of this certification process was performed by COMOPTEVFOR. Testing performed by the developing agent might suffice for some other parts, if the methodology and safeguards met the approval of COMOPTEVFOR. This was the easy part. Success was assured if the system and its operators perform as specified. The hard part was getting approval for mandatory planning, scheduling, and preparation that required lead times of as long as 5 years. In the context of a 1-year, quick-reaction development, this is difficult to achieve. A checklist with approximately 150 approval signature blocks was provided, most of which addressed logistic considerations. A typical question might be

Training facility requirements have been requested 5 years in advance: yes or no.

If the answer was no, the application failed. Another example was

An increase to the total manpower allocation to the Navy (to cover the time operators/maintainers spent training) has been requested and approved.

No procedures were in place to facilitate quick-reaction developments. The approving infrastructure had heard every excuse from other programs in the past, sympathy was in short supply. The NSWCCD team, consisting of one physicist, one electronics engineer and one technician concluded that creative solutions would be required to get the system approved for service use and production. The close

relationship that had been developed with COMOPTEVFOR during earlier testing and during the development proved to be critical. They were well aware of the system, its capabilities, and the opinions of the operators. COMOPTEVFOR became a major supportive force in a process that otherwise was exclusionary in nature. Obviously, no classroom training of operators/maintainers would be possible, due to the requirements for prior planning, notice, and manpower allocation. A training package consisting of videotapes, a "comic book"⁷ (see Figure 9), and a draft technical manual⁸ were developed and used to train the crew that performed the operational evaluation (OPEVAL). The videotapes and comic book were the most popular and effective training aids. The technical

How to USE and MAINTAIN the CHEMICAL WARFARE DIRECTIONAL DETECTOR AN/KAS-1

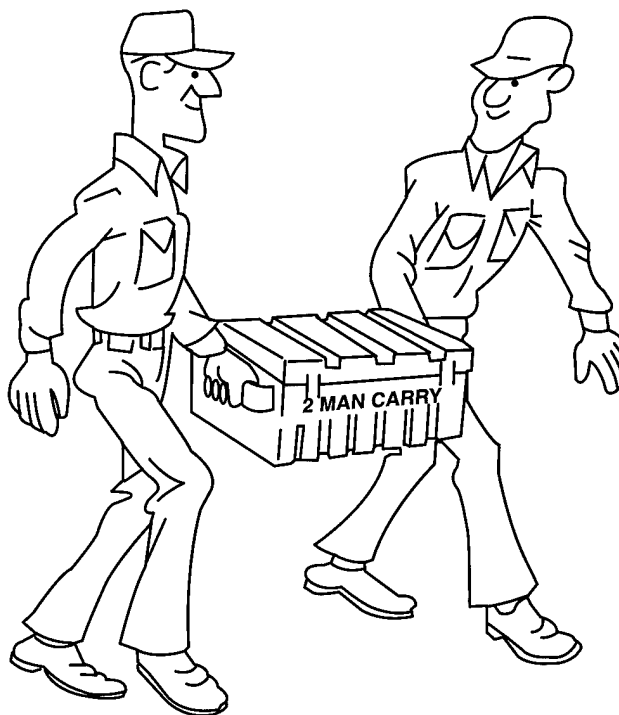


Figure 9—AN/KAS-1 "Comic Book" Manual

manual was later adopted without change. No logistics network existed for the AN/KAS-1. No infrared sensor of any kind was in use on Surface Navy Ships, although they were widespread on naval aircraft. NSWCDD recommended that NWSC, Crane, Indiana (now the Crane Division of NSWC) be the In-Service Engineering Agent (ISEA) for the AN/KAS-1. Spare parts and consumables sufficient to support early production rates for 2 years were purchased as part of the development effort and pilot production contract. Critical items were entered into the naval supply system prior to OPEVAL. The system was packaged in a container that contained all the supplies required for operation for 6 months at sea (see Figure 10). Each

each day brought its new list of surprises. It seemed at times that a huge bureaucracy existed solely to prevent systems from ever getting into production. Of course, it was established to prevent systems that could not be supported or maintained from being delivered to the fleet. Despite our best efforts to become "instant experts" and to create solutions that would meet both the spirit and letter of regulations, some approvals were never obtained. The integrated logistic support plan and the associated approval sheet were signed by the senior flag officer in charge of the approval process. This effectively overruled the objections of his subordinates. We now almost relaxed, thinking that the system was ready for OPEVAL.

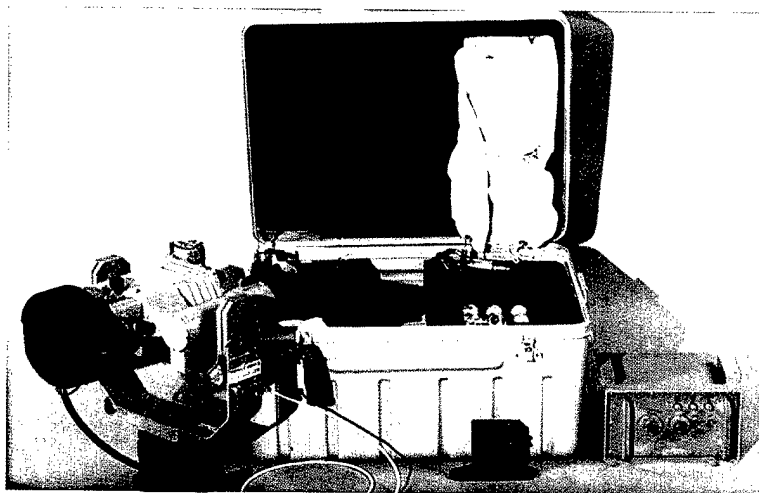


Figure 10—AN/KAS-1

question on the sign-off sheet was addressed in a like manner. Where something did not exist or could not be made to happen in the time allowed through normal channels, a replacement was created and either entered into the supply system, delivered as part of the system, or both. Operation and maintenance funding for projected production was obtained through a brief to the Comptroller of the Navy. The tempo of activity during this accelerated engineering development phase was incredible, and

READINESS FOR OPEVAL

Prior to entering OPEVAL, one additional certification of readiness was required. The Naval Sea Systems Command (NAVSEA) and the Naval Material Command (NAVMAT) (later disestablished) had to review all documentation and to conduct a final review presented by the NSWCDD team. Despite a component design

problem discovered and corrected during Technical Evaluation (TECHEVAL) of the system at sea, the system was as ready as we could make it. Then the issue of shock testing was raised. The waiver of shock testing was ruled invalid, since the AN/KAS-1 was considered mission-critical equipment. Everything came to a halt while this was pondered. Further slippage of OPEVAL would result in loss of production funds for the next year and possible termination of the program. The system could not be hardened to shock without a major effort. Finally, an agreement was reached between NAVMAT, NAVSEA, and NSWCCD. The system would be allowed to go through OPEVAL without passing shock tests, and NAVSEA would fund the follow-on work to harden the AN/KAS-1 to meet the most demanding shock requirements. If OPEVAL was passed successfully, pilot production would be allowed, with the shock hardening modifications to be installed during pilot production. By now the window for OPEVAL was so short that even a single failure would have required the test to be extended such that pilot production funds would be lost. COMOPTEVFOR ruled that all the testing during TECHEVAL would count towards the reliability testing budget, and that the testing at Dugway Proving Grounds would suffice to demonstrate performance against interferences and agents. All the ancillary functions of the sensor were demonstrated during OPEVAL, and the system operated flawlessly through the test's end.

THE REST OF THE STORY

After completion of OPEVAL, the shock problem was solved through a redesign of the sensor support structure. The cost of this change was nearly as much as that of the initial development. The planned one-year development took 18 months, but production stayed on schedule. After review by OPNAV, a letter was issued providing Approval for Service Use (ASU) without restrictions. The sensation of satisfaction was profound and still remains. Pilot Production created its own challenges, as did transition of responsibilities to the ISEA. NSWCCD remained an integral part of the production team for several years beyond the formal transition of responsibilities, providing technical advice and

support when needed. This sometimes included responding to unusual requests such as a casualty report from USS *New Jersey*, which was bombarding Lebanon. The captain wanted his AN/KAS-1 units fixed *now*. We had not foreseen the effects of sensor placement a few feet from the muzzles of elevated 16-inch guns. Users with numerous special applications continued to require technical solutions. Eventually, the ISEA developed the capabilities to respond to these requests without assistance and added improvements such as a remote display capability. A total of 1,029 AN/KAS-1 units were produced. Over 600 are in active use on surface ships and special operations craft. The large logistic supply pool is frequently called upon to provide units for special applications by military and law enforcement users.⁹

SUMMARY

Transition of a good technology into the fleet is a process that requires a great amount of personal conviction and a willingness to deal with whatever presents itself along the way. The process starts with a strategy to demonstrate the technology in a way that will be attractive to its eventual users. The most difficult part occurs well after the science is proven and the most challenging engineering problems are solved to the investigator's satisfaction. Unless the technology is subsumed into a larger program, which will carry the load associated with obtaining production approval, the experience can be protracted and intense. In any case, the satisfaction of carrying a good idea to fruition and seeing it in use by the fleet is well worth the effort.

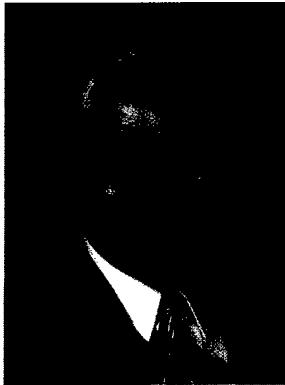
REFERENCES

1. Taczak, W.J. et al., *The Experimental Evaluation of an 8-12 mm FLIR as a CW Agent Detector*, NRL, TR-2850, Feb 1973.
2. Naval Ship Systems Command Task 14583 under ADO 4809.
3. Project No. SSL-80, Program Element 64506.

4. Horman, S.R., *Remote Identification of CW Agents by Spectral Techniques: Calculation of Cloud Emission in the Infrared*, NSWC/DL TR-3457, Jun 1976.
5. Horman, S.R. et al., *Spectrally Filtered FLIR as an Advance Warning Sensor of Chemical Agent Attack*, NSWC/DL TR-3706, May 1978.
6. Taczak, W.J., et al., *Technical Evaluation of the Spectral Filter Wheel Concept for Chemical Warfare Advance Warning Against High Explosive and Chemically Filled Projectiles*, NSWC/DL TR-3894, Nov 1978.
7. *How to Use and Maintain the Chemical Warfare Directional Detector AN/KAS-1*, NSWCDD SW073-AA-TRN-010.
8. *Technical Manual, Description, Operation and Maintenance Instructions, Chemical Warfare Directional Detector AN/KAS-1*, NAVSEA SW073-AA-MMO-010, 1 May 1983.
9. Personal Communication with Mr. Randy McAtee, AN/KAS-1 ISEA Engineer, NSWC, Crane Division.

THE AUTHOR

MR. S. ROGER HORMAN



Mr. S. Roger Horman earned a B.S. in physics from Randolph-Macon College in 1968. After 2 years in the Army as a meteorologist, he studied and taught physics at Williams College while performing research for his thesis at M.I.T. He was awarded an M.A. in physics from Williams College in 1973, after which he came to NSWCDD. He pioneered the naval use of E-O sensors for remote sensing of chemicals. He also headed the effort that developed the high resolution E-O target signatures system, having significant impacts on Navy High-Energy Laser and AIM-9(L&M) seeker programs. He headed the Electro-Optical Systems Branch for 6 years. Additionally, he developed several quick-reaction capability EO weapons that were fielded in the Persian Gulf. He holds two patents—one for the AN/KAS-1, the other for an imaging IR sensor using advanced optical and signal processing. He has authored over 50 technical publications.

THE DEVELOPMENT AND APPLICATION OF THE SHIPBOARD COLLECTIVE PROTECTION SYSTEM (CPS)

Mr. Dale W. Sisson, Jr.

Since the early 1980s, U.S. armed forces have faced an ever-increasing threat from the employment of chemical and biological warfare agents. To this end, the Naval Surface Warfare Center, Dahlgren Division (NSWCDD) has been charged with developing and maintaining chemical and biological detection apparatus; and chemical, biological, and radiological (CBR) protection equipment for Navy and Marine personnel. As this article attests, the centerpiece of the Navy's CBR warfare countermeasures program is the Collective Protection System (CPS). Originally designed and developed at NSWCDD for shipboard use, CPS has since been incorporated into the fleet, as well as vital land-based sites around the globe. In addition, variations of CPS can be found throughout the services in a number of applications.

As an essential component of new-construction ships, CPS is a prime example of an NSWCDD design progressing to the manufacture level. The engineering and testing performed by NSWCDD personnel not only provides the Navy fleet with a CBR protection system of high confidence, but the filtration technology developed and maintained benefits an array of applications across the joint arena.

INTRODUCTION

In 1980, the threat of applied CBR warfare to ship activities was conveyed by the Office of the Chief of Naval Operations (OPNAV). To counter this threat, OPNAV and the Naval Sea Systems Command (NAVSEA) initiated development of a shipboard CPS. Its primary goal was to ensure ship survivability during CBR contamination (based upon the original Navy CBR Defense Operational Requirement, S0410-SL).¹ By directive, the function of CPS is to provide a safe haven in which the unencumbered performance of mission-essential operations can be executed while present in a CBR threat or contaminated environment. This directive tasked NSWCDD with designing the first shipboard CPS and, hence, led to the design, development, installation, and testing of the prototype CPS aboard USS *Belleau Wood* (LHA-3) (see Figure 1).¹ Tagged to serve as the prototype CPS test platform, USS *Belleau Wood* maintained her test ship status from 1984 to 1990. This extended-duration test period afforded NSWCDD engineers the opportunity to implement continuous design improvements en route to obtaining valuable reliability, operability, maintainability, and environmental hardiness data.

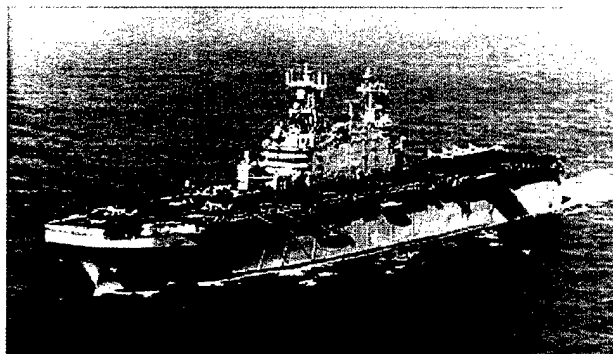


Figure 1—USS *Belleau Wood*, LHA-3 (First CPS Installation)

Today, 25 or more countries are known to be, or suspected of, developing and maintaining chemical warfare capabilities.² Biological weapons programs are known to exist in 10 nations and are suspected of being active in as many as ten more.² The goal of many of these countries is to develop chemical and biological agents of increased potency and lethality. Due to the relative ease of developing chemical and biological warfare capabilities (including delivery), these numbers are expected to continually increase.

In addition to the offensive chemical and biological programs sponsored by foreign governments, there is a growing threat presented by the potential use of chemical and biological agents by terrorist activities. Recent events in history, such as Operation Desert Storm in 1991 (and continuing with the potential dangers presented by Iraq today), as well as incidents such as the Sarin gas attack on a Tokyo subway (March 1995), highlight the worldwide presence of such threats. Chemical and biological agents, when deployed effectively, have the capability to inflict substantial casualties. Therefore, Department of Defense (DoD) policy and OPNAVINST S3400.10E require deployable U.S. surface ships and high-threat overseas shore installations to possess CBR defense capabilities.²⁻⁵

DEVELOPMENT/HISTORY

Chemical and biological defense consists of two primary subcategories: detection and protection. The fusion of these two defense mechanisms is key to effective CBR defense and, therefore, *ship survivability*. Prior to the development of CPS, the only protection afforded the ship's crew was the donning of protective suits, or Individual Protection Equipment (IPE). The utilization of the IPE suits can be time-consuming and, once in place, prohibitive of the performance of certain essential shipboard activities. Therefore, CPS was developed to provide contaminant-free boundaries (i.e., zones) within ships' spaces such that mission-essential operations can be carried out by the crew without suffering the effects of a CBR attack.

As stated previously, OPNAV directed the development of a shipboard prototype CPS system in 1980. This effort was undertaken based on the original Navy CBR Defense Operational Requirement, S0410-SL. Successful prototype development, installation, and evaluation (DT-II and OT-IIA) efforts were completed aboard USS *Belleau Wood* in 1984. In response to the successes achieved in DT-II/OT-IIA, the OPNAV Ship Characteristics Improvement Board (SCIB) issued the directive that CPS installations be included on all planned new-construction ships. Ship classes covered by this directive included the LSD, LHD, DDG, and AOE. Per Test and Evaluation Master Plan (TEMP) 554-5, a formal OT-II/operational evaluation (OPEVAL) was to be conducted in 1989 using the first new-construction ship available.⁶

Further instructions were then provided by OPNAV to proceed with a full OPEVAL on a new-construction ship prior to proceeding to Milestone III. In 1990, USS *Gunston Hall* (LSD-44), as the first new-construction ship available, was selected for shipboard DT-IID/TECHEVAL and OT-II OPEVAL.⁶

DT-IID/TECHEVAL was then conducted aboard the LSD-44 while underway during the period May/June 1990. The CPS requirements defined by TEMP 554-5, Revision I were successfully met,

indicating that CPS was ready for formal OPEVAL.⁷ OT-IIC/OPEVAL was successfully completed on USS *Gunston Hall* in March 1993. Official Milestone III approval for CPS was then authorized by the Assistant Secretary of the Navy (Research, Development, and Acquisition) (ASN (RDA)) in July 1993 by the Navy Program Decision Memorandum (NPDM) for CPS.¹

Since the successful installation of the prototype CPS aboard USS *Belleau Wood* in August 1983, over 40 ships in the Navy's fleet have been outfitted with CPS (see Figure 2). Including both new-construction CPS and back-fit Selected-Area CPS (SACPS) installations, this number is projected to surpass 60 by the year 2002.

SYSTEM DESCRIPTION AND CAPABILITIES

From an analogous standpoint, a CPS environment can be likened to the pressurized cabin of an aircraft. CPS spaces are slightly overpressurized (by approximately 2.0 inches water gauge (IN. WG) for CPS and 1.0 IN. WG for SACPS) to prevent the

ingress of any chemical or biological contaminants. Sufficient replenishment air is pumped into the system to maintain the necessary overpressure. Pressure control valves (PCV), in place to prevent the buildup of excessive air pressure, automatically open when internal air pressure exceeds 2.0 IN. WG. The resultant pressurization allows air to enter the protected only zones through the CBR filter banks. In effect, CPS provides a clean-roomlike environment by subjecting all incoming air for a CPS zone to the CBR filter banks.

While the vaneaxial fans must supply a steady airflow, the most important element of the CBR filtration system is the filter bank. Air filtration (for a total protection (TP) zone) is accomplished using an array of housing assemblies, each containing three 200 cubic feet per minute (CFM) CBR filter sets plus prefiltration. Each of the filter sets includes two components (see Figure 3):

- ◆ 200-CFM, charcoal charged gas adsorber
- ◆ 200-CFM, high-efficiency particulate arresting (HEPA) particulate filter

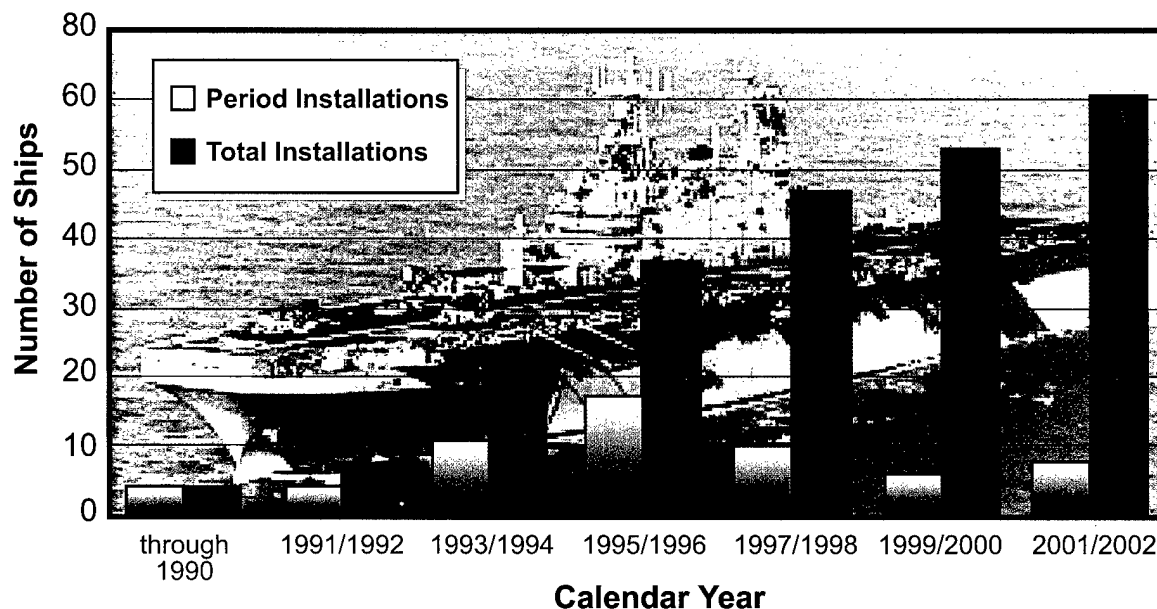


Figure 2—Shipboard Collective Protection System Installations

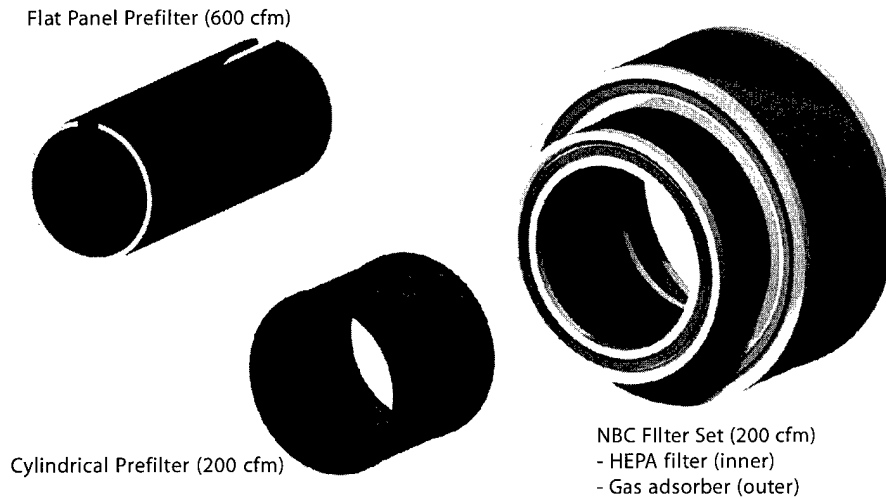


Figure 3—Nuclear, Biological, and Chemical (NBC) Filters and Prefilters

Prefiltration is accomplished via either of the following configurations:

- ◆ Three cylindrical (paper media) prefilters per housing
- ◆ One flat (HEPA media) prefilter with a polyester encapsulating bag filter

From the inlet plenum, incoming airflow is supplied by specially designed vaneaxial fans (notice the fan-room layout as shown in Figure 4). Air enters the prefilter and flows radially outward through the HEPA filter and gas adsorber in succession (see Figure 5). The gas adsorber guards against chemical warfare gases, while the 200-CFM HEPA filter prevents solid and aerosol CBR agent penetration. Prefilters are installed primarily to remove relatively large particulate matter from the incoming airstream and, thus, increase the service life of the 200-CFM HEPA filters. This filtration configuration guarantees protection from a sustained chemical attack. Also, filtration capabilities are maintained and, therefore, not compromised, even after CBR contamination.

With recent advancements in prefiltration media, HEPA filtration media, and gas adsorber charcoal longevity, expected filter service life is now approaching 3 years. Ongoing filtration research and

development will lead to development of a filter with a service life well exceeding the current 3-year benchmark.

CPS zones may be accessed only through air locks, pressure locks, or decontamination stations. Equipped with air sweeps to continuously purge any airborne contaminants, air locks are small, controlled chambers that are utilized to protect zone integrity (see Figure 5). Pressure locks, which do not include air sweeps, are designed to allow access to CPS zones without reducing zone pressurization. As CPS zone pressure is constantly maintained at 2.0 IN. WG, air locks are provided for personnel ingress/egress under normal operating circumstances. Under threat situations, contaminated personnel must enter through decontamination stations, which also maintain air-lock functions.

Two distinct CPS zone categories are implemented into the design of CPS-equipped ships:

- ◆ *Total Protection (TP)*
- ◆ *Limited Protection (LP)*

The purpose of each zone design, as can be inferred, is to provide the level of protection required for the ship space in question. LP and TP zones are applied to appropriate ship classes as

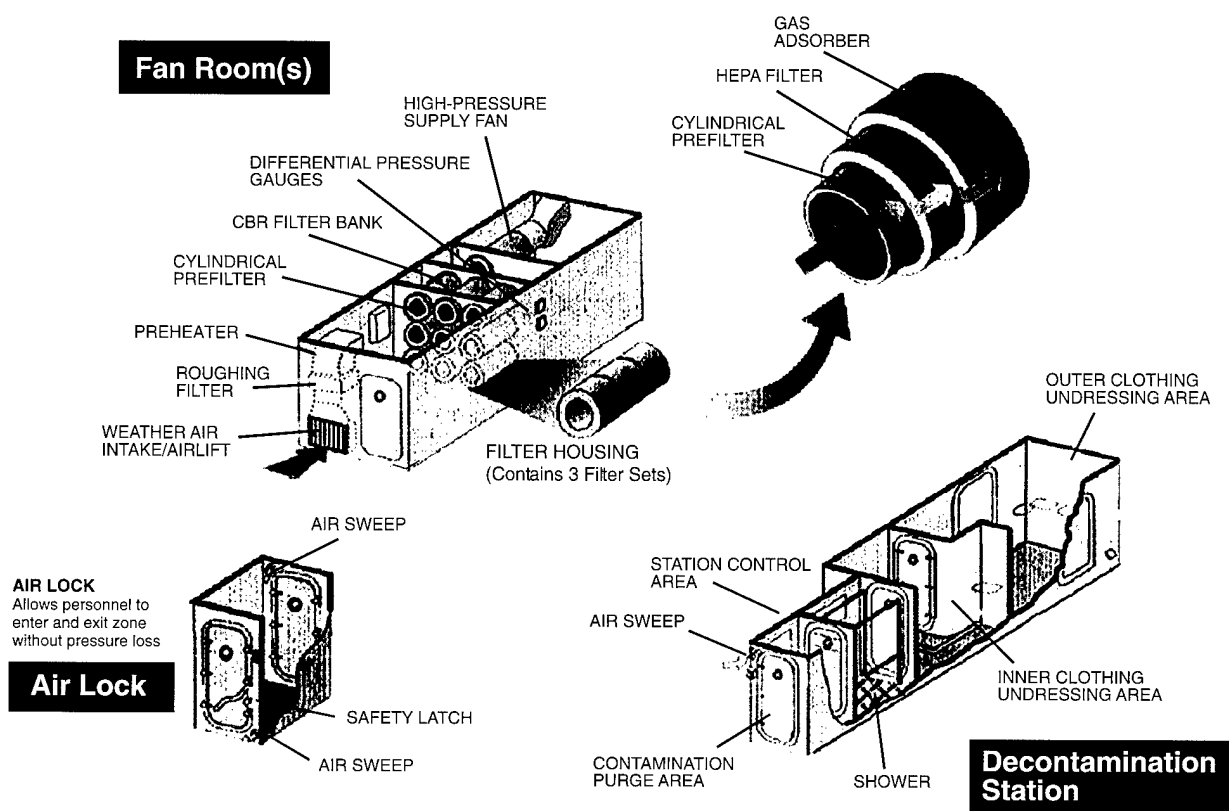


Figure 4—Key CPS Components

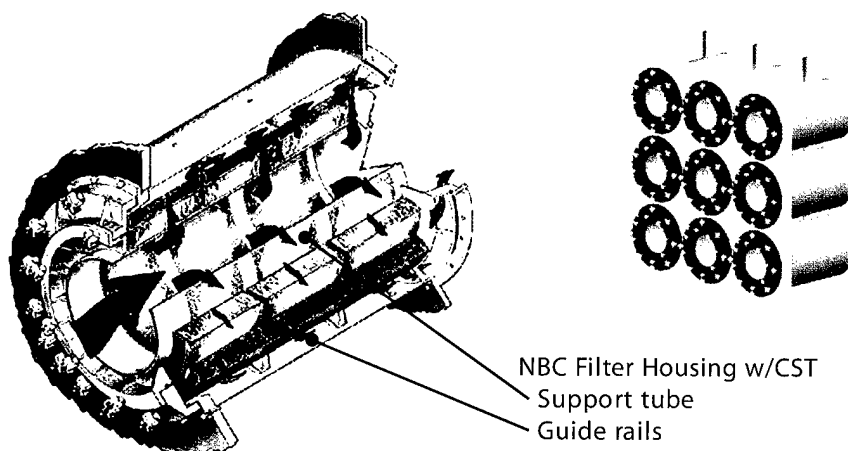


Figure 5—CPS-Filter Housing with Center Support Tube (CST)

shown in Figure 6. Figure 7 depicts a more detailed layout of a TP zone. As the zone descriptions indicate, the primary difference between the two zone classifications is the type of protection provided.

Protection within a TP zone is complete. That is, no IPE usage is required within a subject zone. Typical examples of TP zones include berthing and mess areas, combat information centers (CIC), and the pilot house. As described earlier, TP zone filtration is accomplished via an array of 200 CFM CBR filter sets (including HEPA filters and gas adsorbers).

LP zones, which are not pressurized, are restricted to use in machinery spaces only (i.e., engine rooms). For LP zones, only HEPA filtration is provided. Thus, LP zones (found only at DDG-51 (see Figure 8) and AOE-6 class engine spaces) maintain particulate filtration only. Therefore, no gas adsorbers are included in the LP zone filter banks (see Figure 9). From an operational readiness standpoint, crew working within an LP zone must wear protective gas masks during threat situations. Protective garments, however, are not required in LP zones.

CPS vs. SACPS

Two variations of shipboard collective protection are utilized to meet shipboard collective protection requirements. While both systems employ the same filter sets and operational methods, some differences exist. CPS and SACPS (see Figure 10) features are summarized as follows.

Shipboard CPS:

- ◆ Full-time CBR-protected zone (pressurized and supplied with filtered air)
- ◆ Enables ship to operate in a CBR-contaminated environment
- ◆ IPE not required in zone
- ◆ Provides safe haven for stand-down relief
- ◆ Integral part of the heating, ventilating, and air-conditioning (HVAC) system
- ◆ Applications: DDG-51, AOE-6, LHD-1, and LSD-41 Classes and LHA-3

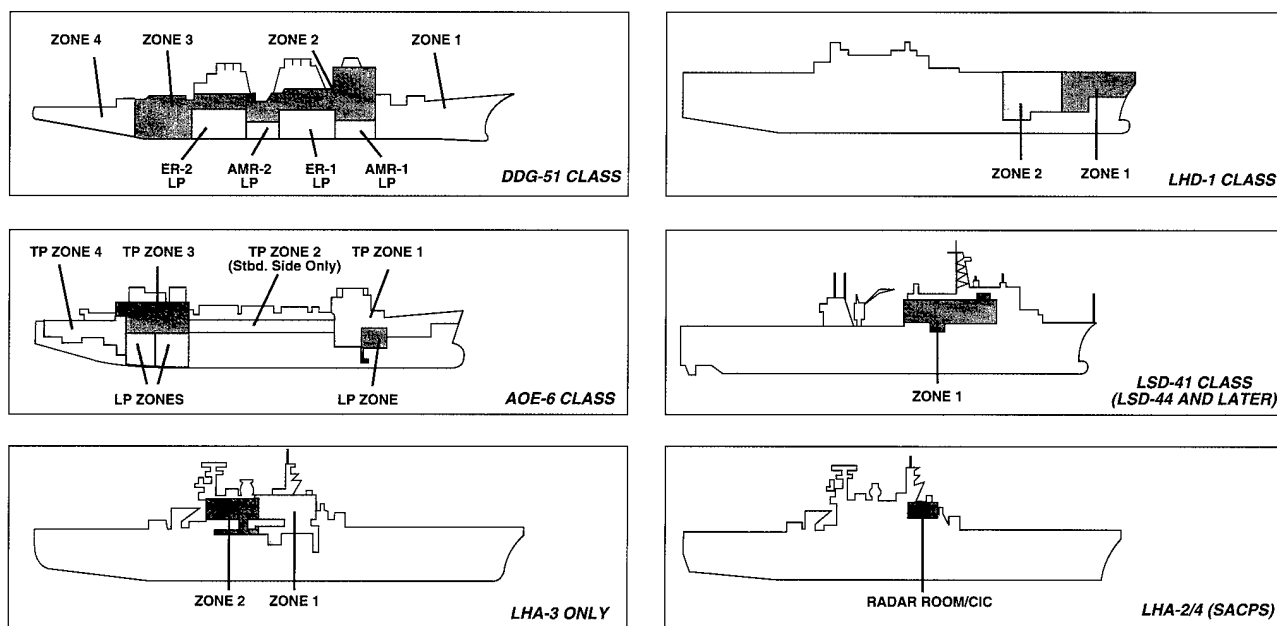


Figure 6—CPS and SACPS Zone Configurations

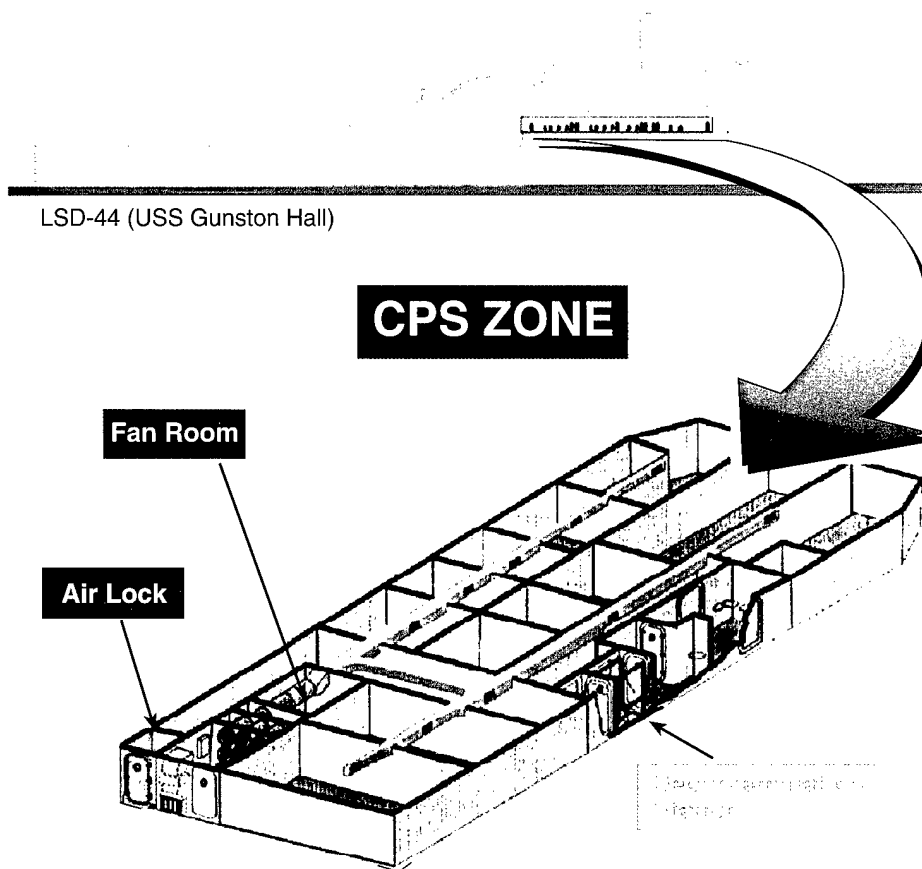


Figure 7—Typical Shipboard CPS Zone Configuration

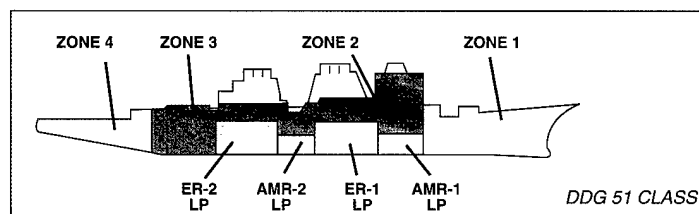
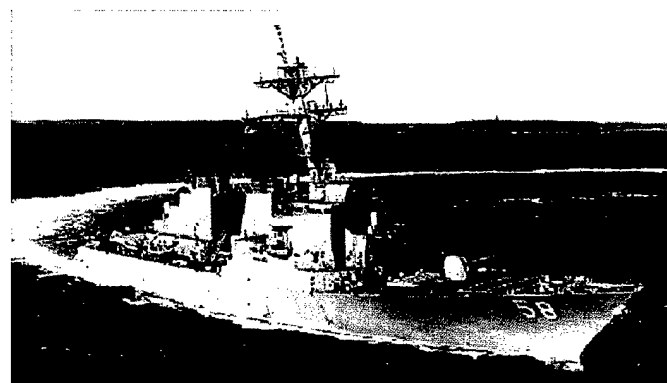
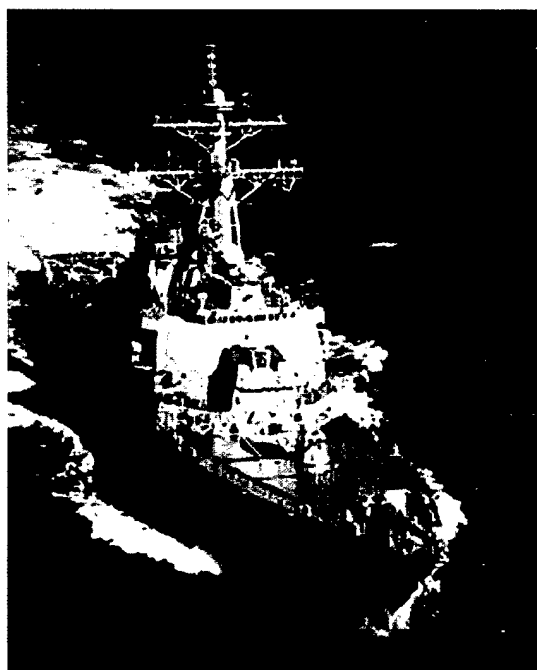


Figure 8—DDG-51 Arleigh Burke-Class Destroyer

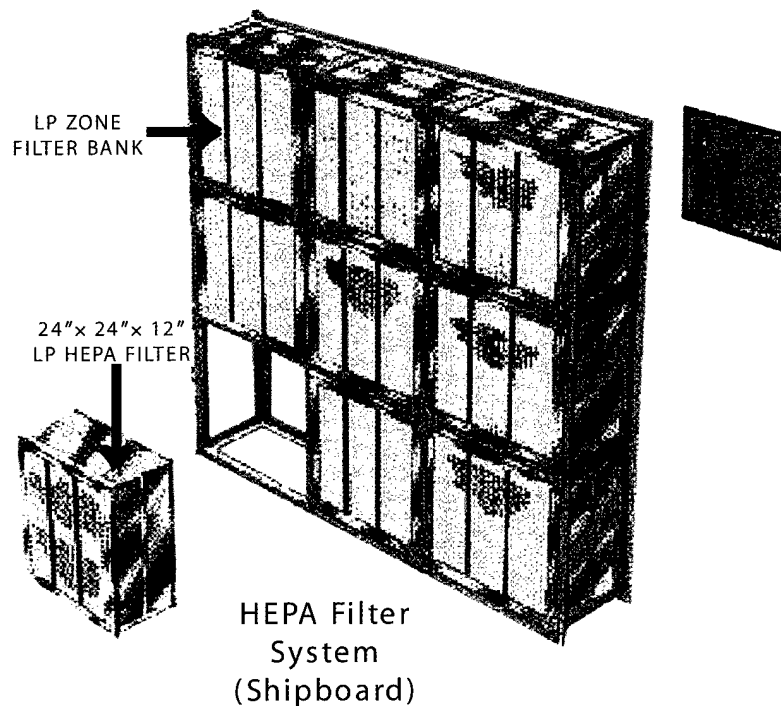


Figure 9—Typical LP Zone Filter Bank

SACPS:

- ◆ Back-fit for existing ships not originally equipped with shipboard CPS
- ◆ Activated on demand to provide CBR Protection of selected ship compartments
- ◆ Modular system designed for application to specific spaces
- ◆ Enables ship to operate in a CBR-contaminated environment
- ◆ IPE not required to be worn in zone
- ◆ Provides safe haven for stand-down relief
- ◆ Current Applications: LHA-2/4

FILTRATION EFFICIENCY MEASUREMENT

Particulate filtration levels of the CBR filter banks must be certified to meet a minimum of 99.97 percent for a nominal particle size of 0.3 micron (.000012"). Following the installation/replacement of CBR filters, filtration capability is verified with

dioctylphthalate (DOP) testing according to the following procedure.⁷

1. DOP (which serves as an agent simulant) is injected into the filter inlet plenum at a concentration of approximately 100 mg/m³ (using a DOP smoke generator).
2. Using a photometer, DOP concentration is measured immediately downstream of the filter bank being tested.
3. Efficiency is calculated as a function of the difference of the upstream and downstream DOP measurements as a ratio of the upstream DOP concentration.
4. Acceptable filter banks are those with efficiency ratings of 99.97 percent or better.

$$\text{Filtration Efficiency} = \frac{\text{DOP}_{\text{UP}} - \text{DOP}_{\text{DOWN}}}{\text{DOP}_{\text{UP}}} \times 100\%$$

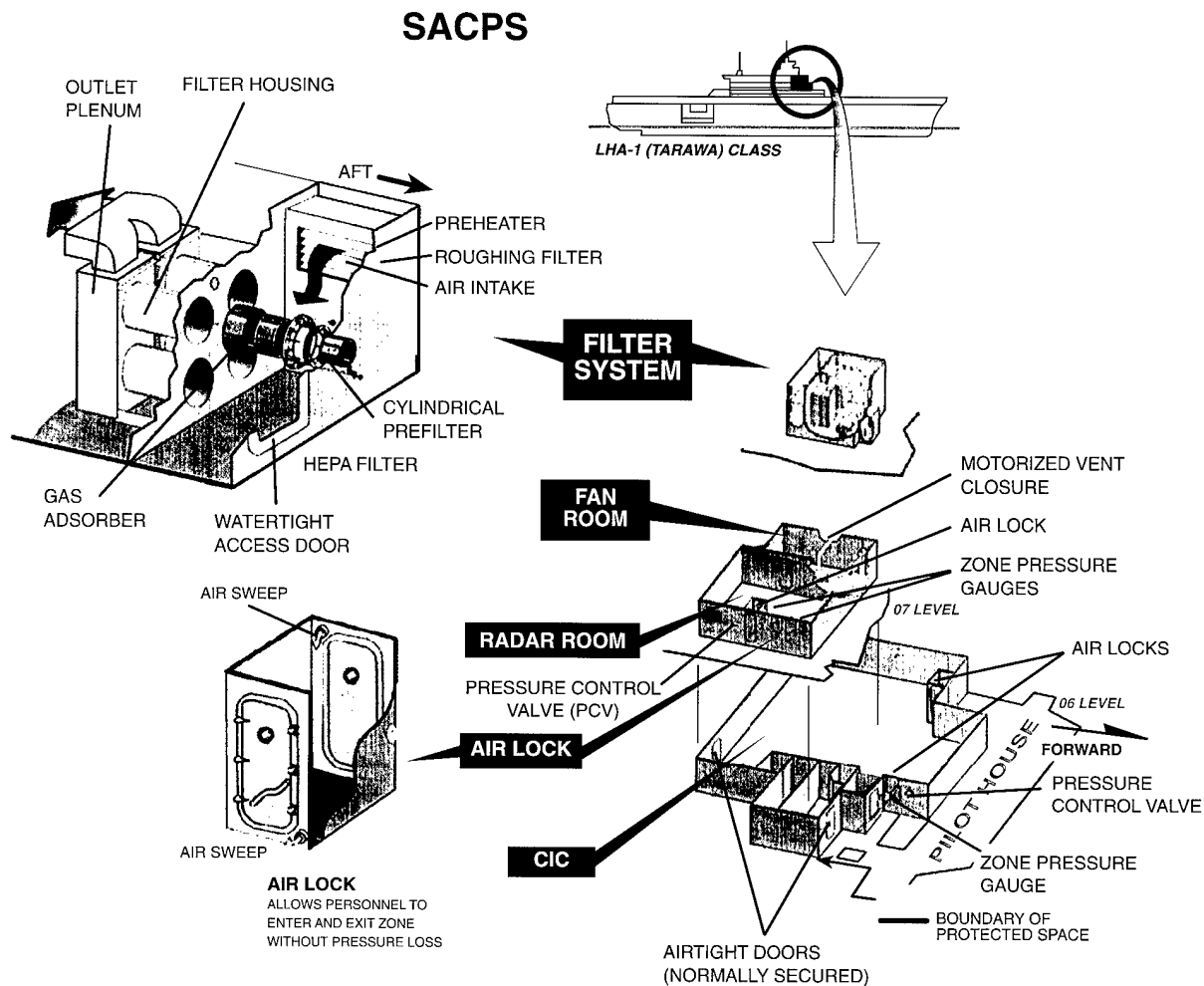


Figure 10—SACPS Configuration

CURRENT APPLICATIONS

To date, shipboard collective protection has been installed in five ship classes, as described in the CPS versus SACPS analysis section of this article. Cumulatively, these ship classes account for over 40 CPS-equipped vessels currently in service. In addition, CPS was also installed in 1990 aboard two container ships: SS *Gopher State* (T-ACS 4) and SS *Flickertail State* (T-ACS 5).⁸ These two container ships were specially equipped by NSWCCD for moving chemical weapons under the demilitarization program.

In addition to the sea-bound collective protection installations, CPS has been implemented into the design of four land-based naval facilities. Final system checkout and filter leak testing were completed by NSWCCD's Chemical Defense Systems Branch (NSWCCD B53) in September 1997 on a new NATO Communications Center at Keflavik Naval Air Station (NAS), Keflavik, Iceland. This was the third such CPS-capable facility to be brought on line at Keflavik NAS. The fourth land-based naval site is found at the Sigonella Naval Hospital in Sigonella, Sicily, Italy. Installation and technical assistance were provided to Sigonella by NSWCCD from 1990 to 1994.⁹ These four shore-based sites all

include the same components as, and are modeled after, the Navy shipboard CPS developed by NSWCCD B53.

The technology developed for shipboard CPS extends beyond the shipboard and land-based Navy installations listed previously. Variations of the shipboard CPS can also be found across the services in transportable CBR shelters, land-based vehicles, liquid oxygen/nitrogen generating plants, and aircraft.

THE FUTURE OF CPS AND NSWCCD'S CONTINUED ROLE

NSWCCD will continue to have an important hands-on role in the advancement of CPS; including both Navy and joint-service interests. Two major advancements currently being undertaken for shipboard CPS are filtration improvements (including alternative filtration methods) and CPS supply-fan redesign.

By designing filters with minimized initial pressure drop and by employing filter regeneration methods, filter service life can be vastly increased. NSWCCD, in conjunction with Army efforts, is developing methods of incorporating commercial technology into the standard 200-CFM HEPA filter design to achieve increased service life goals. NSWCCD is also in the process of providing the Navy with an LP HEPA filter that is expected to increase the service life of the LP HEPA filters by more than 100 percent.¹⁰

While much of the in-process filtration development centers on filter media and assembly configuration, NSWCCD is also investigating methods of providing an economical biological deactivation system for shipboard use. Ultraviolet-light biodecontamination systems are being evaluated for their potential effectiveness in shipboard ductwork applications. This alternative biological agent deactivation approach has the potential to provide a modular, flexible, and cost-effective method of protecting selected ship spaces from biological attacks.

Current CPS supply-fan noise emissions exceed acceptable levels (as defined by the Occupational Safety and Health Administration, or OSHA). In conjunction with fan redesign and development efforts performed by the Naval Surface Warfare Center, Carderock Division, NSWCCD will procure, direct the manufacture of, and install the first prototype of the next-generation vaneaxial fan at the end of FY98. The redesigned, acoustically improved supply fan will provide living conditions that are 10 to 20 dBA quieter for ships' crews. In addition, the fan redesign offers a significant increase in efficiency, resulting in energy savings to the ship. NSWCCD is developing the manufacturability of the new fan such that fan improvements will be realized without a significant procurement cost increase.

The application of variable-speed drive (VSD) motors is also being investigated for future CPS supply-fan implementation. Again concentrating on a theme of cost effectiveness, VSD motors would allow CPS fans to adjust operating speed to specific load conditions. Thus, efficiency is maximized and performance optimized.

As all new-construction ships will include the installation of CPS, the breadth of NSWCCD's contribution to the fleet will be expanded. NSWCCD will direct the planned back-fit of CPS to key areas (such as medical spaces) of amphibious ship classes not already included in the CPS envelope. Possible future consideration may also include CPS application to the fleet's aircraft carriers. Throughout the ascertainable future, NSWCCD will continue to serve as the Navy's technical expert for the development and enhancement of CBR collective protection.

SUMMARY

Collective protection developments engineered by NSWCCD are vital to the sustainability and survivability of U.S. naval forces within a CBR arena. The contribution of CPS to the Navy's CBR defense will increase as new-construction ships are brought into the fleet. By combining joint service research and development efforts with technologies

offered in the commercial and industrial marketplace, effective *and efficient* Collective Protection Systems will remain at the forefront of the Navy's CBR defense program.

REFERENCES

1. Pompeii, M.A. and LaMoy, C.S., *Developmental Testing (DT-III A) of The Collective Protection System (CPS) Aboard the USS Curtis Wilbur, DDG-54*, NDWCDD/TR-94/243, Dahlgren, VA, Dec 1994.
2. Driscoll, D.C. and LaMoy, D.H., "Shipboard Chemical Warfare Agent Detection," *NSWCDD Technical Digest*, Dahlgren, VA, 1996 Issue.
3. *Surface Ship Survivability*, Chief of Naval Operations (N86D), NWP 62-1 Rev D, Jan 1993.
4. *Naval Ships Technical Manual*, Chapter 470, "Shipboard BW/CW Defense and Countermeasures," S9086-QH-STM-000/CH-470, 1 Sep 1991.
5. *Chemical, Biological, and Radiological Defense for Surface Ships*, Chief of Naval Operations (N11), NTP X-00-8201B, 7 Aug 1992.
6. Pompeii, M.A. and LaMoy, C.S., *Developmental Testing (DT-IID) of the Collective Protection System (CPS) Aboard USS Gunston Hall, LSD-44*, NAVSWC TR 91-747, Dahlgren, VA, Jan 1991.
7. *Technical Manual for Navy Shipboard Collective Protection System (CPS), System Description, Operation, and Maintenance*, SS2200-AF-MMM-010, Dec 1992.
8. Culbertson, D.W., *Collective Protection and Cargo Hold Containment/Filtration Systems for the SS Gopher State (T-ACS 4) and SS Flickertail (T-ACS 5) Containerships. Final Report*, Naval Surface Warfare Center, Dahlgren, VA, 30 Nov 1990.
9. Culbertson, D.W., *Installation and Testing of Chemical, Biological, and Radiological (CBR) Filtration System and Inspection of Decontamination Modules for Sigonella Naval Hospital, Sigonella, Sicily, Italy*, NSWCDD, Mar 1994.
10. Sisson, D.W., *Follow-Up Environmental Testing of Limited Protection (LP) HEPA Filters*, NSWCDD/TR-98/25, Jan 1998.

THE AUTHOR

MR. DALE W. SISSON, JR.



Mr. Dale W. Sisson, Jr., joined the Chemical Defense Systems Branch of the Systems Research and Technology Department as a mechanical engineer in May 1997 after gaining 5 years of engineering experience in the industrial sector. A 1992 graduate of Virginia Polytechnic Institute and State University (B.S. mechanical engineering), Mr. Sisson has worked as a project/manufacturing engineer in the bearing industry and as a product design engineer for a world-leading CNC machine tool manufacturer. Mr. Sisson's efforts are currently concentrated in the area of Collective Protection Systems. He also serves as the Navy's representative to the Joint Collective Protection Equipment (JCPE) and the Joint Collective Protection Shelter (JTCOPS) Integrated Product Teams (IPT). As a member of the American Society of Mechanical Engineers, Society of Automotive Engineers, and the National Society of Professional Engineers, Mr. Sisson is a licensed professional engineer.

MAGIC LANTERN DEPLOYMENT CONTINGENCY

Dr. Jack M. Lloyd, Jr.

This article describes the Magic Lantern System, which has recently entered service as the first electro-optic minehunting system to be fielded. This capability is put into its proper perspective as an Air Mine Countermeasures System by examining the history of airborne mine countermeasures (AMCM) capabilities and projects the immediate future of AMCM as it migrates from a dedicated platform/dedicated mission capability to one organic with the fleet.

INTRODUCTION

On Saturday, December 7, 1996, an important milestone in deploying electro-optic minehunting within the U.S. Navy was reached with the Roll-out of the Magic-Lantern-configured SH-2G Lamps Mk I helicopter (see Figure 1). This ceremony marked the formal introduction of electro-optic minehunting into the available suite of AMCM equipments. Presently, the Magic Lantern capability has been provided to HSL-94 to support such AMCM missions as are required.

The existing capability in HSL-94, a Naval Reserve Air Squadron, includes a number of Magic Lantern systems, specially modified SH-2G aircraft, training and tactical aids, and a limited number of system spares. This capability is not fully integrated into the standard Navy supply and support systems; it is a "deployment contingency" capable of providing a much-needed capability to the fleet during the period in which the Airborne Laser Mine Detection System (ALMDS)¹ is undergoing Engineering Development to provide a fully-supported capability to the fleet. This approach, which provides for early availability of important new capabilities for fleet support, is one of the innovative approaches arising from the altered procurement strategies implemented over the last few years.

PRINCIPLE OF OPERATION

Magic Lantern is an imaging lidar system. It transmits a short (order of 10 ns) pulse of blue-green light through an optical train that shapes the beam spatially into a uniform energy density (top-hat) distribution, which is well-matched to the receiver field of view. This pulse propagates through the air to the water surface, passes the surface, and continues propagating into the water column. This is shown in Figure 2, where the location of successive beam

centroids are shown. The receivers, which are gated intensified digital cameras, each are triggered on a separate depth bin. All receivers are boresighted so that they are coregistered on the same laser spot. A receiver that receives reflected energy from a target will show a highlight image, with the target giving a higher energy return than that of the surrounding water. This occurs when the receiver is gated at the depth of a target. A receiver that is gated below a target will not receive the reflected energy from the

each target can be derived to a position whose location accuracy is limited primarily by the inaccuracy in the GPS position. These localization capabilities permit a high degree of precision in later target reacquisition for neutralization.

In normal operating conditions, the primary attenuations suffered by the beam occur at the water's surface—where some energy is reflected, and other energy is scattered—and then in the water,



Figure 1—SH-2G LAMPS Mk-I Helicopter with Magic Lantern Pod Attached

target; rather, the target will obscure the light that would have been returned from the illuminated water volume. This produces a “negative” image, where the detected target will show as a dark spot within the water-return image.

From a knowledge of the gating time relative to the water surface, the approximate depth of the detected target can be determined. Since the location of each laser spot is known to high precision relative to the Global Positioning System (GPS)-derived aircraft position, the geographic location of

where energy is both absorbed and scattered. In order to compensate for the in-water attenuation, Magic Lantern incorporates an automatic gain control that functions independently for each camera, while maintaining the information required to normalize each camera's return to those of the other cameras. Achieving the high degree of accuracy required substantial calibration to ensure that data could be interrelated between cameras. One use for this data is in calculating the system attenuation coefficient. Light is attenuated logarithmically, so that the intensity at a depth z

(more strictly speaking, a slant range z) is related to that just under the surface by $I(z) = I(0) \exp(-kz)$, where k is the system attenuation coefficient. For Magic Lantern, the system attenuation coefficient is very similar to the diffuse attenuation coefficient for the attenuation of downwelling sunlight in water.

was then tested at the Naval Surface Warfare Center, Dahlgren Division (NSWCDD) Coastal Systems Station (CSS) in July of 1988. These tests were executed with the system mounted on an SH-2F aircraft, which was operated by Navy personnel from Rotary Wing Air Test Unit at Patuxent River,

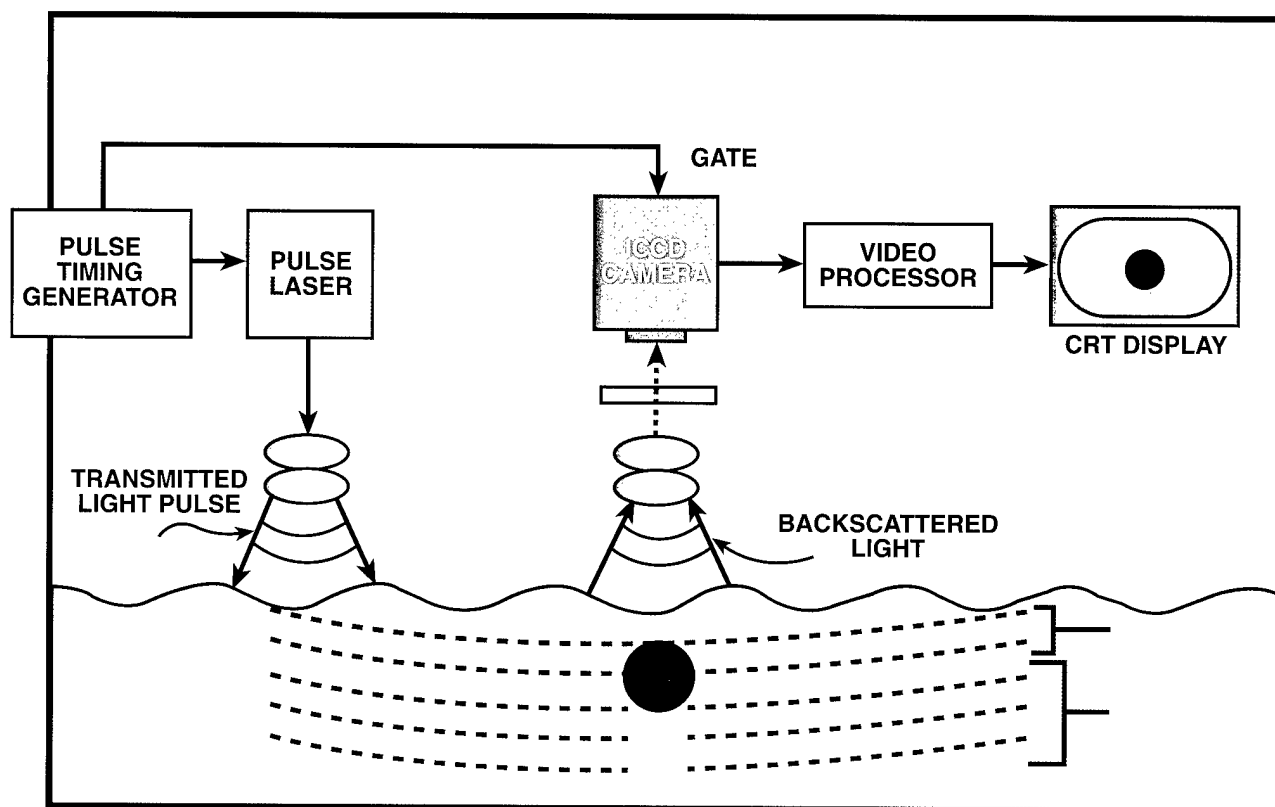


Figure 2—Magic Lantern Principle of Operation

MAGIC LANTERN PROGRAM HISTORY

The Magic Lantern Program began at the start of FY 1988 as a Kaman Aerospace Corporation Independent Research and Development (IR&D) project. Following pier testing of the initial system concept using commercial subsystems, a revised system was fabricated and integrated into a brassboard, which

Maryland, and from the VX-1 Air Test Unit of the Operational Test and Evaluation Force (OPTEVFOR). While this brassboard showed substantial promise by achieving a high probability of detection, and successfully demonstrated the feasibility of the technical approach, various operational limitations suggested that additional development was needed to give the system the overall performance expected of a fielded AMCM system.

The greatest performance drawback to the system at this stage was a very limited swath width, so limited that available aircraft navigation could not ensure that contiguous tracks over an area without unexamined gaps could be achieved. Since the system had achieved successful detection of targets at depths ranging from surface to bottom, it was clear that additional development could result in a much-needed minehunting capability.

Additional development work during FY 1989 and 1990 resulted in useful data gathering in field tests conducted both at CSS and at the Atlantic Underwater Test and Evaluation Center (AUTEC). This process of development, coupled with an increasingly sophisticated ensemble of sea-truth measurements, significantly increased the awareness of the ocean optics differences encountered in the littoral waters in which mine countermeasures operations are conducted from those encountered in the open ocean waters in which antisubmarine warfare (ASW) operations are normally found. In particular, the role of scattering in littoral waters had previously been substantially underestimated as a source of optical signal return. In the process of developing Magic Lantern, it was found desirable to utilize the returned signal to estimate the ambient ocean optical parameters as a measure of probable system performance. This feature was successfully implemented and has become a standard feature of subsequent electro-optic systems.

In late 1990, the Navy directed that the Magic Lantern brassboard, after undergoing certain modifications to improve operability, be fitted-out for operation during Operation Desert Storm. This version, referred-to as ML(30), was then deployed in early February of 1991 to USS *Vreeland* (FF-1068) and operated by personnel of HSL-36. System maintenance and operational support was provided by Kaman Aerospace Corporation. Within a short period of time, ML(30), while searching an area previously examined and declared "safe" by an allied passive electro-optic system, detected an Iraqi-laid mine line. This was the first time an electro-optic system had been used by the U.S. Navy for a successful minehunting mission. Later, the system was transferred to USS *Kidd* (DDG-991), under operation by HSL-34 personnel, where it continued to

operate successfully. The deployment ended in May 1991.

Continued development of Magic Lantern ensued, directed at improving swath width, providing increased area search rate, and replacing components and subsystems with ones that were more robust and fieldable. Improvements included:

- ◆ Incorporation of a scanner to improve swath and area coverage
- ◆ Multiple receivers to improve depth coverage
- ◆ A high-power, all solid-state transmitter
- ◆ Improved processing capability to handle the higher throughput

Concomitant with the higher throughput was the development of an automatic target recognition (ATR) suite to keep operator workload within acceptable limits. Each of these individual improvements represented a significant advance over the previous version; taken together, they provided a very substantial performance improvement. Developmental testing was conducted at CSS in 1994 and, after incorporating changes suggested by these tests, again in 1995. In these tests, the sensor system demonstrated performance that significantly exceeded those contractually specified. As the SH-2F aircraft on which the system was operated was being phased out of the Navy inventory, modifications were taken in hand to adapt the system to operation from the SH-2G. This testing series was rounded out with the conducting of an Operational Assessment, which was also passed successfully, demonstrating the capability on the SH-2G.

OTHER FEATURES AND VERSIONS

The deployed Magic Lantern is augmented by a Tactical Planning and Evaluation Tool, developed by a CSS and Metron, Inc., team, which is used for premission planning and postmission performance analysis and reporting. Additionally, changes in the

aircraft navigation system to permit flying the precision tracks needed for successful AMCM operation have been made. These changes include modification of the AN/ASN-150 TACNAV and addition of a GPS receiver to the SH-2G.

Magic Lantern has also been modified to permit operation from an inboard mounting in an MH-53E. This configuration was operated successfully at CSS, showing no performance degradation over that in the SH-2G configuration.

At Congressional direction, the Magic Lantern design was also modified for operation as a Technology Demonstrator in the surf zone and foreshore regions of an amphibious operating area. These modifications included:

- ◆ Redesigning the receiver to allow a greater area coverage (at the expense of the depth coverage, which is not needed in this operating environment)
- ◆ Providing resolution improvement to accommodate the significantly smaller targets
- ◆ Improving processing throughput

This configuration has also been tested successfully, although the more challenging environment found in the surf zone suggests that additional improvements to deal with adverse conditions would be helpful to make the system more robust in this mission. This result is not surprising, as the original systems design was for a different, somewhat more benign environment, and Congressional direction did not provide for extensive modifications or redesign.

ROLE OF AIR MINE COUNTERMEASURES

To better see how the Magic Lantern Deployment Capability fits into the Navy concept of operations, an appreciation of the overall role of AMCM is needed.

The earliest documented use of minehunting from an airborne platform is a visual minespotting operation conducted by the Italians in 1911. Minespotting, the locating of sea mines by direct visual observation from an aircraft, remained the most usual form of AMCM until after the Korean War. It had been recognized as early as the First World War that if mine countermeasures operations (such as minesweeping) could be conducted from the air that it would be a safer operation than the use of surface craft for such operations. However, it was not until the advent of the helicopter that an airborne platform suitable to the AMCM mission was available. In 1952, an HRP-1 helicopter was equipped with minesweeping gear and successfully tested to demonstrate a capability for sweeping moored contact mines.² AMCM developments continued over the next two decades, at a pace dictated more by fiscal than technical considerations. These developments produced several minesweeping suites for AMCM use, which were employed in Operation End Sweep at the end of the Vietnam War for clearing areas mined by U.S. forces. Since these high-priority developments required all available funding, minehunting development was performance postponed until their completion.

The next advance taken in-hand by the Program Manager (PM) for Air Mine Countermeasures (originally PEO(A)/PMA-210, now PEO(MIW)/PMS-210) was the development of a minehunting sonar. This resulted in the AN/AQS-14 system. CSS has served as the lead laboratory for AMCM developments.

AMCM forces, consisting primarily of two helicopter squadrons, HM-14 and HM-15, serve as the Navy's "first response" mine countermeasures force. These squadrons are capable of deploying to a combat zone within 72 hours, and to begin mine countermeasures operations within seven days of the order to deploy. The designated AMCM helicopter is the MH-53E (see Figure 3), which is capable of operating all AMCM equipments to their full design capability.

In FY 1984, PMA-210 funded CSS to examine the potential of electro-optics as the basis of a minehunting system. This examination showed the

feasibility of such a system, but further development at the time was constrained by lack of funding. This remained the situation at the start of Operation Earnest Will in 1987. During that operation, CSS tested eight separate optical systems and techniques for their performance against moored contact mines, looking primarily at mines similar to the M-08 copies, which represented the bulk of the threat encountered. Of these, Magic Lantern showed the greatest promise for development into a fielded AMCM minehunting system.

step is the identification of a mine-like object as actually being a mine. Once it is determined that a threat mine has been located, the mine is either cleared by standard Navy procedures, or the decision is made to avoid the mined area. This decision is made based on tactical considerations under which the operation is being carried out.

As is documented elsewhere,³ Magic Lantern is quite capable of detecting other things in the water besides mines. One of the development challenges



Figure 3—MH-53E Mine Countermeasures Helicopter

THE MINE DETECTION MISSION

Mine detection, in the sense it has been used in this article, comprises several steps, each more demanding than the previous. First is detection of an object in the water. Next is the determination that the detected object is mine-like; this step is referred to as classification. The most demanding

was the development of robust ATR algorithms and operator aids to correctly classify those objects that were detected as being mine-like. CSS, working in conjunction with Metron and Kaman, developed and implemented the basic algorithms used for this purpose. The very wide range of sizes (for sea mines, from around 12 to more than 40 inches in diameter) and shapes (from spheres to elongated torpedo shapes) made this task much more complex than

would have been required if all mines were the same size and shape. The success of the ATR algorithms in tests against variously sized and shaped mines demonstrates the overall robustness of the software implementation.

ORGANIC AMCM

The 1988 mining of USS *Samuel B. Roberts* (FFG-58) in the Persian Gulf showed the desirability of a mine countermeasures capability that could deploy in conjunction with various Navy Task Groups, which did not provide landing decks for the large MH-53E AMCM helicopters. The advent of Magic Lantern operating on the SH-2G is a first step in realizing such a capability. When followed by the ALMDS mounted on a seagoing H-60 variant, the fleet will have a minehunting capability that will

materially aid in the Navy's execution of the *Forward...From the Sea* strategy.

NOTES AND REFERENCES

1. The name "Magic Lantern" is a registered trademark of Kaman Aerospace Corporation; the Navy program name ALMDS is nonproprietary.
2. Tamara Moser Melia, "Damn the Torpedoes," *A Short History of U.S. Naval Mine Countermeasures, 1977-1991*, Contributions to Naval History #4, Navy Historical Center, Washington, DC, 1991, p. 85.
3. J. Lloyd et al., *Proceedings of the SPIE Conference on Mine Warfare*, SPIE v. 2765, p. 466 (1996).

THE AUTHOR

DR. JACK M. LLOYD, JR.



Dr. Jack M. Lloyd, Jr., received his B.S. in physics from Birmingham-Southern College in 1966, and M.S. (1971) and Ph.D. (1977) degrees in physics from Auburn University. He has been at the Coastal Systems Station since 1979, working in the areas of electro-optics, remote sensing, and related disciplines. He is currently Branch Head for Air Systems Development in the Air Mine Countermeasures Division.

REMOTE MINEHUNTING SYSTEM (RMS) AN/WLD-1

Mr. Guy A. Santora

The U.S. Navy has formed a system development team with mine warfare (MIW) experts at PEO-MIW (PMS407)—the Naval Surface Warfare Center, Dahlgren Division (NSWCDD) Coastal Systems Station (CSS) and Lockheed Martin—to produce the Remote Minehunting System (RMS). The RMS will conduct forward-area reconnaissance well in advance of the arrival of other naval forces, thus providing an early assessment of the threat conditions. The RMS is a high-endurance, offboard, low-observable system, which is launched, operated, recovered, and maintained from a host ship. The host ship will be equipped to perform data processing, display, recording, and mission analysis functions. Processed data will be used to support host ship operations and is passed to the task force for integration into the comprehensive tactical picture.

An operational prototype, RMS (V)1/(V)2, has been developed and demonstrated on board USS John Young, during Exercise Kernel Blitz 95, and on board USS Cushing, during a Middle East deployment with the Kitty Hawk Battle Group. A new RMS vehicle is currently under development by a joint Lockheed Martin/Navy team. Scheduled for completion in early FY99, the new vehicle will utilize the same mine countermeasures (MCM) sensor as (V)1/(V)2, the AN/AQS-14 Airborne Mine Reconnaissance Sonar. The new vehicle supports growth to future MCM system requirements. The AN/WLD-1 system, including the new vehicle and MCM systems, is scheduled for Operational Evaluation (OPEVAL) in FY02 and will meet the full operational requirements for RMS.

INTRODUCTION

The United States' new maritime warfare strategy, articulated in the Navy-Marine Corps policy document, *Forward...From the Sea*, emphasizes the shift away from the open-ocean strategy of the Cold War toward a focus on rapid-response operation conducted *from* the sea. The key to the implementation of this new strategy is the ability of naval forces to conduct *operational maneuvers* in coastal waters. Battlespace dominance, the heart of naval warfare, requires that the operating area be clear of all threats that might be faced in these littoral waters. In these areas, adversaries have the opportunity to concentrate and layer their defenses. Perhaps the most effective defensive weapons of Third World nations are sea mines, which are employed in an effort to "shape the battlespace" and oppose any operation from the sea. Technically advanced mines are readily available at relatively low cost.

MCM capabilities that are beyond the scope of the traditional, dedicated MCM platforms—such as the MCM-1 ship and MH-53E helicopter and their mine-clearing systems—must be developed, and in many cases, these assets are not available to forward-deployed ships or groups. There must be an organic MCM capability to provide surface ships with a self-defense from mines.

The high-endurance, offboard low-observable (RMS AN/WLD-1) is launched, operated, recovered, and maintained from a surface ship (see Figure 1). The host ship will be able to perform data processing, display, recording, and mission analysis functions. Host ship operations will be supported by processed data, which is passed along to the task force to be integrated into the common tactical picture. The system will enable rapid mine reconnaissance from the deep-water region (greater than 200 ft) to the very-shallow-water region (less than 40 ft). RMS, on board a surface combatant, will conduct forward-area reconnaissance well in

advance of the arrival of other naval forces, thus providing an early assessment of the threat conditions. RMS will enable in-theater forces to respond to regional contingencies with a capability to quickly assess the sea mine threat without impacting the primary mission of either the host ship or the task force.

THE PROGRAM

To facilitate the development of the system, the U.S. Navy has formed a Mine Reconnaissance Integrated Product Team (IPT). This IPT, led by PEO(MIW) and consisting of members from PMS407 and CSS, received the Department of Defense/Assistant Secretary of the Navy (DoD/ASN) Award for Acquisition Reform last year. This award was given in recognition of the many acquisition streamlining initiatives achieved by the program. These include:

- ◆ Elimination of the majority of military specifications and standards
- ◆ Extensive use of commercial off-the-shelf (COTS) and nondevelopmental items (NDIs)
- ◆ Use of a Single Acquisition Management Plan (SAMP)
- ◆ An interactive electronic technical manual (IETM)
- ◆ Use of a Website-based electronic data exchange
- ◆ Active contractor membership in the IPT

The IPT employed an evolutionary acquisition strategy that is reducing risk through incremental developments, while fully meeting the requirements of the Operational Requirements Document at an affordable cost.

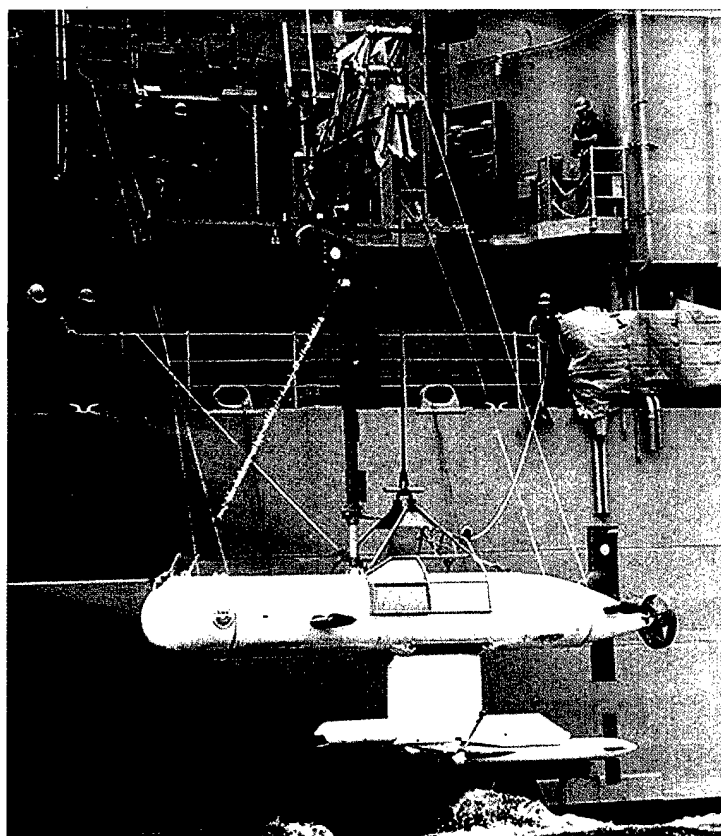


Figure 1—RMS (V)2 On Board USS *Cushing*

An operational prototype, RMS (V)1/(V)2, was developed at CSS to demonstrate the proof of concept and to provide for a contingency system. The system was demonstrated on board USS *John Young* (DD 973) during Exercise Kernel Blitz 95 in March 1995, and on board USS *Cushing* (DD 985), during a Middle East deployment with the *Kitty Hawk* Battle Group in January 1997. While in the Arabian Gulf, the system participated in the Ship's Antisubmarine Warfare (ASW) Readiness Effectiveness Measurement (SHAREM) 119 exercise.

The RMS (V)1 system relied on a shore-based launch and recovery subsystem (L&RS) and was operated by a civilian crew. It was produced through an integration of existing fleet assets with commercial equipment. The semisubmersible vehicle, originally produced by International Submarine Engineering Research, was modified to accept the AN/AQS-14 Airborne Mine Reconnaissance Sonar. Full sonar performance is achievable at mine-hunting speeds of approximately half the aircraft's tow speed. A high data-rate ultrahigh frequency (UHF) link, with a bandwidth of 10 MHz, transmits a full-fidelity, sidescan sonar; forward-looking sonar (FLS); and video to the system operators for evaluation. In this system, the range from the remote minehunting vehicle (RMV) to the mission control and display subsystem (MC&DS) is limited to line of sight (LOS).

RMS (V)2 is an upgrade to (V)1 that focused on improving the operability of the system. Improvements are in three specific areas: L&RS, ship connectivity, and mission analysis. An L&RS system was developed to deploy (V)2 from a *Spruance* class ship. The system utilizes a modified single-arm gravity davit and replaces the boat on the port side of the ship. Building on proven techniques, the L&RS system performs safely and reliably without using offboard personnel (e.g., swimmers or persons in rigid inflatable boats (RIB)). Connectivity is made to the ship's combat information center (CIC) via a remote login over the display local area network (DLAN) Ethernet link to the AN/SQQ-89 ASW system. Specifically, information is shared with the AN/USQ-132 Tactical Decision Support Subsystem (TDSS). Using the TDSS display, the Combat

Systems Officer (CSO) views RMV position and route plans, and locations of any mine-like contacts (MLCs). Mission analysis is enhanced by the addition of several features. Automating contact marking on the AN/AQS-14 sonar console significantly reduced operator workload. A contact data base allows sonar images to be stored digitally, where they can be reviewed and compared in postmission analysis. MIW reports, which are sent off the ship to report the results of an RMS mission, are computer generated.

The Mine Reconnaissance IPT has matured into a Navy/Industry partnership with the addition of Lockheed Martin (Ocean Radar & Sensor Systems, Syracuse, New York) to the team. The initial phases of the contract focused on the development of the RMV. In early fiscal year (FY) 1999, a follow-on contract will be awarded to integrate a new variable depth sensor (VDS) package (which will replace the AN/AQS-14 sonar) to the system and also integrate the system to an *Arleigh Burke* class destroyer (DDG 91).

THE SYSTEM

The RMS comprises six major subsystems that include:

- ◆ RMV
- ◆ L&RS
- ◆ MC&DS
- ◆ Maintenance support subsystem (MSS)
- ◆ Transportation support subsystem (TSS)

See Figure 2.

The RMV is a diesel-powered semisubmersible containing the mine reconnaissance sensors; navigational, guidance, and control equipment; and sensor data-processing computers. The navigation system utilizes the military P(Y) code Global Positioning

System (GPS). The RMV automatically follows predetermined waypoints for transit and mine-hunting tracks. It can also be manually controlled for near-ship operations. An ahead-looking sonar and a mast-mounted camera provide for obstacle avoidance.

The RMV being developed by Perry Technologies, Riviera Beach, Florida, is 23-ft long and 48 in. in diameter. It weighs approximately 14,000 lb fully fueled. Powered by a 370-hp marine diesel, the RMV carries enough fuel (DFM or JP-5) for extended operations. A highly efficient, low torque pump jet propels the RMV. With 13 preswirl stators and 16 rotor blades turning at 250 rpm, the propulsor achieves 85 percent efficiency—considerably higher than conventional boat propellers. The hull is a modular design that contains five separate sections: propulsion, winch and capture, fuel, electronics, and nose. The forward nose section contains the FLS used for volume mine detection and obstacle avoidance. A 50-ft³ electronics module contains all

vehicle processors and electrical equipment. Additional volume is reserved for future electronics.

The vehicle runs at a nominal distance below the sea surface, where “wave-making drag” is at a minimum, and the surface sea state has little effect on RMV motions. This provides a high-speed, high-endurance, and high-stability platform towing the MCM sensor(s). The surface-piercing mast provides for both air intake to a diesel engine, as well as a platform for the communication link antennae. The RMV has the ability to operate autonomously with no communications or via one of two data links. These data links provide a reliable, real-time data exchange between the RMV and the system operators, and allow for rapid assessment of the area being searched. An LOS UHF data link is used for L&R and near-ship operations, and a high-frequency (HF) or satellite data link for over-the-horizon (OTH) operations can provide real-time communications. An onboard mission and sensor data recorder is provided as a backup to the data

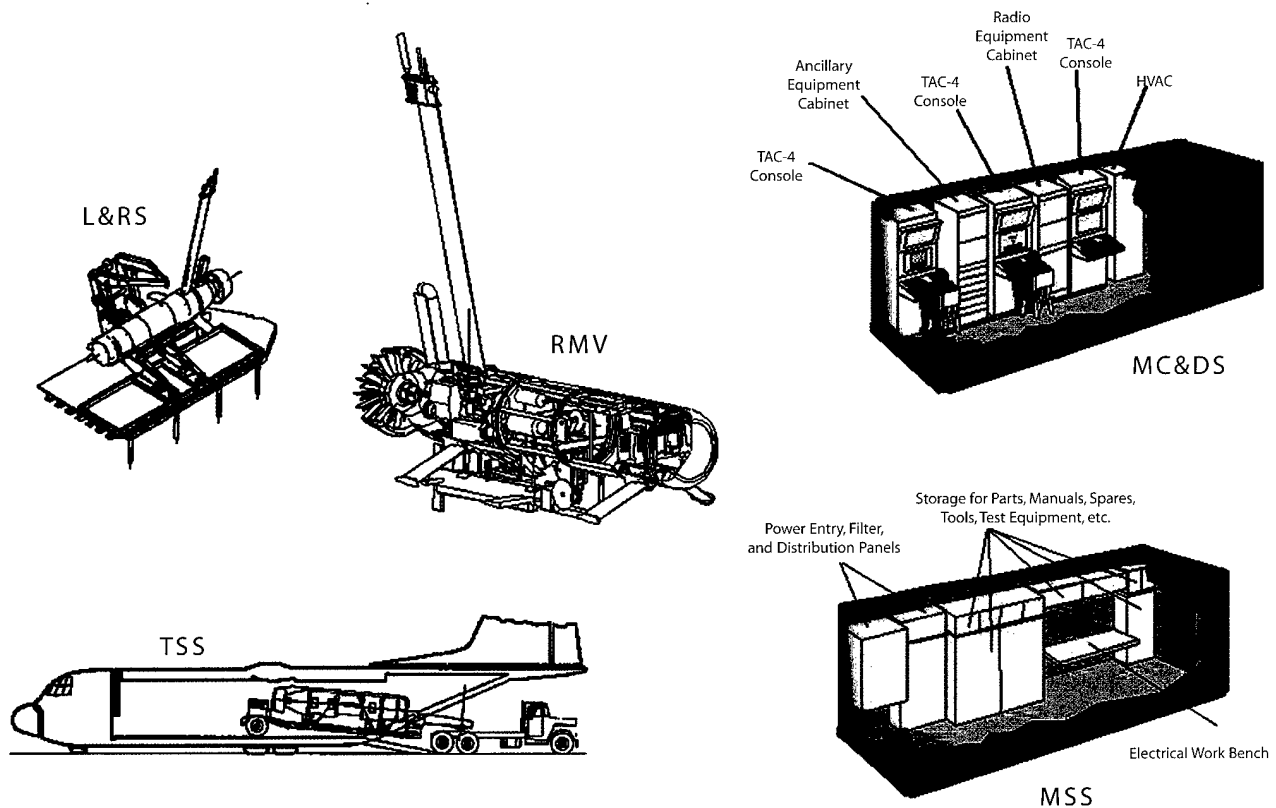


Figure 2—RMS Subsystems (Modular Version)

links and for the autonomous mode. Multiple operating modes and states, redundant sensors and systems, and autonomous fail-safe processing for various conditions provide flexibility and minimize impact to ship operations. The system will attempt to mitigate conditions like high engine temperature in order to continue the mission, and in the event that it is unsuccessful, will abort the mission and endeavor to exit the minefield area and return to a recovery point in safe waters. If the ship cannot immediately recover the RMV (in either a casualty or noncasualty condition), it can place itself in standby states to conserve fuel and maintain its position.

A variable depth capability is provided to the MCM sensors by a hydraulic winch within the RMV. This allows the VDS to optimize their performance against specific mine types within the acoustic environment. The VDS is an actively controlled tow body with automatic depth or altitude control. Acoustic sensors provide coverage of the full water column for detection and classification of MLCs. An electro-optic (EO) sensor is used for identification of MLCs as a mine or nonmine. The VDS relies on computer-automated detection and classification to determine the presence of an MLC that must be identified with the shorter-ranged EO sensor by reacquiring the contact.

The MC&DS contains all mission planning and analysis equipment; and system processors, controls, and displays. The MC&DS is an 8- by 20-ft van containing three identical Tactical Advanced Computer consoles (TAC-4s). Used for system control and data processing, recording, display, and mission analysis, these consoles have common functionality and operator tasks, and can be tailored to specific mission requirements and operator skill levels. The system is designed to maximize commonality with the AN/SQQ-89 ASW system, and the console operator machine interface (OMI) is based on the AN/SQQ-89 style guide. The MC&DS is connected to the host CIC via the AN/SQQ-89(V)6 DLAN, which is used to communicate with TDSS. Data exchange with TDSS is in the form of RMV position, contact reports, and mission plans from RMS to TDSS, with the common tactical picture provided by TDSS to RMS. TDSS also provides connectivity

to offboard communications by formatting and transmitting position and contact reports to the Joint Maritime Command Information System (JMCIS).

On board the AEGIS destroyer, this function will be performed within the AN/SQQ-89 ASW Combat System. The RMS will use two AN/UYQ-70 consoles in the Sonar Control Room and the Computer-Aided Dead-Reckoning Tracer in CIC for these functions.

The L&RS consists of:

- ◆ An RMV cradle
- ◆ Overboarding gear (davit and winch)
- ◆ Kingpost and boat boom
- ◆ Associated winches and control systems

The overboarding gear is being developed by Lake Shore Incorporated, Iron Mountain, Michigan. The L&RS is capable of launching and recovering the RMV with no in-water personnel.

Twenty months into development, the program is well on its way to placing another "arrow in the quiver" of the expeditionary warrior. A prototype RMV underwent hydrodynamic testing at the Perry Technologies facility, which proved the vehicle, propulsor, and control system design. Prototype testing has demonstrated that the RMV will meet or exceed all requirements. The overboarding portion of the L&RS recently passed factory acceptance testing at the Lake Shore facility, where the unit was operationally certified under static and dynamic-load conditions. The program to deliver the fully capable system to an *Arleigh Burke* began in earnest this year with the development of a system specification.

The transition to AN/WLD-1(V)1 is highlighted by two major events: the integration into the AEGIS ship, DDG 51 Flight IIA, and the insertion of the next-generation sensor technologies that will

dramatically increase the minehunting effectiveness of the system. For effective mine reconnaissance and to minimize ship delay time, increased coverage rates and high-resolution sensors are required. These sensors must be able to cover the full water column, and perform detection (POSMINE) and classification (PROBMINE) for both volume and bottom mines in a single pass. AN/WLD-1(V)1 will be capable of coverage rates as great or greater than is achievable with current MCM sensors. Aside from sonars, EO sensors will be employed to perform identification (CERTMINE). A second pass will likely be required for identification due to the short effective range of these sensors, relative to sonars.

ADVANCED SENSORS

The Advanced Sensors are a result of a long development effort carried out by the Office of Naval Research (ONR), for which the ultimate objective is to create mine detection capabilities for use on platforms like AEGIS Flight IIA and the DD 21. Sea mine reconnaissance and hunting pose notoriously challenging technology problems due to the size of areas being searched, the small sizes of mines, the acoustically reverberant environment,

and the frequent occurrence of acoustic or magnetic clutter. To address this technology challenge, ONR established a robust exploratory development effort that will yield sensor designs and technologies directly applicable to the RMS next-generation sensor suite.

Acoustic minehunting sonars are active sonars that can be divided into detection sonars and classification sonars. As seen in Figure 3, the sonars cylindrically project around the axis of the vehicle, out to the side, or ahead. Detection sonars are generally characterized by very large ranges (several hundred meters) and by many narrow receive beams, so that as small an area as possible is illuminated to minimize reverberation returns. The mine generally subtends an angle much smaller than the angular widths of the beams, so no shape information is gleaned (hence the descriptive term "detection sonar").

On the other hand, classification sonars are imaging sonars that typically have a many-element line array producing one vertical beam and many horizontal beams along the length of the array. They generally are used in the near-field of the array,

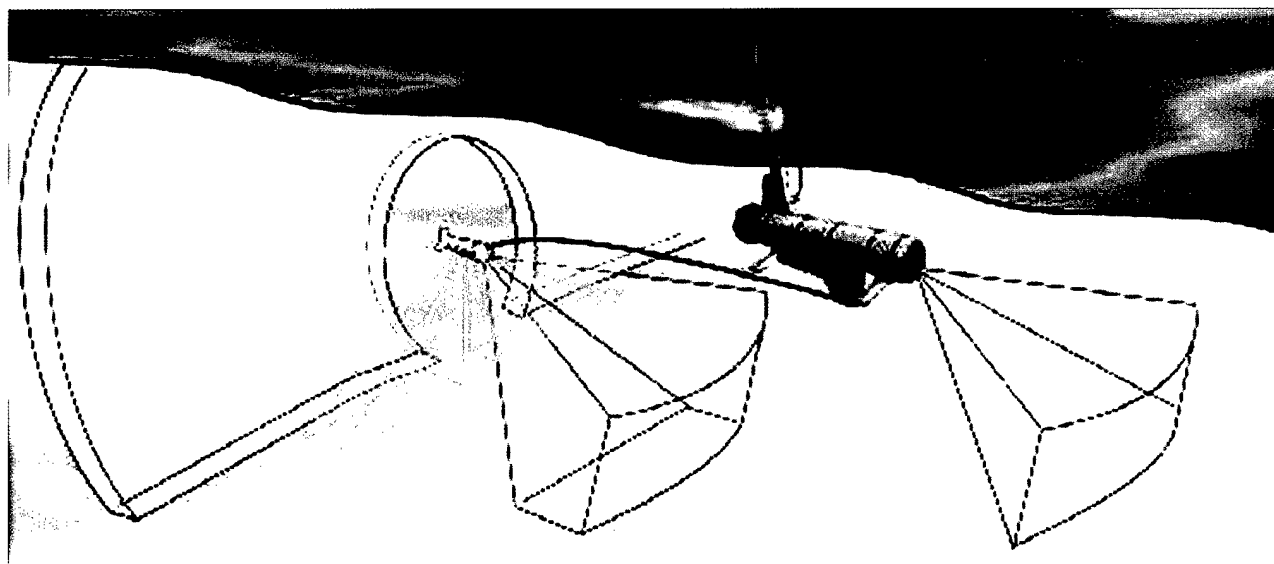


Figure 3—Sonar Projection Schemes

where the resolution in the azimuthal direction (along the length of the array) is constant. The ranges of real-aperture imaging sonars are typically 150 m or less (ranges are limited by practical constraints on array length), and resolution is typically 20 cm or larger. Synthetic-aperture imaging sonars, on which CSS began development in the 1970s, can have very large ranges and very high resolution. Classification sonars can be either ahead-looking, real-aperture, or side-looking real- or synthetic-aperture sonars (SAS).

Optical mine sensors for MIW range from simple camera systems that rely on natural light or floodlights for illumination to sophisticated range-gated and laser line-scanning sensors (LLSs). The ranges of these sensors run from about one optical attenuation length for the simple camera-based systems, to five or more attenuation lengths for the LLSs. (Attenuation lengths can vary from 1 m or less at murky very-shallow-water sites to 5 m or more at deep-water sites.) The resolution deteriorates with increasing range, but typically, 1-cm resolution or better can be obtained. Resolution of this size provides an excellent identification capability.

The ONR exploratory development program has systematically pursued development of the most capable technology within reach in each of these areas. A wide variety of contractors with specialized capabilities and skills have been used.

TOROIDAL VOLUME SEARCH SONAR (TVSS)

The principal sensor in the suite, designed for deep water, is the TVSS. The TVSS encircles the underwater sensor body. It is a long-range, medium-resolution search sonar designed to detect all targets located in the water column.

The TVSS, seen in Figure 4, is the first minehunting sonar ever built with a toroidal geometry. It is designed to form 120 three- by three-deg conical beams and provide a 750-yd detection range (1,500-yd swath width) against volume and close-tethered mines in water depths as shallow as 60 ft. The 120 beams are formed simultaneously to provide 360-deg coverage on each ping. Because the signal-to-noise ratio (SNR) is greater than 15 dB for the range of interest, the TVSS produces a very high

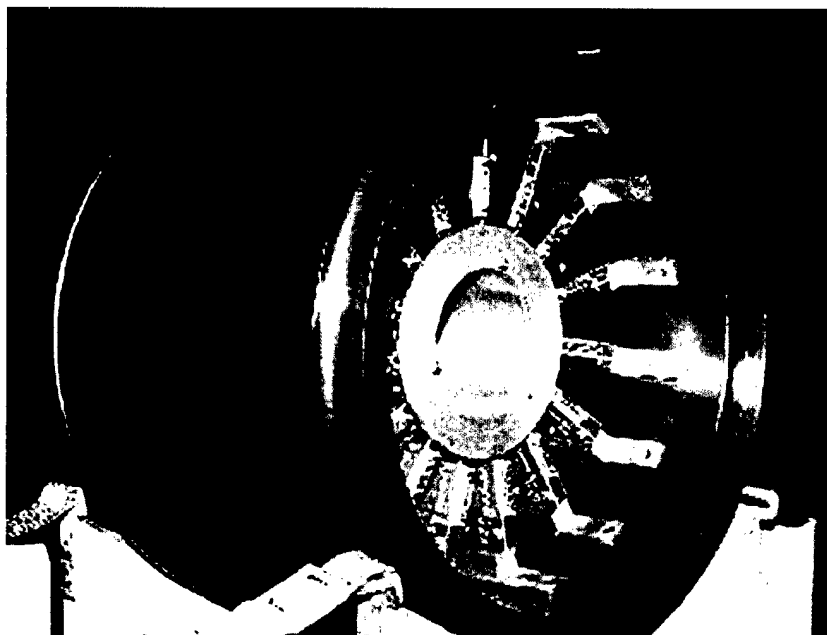


Figure 4—Toroidal Volume Search Sonar

single-pass probability of detection (P_d), thus eliminating the need for multi-ping integration to improve SNR.

The length of the TVSS arrays is 29.94 in.. The projector consists of 32 staves (1.94 by 12.06 in.) spaced on 11.25-deg centers. Each staff comprises four bizonally wired elements (1.94 by 3.25 in.), which sum to give a nearly omnidirectional transmit beam in the roll plane and a 3.7-deg beam in the pitch plane. Raytheon fabricated the projector array. The receive array, also fabricated by Raytheon, is a ceramic array with 120 individual elements spaced on 3-deg centers. The array was constructed from traditional ceramic material.

Extensive sea testing of the TVSS used motion compensation techniques to minimize the adverse effects that even small amounts of motion can have on the data, especially in shallow water. In deep water, the nonmotion-compensated 3-deg beam, regardless of the signal transmitted, exceeded the performance requirements. Because of this, deep-water performance was determined based on the 3-deg and the gated, continuous wave (CW) signal, which is the simplest configuration. A 2-deg beam, formed by a newly developed algorithm employing the entire aperture and neglecting errors due to cylindrical array geometry, with a linear frequency modulation (FM) transmit signal and motion compensation, performed the best in shallow water.

Advanced signal processing and beamforming techniques to improve the signal-to-reverberation ratio (SRR) in shallow water will be incorporated as they become available.

SIDE-LOOKING SONAR (SLS)

The SLS is a sonar capable of very high-performance and high-speed minehunting of mines on the sea bottom. The SLS will provide a 200-yd detection range (400-yd swath width) against close-tethered and bottom mines. Its very high spatial resolution (8 by 8 in. at 200 yd) will provide a minimum of 5 pixels/yd in both cross-track and along-track directions for all ranges. Its 30-dB

side-lobe suppression and 15-dB SNR will provide high-contrast imagery and improve detection and classification performance.

One SLS receive line array consists of 38 ceramic elements centered 4 in. apart. The array is 12.5 ft in length. The central operating frequency of the SLS is 400 kHz. Theoretical pixel resolution is 4 by 4 in. out to 100 yd. Northrop Grumman Oceanic Systems (NGOS) developed the SLS. During initial at-sea testing in FY97, raw data was collected and passed by high-speed fiber-optic data communication link to a tow vessel and an Ampex digital recorder. In operational situations, an embedded computer will process the sonar data, and detections will be forwarded to the surface for evaluation.

The development approach to the SLS and the TVSS has been to design and fabricate highly capable and flexible (research-oriented) system hardware and then to use the comprehensive data set collected during sea testing to develop sophisticated sonar signal processing and beamforming algorithms that maximize the overall system performance. Based on previous experience, it is anticipated that separate sets of algorithms will be required to maximize system performance for significantly different operational environments. A preliminary set of sonar signal processing and beamforming algorithms is being developed and used to determine a baseline system performance capability.

Unlike any previous sidescan sonar of similar general design and size, the SLS receive channels are all fully bandwidth sampled. This makes the SLS a complete research tool for experimentally investigating target classification performance as a function of resolution, real aperture versus synthetic aperture, beamforming schemes, motion-compensation techniques, etc. In real-aperture mode, the best achievable azimuthal resolution of the SLS in 10 cm is out to a range of 90 m, and this increases linearly to 20 cm at 180 m. In synthetic-aperture mode, the best achievable resolution is 5 cm out to the full 180-m range. As a research tool, the SLS will be used to conduct critical experiments that would provide a much-needed understanding of the relationships

between sonar beamwidth (resolution), sidelobe level, signal bandwidth, signal design, beamforming, spectral averaging, motion compensation, image quality, image statistics, P_d , P_c , and other sonar performance parameters.

SYNTHETIC-APERTURE SONAR (SAS)

Synthetic-aperture techniques can be applied to SLSs to achieve greater ranges and/or higher resolution. The SAS sonars developed under the ONR program are shown in Figure 5. They are a combination high- and low-frequency SAS (HF/LFSAS), with operating frequencies of 180 kHz and 20 kHz, respectively. The HFSAS has a linear array of 11 piezo-rubber receive elements, each 5-cm long for 2.5-cm azimuthal resolution. The ceramic HFSAS projector has a 30-kHz bandwidth for 2.5-cm range resolution and is located near the center of the receive array, which research has shown is the optimal location for motion compensation using autofocusing techniques. The LFSAS has a linear array of 16 piezo-rubber receive elements, each 3.75-cm long (this is half a wavelength at 20 kHz), that allows for beam steering through one

radian. The ceramic LFSAS projector has a 10-kHz bandwidth for 7.5-cm range resolution, which matches the LFSAS azimuthal resolution and is located forward of the receive array. (The LFSAS is motion compensated by the HFSAS, which is capable of more accurate motion estimates.) The 21-in. section in which the sonar is housed is 90-cm long. The sonar consumes less than 400 W of power.

The HF/LFSAS has a range of 40 m and an area search rate (ASR) of 0.32 nmi²/hr at 8 knots. The range and ASR would be larger if the array was longer. The HF/LFSAS receive channels are all well oversampled at 160 kHz. With the development of new projector technology, this allows for a large planned increase in the bandwidth of the projectors.

The LFSAS's 20-kHz, bottom-penetrating operating frequency, its very large horizontal beamwidth and resultant novel multiaspect capability, and its high-resolution promise excellent performance against buried as well as proud and volume mines. The HFSAS provides sufficient resolution to provide a near-identification capability. Its higher operating frequency will produce better shadows of proud mines than the LFSAS and

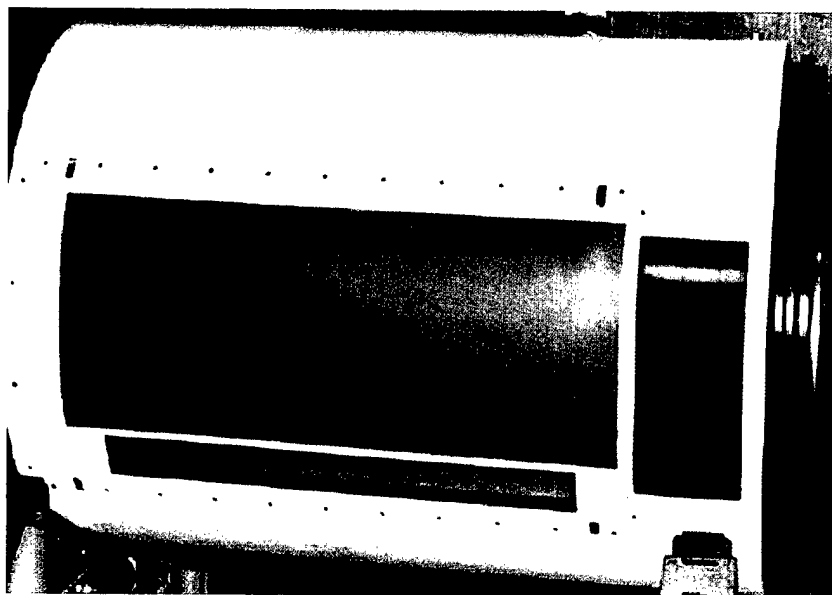


Figure 5— Synthetic-Aperture Sonar

will also produce complementary shape information from returns directly off of mines or mine-like objects, when their specularly makes shape determination from direct returns difficult.

ELECTRO-OPTICS IDENTIFICATION (EOID) SENSOR

The EOID Sensor provides high-resolution (6 mm), long-range (five optical attenuation lengths) performance in a 21-in. section only 81-cm long, consuming only 285 W of power.

The sensor uses a CW blue-green laser to illuminate a small spot that is synchronously scanned by a photomultiplier receiver to build up a raster-scanned image, as shown in Figure 6. It represents an enormous improvement in performance over the simple optical systems that have been used for mine identification in the past.

The sensor's field of view is 70 deg, which is augmented by a rotator mechanism that can turn the sensor to the left or right side, producing a field of regard of 130 deg.

The EOID sensor's relatively long viewing range is especially valuable, as it greatly reduces the positional accuracies required in the difficult target reacquisition process. The enhanced range will also increase the security of the package when viewing an explosive device.

Technologies developed under these ONR programs will begin transition into the RMS program this year. These technologies will be applied to previously demonstrated sensors to provide a low-risk sensor solution for RMS.

Because of the high coverage and high resolution of these sensors, a tremendous amount of data reduction is required to bring the data rates down to manageable size. AN/WLD-1(V)1 will rely on advanced data processing, and data reduction and compression techniques, and extensive use of computer detection and computer-aided classification (CD/CAC) algorithms. On board the RMV, real-time processing will be incorporated to automatically select contact images to be transmitted and presented to the operator for verification. In this fashion, real-time, OTH reconnaissance operations can be achieved.

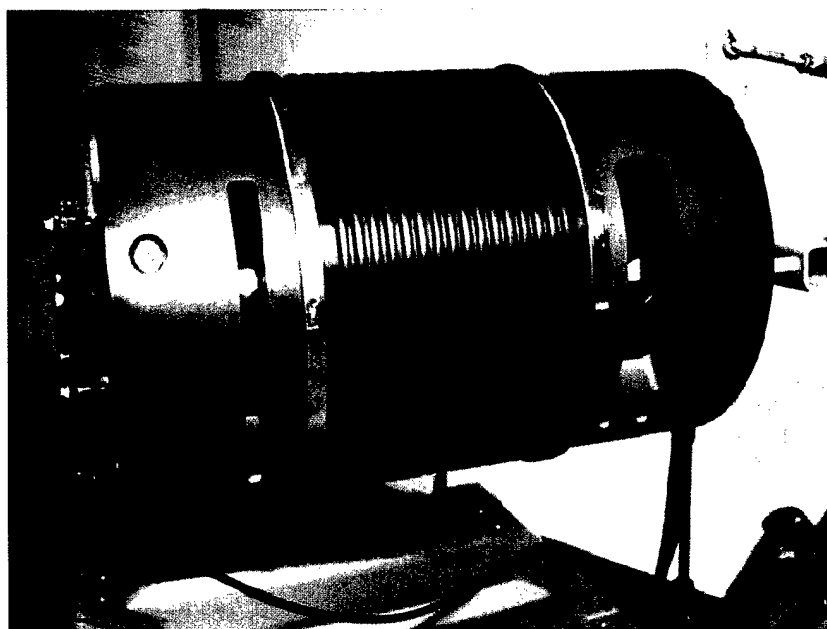


Figure 6—Electro-Optic Identification Sensor

Human operators of the RMV will reside on a host ship. The RMV will communicate with the ship via a radio link capable of transmitting digital data. There will be little sensor data processing on board the host ship. The bulk of the automatic data processing on the acoustic and magnetic data will be performed in the embedded computer within the RMV and sensor body. The contacts deemed to be mine-like objects will be transmitted to the ship with their positions. The EOID data will be transmitted directly to the ship and processed both automatically and by personnel on the ship. The final mine declarations will subsequently be furnished to the task force.

AEGIS

The AN/WLD-1(V)1 system is targeted primarily for installation on DDG-51 Flight IIA ships (see Figure 7). The MC&DS is eliminated, and its functions will integrate with the AN/SQQ-89(V)15 ASW combat system. RMS will share the use of the

AN/UYQ-70 ASW acoustic display consoles. The Recon IPT has been working closely with both the ship designers and builders to integrate RMS with the next procurement of *Arleigh Burke* class ships.

Due to radar-cross-section (RCS) requirements of this ship, the RMV installation design has the vehicle within the skin on the ship. The location is the starboard side where the aft RIB is currently located. The displaced RIB will be located forward and stacked above the forward RIB. A separate, environmentally controlled, maintenance area is immediately aft of the RMV that provides facilities for maintaining and repairing the VDS and RMV. For the remainder of the installation, equipment will occupy existing ship spaces. The RMS telemetry links—consisting of the OTH receivers and exciters, and the LOS radio with encryption gear—will occupy one standard equipment rack in the communication center. The OTH link will interface with the AN/URC-131 and use existing ship antennas. RMS command and control is provided through the AN/SQQ-89(V)15. Existing AN/UYQ-70 consoles in

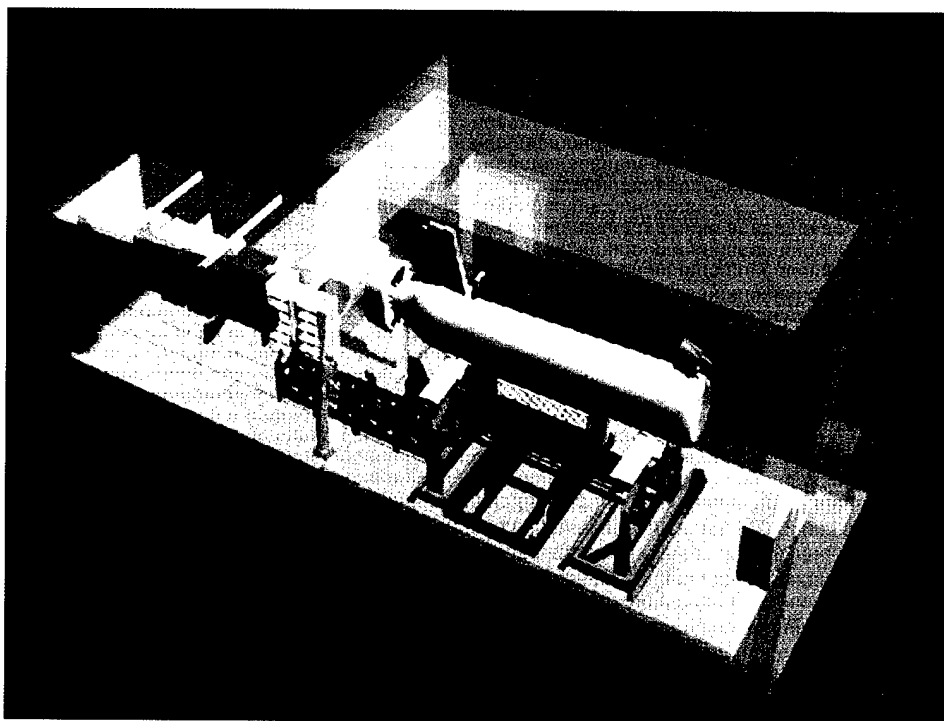


Figure 7—RMV Installation on DDG 91

the sonar control room will be used. Up to two of these consoles may be used for intensive missions but can be reduced down to one console, or even none at all, with the RMV in the autonomous data recording mode.

THE MISSION

The RMS versions have evolved systematically from the proof-of-concept devices of RMS (V)1 and (V)2, to the new (V)3 RMV, to AN/WLD-1(V)1, which will fully meet the fleet's long-term requirements. Figure 8 graphically depicts how this type of

system will provide a substantial enhancement to the safety of ships. In the study, whose results are shown in this figure, two ships are assumed to be conducting ASW operations in an area that may be mined. Whether the threat is bottom or moored mines, it has been found that the ships could not survive using only onboard systems, even the Advanced Mine Detection System (AMDS). AMDS is a hull-mounted, HF, small-object-detection sonar designed for the new-generation surface combatants. Since onboard systems cannot detect every mine, and ships must make multiple passes through the minefield, the undetected mines would soon strike the ships.

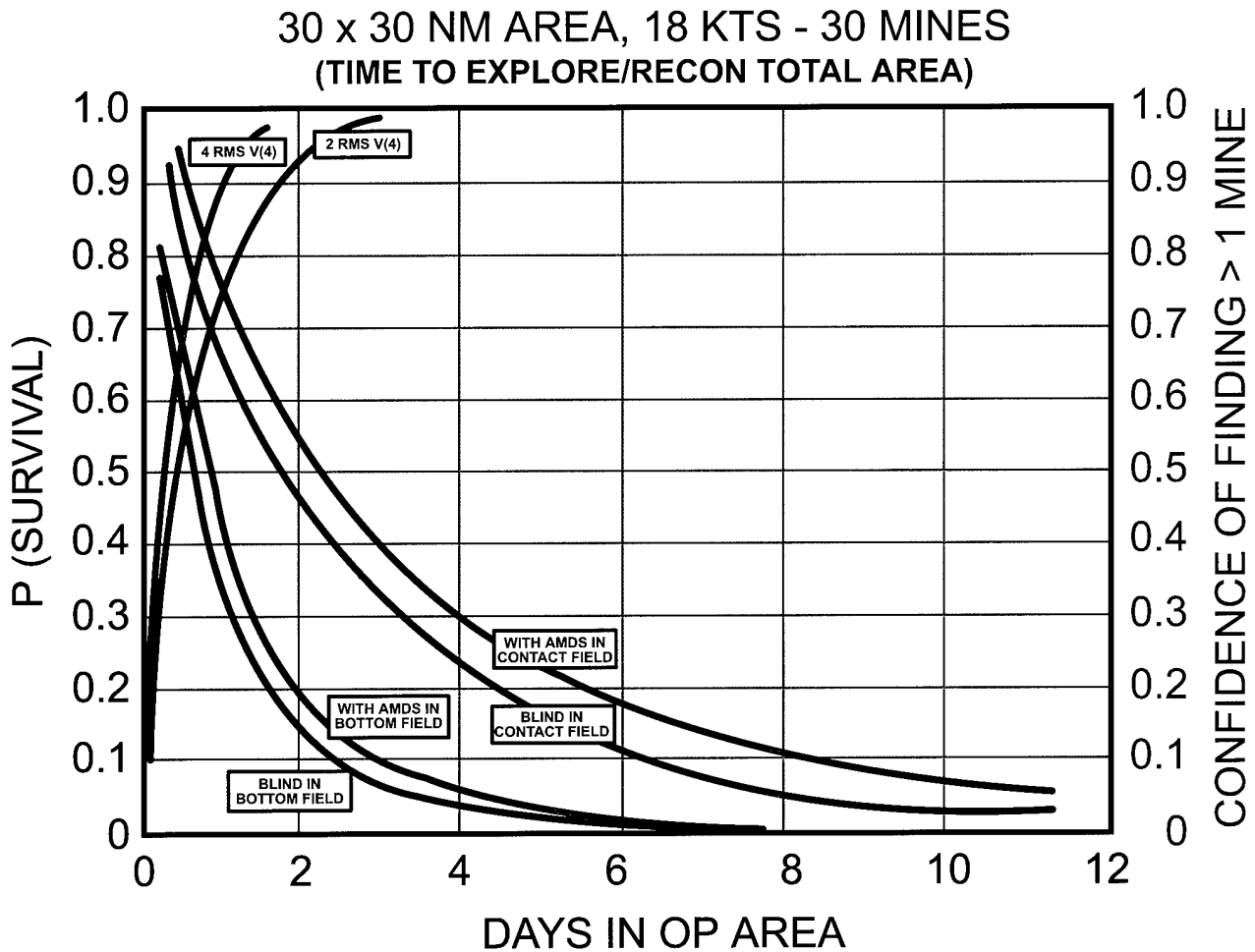


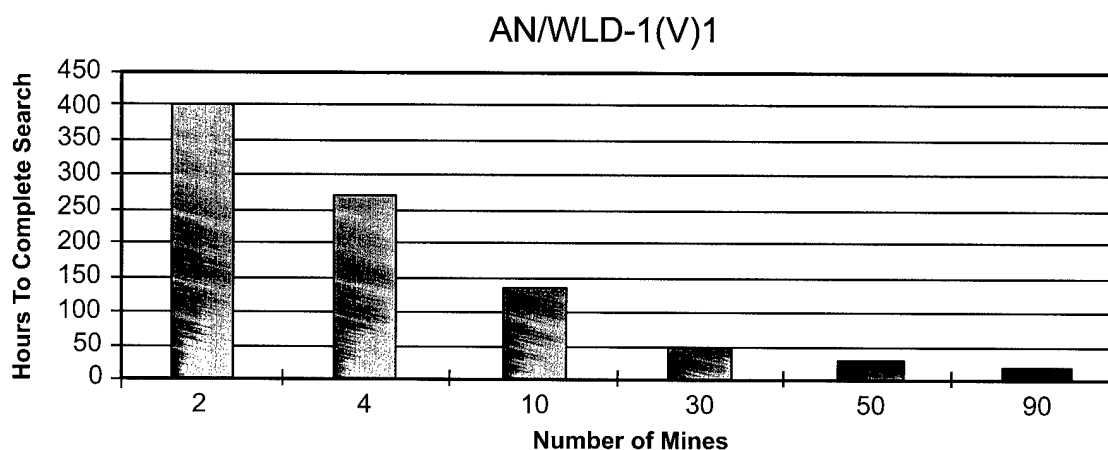
Figure 8—Survival Probabilities Vs. System Types for DD-21 ASW Sweep

The offboard sensors, such as those employed by the RMS can, however, be used to conduct reconnaissance of the area, detecting and identifying mines before the ships enter the area. If the area is found to be not mined, the ship can move in to conduct the ASW sweep, with little chance of encountering a minefield. If mines are discovered, the ships can stand off until mine clearance assets arrive.

Figure 9 presents the time required for the RMS to search the 30- by 30-nmi area in this scenario for several densities of mines. As a rule, the more mines that are present, the shorter the time it takes to determine that the area has been mined. Even assuming a very low threat density of one mine per nautical mile (30 mines total), it would take less than 52 hours to search the area to a 95-percent confidence level; i.e., if a number of mines had been there, at least one would have been detected.

CONCLUSIONS

MIW presents a most severe threat to operations of the Navy. It is the only threat capable of stopping naval operations that is within easy technical and financial reach of all potential adversaries, regardless of their size. Therefore, it must be assumed that in any future conflict, the Navy will encounter numerous and advanced mines, whatever their specific assignment. As discussed in the system descriptions, no one system is totally effective against all threats. For example, airborne EO systems are good against mines at or very near the surface, where sonar system performance is poor at significant sea states. Likewise, sonars are excellent for the detection and classification of other moored and proud bottom mines. A combination of systems is required to provide a high level of safety to a ship or battle group.



2 AN/WLD-1(V)1 vs. Bottom Mines

4 NOMBOs nmi²
5 Min to ID MLCs

Search Pattern Will Find, to a 95% Assurance,
at Least One Mine of Given Minefield

Figure 9—Time Required to Complete Search

THE AUTHOR

MR. GUY A. SANTORA



Mr. Guy A. Santora received a B.S. degree in oceanographic technology from the Florida Institute of Technology in 1980 and an M.S. degree in aerospace and ocean engineering from Virginia Polytechnical Institute and State University in 1985. He has been employed at CSS since 1983. He has served as project engineer on the Remote Minehunting System (AN/WLD-1) since 1990. Mr. Santora has been a leader in the Navy's efforts to mainstream mine countermeasures and put organic MCM capabilities in the Surface Fleet. He has been awarded the Navy Meritorious Civilian Service Medal for his efforts and the Bronze Medal Award from the American Defense Preparedness Association (ADPA), specifically for leading the Remote Minehunting Program.

UPGRADING THE FLEET AN/PQS-2A DIVER-PORTABLE SONAR

Dr. Joseph L. Lopes

Presently, military divers use the AN/PQS-2A audio output, handheld sonar to hunt for and locate underwater objects such as mines. Recently, the sonar was upgraded by integrating a spectral processing computer with the sonar. The computer is used to create a video representation of the sonar's audio signal. Thus, the upgraded AN/PQS-2A provides sonar operators with a combined audio and visual detection capability. This article presents a description of the hardware and software used to develop prototype units. Examples of the spectrally processed data that are displayed to the operators are illustrated. The importance of providing the sonar operator with a combined audio plus visual detection capability is described.

In addition, the AN/PQS-2A target echo backscatter discrimination capability is discussed. Lastly, the results of this work, including transitions to the fleet for testing and evaluation, civilian usage, and fleet diver recommendations for improvements, are presented.

INTRODUCTION

In performing their missions, Naval Special Warfare (NSW), Explosive Ordnance Disposal (EOD), and Marine Corps divers have the responsibility to detect, classify, localize, and identify underwater threats. The underwater threats are usually either moored or bottom sea mines. Presently, Navy divers conduct their missions using the AN/PQS-2A, aural output, diver-portable sonar. This sonar produces a long, continuous transmission of a frequency-modulated (CTFM) sinusoidal signal. The diver detects a target by horizontally sweeping the sonar while listening for a tone generated at a frequency that is obtained by multiplying (or mixing) the transmitted pulse with the backscattered signal. This detection scheme is completely dependent on the diver's ability to discern the characteristics patterns in the sonar's aural output. Performance has been found to depend strongly upon diver training and experience.

Issues associated with performance of the AN/PQS-2A have been addressed in two efforts sponsored by the Office of Naval Research (ONR) under the NSW Technology Program and conducted at the Naval Surface Warfare Center, Dahlgren Division (NSWCDD) Coastal Systems Station (CSS) in Panama City, Florida. In the first effort, improvements in detection

performance were obtained by modifying the AN/PQS-2A sonar. Modification consisted of using a computer to spectrally process the aural signals such that sonar operators were able to view a video representation of the sonar's audio output on a display. Thus, the upgraded sonar provided operators with a combined audio and visual detection capability. In the second effort, the target echo backscatter discrimination capability of the AN/PQS-2A was explored. Such discrimination would enable a sonar operator to determine if a contact was mine-like or not, thereby providing an improved classification capability.

A summary of these two efforts, as well as related topics, are described below. This article is organized as follows:

- ◆ In the first section, a description of the upgraded sonar's instrumentation is provided; this description also includes a discussion of the background operation of the AN/PQS-2A sonar.
- ◆ The second section provides a description of the method to create a video representation of the audio signal.

- ◆ In the third section, examples of the images displayed to divers are illustrated.
- ◆ The fourth section highlights the importance of a combined audio plus visual detection capability.
- ◆ In the fifth section, the AN/PQS-2A target echo backscatter discrimination capability is discussed.
- ◆ In the final section, the results of CSS efforts, including transitions to fleet for testing and evaluation, civilian usage, and fleet diver recommendations for improvements, are presented.

UPGRADED AN/PQS-2A SONAR INSTRUMENTATION

Figure 1 illustrates a diver with a prototype of an upgraded AN/PQS-2A sonar. The prototype unit consists of a leak-tight canister (6-in. diameter, 12-in. long) attached to the AN/PQS-2A sonar by a pair of mounting brackets. The audio bulkhead connector of the sonar has been changed such that the sonar's audio signals are cabled to off-the-shelf



Figure 1—Diver Outfitted with Upgraded Sonar

electronic instrumentation packaged inside the attached canister. The electronic instrumentation consists of a computer system with a small color monitor, and a tilt-and-compass sensor. A description of the components composing the instrumentation, as well as a brief discussion of the operation of an AN/PQS-2A, are provided below.

The AN/PQS-2A sonar has a transducer face consisting of an inner circular section and an outer ring, which is concentric with the inner section. The inner section is used as the projector, while the outer section is used as a receiver. The sonar transmits a CTFM pulse with a frequency bandwidth of about 30 kHz. The pulse length of the CTFM signal is either approximately 0.3, 0.9, or 1.8 s corresponding to either the 20-, 60-, or 120-yd range scale setting of the sonar, respectively. This sonar relies on the fact that the backscattered return from a target is coherent, which implies that a target echo return replicates the transmit signal in frequency over the pulse length. The sonar then electrically processes acquired data by multiplying the transmit signal with the backscattered return, thereby producing a signal with a difference frequency component. This

difference frequency component is amplified and then cabled via a volume control knob to the diver's headset. The diver perceives this signal as an audible tone.

The sonar operator may estimate the range of a backscattered return by noting the frequency component of the tone. This point can be understood using the graph in Figure 2, which depicts sonar bandwidth frequency versus ping time for transmit and receive signals. A return from a target will begin at a particular ping time, which will correspond to a particular difference frequency signal or tone. If the target was at a different range, then the start of the receive signal will arrive at the sonar at a different ping time, which in turn, will change the difference frequency component. Thus, by listening to the frequency of a tone, an operator using the AN/PQS-2A may estimate the range of a target.

The audio output of the AN/PQS-2A ranges in frequency from 0 to 2.5 kHz. The higher frequency corresponds to a detection occurring at the full-range scale setting (either 20, 60, or 120 yd) of the

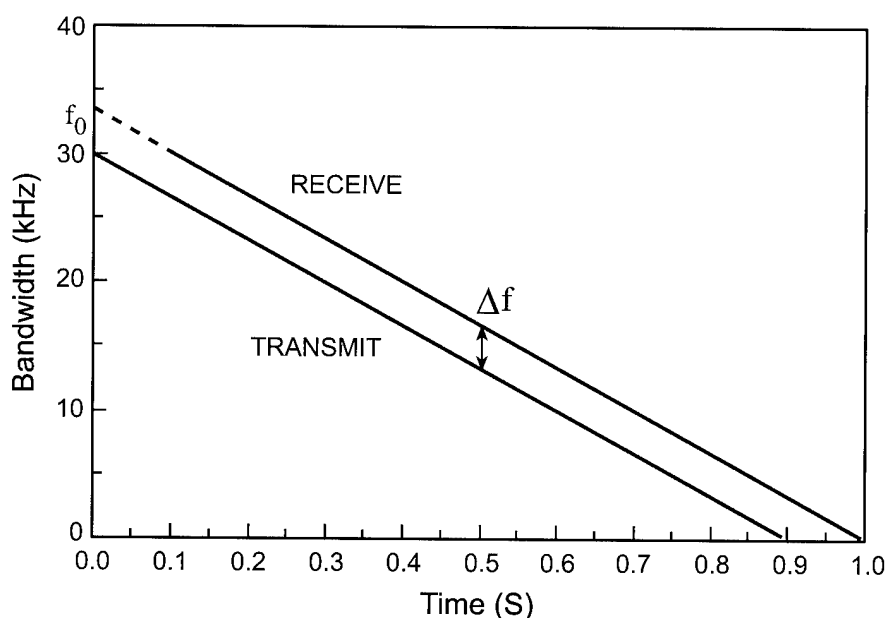


Figure 2—Sonar Bandwidth Frequency Versus Ping Time

sonar. Thus, the range of a detected target can be determined from the tonal frequency, pulse length, and speed of sound in water by:

$$r = tcf / 60000 \quad (1)$$

where r is the range of a target in yards, t is the length of the pulse (i.e., either 0.3, 0.9, or 1.8 s corresponding to the appropriate range scale setting of the sonar), c is the speed of sound in water in yards per second, and f is the frequency of the tone in Hertz. The audio signal prior to amplification is cabled to the instrumentation that is used to digitize, process, and display the sonar's audio output signal.

A block diagram of the electronics used to digitize, process, and display the output signals of the AN/PQS-2A is shown in Figure 3. A trigger, which is produced by the modified AN/PQS-2A and synchronized with the beginning of the CTFM pulse, initiates aural data acquisition by a PC/104 format, 486SLC 33-MHz host computer. The aural signal is digitized at a sample rate of 8 kHz and

processed with the aid of a DSP32C (analog-to-digital (A/D) converter and a 50-MHz digital signal processing (DSP) board). The aural data are processed into their frequency components, which are next mapped into a video image. The video graphics array (VGA) output signal of the computer is then passed through a converter that outputs a National Television Standards Committee (NTSC) signal. This signal is displayed to a sonar operator via a 4-in. diagonal, color, liquid-crystal display (LCD). These components (and associated processing algorithm) provide a near real-time capability in displaying the video image of an aural signal. All of the components are battery powered.

A clinometer and a digital compass are also employed in the upgraded system. These electronics are provided as aids to the sonar operator. Their respective outputs are cabled to the serial port of the PC/104 format host computer. The clinometer is used to measure the inclination angle of the sonar's acoustic beam; the inclination angle is displayed as a false-horizon indicator on the screen. The compass is used to determine the bearing of the acoustic beam, which is shown to the sonar operators in both

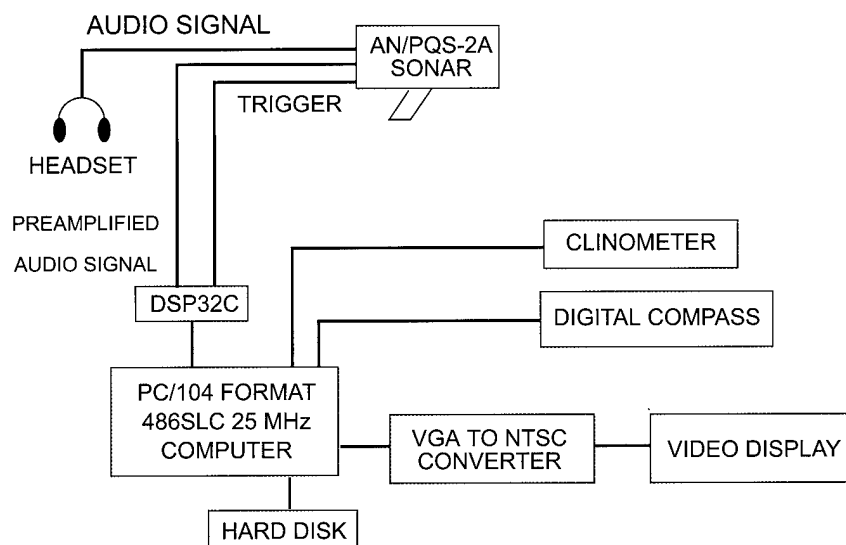


Figure 3—Block Diagram

analog and numeric form. In addition, the computer utilizes the output from the compass sensor to calculate the rate at which the sonar operator rotates the upgraded sonar while scanning through a target field. The scan-rate information is displayed to the sonar operator using three small bars (left, right, and middle) on the monitor and is provided to the sonar operator as an aid to ensure that the sonar transmits and receives acoustic signals at the same bearing, thereby eliminating regions in the target field that are not searched.

VISUAL REPRESENTATION OF AUDIO SIGNAL

The spectrogram processing technique is employed to display the audible tone produced by a backscattered return. A spectrogram is an amplitude contour plot of frequency versus time in a time-windowed ping trace; here a ping trace refers to the waveform of an audible signal corresponding to one CTFM transmit pulse.

The processing methodology to form the spectrogram is as follows. Between sonar triggers, the sonar's audio output signal is digitized and stored in the DSP32C's memory until enough sample points are present to be spectrally analyzed by performing a Fast Fourier Transform (FFT). (In the present configuration, the time window corresponds to 128 sample points). This spectrally processed data is stored in another memory location, and the processing procedure is repeated until the next trigger occurs. When a trigger signal from the sonar is received, the spectrally processed data for a time period corresponding to one period of the previous CTFM pulse are uploaded to the host computer. The host computer first calculates the appropriate decibel (dB) amplitude level of each time-window segment and next assigns a color to the calculated spectral amplitudes, which are then displayed to the diver via the color monitor.

The spectral amplitude levels are displayed on the monitor to the sonar operator using 256 colors. In the current system, the maximum level is assigned red in color, while the background level corresponds to the color blue. Thus, when the

AN/PQS-2A sonar detects a target, it emits an audio signal which is displayed on the monitor as a bar color that horizontally extends across a significant portion of the screen that displays the sonar's audio signal. If the audio signal is very high, the color will be red, whereas a lower amplitude signal will be either yellow, green, or light blue in color. A range scale associated with the proper range-scale setting of the sonar appears to the right of the displayed sonar data. This color assignment was empirically determined during initial testing of the upgraded AN/PQS-2A.

IMAGES DISPLAYED TO DIVERS

Figure 4 depicts four examples of spectrogram-displayed images shown to divers. These images correspond to backscatter data obtained while testing the upgraded sonar in a very-shallow-water (VSW) region. In each instance, the y-axis is the tonal frequency that has been converted to range using the appropriate parameters in Equation (1); the x-axis is the ping time for one pulse length (i.e., time for one transmitted frequency sweep) and is not labeled in any of the figures since the sonar operators do not need this information. In images A, B, and C, high-amplitude returns that had horizontally extended over a significant portion of the ping time appear at 25 yd (image A), 32 yd (image B), and at 22 and 32 yd (image C). In addition, a low amplitude return appears at 15 yd in image D; this return is due to a low target strength, low observable object.

IMPORTANCE OF COMBINED AUDIO PLUS VISUAL DETECTION CAPABILITY

Complementing the current AN/PQS-2A aural output with a visual spectral display is important for two distinct reasons. First, the visual display confirms the audio signal heard by an operator. The combined audio-plus-visual detection method enables operators to use two senses (ears and eyes) when mine searching. Both senses are especially important in situations when an operator is unsure of audibly detecting a low-amplitude signal, such as a return from a low observable object. The

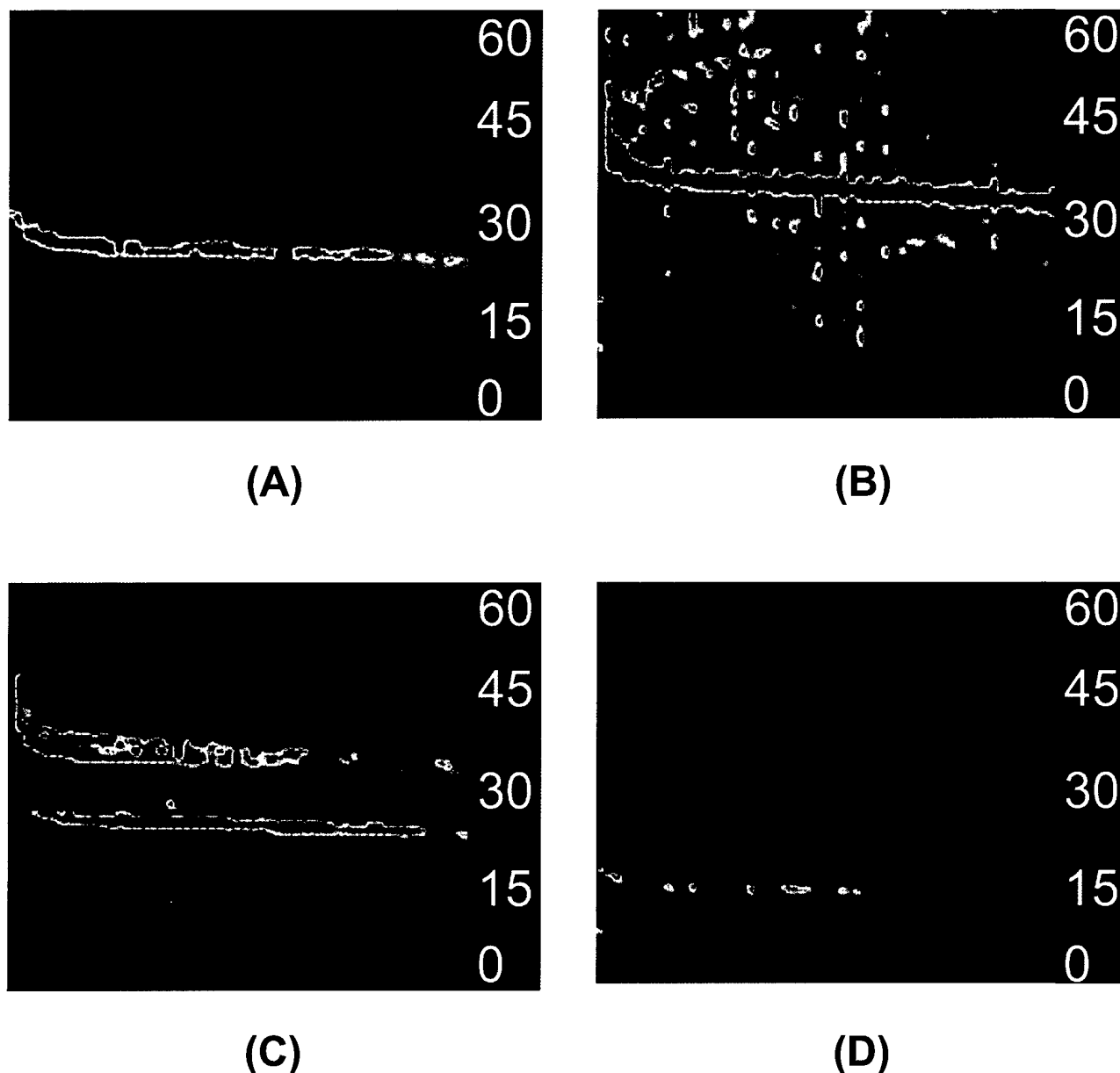


Figure 4—Spectrograms Displayed to Diver

combined method has been demonstrated to reduce training requirements, improve detection performance, and reduce variation in operator performance.

A second important reason to supplement the aural output with a spectral display is that the display provides both detection and location (i.e.,

range) information. In principle, aural ranging with the unmodified AN/PQS-2A is possible; however, it is not reliable, and presently, an operator using this sonar usually swims within visual range of every contact. Thus, by viewing the range of a detected object, sonar operators can tell if a contact is within their search area. If it is not, then the operators do not swim to the target, thereby saving mission time.

TARGET ECHO BACKSCATTER DISCRIMINATION CAPABILITY

Interestingly, the returns seen in each of the spectrogram images shown in Figure 4 are not sharp lines with uniform amplitudes that extend horizontally across the images. Thus, these images indicate that the returns from the various targets exhibit some structure in the audible signal heard by a sonar operator. Such structure may be used to discriminate the backscatter return from one object with that of another.

As a result of this observation, CSS also investigated the AN/PQS-2A capability to discriminate one target from another using target echo backscatter. In

this work, AN/PQS-2A backscatter aural data were recorded for different objects. Examples of time-waveform audio signals and their corresponding frequency spectra of an air-filled barrel, as well as that of a water-filled barrel, are illustrated in Figure 5. These data clearly show that the audio signal from the water-filled barrel is amplitude-modulated, and the associated spectra indicate that there are two frequency components in the aural signal; these two frequency components are the result of backscatter from the front and back of the barrel. On the other hand, the aural signal from the air-filled barrel is not amplitude-modulated, and the corresponding spectra indicate that there is only one frequency component in the audio signal; this frequency component is due to backscatter from the front of the barrel. Since this barrel is air-filled, virtually

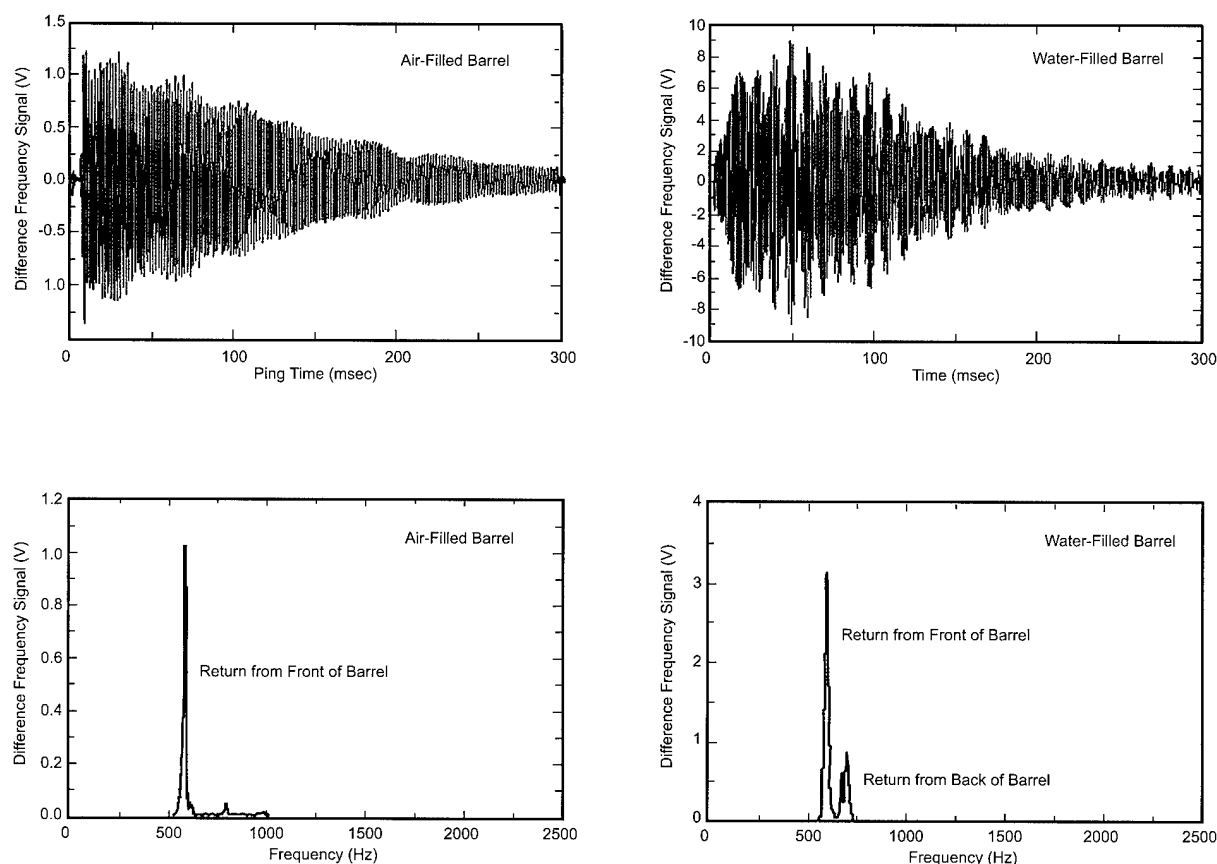


Figure 5— Time Waveforms and Corresponding Frequency Spectra for Air-Filled and Water-Filled Barrels

none of the projected acoustic beam can propagate through the air to the back of the barrel, whereas a significant amount of the projected beam can propagate to the back of the water-filled barrel. This is a reason for the different aural signals, which divers can easily differentiate.

This effort has shown that backscatter returns from different targets produce different amplitude-modulated aural signals. These signals are dependent upon aspect angle, target fill material, and target geometry. This work has indicated that the amplitude-modulated signals are caused by multiple scatterers within the sonar's beamwidth. Thus, by implementing an appropriate advanced processing method, the upgraded AN/PQS-2A may be further enhanced to provide an improved classification capability. Such advanced processing methods may include:

- ◆ Pseudophoneme and filter processing techniques
- ◆ Target physics-derived features and reconfigurable hybrid classifier techniques
- ◆ Classic match filtering approaches such as a finite impulse response (FIR) filter, an adaptive clutter filter, maximum discrimination filters, and pseudo deconvolution techniques

RESULTS OF EFFORT

With the aid of Navy divers, CSS has conducted extensive tests that compared detection performance of the upgraded AN/PQS-2A sonar with that of an unmodified sonar. Results of these tests have demonstrated that the upgraded sonar provides improved detection and localization capability, reduced variation from operator to operator, and reduced training requirements.

The prototype units were demonstrated to the Program Management Office - Explosive Ordnance Disposal - Two (PMS-EOD-2) in Panama City, Florida, and in Coronado, California, at the

NSW Center, NSW Group ONE, EOD Group ONE, and EOD Mobile Unit THREE. As a result of these demonstrations, the NSW Technology Program was requested by PMS-EOD to develop four additional prototype units to be tested and evaluated by the personnel from the VSW MCM Test Detachment in Coronado, California.

In addition, the prototypes of the AN/PQS-2A upgrade with visual display were used in several civilian applications. In the most notable application, the upgraded sonars were used by Navy Salvage Divers at the TWA Flight 800 crash site off of Long Island. Recently, these sonars also have been used by Panama City, Florida police department divers who were searching for evidence on the bottom of a lake.

Three recommendations have been suggested by military divers to improve the upgraded AN/PQS-2A sonar:

1. Reduce the size of the present prototype system by placing all of the instrumentation (sonar's electronics, spectral processor, clinometer and compass sensors, batteries, etc.) in one housing. This would reduce drag effects and make it easier for divers to swim with the unit.
2. Incorporate target echo backscatter discrimination processing techniques to the upgraded sonar; such techniques would provide an improved classification capability.
3. Improve the method of displaying the sonar data to the diver by using an image sector scan display instead of the spectrogram presentation method

An image sector scan is a two-dimensional picture in which color magnitudes derived from acoustic returns are mapped into their proper spatial locations. The upgraded AN/PQS-2A processing code can easily be modified such that the sonar's audio output signals can be displayed to a diver in a fashion similar to the image sector scan shown in Figure 6; this image was obtained from

processed AN/PQS-2A data acquired while testing in a VSW area. The image was formed by the following procedure. For each transmitted pulse, the upgraded AN/PQS-2A sonar's host computer recorded the sonar bearing, and the sonar's aural signal was spectrally analyzed, with the amplitude being assigned a color (such as red for a high-amplitude return and blue for a low-level return). The audio frequency was then converted to range using Equation (1). This processed data (back-scattered amplitude and range information) and the sonar bearing information were stored in memory. The image was formed by accessing the information stored in memory and then plotting the processed sonar signals into their proper spatial locations. This method of display has the effect of painting a picture for the diver and shows where the diver has

already scanned and where the diver is presently pointing the sonar.

Presently, CSS is planning to reconfigure the processing code such that an image sector scan will be displayed to divers. This improved display method will then be demonstrated to, and assessed by, Navy divers. Future CSS efforts call for determining the appropriate advanced processing method for an enhanced classification capability, implementing this method, and then developing the instrumentation to reduce the size of the upgraded sonar. With these efforts, the upgraded AN/PQS-2A will provide fleet divers with a handheld sonar that will improve the current detection, classification, and localization capability; reduce variation from operator to operator; and reduce training requirements.

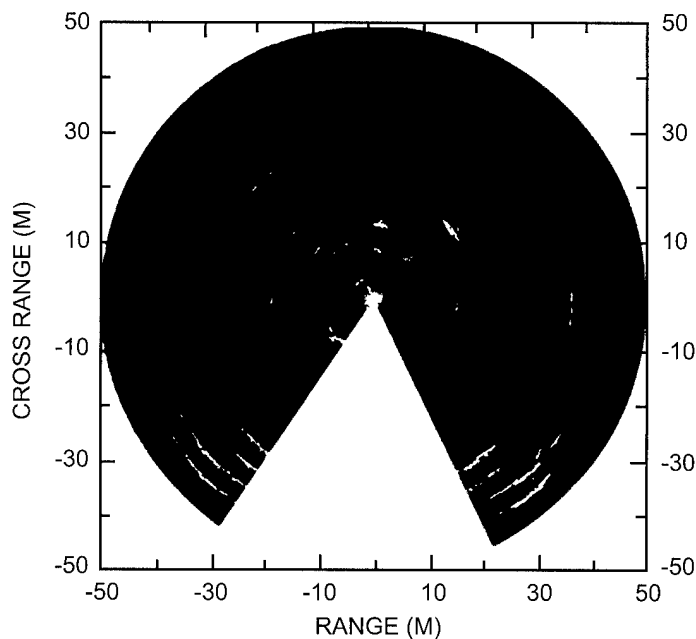


Figure 6—Image Sector Scan

THE AUTHOR

DR. JOSEPH L. LOPES



Dr. Joseph L. Lopes received B.A. degrees Summa Cum Laude in mathematics and physics at Rutgers University. He has also received M.S. and Ph.D. degrees in physics from Stevens Institute of Technology. For the past decade, Dr. Lopes has worked as a research physicist in the Research, Technology, and Analysis Department at CSS in Panama City, Florida. While at CSS, he has conducted research in programs dealing with: (1) VSW acoustic characterization and sonar performance measurements, (2) developing and assessing the modified AN/PQS-2A against targets in the VSW regime, (3) investigating acoustic, magnetic, and electro-optics technologies in support of developing a diver-portable classification capability for non-buried targets, and (4) investigating effects of sediment loading on the acoustic backscatter signals from a buried target. Presently, Dr. Lopes is developing technology in support of a diver-portable buried minehunting sensor system. He has published numerous reports describing his research and has presented his work at various symposia and conferences.

THE EVOLUTION OF AIR TARGET WARHEADS

Mr. Samuel S. Waggener

Warheads have evolved from simple designs that projected nonoptimized size fragments in a symmetric pattern about the roll axis of the missile to those that aim optimized fragments in a concentrated beam in the target direction. Evolution has been driven by the changing target threat and is made possible by advances in warhead explosive initiation system and target detection (fuze) technology, in conjunction with the maturity of target vulnerability descriptions and methodology.

INTRODUCTION

Investments in warhead technology over the past few decades have resulted in transitions of advanced concepts that have increased the lethality of many antiair missiles. The investments and the resultant transitions have produced an evolution of air target warheads driven by changes in the characteristics of the targets (size, speed, and hardness) and interceptor missiles (speed, agility, and fuzing) and by the ability to describe the vulnerability of the target with increasing fidelity.

A typical air target warhead consists of an explosive charge surrounded by a fragmenting metal case. The warhead is carried to the target by the intercept missile. There would be no need for a warhead if the interceptor could achieve a direct hit of the target. The interceptor's kinetic energy alone would cause target breakup (except perhaps for small, shoulder-launched missiles). Except for short-range, shoulder-launched missiles, direct hits are rare. As range requirements increase, missile size increases, and missile agility decreases. The result is a requirement for a warhead—an item that can eject high-speed, lethal fragments at the target near the point of closest approach.

Air target intercepts can result in target/interceptor closing velocities of up to 9000 ft/s for cruise missiles and even greater velocities for tactical ballistic missile targets. Existing target detecting devices (TDDs), sometimes referred to as fuzes, require that the warhead fragments be quickly accelerated to velocities similar to these closing velocities in order to hit the target. This magnitude of acceleration and final velocity can be achieved only through the use of explosives.

A typical pure explosive is a solid composed of molecules consisting of a carbon or carbon-nitrogen backbone with attached oxygen sources. These sources are either nitro groups (NO_2), nitrate ester groups ($-\text{ONO}_2$), or nitromine groups ($-\text{NH}-\text{NO}_2$). These explosives can be considered metastable materials that, given the proper stimulus, will decompose at the molecular level into gaseous H_2O , CO_2 , CO , and N_2 . Decomposition occurs so rapidly (with

reaction propagation rates up to 30,000 ft/s) that the solid explosive mass can be considered to instantaneously convert to gas, with an energy release of 1000 to 1500 cal/gm. The energy released heats the gases to between 3000 to 4000 K with resulting pressures between 4 and 5 million psi! If the explosive has been encased in metal, the expansion of the gases will accelerate the casing to several thousand feet per second in a few microseconds.

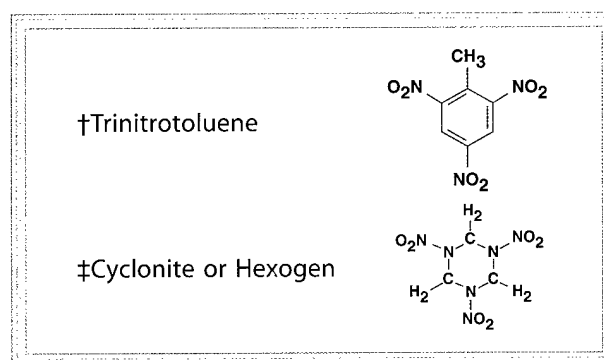
AIR TARGET WARHEADS OF THE 1950s

Examples of antiair missile warheads in service during the 1950s are warheads employed on the air-launched SIDEWINDER 1A and the ship-launched RIM-2 TERRIER missiles. Both warheads produced a fragment pattern that was symmetric about the roll axis of the missile. The SIDEWINDER 1A warhead was a simple, smooth steel tube filled with explosive. A plastic grid was placed between the case and the explosive. The grid was designed in such a way that upon detonation of the explosive, the gases at the interface would be focused to score the case in a square pattern. As the case expanded, it broke along these score lines. The TERRIER warhead was constructed of adjacent, square wire rings that were notched to provide lines of fracture upon explosive detonation. The warhead was tapered at one end to produce a relatively wide polar spray pattern (see box below). Both the SIDEWINDER and TERRIER warheads were designed to produce a large number of relatively small fragments.

Targets for these early missiles were relatively light fighter and bomber aircraft. Warhead design philosophy was to throw many small fragments at these targets to achieve a high probability of striking

a vulnerable component. Unless detonated close to the target, these warheads would achieve a "K" type kill in which the damaged component(s) would cause the aircraft to lose control within 30 s of engagement.

Explosives of the era were usually mixtures of TNT[†] and RDX.[‡] TNT, the first of the modern explosives, was developed prior to World War I. It is a relatively inexpensive melt-castable explosive, but by today's standards, it has relatively low performance. RDX was discovered in the early 1900s but was not used in military applications until World War II. It has 10 to 20 percent greater performance than TNT (performance related to power output minus the energy release rate).



THE CONTINUOUS ROD (CR) WARHEAD ERA

The CR Warhead was conceived at New Mexico Institute of Mining and Technology (NMT), Socorro, New Mexico, during the early 1950s. Its genesis was from early tests of discrete rods in which the rods were shown capable of slicing through

THE POLAR ANGLE IS THE ANGLE MEASURED WITH RESPECT TO THE LONGITUDINAL AXIS OF THE WARHEAD, WHICH USUALLY CORRESPONDS TO THE LONGITUDINAL AXIS OF THE CARRIER MISSILE. THE AZIMUTH ANGLE MEASURES THE ANGLE AROUND THE ROLL PLANE OF THE MISSILE.

aircraft skin and damaging internal structure. The CR concept was a means of producing a rod long enough to slice through the entire fuselage or wing to cause catastrophic breakup of the aircraft. The CR warhead consists of a double bundle of steel rods running lengthwise around the circumference of an explosively filled cylinder. The rods are welded together at alternate ends. Upon detonation of the central core of explosive, the rods are projected radially outward, forming a lattice, as illustrated in Figure 1. The rods continue to expand, reaching what is called *full open radius*, the stage at which the hoop is fully extended. As the hoop continues to expand, the rods fracture. After fracture, the rods are still capable of causing component damage, but not catastrophic structural damage. Figure 2 illustrates the desired target interaction at intercept.

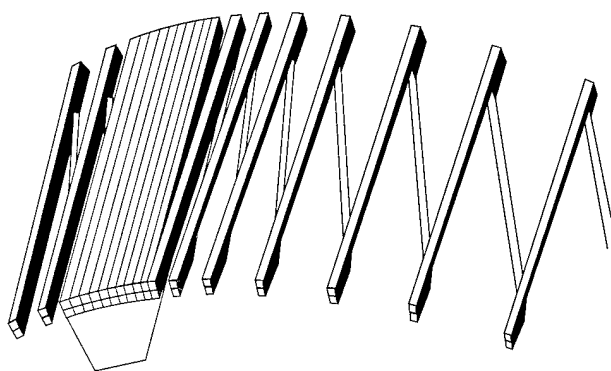


Figure 1—Section of Cylindrical CR Case Showing Initial Rod Bundle Configuration and Expansion

All Navy anti-air missiles employed the CR concept during the 1960s and into the 1970s. A SIDEWINDER version was developed at the Naval Air Warfare Center, Weapons Division (NAWCWD) at China Lake, California. SPARROW, TERRIER, TARTAR, TALOS, STANDARD and PHOENIX versions were developed at NSWCDD, with contract support from the Applied Physics Laboratory, Johns Hopkins University. Unfortunately, this novel concept became ineffective shortly after service introduction. Development testing had been conducted against 1950s-type aircraft, which could be effectively damaged by the CR kill mechanism. The target fighters and bombers in service during the 1960s were of heavier construction and more

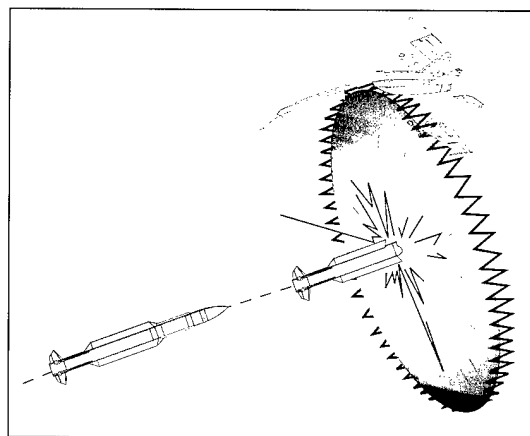
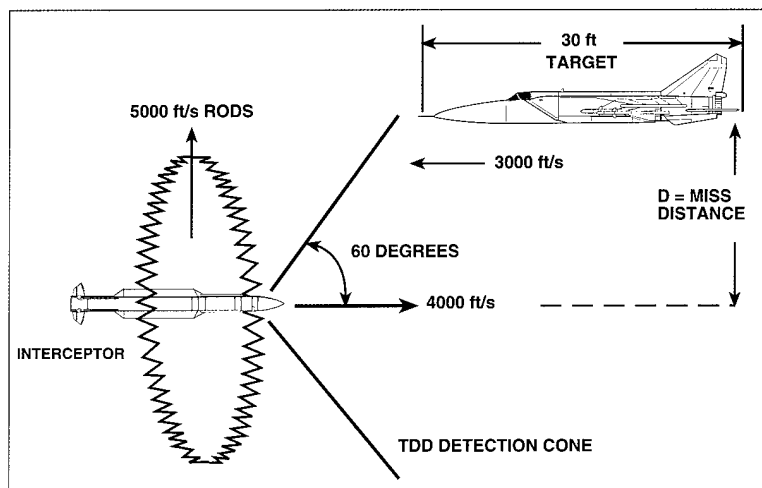


Figure 2—Target Intercept Using a CR Warhead

densely packed with components. So it was difficult for the CR to achieve the desired structural kills against these targets. The rods could still inflict damage to components; however, the single narrow rod meant impact at only one location, and if there was not a vulnerable component at this location, the target would not be killed.

The CR had one other problem—a limitation in rod ejection velocity. Ejection velocities were limited to a maximum of 4000 to 5500 ft/s due to an impulse restriction to keep the rods intact at launch. These ejection velocities were adequate to engage targets of the 1950s; however, during the 1960s the Soviets introduced cruise missiles with double or triple the speed of the fighter and bomber aircraft that the CRs were developed to counter. At the same time, US interceptor missiles were also increasing in speed. The results were closing velocities that could reach 6000 to 7000 ft/s. Even the most advanced TDDs had minimum half-cone detection angles of 45 to 60 degrees, which limited response time after target detection. The result of low rod ejection velocity coupled with high closing velocity and TDD detection cone angle limitations could result in the rods passing behind the target for a complete miss, as illustrated in the example of Figure 3.

In this example, the rods will pass behind the target at miss distances greater than 35 ft. Shorter, faster targets; larger TDD cone angles; TDD target detection beyond the target nose; finite



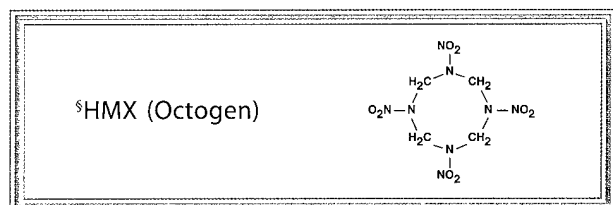
TIME FOR RODS TO REACH TARGET: $t_1 = D/5000 \text{ ft/s}$
 TIME FOR TARGET TO BYPASS RODS: $t_2 = (30 \text{ ft} + D \text{ CTN } 60^\circ) / (3000 + 4000 \text{ ft/s})$
 LET $t_1 = t_2$; SOLVE FOR D; D = 35 ft

Figure 3—Example of a Parallel Encounter With 7000 ft/s Closing Velocity (Rods will completely miss target at any miss greater than 35 ft)

fuse-integration times; faster interceptors, and interceptor angle of attack at warhead burst all produce a rod miss at much closer miss distances.

AIR TARGET WARHEADS OF THE 1970s AND 1980s

The 1970s and 1980s saw the return of fragmenting warheads, with emphasis on higher velocity and improved fragment-size control methods. Higher fragment velocity could be obtained by increasing the relative mass of explosive and by using higher performing explosives containing RDX or HMX.[§] HMX has 10 percent greater performance compared to RDX. It was initially a by-product of RDX production, and as such, its supply was limited. It soon could be separately synthesized and became



the explosive ingredient of choice, and it remains so today.

The Navy's emphasis during this period was the defeat of Soviet cruise missiles. At the same time, cruise missile vulnerability descriptions and target vulnerability methodology reached a high level of advancement, allowing optimization of fragment size. Two of the most popular size control methods were the Pearson notch and the opposed notch techniques. Both methods allowed use of a solid steel casing whose residual strength after notching could carry the missile flight loads, if required, and provide for case expansion before rupture to obtain high fragment velocity.

John Pearson at NAWCWD developed the Pearson notch, also referred to as the shear-control method, during the 1970s and 1980s. The inside of the steel, cylindrical case is notched in a diamond pattern, as illustrated in Figures 4 and 5. Even though the notches are shallow, they are effective in initiating a fracture trajectory that travels to the outside of the case as

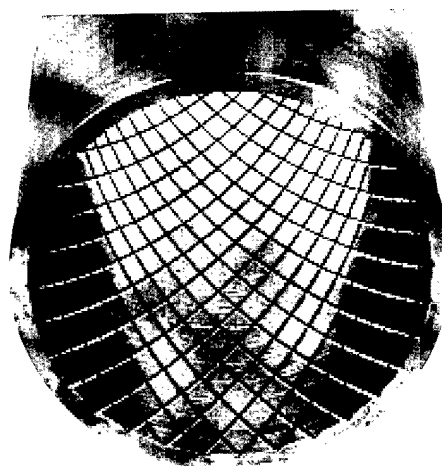


Figure 4—Steel Cylinder Showing Inner-Surface, Diamond-Pattern Grid (Figure 1 from Reference 1)

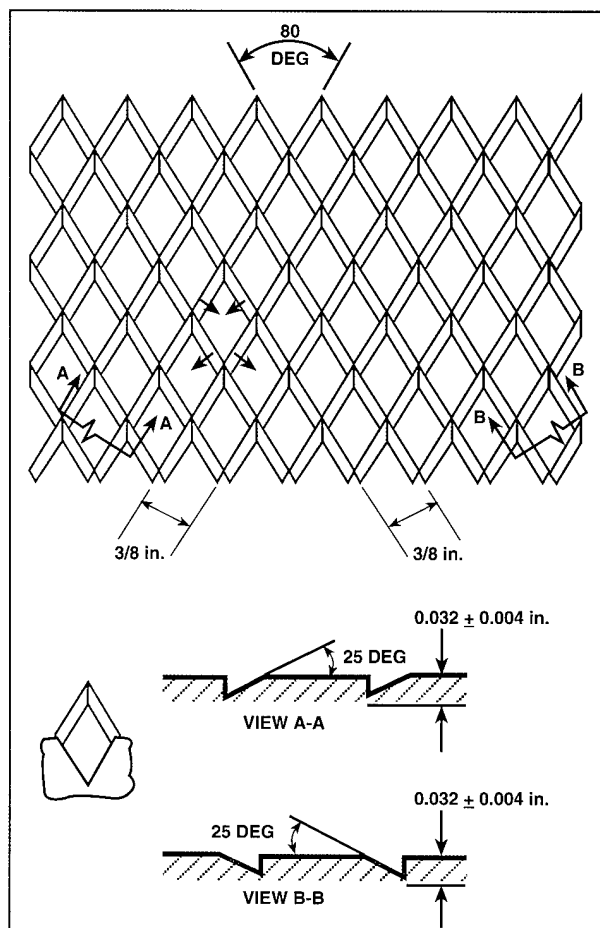


Figure 5—Diamond Grid Design with Nonsymmetrical Profiles (Figure 6 from Reference 1)

the case begins to expand upon detonation of the core explosive. This process is illustrated in Figure 6. A sample of resulting fragments is shown in Figure 7. This method is effective for certain ratios of case thickness to notch spacing. For optimum ratios, 80 percent of the case mass can be controlled to the desired size.

The opposed groove method was developed at NSWCCD during the 1970s and is still being refined to this day. As the name implies, it consists of narrow, tapered, or straight grooves cut on the inside and outside of the case directly opposite one another. The grooves are cut to a depth, and the radius at the bottom of the groove chosen such that the thickness remaining between the grooves provides the required case strength and rigidity,

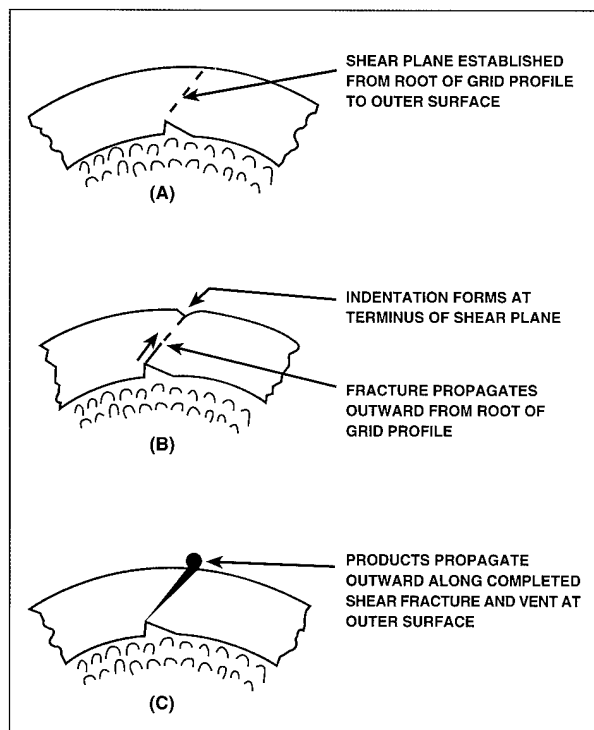


Figure 6—Dynamics of Shear Trajectory Formation (Figure 4 from Reference 1)

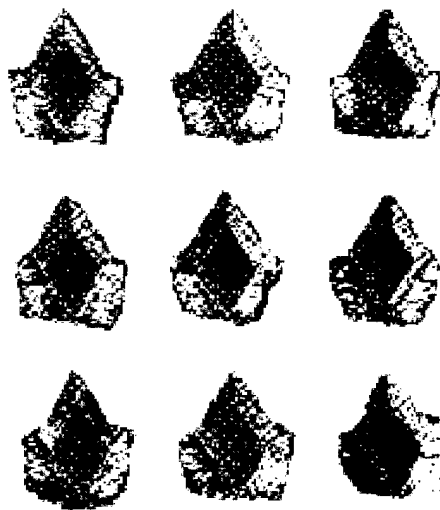


Figure 7—Fragments Formed by the Pearson Notch Method (Figure 7 from Reference 1)

while also assuring that the case will break cleanly between opposing grooves upon explosive detonation. The opposed groove technique allows for a wider choice of fragment size, but the case is weaker compared to the Pearson notch technique. The opposed groove technique can yield 90 percent or more of the case mass into the desired fragment size. Figure 8 shows recovered fragments from a warhead using this control method.

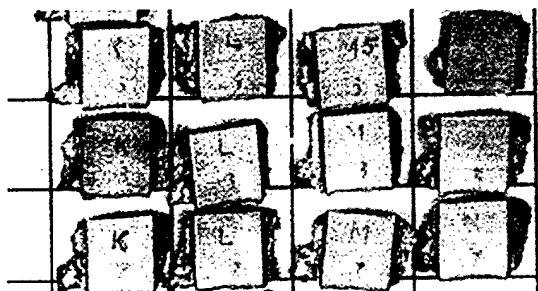


Figure 8—Fragments Formed by the Opposed Notch Method

THE AIMABLE WARHEAD ERA

During the late 1980s and into the 1990s, advanced development began on aimable warheads. Up until this time, deployed air target warheads were axisymmetric; i.e., they produced a fragment pattern that was the same in all azimuth directions. The first-generation aimable warhead is the Asymmetric Initiated (AI) Warhead. An AI warhead is a

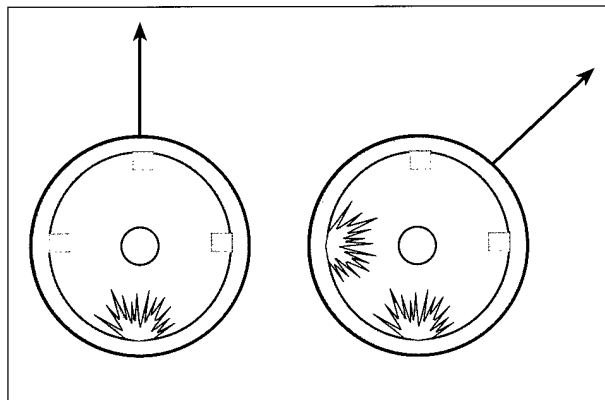


Figure 9—Operation of the AI Warhead

cylindrical warhead in which initiation occurs on a line or lines at the explosive/case interface opposite the direction of aim, as shown in Figure 9.

Asymmetric initiation produces an asymmetrical fragment pattern with a 20 to 30 percent higher velocity in the direction of aim compared to the same warhead initiated along the central axis. Figure 10 shows the fragment pattern resulting from this type of initiation scheme. In practice, the aiming of such a warhead can be accomplished by initiation of 1, 2, or 3 lines of initiators from a warhead containing 4 to 16 equally spaced lines of initiators. An azimuthal sensing TDD would be used to signal the choice of initiator lines to direct the maximum kill mechanism on the target. This type of aiming system requires no physical orientation of the warhead prior to detonation. Therefore, the time between determination of the required aim direction and warhead detonation can be zero.

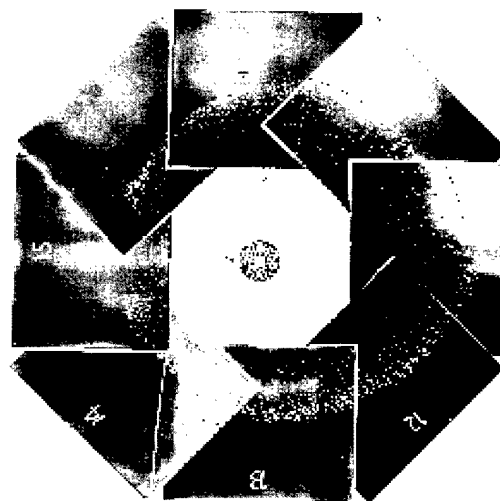


Figure 10—Radiograph of Fragment Pattern from an AI Device Showing Enhanced Velocity in Aim Direction (directly to the right of the original charge position)

AI technology had been around for several years, having undergone exploratory development by the Air Force at Eglin Air Force Base (AFB), Florida, during the 1970s and intermittently at NSWCDD from the late 1960s to the late 1980s. These efforts explored the effects on fragment velocity versus central cylindrical explosive voids; single, multiple,

and sequential multiple-line initiation; and a number of initiation points along each line. AI technology was implemented at NSWCDD during the early 1990s when the warhead was integrated with an advanced initiation system and an azimuthal-sensing TDD. The impetus for this development was a need for higher fragment velocities than could realistically be achieved from axially initiated warheads.

The enhancement through asymmetric initiation can be measured by two methods:

1. Fragments can be ejected in the direction of aim at velocities 20 to 30 percent higher than normally possible.
2. A fixed-weight warhead system can devote more relative weight for the case and less for explosive and project more fragment mass in the direction of the target at a velocity equal to that produced by an axially initiated warhead.

It is this latter measure that is the most useful.

Fragment velocities from an axially initiated cylindrical warhead can be estimated from the well-known Gurney formula:²

$$V = A \left(\frac{1}{2} + \frac{M}{C} \right)^{-1/2}$$

where V is fragment velocity, A is a constant depending on the type of explosive used, M is the case mass, and C is the explosive mass. This equation becomes:

$$V = (1.25)A \left(\frac{M}{C} + \frac{1}{2} \right)^{-1/2}$$

in the direction of aim for the AI warhead. A typical value for A is 8500 ft/s. Figure 11 is a graph-plotting relative mass that can be projected at a target as a

function of desired initial fragment velocity (AI relative to an axially initiated warhead of equal weight). Relative mass is found by determining the M/C ratio, which gives the desired fragment velocity for each of the two types of warheads. For a fixed-weight system, the fraction of weight that can be devoted to the case for this desired fragment velocity is:

$$M = 1 / (1 + C/M)$$

The relative values of M for the AI compared to the axially initiated warhead are found along the ordinate in Figure 11. When the required fragment velocity is high, the advantage of employing the AI warhead is apparent. This occurs when the miss distance is large, closing velocities are high and/or when the target is short (as per discussion of the CR's demise and as shown in Figure 3).

The second-generation aimable warhead is currently undergoing advanced development at NSWCDD. This warhead is referred to as the Deformable Warhead, it is part of an integrated Directional Ordnance System (DOS), which includes a safe and arm device, and an initiation system that is being developed at NAWCWD.

The warhead concept is illustrated in Figure 12. It consists of an explosively filled, fragmenting cylinder that may contain an explosive void. The

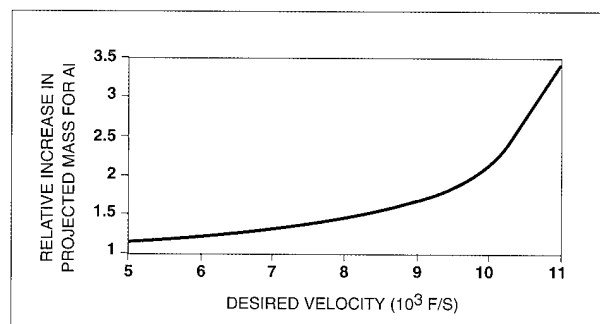


Figure 11—Relative Fragment Mass Projected in Aim Direction by AI Compared to Axially Initiated Warhead of Equal Total Weight

fragmentation cylinder is surrounded with a layer of explosive that is divided radially and buffered so that the resulting strips can be initiated independently. The desired operation of the warhead is shown in Figure 12. Upon determining the desired direction of aim, a number of the outer explosive strips—called deforming charges—are initiated (3 out of 12 are shown in the figure). Detonation of the strips causes deformation of the fragmenting case so that, at some later time, a large portion of the case is flattened; at the same time, the void that may have been present in the main charge

This allows the warhead to achieve kills at double the miss distance or to achieve a higher quality of kill (catastrophic versus slow kill) at the same miss distance compared to an ordinary warhead.

The inflight operation of a DOS, illustrated in Figure 13, shows that an azimuthal-sensing TDD predicts target/warhead relative orientation at intercept. After an optimal time delay, specific deforming charges are initiated to flatten the case on the side nearest the target. After an appropriate time delay to allow the case to deform into a “D” shape,

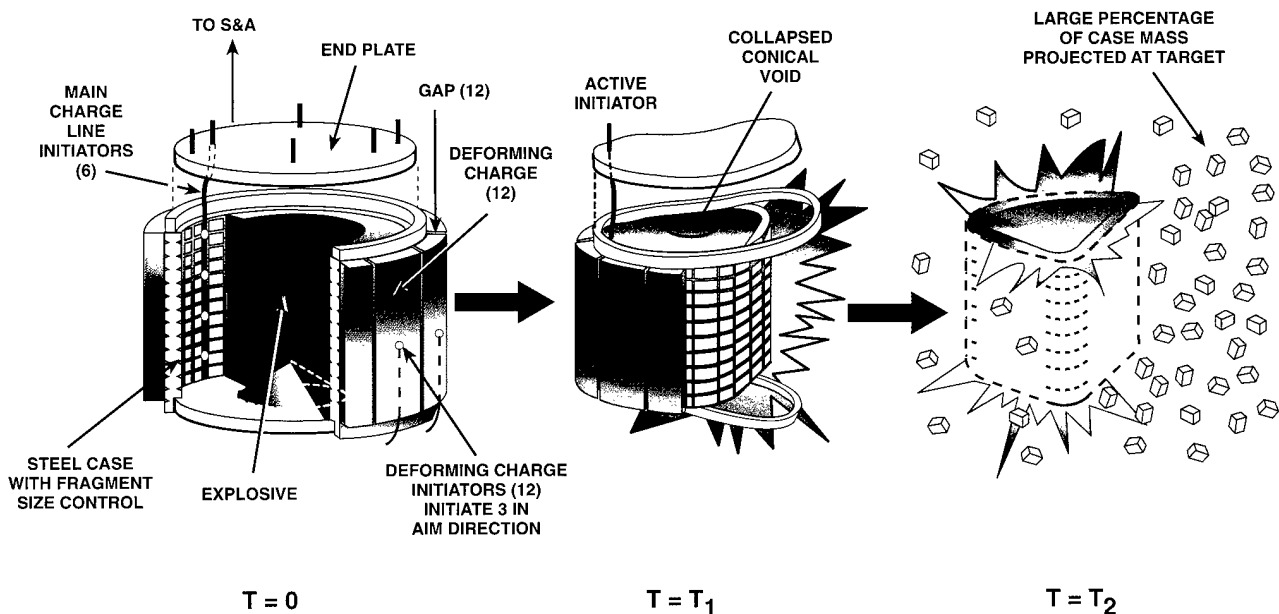


Figure 12—Sequential Operations of a Deformable Warhead

explosive is collapsed. This ensures that the explosive is in compression, at which time the main charge is initiated by a line initiator on the side opposite case deformation. The flattened portion of the case is projected at the target at high velocity. As a first-order approximation, fragments are ejected in a direction normal to their outer surface; thus the fragments originating from the flattened portion of the case can be projected in a tight beam at the target. The beam tightness can be controlled and is optimized to the azimuthal resolution of the TDD. The beam typically contains three to five times the fragment mass compared to an ordinary warhead.

the main high-explosive charge is initiated to direct a concentrated beam of fragments toward the target.

The idea of a deformable warhead has been around for a long time. NMT and NAWCWD undertook an exploratory development of the concept during the 1970s. Efforts were hampered by sympathetic initiation of the main charge explosive, lack of fragmentation control, and a poor understanding of the deformation dynamics (due to immaturity of Hydrocode modeling). Exploratory development of the warhead was reinitiated at NSWCCD during the late 1980s and transitioned to

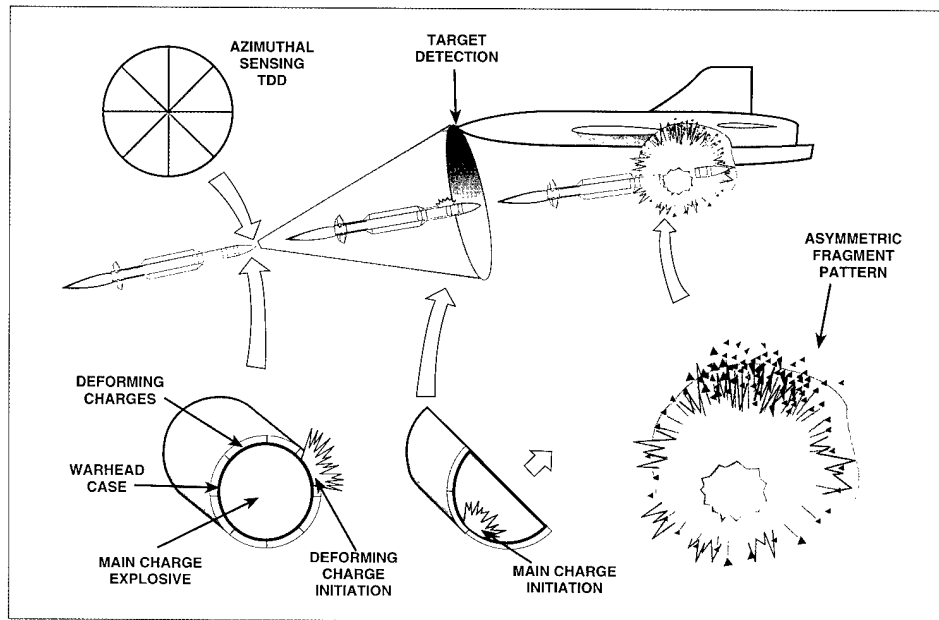


Figure 13—In-Flight Operation of Ordnance System Employing a Deformable Warhead

advanced development in the early 1990s. Success of this effort was due to development of a new shock-insensitive explosive at the Naval Surface Warfare Center, Dahlgren Division (NSWCDD), White Oak Detachment; an understanding of deformation dynamics through Hydrocode simulations; and development of successful fragment control techniques.

SUMMARY

Air target warheads have evolved through the years in response to the changing target threat, increases in explosive output, advancements in associated ordnance components, and refinements in target vulnerability descriptions and methodology. Warheads have changed from designs using simple fragment-size control techniques—whose size was chosen with little basis, and which produced roll-symmetric fragment patterns—to those

incorporating sophisticated optimized fragment-size control and that can bias fragment velocity or fragment mass at the target. Warhead technology transitions will continue to evolve into devices that direct narrow, concentrated fragment beams at a specified area on the target. These warheads will be part of a unified system that will consist of a precision, forward-looking TDD integrated with the guidance and airframe control components.

REFERENCES

1. Pearson, John, *A Fragmentation Model Applied to Shear-Control Warheads*, Naval Weapons Center, China Lake, NWC TP 7146, May 1991.
2. Gurney, R.W., *The Initial Velocities of Fragments from Bombs, Shells, and Grenades*, BRL Report 405, Sep 1943.

THE AUTHOR

MR. SAMUEL S. WAGGENER



Mr. Samuel S. Waggener graduated from the University of Colorado with a degree in physics in 1965. Coming directly from college to NSWCDD, he has spent his career in the exploratory development of new warhead concepts. These efforts have transitioned to the in-service PHOENIX WDU-29/B and STANDARD Missile MK 115 and MK 125 Warheads as well as to advanced development of the Deformable Warhead.

THE APOBS MK7 MOD 1 MOVES ASSAULT BREACHING OPERATIONS AND EXPEDITIONARY WARFARE INTO THE 21ST CENTURY!

Mr. Robert C. Woodall, Jr., and Mr. Felipe A. García

Historically, assault breaching operations have been highly dangerous because the previous tools and methods employed exposed the assault team to direct enemy fire for a long period of time at a location most advantageous to the enemy. They also exposed the assault team to the fragment and blast effects of mines disturbed during the assault breaching operation.

The MK7 Mod 1 Antipersonnel Obstacle Breaching System (APOBS) is a man-portable, rocket-propelled weapon system designed to destroy antipersonnel mines and wire obstacles during assault breaching operations. APOBS creates a 45-m long by 0.6-m wide pathway through antipersonnel mines and wire obstacles, provides a lifesaving standoff of approximately 35 m from enemy-controlled mine and wire obstacle fields, while exposing a two-man team for less than 60 s!

APOBS moves assault breaching operations and expeditionary warfare into the 21st century by eliminating the need for the user to detect antipersonnel mines with probes and detectors, cut antipersonnel wire obstacles by hand, employ the operationally burdensome M1A2 Bangalore Torpedo, and accept the human toll and suffering inherent with the use of the old assault breaching tools and methods. Although APOBS weighs approximately 120 lb (a fraction of the 390 lb needed using Bangalore Torpedoes), APOBS makes up for the weight difference with innovative warhead technology that meets all the insensitive munition (IM) system requirements of NAVSEAINST 8010.5 while packing a powerful punch capable of effectively neutralizing antipersonnel mines and wire obstacles.

ASSAULT BREACHING

Assault breaching of antipersonnel mines and wire obstacles just got a lot simpler, a lot lighter, and a whole lot faster. With a final reliability demonstration and subsequent commencement of its production process, the APOBS MK7 Mod 1 has moved man-portable assault breaching and expeditionary warfare into the 21st century. The APOBS MK7 Mod 1 transition into production took place on March 3, 1997, after years of development. During

the development of APOBS, the U.S. Marine Corps acted as the Lead Service and the Naval Surface Warfare Center, Dahlgren Division (NSWCDD) Coastal Systems Station (CSS) Marine Corps Project Office acted as the Principal Development Agent, Technical Direction Agent, and Fuzing Design Agent (DA), in cooperation with other Naval Surface Warfare Divisions and the Department of the Army. In February, 1998 APOBS met another milestone, when a preliminary Request for Proposal (RFP) was issued by the Marine Corps. This preliminary RFP is the initial vehicle by which APOBS will be fabricated for use by the Marine Corps and the Army, and will eventually lead to foreign military sales.

The Marine Corps recognized for many years the need to provide infantrymen and combat engineers the ability to perform assault breaching operations without the support of tanks or amphibious assault vehicles. The Marine Corps also recognized that a successful nonmechanized assault breaching operation must negate the significant advantage provided to enemy forces by the lethal combination of antipersonnel mines, antipersonnel wire obstacles, and direct arms fire when used in conjunction with terrain features of the local topography. Figure 1 shows a close-up of a triple standard concertina wire obstacle. Figure 2 shows successive belts of mines and wire obstacles.



Figure 1—Ssgt William "Bill" Fuller, US Army National Guard, with Team Engineer, 578th Engineer Battalion, Kearney Mesa, California, looking into the obstacles on Red Beach during Exercise Kernel Blitz 97

Successive belts of antipersonnel mines and wire obstacles work in unison to channel and hinder the advance of nonmechanized assault breaching echelons. If the threat was limited only to surface-laid or trip-wired antipersonnel mines, creating a small pathway would be a relatively easy task. A lightweight detonating cord charge could get the job done. Several explosive weapon systems have been developed and marketed to accomplish just that, with a total system weight of approximately 20 lb and requiring only one person to emplace and deploy them. However, the threat that assault breaching teams face is much more complex than just surface laid or trip-wired antipersonnel mines.



Figure 2—Marines cross the beach on D-Day during Exercise Kernel Blitz 97

Heavy, blast resistant, and buried antipersonnel mines represent a much more difficult threat, and inexpensive, low-technology, hardened, antipersonnel wire obstacles represent the unique threat of both a physical and psychological barrier. Although each type of threat has its own set of strengths, their combined use produces a formidable barrier. Successive belts of antipersonnel mines and wire obstacles work in unison, compounding the technical problem because the mine belts are protected by wire obstacles like triple standard concertina. The mines are effectively underneath and protected by the wire obstacle itself when viewed from the typical airborne countermeasure deployment angles. Finally, but of foremost technical significance, nonmechanized assault breaching operations require not just a small cleared pathway, they require a continuous path that is wide enough for

combat-loaded personnel to traverse while under direct enemy fire, under all environmental combat conditions—day or night.

As a result of these operational requirements, APOBS Warhead Designers had to overcome significant technical problems:

- ◆ **Blast resistant mines**, to say the least, are blast resistant.
- ◆ **Wire obstacles** are strong, with very low cross-sectional and surface areas, making them blast resistant.
- ◆ **Soil** is a great ablative material that protects buried mines and buried metallic wire supports.
- ◆ **Blast effects** take the path of least resistance and, most often, away from the intended target.
- ◆ **Fragments** travel underground very inefficiently.
- ◆ **Targets** with very low cross-sectional and surface areas, like wire obstacles and some mines, have a low probability of hit.

But, most important of all technical problems,

- ◆ **The Warhead** had to be lightweight but at the same time very powerful to ensure that a two-man team could transport and deploy APOBS to create a continuous path wide enough for combat-loaded personnel to traverse while under direct enemy fire.

APOBS had to be lightweight and neutralize antipersonnel mines and obstacles exceedingly well to be suitable for use in support of nonmechanized assault breaching operations. Additionally, successful assault breaching operations must also negate the enemy forces' ability to control the battlefield. Historically, obscurants and overwhelming fire

support have been the traditional means to achieve this objective. The Marine Corps created a better vision. They envisioned APOBS not only to provide a superb clearance capability while being lightweight, but they also recognized the operational significance of performing the assault breaching of antipersonnel mines and obstacles from a lifesaving standoff from the enemy-controlled obstacle field.

To effect optimal standoff, the APOBS System Engineer traded standoff versus payload, resulting in a standoff of approximately 35 m, with a 45-m long, fragmenting-warhead line charge. Using the 35-m standoff and the inherent standoff provided by the 45-m long line charge, the assault breaching team gained 80 m of lifesaving standoff, which when employed in combination with obscurants and overwhelming fire support, negates the ability of the enemy forces to control the battlefield. Using APOBS, the assault breaching team gained the ability to use 80 m of the battlefield terrain to their full advantage. For example, an assault breaching team facing a 20-m long mine and obstacle field can select an APOBS standoff firing location up to 60 m away from the enemy-controlled obstacle field. A tree stump, a large rock, a sand dune, or a ravine becomes a lifesaving parapet, and for this example, provides 60 m of lifesaving standoff from enemy-controlled positions.

The Marine Corps also recognized that—in the battlefield—speed is life. As a result, the APOBS System Engineer and Safety Engineers traded off designs until a design was reached that balanced combat operational safety versus system complexity and the inherent need for ease of use while under direct enemy fire. The trade-off resulted in a safe, simple, and highly reliable fuzing system that provides outstanding shipboard safety and minimizes system employment times. During operational test conditions using inert systems, APOBS was employed in under 30 s. Live system tests showed that APOBS could be safely deployed in less than 60 s.

Once the APOBS development team completed their task, the resulting weapon system was found to be far superior to the previous nonmechanized assault breaching methods.

A COMPARISON

As shown in Table 1, manual breaching methods impose an extremely heavy human toll because of the lack of standoff and the extremely high-employment engagement times that result. For example, a 12-man assault breaching team under average conditions of visibility and moderate enemy activity (with normal use of artillery support, substantial suppressive fire, and the use of obscurants to protect the assault breaching team) will require approximately 50 min to clear a 45-m safe pathway using probes and wire cutters.

As a result of this clearly unacceptable situation, the Bangalore Torpedo was introduced more than 60 years ago. However, using the Bangalore Torpedo, shown in Figure 3, still represented a heavy human toll because of the lack of standoff from enemy-controlled positions, the payload weight of 390 lb, and the high-employment engagement times that result. A 12-man assault breaching team under the aforementioned average conditions will require 390 lb of Bangalore Torpedoes and approximately 15 min to clear a 45-m pathway.

Although, the Bangalore Torpedo reduced employment time from 50 to 15 min when using a 12-man team, the Bangalore Torpedo still provided no standoff and required the hauling of 30 M1A2 Bangalore Torpedoes consisting of 390 lb of mostly Composition B and TNT, melt-cast explosives that have shown to detonate reliably when exposed to standard issue rifle and machine-gun fire. If one Bangalore Torpedo detonates during employment, either due to direct enemy fire or due to the inadvertent actuation of a mine while pushing together the 45 m of Bangalore Torpedoes, the assault breaching team will not survive.

Note that for assault breaching methods like manual breaching and the Bangalore Torpedo, employment time is a function of manpower. Based on the data in Table 1, Table 2 illustrates how these methods compare to APOBS on an equal manpower basis.

As noted above, APOBS marks a technological breakthrough by being the first man-portable assault breaching system that provides a standoff from its firing position to the enemy-controlled

Table 1—Breaching Method Comparison (45-m long by 0.6-m wide safe pathway)

BREACHING METHOD	SYSTEM WEIGHT (lb)	STANDOFF DISTANCE (m)	EMPLOYMENT TIME (MAN-MIN)
Manual Probes, Detectors, and Wire Cutters	Insignificant	None	594 ¹
M1A1 or M1A2 Bangalore Torpedo	390	None	180 ¹
AP OBS MK7 Mod 1	120	Minimum: 35 Maximum: 80 ²	2

¹ Reference: FM 5-34, Engineer Field Data, Sep 1987

² Note: Maximum distance is a result of (a) the minimum 35-m standoff from the firing position to the APOBS Rear Fuze and (b) the inherent standoff provided by a 45-m long line charge.

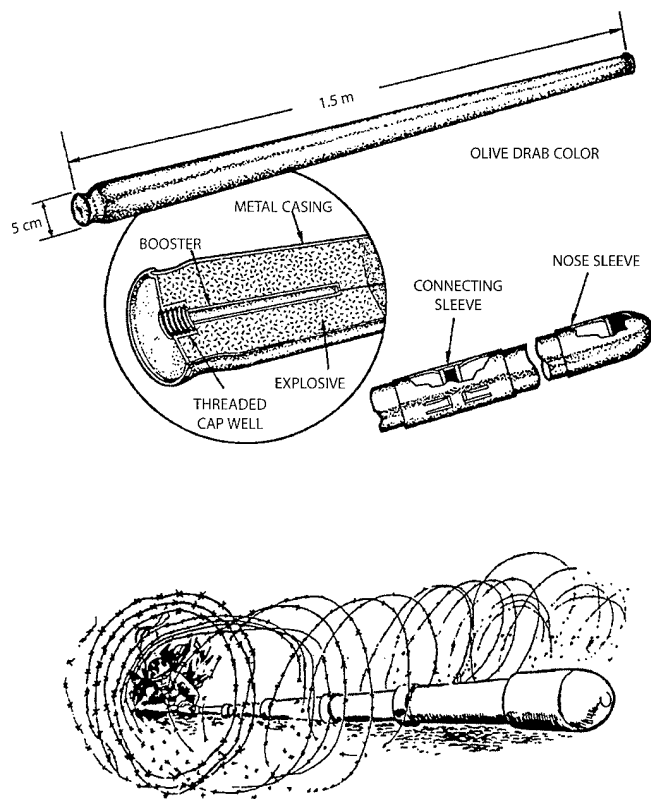


Figure 3—Bangalore Torpedo

obstacle field. APOBS also marks a second and prestigious technological breakthrough by being the first explosive weapon system to meet all the IM system requirements of NAVSEAINST 8010.5. As a result, APOBS eliminates, with IM design features, the real and serious threat of warhead detonation due to direct enemy fire during assault breaching operations. APOBS' ingenious and innovative IM warhead technology meets all IM system requirements, while packing a powerful punch capable of clearing a 45-m long by 0.6-m wide safe pathway through both antipersonnel mines and wire obstacles:

- ◆ Using a 100-lb distributed warhead (120-lb total system weight) rather than 390 lb for the Bangalore Torpedo
- ◆ Requiring 60 s to employ rather than 5,400 s as with the Bangalore Torpedo
- ◆ Providing at least a 35-m standoff, rather than none

Table 2—Breaching Method Comparison Using a Two-Man Assault Breaching Team
(45-m long by 0.6-m wide safe pathway)

BREACHING METHOD	SYSTEM WEIGHT (lb)	STANDOFF DISTANCE (m)	EMPLOYMENT TIME (TOTAL MIN)
Manual Probes, Detectors, and Wire Cutters	Insignificant	None	297 ¹ (Null Option)
M1A1 or M1A2 Bangalore Torpedo	390	None	90 ¹
APOBS MK7 Mod 1	120 (30% of 390)	Minimum: 35 Maximum: 80 ² (35/0 = + ∞) ³	1 (1.1% of 90)

¹ Reference: FM 5-34, Engineer Field Data, Sep 1987

² Note: Maximum distance is a result of (a) the minimum 35-m standoff from the firing position to the APOBS Rear Fuze and (b) the inherent standoff provided by a 45-m long line charge.

³ Note: APOBS marks a technological breakthrough by being the first U.S. nonmechanized assault breaching weapon system effective against both antipersonnel obstacle mines and obstacles that provides an operationally significant standoff distance of 35 to 80 m.

SYSTEM DESCRIPTION

The APOBS MK7 Mod 1, shown in Figures 4 and 5 ready for firing, is a two-man, backpack-trans-portable explosive weapon system designed to destroy antipersonnel mines and wire obstacles during assault breaching operations, without the need of mechanized support. APOBS consists of the following components:

- ◆ A Rocket Motor and Front Fuze Assembly
- ◆ A Front Backpack Assembly containing 60 fragmentation grenades, equally spaced along a 25-m detonating cord and Nylon Rope Line-Charge Assembly
- ◆ A Rear Backpack and Rear Fuze Assembly, containing 48 fragmentation grenades equally spaced along a 20-m detonating cord and Nylon Rope Line-Charge Assembly
- ◆ An extruded aluminum system shipping and storage container

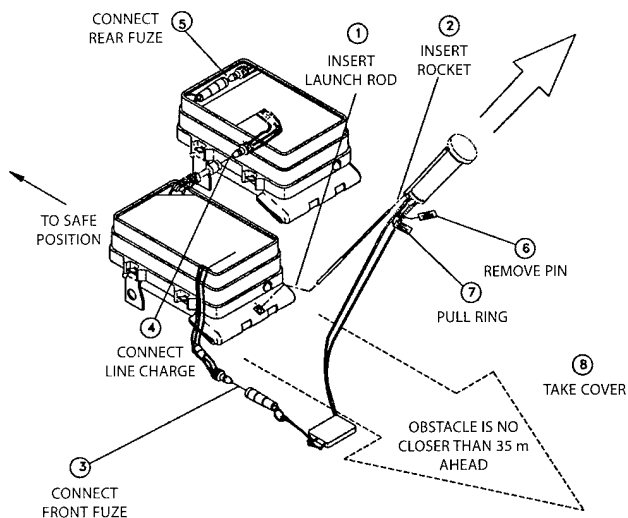


Figure 4—APOBS MK 7 Mod 1



Figure 5—Ready to Fire APOBS

APOBS can be deployed using either command or delay-mode initiation of the rocket. Rocket launch provides the necessary setback forces to arm each fuze subsystem and initiate a pyrotechnic delay therein. After rocket launch the system flies over and drapes across the mine and obstacle field, as shown in Figures 5 through 9. Figure 6 shows the launch phase of APOBS deployment, with the Rocket Motor and Front Fuze Assembly in clear view, and the Front and Rear Backpack Assemblies somewhat obscured by the Rocket Motor Igniter/Thruster exhaust plume.

To minimize man-weapon separation distance requirements, the APOBS design team, through the manipulation of external and internal ballistics and unorthodox energy absorption mechanics, designed APOBS such that it creates a very small launch

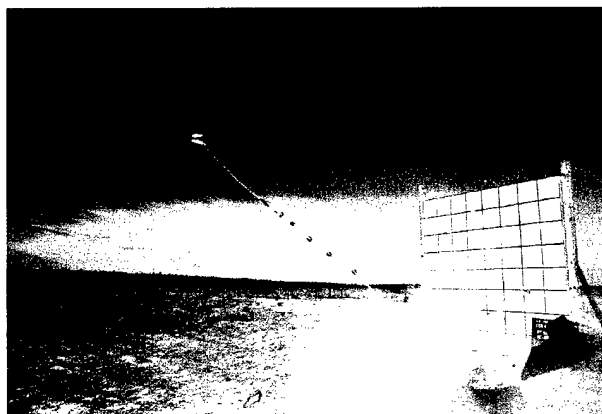


Figure 6—Launch

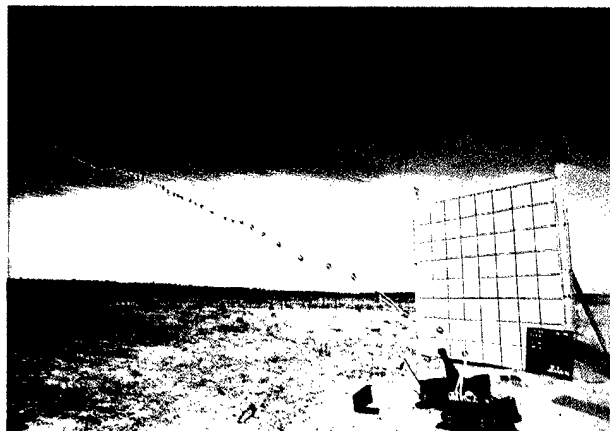


Figure 7—Rocket Motor Burnout



Figure 8—Rear Backpack Liftoff

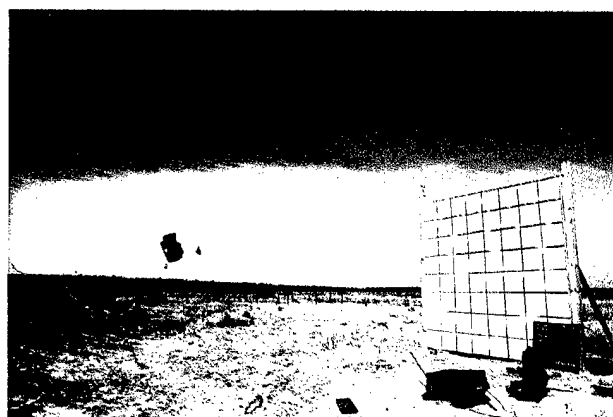


Figure 9—Landing Phase

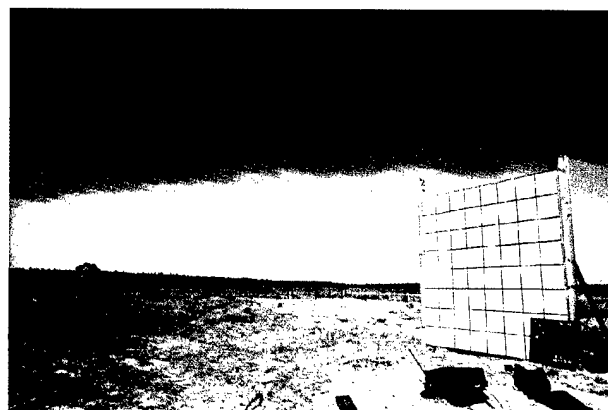


Figure 10—APOBS Landing

signature. Figure 6 shows in detail the extremely small launch signature, allowing the user to remain very close to the system during its deployment process. This would be useful if APOBS is being fired from a protected position such as a tree stump or a large rock. Figure 7 shows rocket motor burnout, indicated by the puff of black smoke. Figure 7 also shows the Front Line Charge Assembly in full flight, with the Rear Line Charge Assembly evolving into its deployment process. By comparing Figures 6 and 7, the extremely small launch signature of APOBS is readily apparent.

Figure 8 shows the instance of Rear Backpack Assembly takeoff with the Rocket Motor and Fuze

Assembly faintly in sight, the warhead in full flight, the Rear Fuze Assembly in clear view, and the Parachute Assembly in its final stage of deployment prior to full inflation. Figure 9 shows the Rear Line Charge Assembly just prior to landing, with the Parachute Assembly fully inflated and acting as a drogue, with the Rear Backpack Assembly in full flight. Figure 10 shows the line charge fully deployed over the wire and mine obstacle field, with the parachute still in flight, and the Rear Backpack Assembly just prior to ground impact.

Although APOBS is designed to produce an extremely small launch signature, once the takeoff thrusting phase is over, deployment is rapid. Note

that Figure 10 shows that APOBS has already landed before some of its foam packing material has had a chance to land beside the remaining Front Backpack Assembly, despite the fact that—as shown by Figure 8—the foam packing material is not propelled very high at all.

Detonation of APOBS is automatic. Detonation of the warhead provides the necessary environment required to clear a lane through antipersonnel mines and wire obstacles using the lightest possible warhead and while allowing the Field Commander to expose the fewest number of personnel for the least amount of time to enemy fire. Figure 11 shows a cleared lane through a triple standard concertina wire obstacle. The significant clearance shown in



Figure 11—Cleared Lane

Figure 11 is impressive when compared to the obstacle shown in Figure 1. Figure 12 shows APOBS Front and Rear Backpacks faintly in the background, with follow-on assault breaching forces negotiating an APOBS cleared lane, which was marked by the initial assault echelon following standard assault breaching doctrine. Figures 13 through 15 show the power of APOBS when detonated.

WEAPON SYSTEM DESIGN FEATURES

APOBS subsystems and components (detonating cord, fuze, rocket, grenades, clamps, strength members and backpacks) are all integrated to provide a lightweight, powerful, and reliable mine

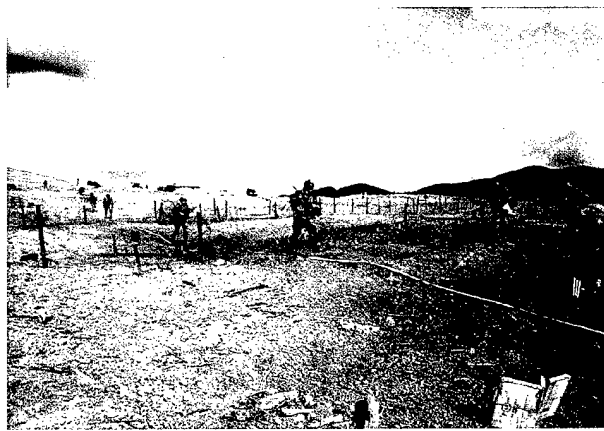


Figure 12—Forces Negotiate APOBS Cleared Path

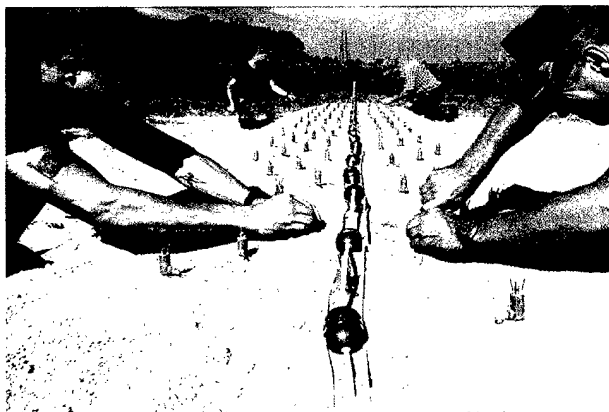


Figure 13—APOBS Warhead Effects

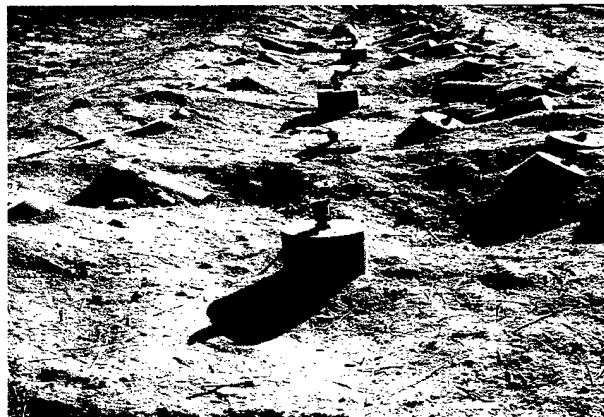


Figure 14—APOBS Warhead Effects

clearance tool. The APOBS team developed many innovations over a period of about six years. The primary driver behind many of the innovations resulting from the APOBS Program was the objective of meeting the requirements of the IM Program of NAVSEAINST 8010.5. This directive delineates numerous goals to make weapons safer to store, transport, and use. Unfortunately, IM goals are nearly impossible to attain in any weapon system.

weave of Type II and Type III polyamide yarns specifically designed for APOBS. This weave is used to enhance the physical properties of the line-charge explosive material and reduce the incidence of material degradation during storage and handling. Over the polyamide yarn weave, a silicone rubber sheath runs the length of the detonating cord to provide environmental protection to the PBXN-8 explosive. Finally, over the rubber sheath is a weave



Figure 15—Additional APOBS Warhead Effects

The basic APOBS IM building block was the detonating cord, which is used to transfer detonation from the fuzing subsystem to the warheads distributed along the line charge. The APOBS detonating cord consists of a specific physical and chemical construction in order to minimize sensitivity to initiations while ensuring reliable explosive transfer during an intended deployment. The detonating cord uses explosive PBXN-8, a new booster explosive developed and type qualified by the APOBS team to provide maximum insensitivity to unintentional initiation, yet also provide for powerful detonation transfer during intentional initiation. Around the explosive is an integrated

of Polyamide Yarn Type I that adds structural stability and protection to the assembly. The combination of polyamide yarns and rubber sheathing provide for structural integrity over storage and operational temperature and humidity extremes. The composite of materials limit the strain that can be imposed upon the explosive found at the center of the detonating cord. Another effect of this particular construction is the direct containment of the shock wave that is produced within the detonating cord during intended function. Sufficient material properties were engineered into the design to reliably control the detonation process of the detonating cord such that it reliably propagates from

one end of the detonating cord to the other while remaining insensitive to unintended sources of initiation. In fact, if the PBXN-8 explosive was not contained in such a fashion, propagation of the detonation wave front would prove much less reliable, and as result, the detonating cord would have to be made from a much more sensitive explosive and, therefore, unable to meet IM requirements.

Once the fuze subsystems have reliably initiated the detonating cord, the cord in turn initiates the APOBS warheads, which are powerful and insensitive. The grenade assembly makes use of innovative design to ensure compliance with IM requirements and provide powerful blast and fragmentation effects. The grenades consist of hollow shells formed from steel sheet and coated with zinc phosphate in order to mitigate corrosion potential in humid salt water environments. The hardness of the shell ensures that critical explosive warhead performance requirements are attained during detonation, ensuring specific blast and high-velocity fragmentation effects to be imparted against mines and obstacles. Thickness, material, and hardness of the grenade assembly were designed in such a fashion as to provide maximized fragmentation mass and velocity, and direct blast energy as necessary to effect simultaneous mine and wire obstacle obliteration.

Pursuing insensitivity and increased performance, the APOBS team also developed and type qualified a new main charge explosive, PBXN-9, providing unmatched insensitivity to unintentional initiation and powerful detonation effects during intentional initiation. Due to the high insensitivity of PBXN-9, the Grenade Assembly houses a Booster Pellet made from a previously developed insensitive (plastic bonded) Booster Explosive PBXN-5. Both the booster and main charge explosives are even more insensitive than the detonating cord used to initiate them. This means that it is virtually impossible to detonate the APOBS warhead unintentionally. To detonate the APOBS grenades, the already insensitive and powerful detonating cord that runs through the center of each grenade must be initiated in proper fashion to achieve the requisite detonation velocity needed to detonate the grenade assembly.

Low-order burning or deflagration of the detonating cord, for example, due to slow or fast cook off environments, will not detonate the APOBS grenade. This effect makes APOBS an extremely safe tool to use since it is not susceptible to detonation singularly or in mass due to enemy arms fire and burning risks associated with war and accidents. This means that APOBS can be stored, transported, and used during wartime and peacetime operations at an unprecedented level of safety for a Class A explosive weapon system.

Another significant technical innovation provided by APOBS is the use of Man-Rated Pyrotechnic Devices to effect explosive weapon system safety. Rather than using mechanical devices of limited conventional reliability (0.99) to preclude premature arming and to preclude premature detonation, the APOBS design team borrowed highly reliable Man-Rated Pyrotechnic Device technology proven in countless aircrew escape systems and NASA Space Shuttle missions. Man-rated pyrotechnic device technology provided several benefits never before realized in a general demolition explosive weapon system:

- ◆ Extremely reliable (0.9999) and accurate pyrotechnic time-delay components proven to meet minimum time-delay requirements, within six standard deviations of the mean functioning time, after environmental exposure, with no lot-to-lot variability, over a temperature range of -25 °F to +125 °F
- ◆ Aerospace quality time-delay pyrotechnic detonators, providing accurate, long delay times (15 s) using very compact delay elements

The APOBS team used a simple and cost effective approach to explosive weapon system safety. The Rocket Motor Assembly contains a Man-Rated Pyrotechnic Device to preclude motor ignition, allowing sufficient time for the APOBS firing team to reach man-weapon separation distance. Upon deployment, both APOBS fuzes arm, and a second Man-Rated Pyrotechnic Device precludes a midair

premature detonation. Using this novel and simplistic approach, weapon system safety was effected using commercial off-the-shelf (COTS) technology.

APOBS Man-Rated Pyrotechnic Devices (Rocket Motor Delay Cartridge Initiator and Front and Rear Fuzes) are proprietary designs of Roberts Research Laboratory, developed by the Roberts Research Laboratory for the APOBS team using COTS technology. APOBS Man-Rated Pyrotechnic Devices were found to be extremely safe, reliable, and cost effective. Using COTS solutions eliminated development costs and helped the Government reap production costs savings by using items already in production for other applications.

EPILOGUE

The fielding of APOBS is a very significant achievement. APOBS, in addition to being a powerful clearance tool, is also extremely insensitive. APOBS is so insensitive that it will not detonate even upon penetration from a 20-mm armor-piercing round. In fact, APOBS is the first and only weapon system in the world to meet all IM Certification Requirements. What this means to a soldier emplacing the system while under direct enemy fire is immeasurable.

The APOBS team now turns its attention toward producing this system and supplying it to Army and Marine Corps expeditionary forces around the world. Additionally, many NATO allies have

expressed keen desire in purchasing the system to meet their own assault breaching requirements, and in support of administrative and humanitarian mine-clearance interests.

CSS, as DA for APOBS, maintained continuous liaison with the Navy's Weapon System Explosives Safety Review Board (WSESRB) and the Army's Fuze Board during development and transition to production. The APOBS Program instituted many safety innovations and shared them with the Defense community. During the final Explosive Weapon System presentation to the WSESRB, seeking concurrence for a Milestone III Approval, the WSESRB commended the APOBS Program "for establishing and performing an excellent system safety program and the commitment of the program manager and program personnel to the safety of APOBS."

CSS personnel were instrumental to innovation within the APOBS Program by establishing fabrication facilities and procedures, implementing strict quality assurance processes, as well as originating many of the innovations that resulted in the APOBS line charge. Many of these innovations are now pending patent by the U.S. Patent and Trademark Office. It is anticipated that commercial enterprises will seek arrangements with the U.S. Navy in order to transfer this technology for other administrative and humanitarian demining uses.

The authors congratulate and express gratitude to the entire APOBS team for their unrelenting commitment to excellence, and for a job well done. Bravo Zulu!

THE AUTHORS

MR. ROBERT C. WOODALL, JR.



Mr. Robert C. Woodall, Jr., is a systems engineer employed at CSS in Panama City, Florida. He received a B.S. degree in mechanical engineering from the University of Maryland, Baltimore County, in May 1989. Employed with NSWCCD since 1988, Mr. Woodall has nurtured a broad background in weapons engineering and has been instrumental in the success of several weapon system development programs. He was a major player in the development and fielding of the "Torch" series of Infrared Antiship Missile Decoys; where he conducted critical failure investigations, led test and evaluation efforts, and implemented numerous design solutions. Mr. Woodall also originated the design for the Launched Expendable Acoustic Device, a torpedo countermeasure launched from the deck of surface combatants. More recently, Mr. Woodall worked as the Systems Engineer and Fuze Program Manager for the successfully completed APOBS Program. Mr. Woodall has received numerous technical excellence and special achievement awards for his contributions. Mr. Woodall has published a number of technical articles, white papers, and official reports that can be found at the Defense Technical Information Center (DTIC). Additionally, he holds five patents and currently has 20 others pending related to innovations in modern expeditionary warfare.

MR. FELIPE A. GARCÍA



Mr. Felipe A. García is a weapons system engineer employed at CSS in Panama City, Florida, supporting concept formulation, system integration, and program execution of command/control/communication weapon systems for amphibious and littoral missions. He received a B.S. degree in chemical engineering from the University of Puerto Rico, Mayagüez Campus, in May 1980. Mr. García's early interest in system simulation, explosives, propellants, and pyrotechnics provided him opportunities as a research assistant during his college years and led him to a job with the Naval Ordnance Station, Indian Head, Maryland, in 1980. There, Mr. García led the SEAWARS Program, in just 2½ years, from concept formulation into production. His technical insight of electronics and electrochemistry resulted in the fielding of the world's first Man-Rated Sea-Water Activated Cartridge Actuated Parachute Release System. In 1983, Mr. García accepted a technical position at the Explosive Ordnance Disposal Technology Center (EODTECHCEN) in support of civilian and military EOD operations. After having the honor of supporting two major national security operations, during Fall 1984, Mr. García accepted a position at CSS, in Panama City, Florida. There, he led the APOBS Program from concept formulation to production. While leading the APOBS Program, Mr. García also led the concept formulations of the SABRE and the Brute-Force Obstacle Breaching programs, weapons systems designed for use during amphibious assault breaching operations. Mr. García has been awarded four patents, one Statutory Invention Registration, a Meritorious Civilian Service Commendation, a Meritorious Unit Commendation, a Citation for Special Achievement in IM Technology, and two Commanding Officer Executive Director (COED) Awards for Special Achievements in Systems Development and Acquisition.

RADIO FREQUENCY COUPLING CHARACTERISTICS OF AVIONICS MEASURED ON A PASSENGER AIRCRAFT AND IN A REVERBERATION CHAMBER

Mr. D. Mark Johnson and Mr. Michael O. Hatfield

A reverberation chamber is a facility used to perform radiated electromagnetic testing, typically at frequencies from 200 MHz to 18 GHz. The operational concept of a reverberation chamber is basically like a very large microwave oven where electronic equipment under test is exposed to microwave radiation from all aspect angles and polarizations without having to rotate the test object.

Until recently, most reverberation chamber testing was Department of Defense (DoD)-related, but today their use is rapidly growing in the mainstream private sector, such as in commercial avionics testing. Demand for reverberation chambers is increasing as testing requirements increase, and companies search for time- and cost-effective test techniques. The Naval Surface Warfare Center, Dahlgren Division (NSWCDD) has pioneered many of the applications of reverberation chambers by testing a wide variety of systems and subsystems to ensure that electronics function properly in their intended environments when needed.

Electromagnetic reverberation tests (funded in part by NASA Langley Research Center) were performed on a decommissioned Boeing 707 aircraft to demonstrate the applicability of reverberation chambers to test avionics installed in commercial aircraft, which fly through high-intensity electromagnetic environments (EMEs). A part of these tests included radio frequency (RF) coupling measurements on selected avionics boxes and a simulated avionics box—when the cockpit, avionics bay, and passenger cabin were excited with RF signals, and mode mixing techniques were used. Follow-on tests with these boxes were performed at the NSWCDD reverberation chamber.

The aircraft and chamber test data are intended to demonstrate that the RF-coupling characteristics obtained on the actual and simulated avionics boxes in a reverberation chamber are representative of the RF-coupling characteristics of those boxes when installed in an aircraft.

INTRODUCTION

Electromagnetic compatibility (EMC) is the ability of an electronic system to function without performance degradation and without causing interference to other electronic devices in its service use configuration. EMC exists when an electronic device operates without performance degradation from exposure to its intended EME and does not contribute interfering electromagnetic energy to its EME.¹ The categories of EMC are:

- ◆ Radiated and conducted susceptibility and emissions
- ◆ Electrostatic discharge (ESD)
- ◆ Lightning
- ◆ Electromagnetic pulse (EMP)

EMC addresses frequencies from dc (0 Hz) to over 40 GHz. Testing to verify EMC is crucial in the design and prototype stages of systems, and is generally a contractual requirement of production configuration systems. Many types of tests and facilities are used in EMC testing. The topic of this article relates to radiated susceptibility testing at frequencies above 100 MHz.

Private industry and the military have both addressed EMC for decades. Historically, though, the military's harsh EMEs, such as those encountered on aircraft carriers and in the battlefield, have necessitated more substantial design and test efforts than those required by industry.

The EME in which military and civilian electronic systems must operate is continually changing in terms of the density of the frequencies intentionally and/or unintentionally emitted, and the intensity of the emissions. Furthermore, the trend in electronics is to produce systems that operate at increasingly higher clock speeds and at increasingly

lower operating voltages. In so doing, electronic devices can become more susceptible and produce more undesired emissions. Avionics on board commercial aircraft are particularly of growing concern because the trend in this industry is to replace previous mechanical functions with electronic functions (e.g., "fly-by-wire" flight controls) and to place these electronic functions under computer control. A further trend is to use greater proportions of composite materials in airframe manufacture. Composite materials generally provide little or no shielding of the electronics from RF energy.

The EME and system design trends underscore the importance of designing in and evaluating electromagnetic immunity. Correspondingly, the number and stringency of EMC test standards and the use of these standards is increasing as is the challenge to perform the required testing within reasonable time and cost schedules. This is particularly true of radiated susceptibility testing at frequencies above 400 MHz.

Reverberation chambers have been used for performing time- and cost-effective radiated electromagnetic susceptibility testing of electronics for over 15 years, especially in the military. As part of a demonstration of the applicability of reverberation chamber techniques for testing commercial avionics, NSWCCD performed measurements of the RF-coupling characteristics of selected unpowered avionics boxes and a simulated avionics box during electromagnetic reverberation characterization measurements on a decommissioned Boeing 707 aircraft.^{2,3} The tests were subsequently repeated with the same unpowered systems positioned in the NSWCCD reverberation chamber. The results discussed in this article are intended to show that the RF-coupling characteristics obtained in the reverberation chamber constitute valid descriptions of the coupling characteristics of those same boxes when installed in an aircraft. Such a demonstration would be expected to support the viewpoint that electromagnetic susceptibility test results of powered aircraft avionics systems obtained in a reverberation chamber are valid descriptions of the avionics when installed in an aircraft.

EME AND RF COUPLING

In general, one can describe the RF-coupling characteristic of a given system under test (SUT) as:

$$\sigma(f, \forall, \theta, \phi) [\text{cm}^2] = \frac{P_{RX}(f, \forall, \theta, \phi) [\text{mW}]}{PD_{INC}(f, \forall, \theta, \phi) [\text{mW}/\text{cm}^2]} \quad (1)$$

where: P_{RX} = power received by instrumenting probe inside or on SUT
 PD_{INC} = power density of incident radiation
 f = frequency
 \forall = polarization of incident radiation
 θ = azimuth angle of incident radiation
 ϕ = elevation angle of incident radiation

Anechoic chambers are a type of electromagnetic test facility that can be used to measure the RF-coupling characteristic of an SUT as a function of frequency, polarization, azimuth, and elevation angle. An example of an RF-coupling measurement made on a twisted wire pair in an anechoic chamber is shown in Figure 1.⁴

While anechoic chambers are useful test tools, detailed coupling measurements (such as shown in

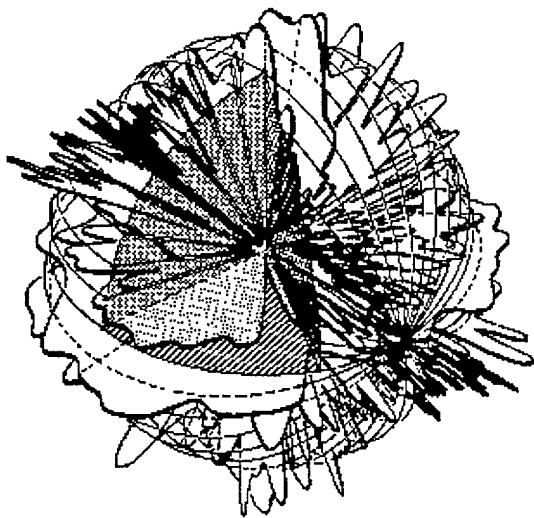


Figure 1—Three-dimensional Graph of RF Energy Coupled to Twisted Wire Pair, Measured in an Anechoic Chamber

Figure 1) are time-consuming. Furthermore, the EME to which aircraft avionics are exposed is not anechoic. The EME within aircraft cavities is complex; i.e., EM energy is contained and reflected within those cavities. The EME of complex cavities is not easily described deterministically; a statistical description is considered more appropriate.

Theory predicts⁵ and measurements support⁶ that the statistical characteristics of the EME are the same in any complex cavity in which a sufficient number of higher-order modes are excited, and adequate mixing techniques are used. Exciting a sufficient number of higher-order modes means the wavelength of the frequency of interest is electrically small compared to the dimensions of the cavity. For the subject of this article, *adequate mode mixing* means one has a method of making substantial changes to the electromagnetic boundary conditions of the cavity. Mode mixing is most commonly accomplished using field-perturbing devices known as paddle wheel tuners. When the conditions of a sufficient number of modes and adequate mode mixing are met, the EME has been shown to be isotropic and randomly polarized. Reverberation chambers, like aircraft cavities, are complex. A result of exposing devices to an isotropic, randomly polarized EME is that directivity effects are lost.⁷ This means that radiation is incident from all aspect angles and polarizations, without having to rotate the SUT. Figure 2 illustrates the qualitative comparison between an anechoic chamber environment and the reverberation chamber environment.

Hence, for an SUT exposed to an isotropic, randomly polarized EME, the RF-coupling characteristic is dependent only on frequency:

$$\sigma(f) [\text{cm}^2] = \frac{P_{RX}(f) [\text{mW}]}{PD_{INC}(f) [\text{mW}/\text{cm}^2]} \quad (2)$$

where: P_{RX} = power received by instrumenting probe inside or on the SUT
 PD_{INC} = scalar power density⁸ existing in cavity where SUT is positioned, derived from an in-band receive antenna measurement

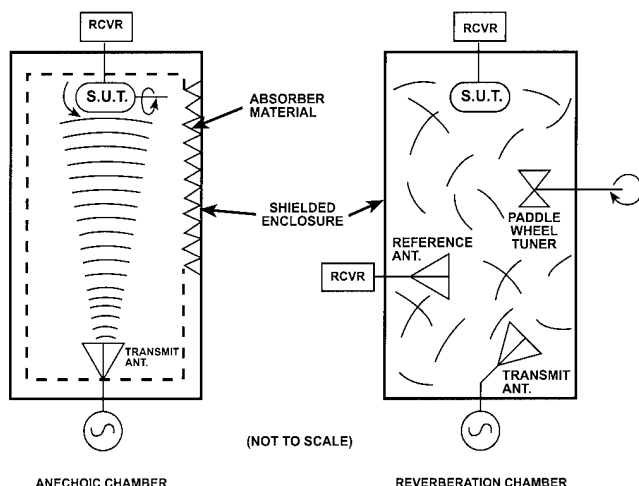


Figure 2—Qualitative Comparison of Anechoic and Reverberation Chamber Electromagnetic Environments

TEST SAMPLES

The RF-coupling measurements were performed on aircraft avionics in two test phases: first on the aircraft, a decommissioned Boeing 707, and then in the NSWCD reverberation chamber.

A total of five boxes from the cockpit instrument panel and avionics bay were extracted for instrumentation prior to testing. For the purposes of this article, only the radar altimeter (RA) will be discussed.

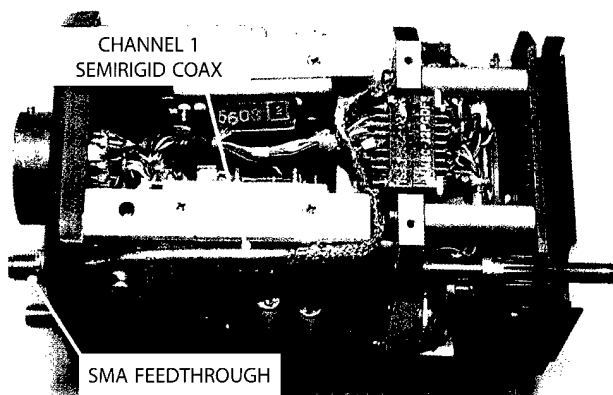


Figure 3—RA Channel 1 Instrumentation

The RA was instrumented to measure the RF energy coupling to an interior wire leading to the aircraft wiring harness (channel 1) and an interior component lead (channel 2).

Instrumentation of the RA was accomplished by drilling two holes at convenient positions on the rear coverplate through which .141-in. semirigid coaxial cable could be routed with SMA feedthroughs. Appropriate lengths of semirigid cable were cut for routing to the point to be instrumented within the RA. Approximately $\frac{1}{4}$ in. of center conductor was exposed at the instrumented end and soldered to a point within the RA. SMA feedthroughs were attached at the opposite end. Details of the channel 1 and 2 instrumentation are shown in Figures 3 and 4.

AIRCRAFT TESTING

RF-coupling measurements to the RA on the aircraft were performed during the Phase II electromagnetic reverberation characterization on a Boeing 707 aircraft. Figure 5 shows the test aircraft at Davis Monthan Air Force Base in Tucson, Arizona; the instrumentation van housing the RF-generating and -measuring equipment, and automating computer can also be seen in Figure 5.

Performing an electromagnetic reverberation test on the aircraft meant treating the cavities as

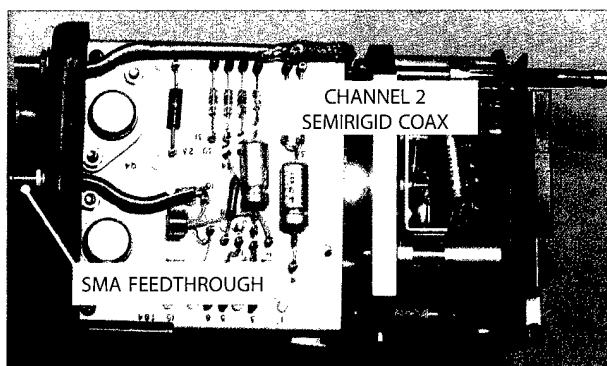


Figure 4—RA Channel 2 Instrumentation

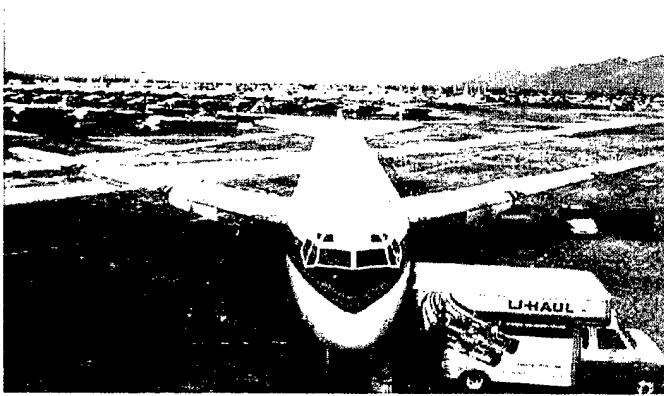


Figure 5—Decommissioned Boeing 707 Aircraft and Test Instrumentation Van

reverberation chambers. Paddle wheel tuners were fabricated on site, and one was positioned in the cockpit. Each paddle consisted of an aluminum-foil-covered, Styrofoam tuner mounted on an aluminum shaft. Each tuner assembly was driven by a shielded dc motor. Figure 6 shows the cockpit paddle wheel tuner. To supply RF signals and dc power to and extract RF signals from the cockpit, holes were drilled in the aircraft skin on the pilot's side of the cockpit. Semirigid coaxial cables with SMA or N-type feedthroughs were then routed through the holes. Figure 7 is a block diagram of the test measurement setup.

Prior to making measurements, the instrumented RA was repositioned in its appropriate location and reconnected to its wiring harness. When the RA was positioned in the aircraft, received power measurements were made in the cockpit. Log periodic antennas were used from 100 MHz to 1.1 GHz, and dual-ridge horn antennas were used for the frequency bands 800 MHz to 2.9 GHz and 2.75 GHz to 6 GHz. During each frequency band excitation, the paddle wheel tuner was continuously rotated as RF signals were transmitted into the cockpit. The RF synthesizer was operated in a stepped-sweep mode. The spectrum analyzer was set to sweep at a much faster rate than the synthesizer sweep.

Received power measurements took approximately 30 minutes per frequency band. Figure 8

shows the power received by the in-band antennas in the cockpit.

When received power measurements with the in-band antennas were completed, semirigid coax receive lines were connected to the channels of the instrumented RA. The sweeps were then repeated using the same settings as during the in-band antenna measurements. The received power measurement for RA channel 1 can be seen in Figure 8 and is representative of the received power data obtained during aircraft testing. All received power measurements were corrected for cable losses and normalized to 0 dBm input power to the cavity.



Figure 6—Paddle Wheel Tuner and Antenna Positioned in 707 Cockpit

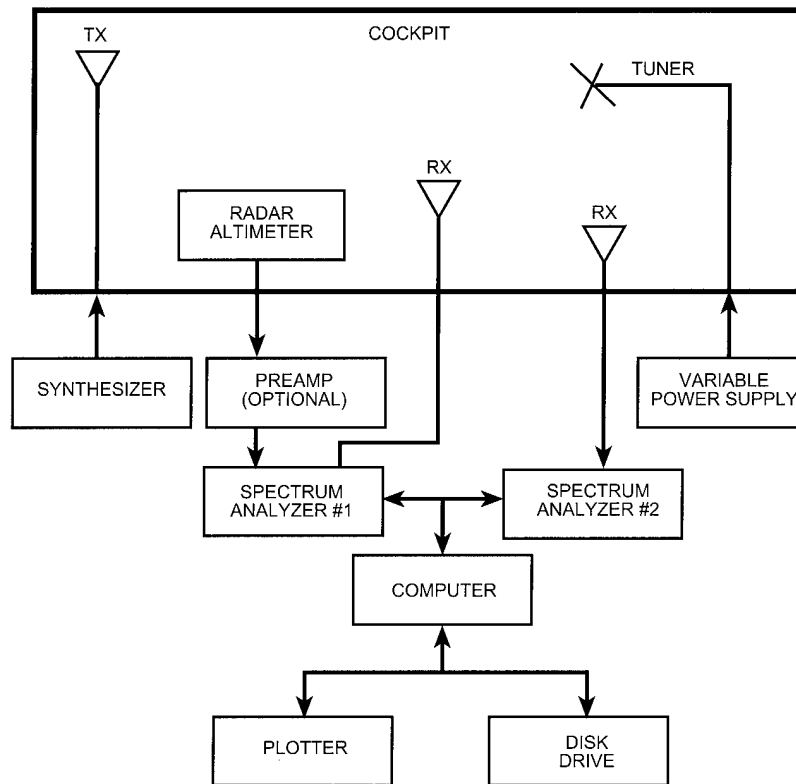


Figure 7—Block Diagram of Aircraft Test Setup

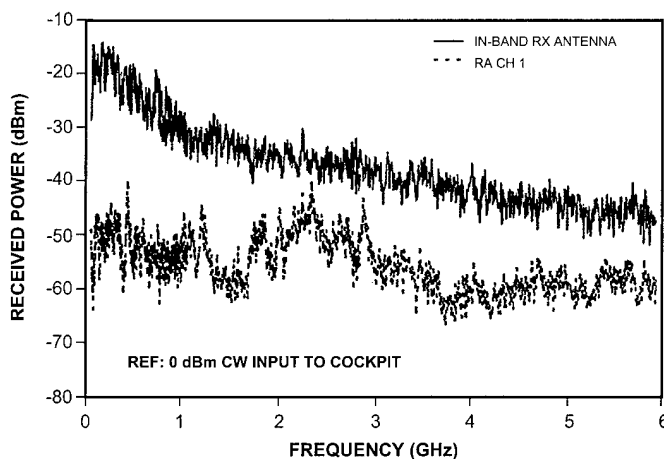


Figure 8—Power Received by RA and In-Band Antenna in Cockpit

REVERBERATION CHAMBER TESTING

When the aircraft tests were complete, the RA with an available length of wiring harness was removed from the aircraft and shipped back to the NSWCDR reverberation chamber.

The NSWCDR reverberation chamber is a 10.82 m × 3.96 m × 5.18 m, RF-tight enclosure constructed of welded solid steel. The chamber has two paddle wheel tuners rotated by means of stepper motors mounted to the chamber ceiling.

The RA, with available lengths of aircraft wiring harness, was tested while positioned on a dielectric block as well as on an aluminum ground plane in the NSWCDR reverberation chamber.

Furthermore, the RA was configured in each of the following variations:

- ◆ Without wiring harness attached
- ◆ With unterminated wiring harness attached
- ◆ With wiring harness attached and terminated in a 50- Ω dummy load
- ◆ With wiring harness attached and shorted to the ground plane

Figure 9 shows the RA configured for testing on a dielectric block in the NSWCDD reverberation chamber.

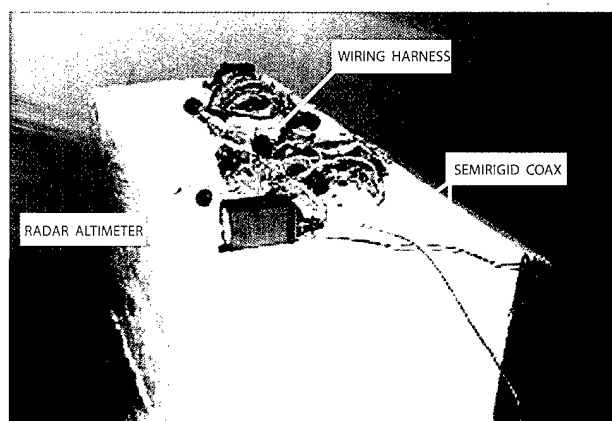


Figure 9—RA Configured for Testing on a Dielectric Block in the NSWCDD Reverberation Chamber

Every effort was made to duplicate the aircraft test setup during reverberation chamber testing. All cables and virtually all the same test equipment used during aircraft testing were employed during reverberation chamber testing. Received power measurements were made using in-band antennas, just as was done during aircraft testing. Figure 10 shows the in-band antenna received power data.

Note that the power received in the reverberation chamber is higher than in the aircraft for the same amount of input power. This is an expected result because the chamber's cavity losses are less than the cockpit's cavity losses. Measurement of the power received by the instrumented channels of the RA

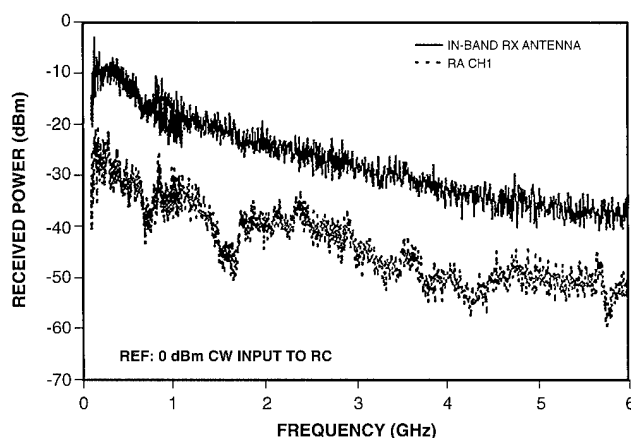


Figure 10—Power Received by RA with Unterminated Wiring Harness on Dielectric Block and In-band Antenna in NSWCDD Reverberation Chamber

were then made for each of the configuration variations described above. Power received by RA channel 1 can be seen in Figure 10, which is representative of the received power data obtained during reverberation chamber testing. All received power data was corrected for cable loss and normalized to 0-dBm input power to the chamber.

COMPARATIVE RESULTS

The RF-coupling transfer function for each instrumented channel of the RA was calculated using the applicable received power data and the derived cavity scalar power density and by applying Equation (2).

The RF-coupling transfer functions for the RA obtained in the cockpit are compared to those obtained in the NSWCDD reverberation chamber as follows:

- ◆ RA channel 1 in the cockpit and on a dielectric block in the reverberation chamber are shown in Figures 11 and 12.
- ◆ RA channel 2 in the cockpit and on a dielectric block in the reverberation chamber are shown in Figures 13 and 14.

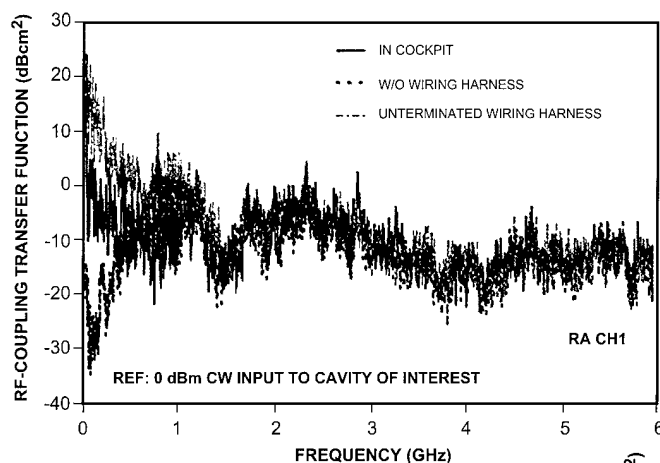


Figure 11—RF-Coupling Transfer Function for RA Channel 1 in Aircraft and on Dielectric Block in NSWCDD Reverberation Chamber

Figure 12—RF-Coupling Transfer Function for RA Channel 1 in Aircraft and on Dielectric Block in NSWCDD Reverberation Chamber

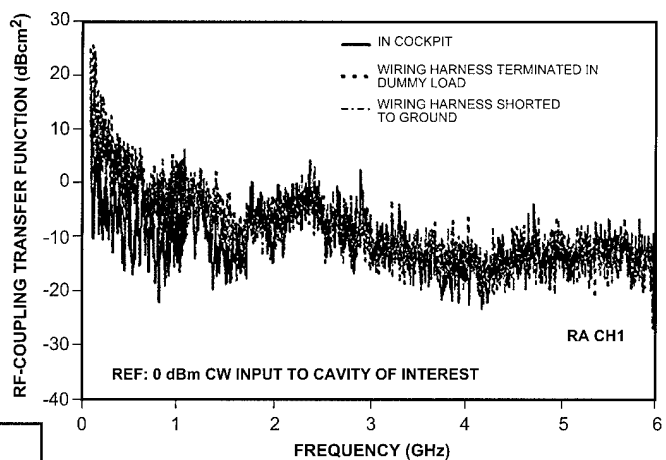


Figure 13—RF-Coupling Transfer Function for RA Channel 2 in Aircraft and on Dielectric Block in NSWCDD Reverberation Chamber

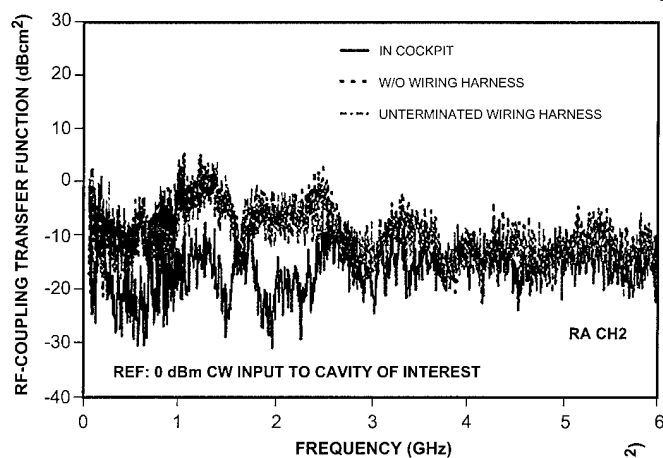
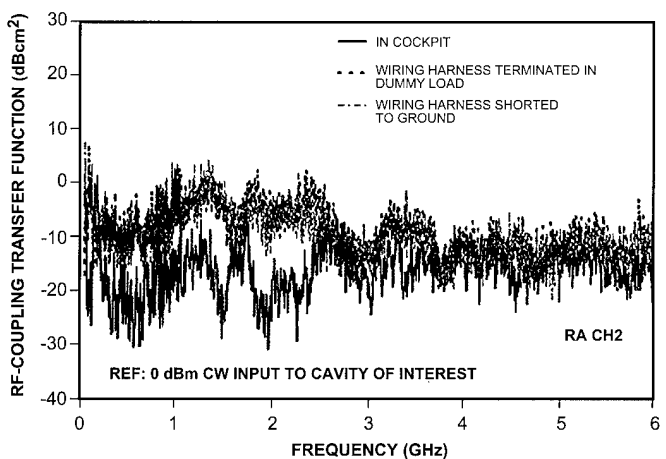


Figure 14—RF-Coupling Transfer Function for RA Channel 2 in Aircraft and on Dielectric Block in NSWCDD Reverberation Chamber



- ◆ RA channel 1 in the cockpit and on a metal ground plane in the reverberation chamber are shown in Figures 15 and 16.
- ◆ RA channel 2 in the cockpit and on a metal ground plane in the reverberation chamber are shown in Figures 17 and 18.

Note that three RF-coupling transfer functions are plotted in each of the RA graphs. Many traces have a large amount of overlap, as the RF-coupling transfer functions obtained typically have excellent agreement.

RESULTS SUMMARY

Summary of the RF-coupling transfer functions obtained for the RA is as follows:

- ◆ Above approximately 1 GHz, the channel 1 RF-coupling transfer function, measured in the reverberation chamber with and without the wiring harness, is an excellent representation of the channel 1 RF-coupling transfer function measured in the aircraft.
- ◆ Below 1 GHz, the channel 1 RF-coupling transfer function measured in the reverberation chamber with the wiring harness bounds the channel 1 RF-coupling transfer function measured in the aircraft.
- ◆ From approximately 300 MHz to 3.7 GHz, the channel 2 RF-coupling transfer function measured in the reverberation chamber with and without wiring harness typically bounds the channel 2 RF-coupling transfer function measured in the aircraft.
- ◆ From 100 MHz to approximately 300 MHz and from 3.7 GHz to 6 GHz, the channel 2 RF-coupling transfer function measured in the reverberation chamber with and without the wiring harness is an excellent representation of the channel 2 RF-coupling transfer function measured in the aircraft.

CONCLUSIONS

RF-coupling transfer functions obtained in a reverberation chamber are an excellent representation of those measured for a variety of avionics systems installed in the cockpit and avionics bay of a large transport aircraft.

Presence of the appropriate wiring harness in the reverberation chamber test setup has the most pronounced effect on the RF-coupling transfer function. The type of harness termination has a distinguishable, but small, effect on the RF-coupling transfer function.

The presence of a ground plane has a distinguishable, but small, effect on RF-coupling transfer function measured in the reverberation chamber.

Testing on a dielectric block in the reverberation chamber yields a reasonable representation of the RF-coupling transfer function.

The authors assert that these RF-coupling results, obtained on unpowered avionics, support the viewpoint that the performance of a powered electronic system tested in a reverberation chamber is an accurate representation of the system's performance in a service-use complex cavity such as an aircraft cockpit. This assertion is also supported by the theoretical and demonstrated statistical equivalence of complex-cavity EMEs, and NSWCCD's experience in testing a wide variety of electronic systems in different types of facilities.

Furthermore, NSWCCD has performed research with a simulated avionics system and demonstrated repeatable susceptibility characteristics of the powered system in several different reverberation chambers. RF-coupling transfer functions were also obtained on the unpowered, instrumented system, in the same way as for the unpowered avionics. The results show the same agreement between RF-coupling transfer functions obtained with the system tested while positioned in the 707 cockpit and when tested in the NSWCCD reverberation chamber.

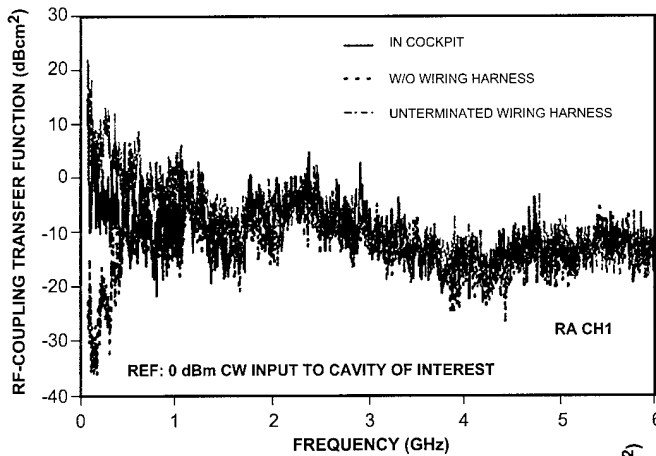


Figure 15—RF-Coupling Transfer Function for RA Channel 1 in Aircraft and on Metal Ground Plane in NSWCCD Reverberation Chamber

Figure 16—RF-Coupling Transfer Function for RA Channel 1 in Aircraft and on Metal Ground Plane in NSWCCD Reverberation Chamber

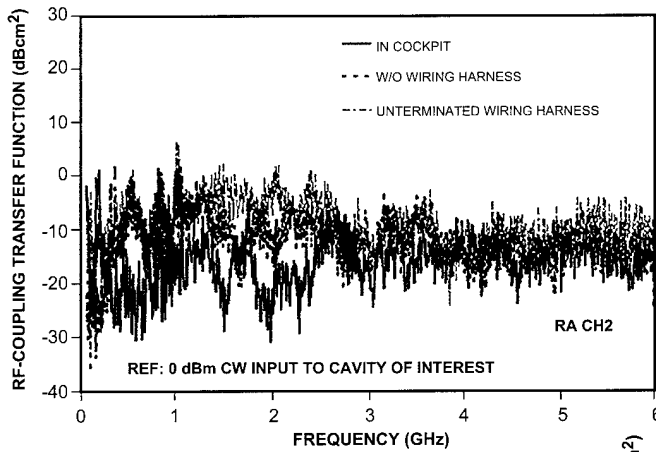
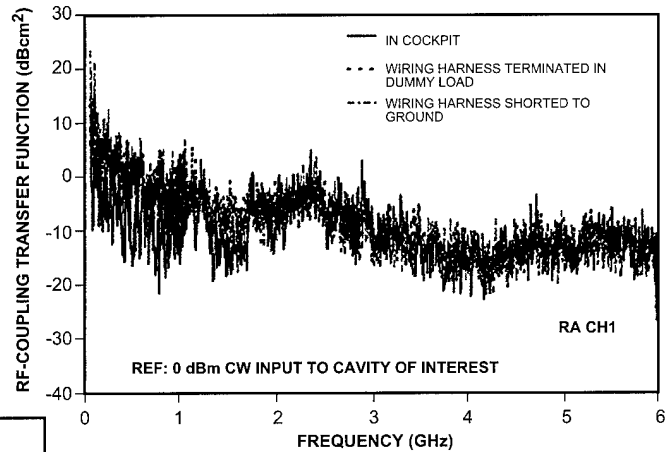
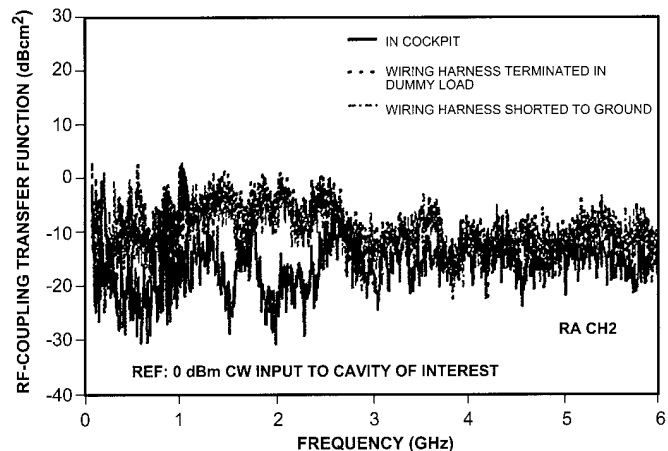


Figure 17—RF-Coupling Transfer Function for RA Channel 2 in Aircraft and on Metal Ground Plane in NSWCCD Reverberation Chamber

Figure 18—RF-Coupling Transfer Function for RA Channel 2 in Aircraft and on Metal Ground Plane in NSWCCD Reverberation Chamber



REFERENCES

1. Ott, Henry W., *Noise Reduction Techniques in Electronic Systems*, J. Wiley & Sons, Inc., New York, 1988.
2. Hatfield, M.O.; Freyer, G.J.; Johnson, D.M. and Farthing, C.L., *Electromagnetic Reverberation Characteristics of a Large Transport Aircraft*, NSWCDD/TR-93/339, Jul 1994.
3. Hatfield, M.O.; Johnson, D.M.; Loughry, T.A.; Ondrejka, A.R.; Johnk, R.T.; Freyer, G.J. and Slocum, M.B., *Phase II Demonstration of the Electromagnetic Reverberation Characteristics of a Large Transport Aircraft*, NSWCDD/TR-97/84, Sep 1997.
4. *Integrated Circuit Electromagnetic Susceptibility Handbook: Integrated Circuit Electromagnetic Susceptibility Investigation—Phase III*, McDonnell Douglas Astronautics Company Report MDC E1929 of 01 Aug 1978.
5. Lehman, T.H., *A Statistical Theory of Electromagnetic Fields in Complex Cavities*, Note 494, USAF Phillips Laboratory Interaction Note Series, May 1993.
6. Freyer, G.J.; Hatfield, M.O.; Johnson, D.M. and Slocum, M.B., *Comparison of Measured and Theoretical Statistical Parameters of Complex Cavities*, presented at the IEEE International Symposium on EMC, Santa Clara, CA, Aug 1996.
7. Crawford, M.L. and Koepke, G.H., *Design, Evaluation and Use of a Reverberation Chamber for Performing Electromagnetic Susceptibility/Vulnerability Measurements*, NBS Technical Note 1092, Apr 1986.
8. J.L. Ladbury, Private communication.

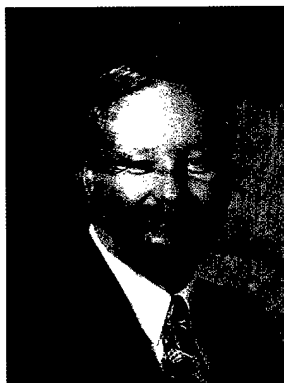
THE AUTHORS

MR. D. MARK JOHNSON



Mr. D. Mark Johnson received his B.S. degree in electrical engineering from the Pennsylvania State University in 1988. He is a candidate for the M.S. in electrical engineering from the Virginia Polytechnic Institute and State University. Mr. Johnson has supported the Systems Electromagnetic Effects Branch at NSWCDD since 1988, until 1996 as a contractor and, subsequently, as a government employee. Mr. Johnson performs or participates in electromagnetic environmental effects testing and analyses of a wide variety of military and commercial systems. Mr. Johnson has experience in performing these testing projects using outdoor ground planes, anechoic chambers, TEM cells and reverberation chambers, although the majority of his work is typically with reverberation chambers. He is also currently participating as the Navy lead for electromagnetic compatibility issues on the EX-171 Extended-Range Guided Munition. Mr. Johnson has presented several papers and authored/co-authored technical reports on topics related to reverberation and anechoic chambers. He is a member of the IEEE EMC Society.

MR. MICHAEL O. HATFIELD



Mr. Michael O. Hatfield received his B.S. degree in electrical engineering from the West Virginia Institute of Technology, Montgomery, in 1979. He has been with NSWCDD since 1979. He was assigned to the Electromagnetic Performance of Aircraft and Ship Systems (EMPASS) project until 1982. Since 1982 he has been in the Systems Electromagnetic Effects Branch where he is in charge of development and operation of the NSWCDD Reverberation Chamber Facility. He is a member of the IEEE EMC Society and has been actively publishing articles about reverberation chambers in the EMC Transactions and at the EMC Symposia since 1988. The IEEE EMC Society awarded Mike the Richard R. Stoddard Award in 1995 for Outstanding Performance and the Laurence G. Cumming Award in 1997 for his work with reverberation chambers.

CONTRIBUTIONS TO THE NAVSTAR GLOBAL POSITIONING SYSTEM (GPS) BY THE NAVAL SURFACE WARFARE CENTER, DAHLGREN DIVISION

Mr. B. Larry Miller, Dr. Bruce R. Hermann, Mr. Everett R. Swift, Mr. Robert W. Hill,
Dr. Alan G. Evans, Mr. James P. Cunningham, and Dr. Jeffrey N. Blanton

This article provides a historical perspective of projects at the Naval Surface Warfare Center, Dahlgren Division (NSWCDD), which contributed directly and indirectly to the development of GPS. Fundamental to these contributions has been the continuing effort to precisely estimate satellite orbit and clock parameters. This work started with the first artificial satellites and continues today. Early work done on the Navy Transit and Timation navigation satellite programs led into the developing GPS program. For the first seven years of GPS operation, NSWCDD generated long-term satellite orbit predictions for the Control Segment. These orbit predictions were updated by the Air Force in near real-time using station tracking data to derive the satellite broadcast messages that enabled real-time user navigation. Since 1985, NSWCDD-developed techniques and software have been used to estimate highly precise GPS orbit and clock parameters for use in geodetic positioning and other military applications. The World Geodetic System 1984 (WGS 84) reference frame in use by GPS was realized by NSWCDD's determination of the operational tracking site antenna locations beginning in 1994. Development of positioning techniques and three generations of GPS receivers, as well as numerous geodetic applications of GPS both supported and were outgrowths of the precise ephemeris work. NSWCDD has supported the incorporation of GPS into satellites, guided missiles, projectiles, and other unmanned vehicles. Precise positioning capabilities have been developed and demonstrated for both test and evaluation (T&E) as well as operational applications. This article reviews all of these developments.

1. INTRODUCTION AND BACKGROUND

By the mid 1960s, NSWCDD (then the Naval Weapons Laboratory) had become a center of expertise in artificial satellite missions and orbit estimation. Earlier work with gun, bomb, and rocket trajectories had established competence in the physical science of *exterior ballistics*. The accurate prediction of ballistic trajectories—especially long-range trajectories—requires the numerical integration of complex differential equations of motion. This need propelled Dahlgren into the development and acquisition of early large electronic computers like the

Naval Ordnance Research Computer or "NORC."¹ During this same time, Dr. Charles Cohen at NSWCDD developed the first six-degree-of-freedom (6-DOF) trajectory simulation and the first rigorous representation of earth's gravity suitable for *geoballistics*, or exterior ballistics on a global scale. Dahlgren became generally recognized as the Department of Defense (DoD) leader for long-range trajectory computations. The ballistics background led to Dahlgren's role in the development of guidance and fire control capabilities for the submarine-launched Fleet Ballistic Missile (FBM) program.² Early satellite work naturally followed. This work included the development, with the Naval Research Laboratory (NRL), of the Naval Space Surveillance System (a tenant facility at Dahlgren, and now part of the Naval Space Command). It also included the development of orbit estimation software for the Navy's new Transit navigation satellite program, which provided worldwide, all-weather navigation support to FBM submarines.

Building on these roles in FBM, space surveillance, and Transit, NSWCDD further developed capabilities for more accurate satellite ephemeris computations and modeling of earth's gravity. The Transit program was based on very accurate measurements of the Doppler shift of signals transmitted by the satellites. Under the direction of Dr. Richard Anderle, NSWCDD not only demonstrated that these measurements could provide the basis for the computation of precise orbits, but also contributed greatly to the development of Satellite Geodesy. By processing Doppler measurements from many satellites simultaneously in a least-squares manner, solutions were obtained for geodetic parameters—such as tracking station coordinates and gravity coefficients—as well as orbit and measurement-related bias parameters. The geodetic parameters obtained in these solutions were the basis for the "World Geodetic System" (WGS), which was adopted for the standard worldwide reference frame by DoD³ and, subsequently, by GPS.

By the end of the 1960s, the need for a three-dimensional, space-based, global navigation system had become apparent throughout DoD. Initial NSWCDD contributions to programs that evolved into GPS began in that time frame with an

assessment of alternative space-based concepts for the Defense Navigation Satellite System (DNSS). DNSS concepts were proposed by all three services. Navy personnel, supported by NSWCDD, met with Air Force and Army representatives in 1973 to develop a joint navigation program that would incorporate the best of all previous proposals. This program became GPS. It included the Navy's concepts of time-based navigation using satellites with constant ground-track orbits, and the Air Force's concept of a pseudorandom noise-coded signal structure. The GPS Joint Program Office (JPO) was formed under Air Force leadership, but with Navy and Army deputies. NSWCDD was tasked (by the Navy deputy) to aid the JPO in areas of constellation design, ephemeris estimation, and geodetic positioning. The Defense Mapping Agency (DMA) (DMA became part of the National Imagery and Mapping Agency (NIMA) in October 1996) was also formed in the early 1970s, and NSWCDD tasking was moved from the Navy deputy to a new DMA deputy in the JPO, where it remained for the formative years of GPS development.

NSWCDD developed earth satellite ephemeris estimation software and used it initially to provide accurate, long time-span trajectories to the GPS Master Control Station, which was originally located at Vandenberg Air Force Base (AFB). The current GPS System Segments are shown in Figure 1. These ephemerides were updated with current tracking data and then uploaded to the satellite's memory, where they became part of the navigation message. In order to obtain this accurate, long-term prediction of the satellite ephemeris, it was necessary to first use observations over some span (usually 1 or 2 weeks) and determine the best-fit trajectory over that observation span. This best fit trajectory (later termed the precise ephemeris) was used in numerous applications. NSWCDD contributed to the development of three generations of GPS tracking stations, which have been used to supply the highly accurate tracking data required for the precise ephemeris. Also, the knowledge and understanding gained from years of processing GPS data have been applied to the navigation and precise positioning of missiles, spacecraft, projectiles, and other dynamic platforms. Geodetic positioning techniques—originally developed to determine precise

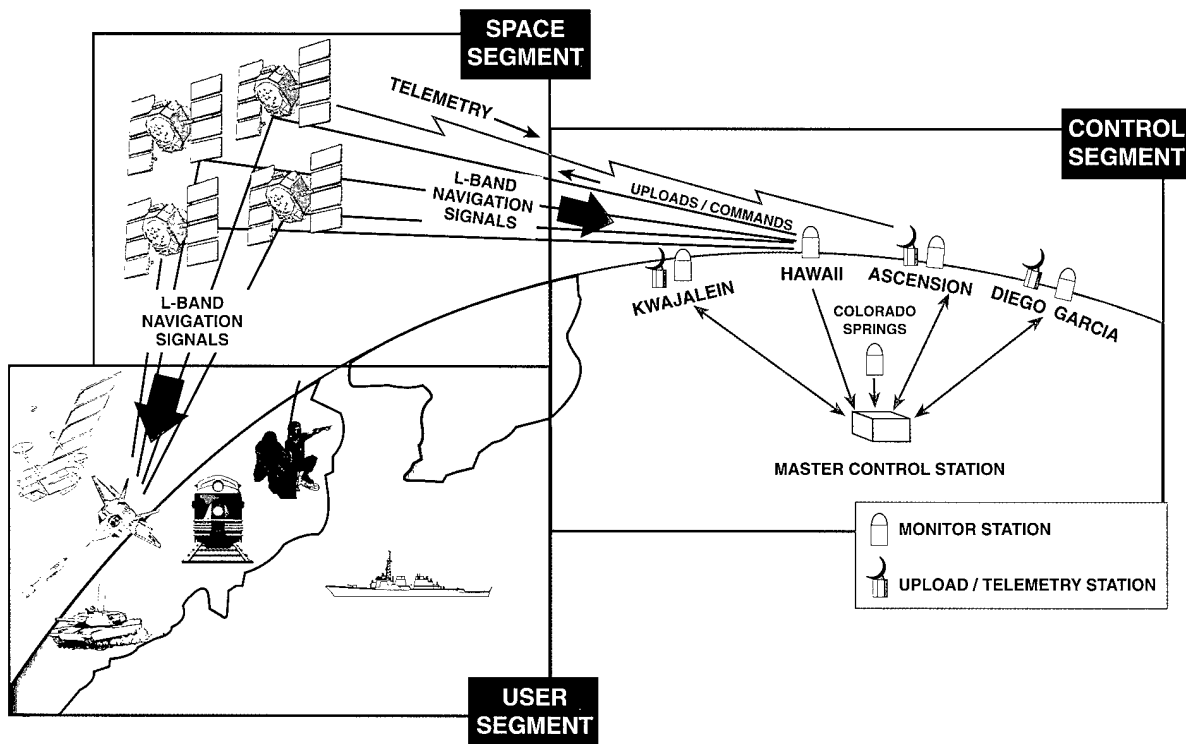


Figure 1—Current GPS System Segments

coordinates of GPS tracking stations—were extended to other less benign positioning problems, for which high accuracy was also needed.

This article describes the historical contributions of NSWCDD personnel to the GPS program. It should be noted that the technology described here—even though it spans three decades and has transitioned to many military and industrial applications—continues to be developed within NSWCDD.

2. CONSTELLATION ANALYSIS

Detailed constellation design studies were begun by NSWCDD in the late 1960s in support of the NRL Timation program and for the proposed DNSS. The primary goal of these studies was to help design a satellite system that would provide *global* navigation coverage. The Navy preferred a lower-altitude navigation system as an easier transition from the Transit system and recommended a constant ground-track constellation with a period of

about 8 hours. A sidereal orbital period of 12 hours was selected as a compromise between the Navy recommendation and the Air Force concept of geosynchronous orbits. Circular orbits were chosen so that the satellite signal level would remain relatively constant as seen from anywhere on the ground. After many studies, a baseline constellation of three equally spaced planes, inclined by 63 deg to the equator, with 8 satellites in each plane—making a total of 24 satellites—was selected.

In 1980, the NAVSTAR GPS Block II operational phase was approved; however, Congress mandated an 18-satellite constellation, which was to be Space Shuttle launched. This would require an orbital inclination change from the desired 63 deg to the Shuttle/Cape Canaveral geographic maximum of 55 deg. The JPO decided on a constellation of six equally spaced planes, with three satellites in each plane. Simulations conducted at NSWCDD, the Aerospace Corporation, and other DoD organizations demonstrated that this mandated constellation would have periodic areas of degraded accuracy. As a result of these studies and the Challenger disaster,

the congressional mandate was relaxed in 1988, and a constellation of 21 satellites, plus 3 active spares, was authorized. The JPO decided to put four satellites into each of the six planes (see Figure 2). The 55-deg inclination, however, was kept to accommodate launches from Cape Canaveral.

3. EPHEMERIS PREDICTION FOR THE BROADCAST MESSAGE

NSWCDD involvement as part of the original GPS Control Segment began in the mid-1970s. The mission of the Control Segment was to operate the satellite constellation. This included maintaining ground-based tracking and upload stations for communication to and from the constellation. The tracking stations (initially located at Alaska, Hawaii, Guam, and Vandenberg AFB) received the satellite signals in the same manner as any user. The data were recorded and transmitted to the Master Control Station at Vandenberg AFB. The latest observations were integrated with a precomputed, predicted satellite ephemeris for each satellite to produce more accurate predictions. The improved ephemerides were then transmitted to the upload station at Vandenberg and, ultimately, to the satellites as they came into view. The improved ephemeris then became the broadcast ephemeris that was a component of the satellite navigation message employed by all navigation users to compute the satellite position.

The GPS ephemeris determination was designed as a two-stage process.⁴ In stage one, GPS tracking network pseudorange measurements, spanning 1 to 2 weeks, were processed at Dahlgren. This processing used an NSWCDD-developed program called CELEST to produce accurate state vectors.

The CELEST orbit computation program had originally been developed to support low-altitude and Transit satellite orbit estimation.⁵ The software was modified to handle both GPS-tracking data types: pseudorange and range difference. CELEST was a batch, weighted least-squares, single-satellite processing program. GPS satellite reference trajectories, spanning 18 days were predicted from these state vectors. In stage two, near real-time observations were used in a sequential (Kalman) processor at the GPS Master Control Station at Vandenberg to determine reference trajectory corrections and associated clock behavior

parameters. These corrections were then propagated along the reference trajectories for about a day to create the satellite upload ephemerides. Stage one of the process was accomplished at Dahlgren for the first 7 years of GPS development.⁶

The modified stage one CELEST was first tested using tracking data from the Navigation Technology Satellite 2 (NTS-2), which was designed and built at NRL, and launched 23 June 1977.

The differences between NTS-2 and subsequent Navigation Development

Satellites (NDS) (later renamed Block I satellites) prevented a complete testing of the GPS concepts. However, the NTS-2 CELEST tests did provide preliminary validation of the stage one process. One significant product of these tests was the verification at NSWCDD of a predicted satellite frequency bias arising from a combination of time dilation predicted by special relativity and a frequency shift predicted by general relativity.⁷

After the launch of the first four Block I satellites in 1978, earlier estimates of errors in the stage one reference trajectories of less than 10 m per day

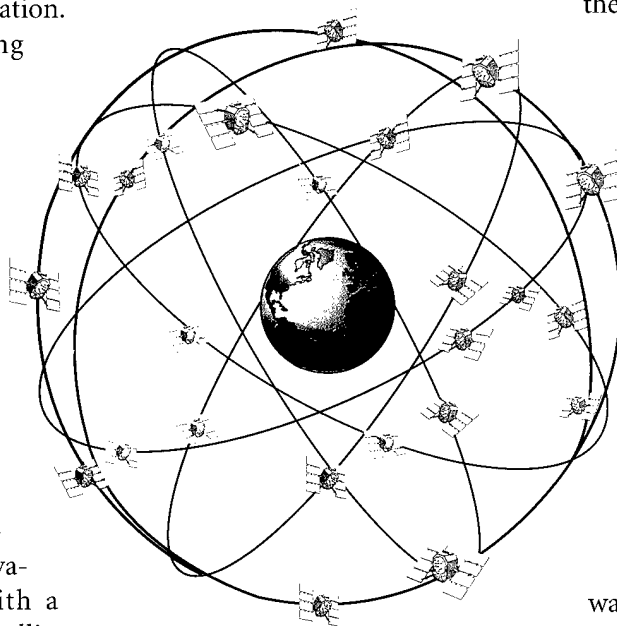


Figure 2—GPS Operational Constellation

proved to be optimistic. In fact, the errors were routinely greater than 100 m per day. Fortunately, the stage two Kalman filter was robust enough to accommodate these larger errors. Some of the error was eliminated in 1979 with a change in satellite momentum dump procedures. In 1980, after extensive analysis by NSWCDD, the Aerospace Corporation, and IBM, it was determined that an empirical acceleration parameter—along the solar array axis (termed the “Y bias”)—could absorb much of the remaining error in the stage one process.

As the number of GPS satellites increased, the overhead of using CELEST on the Control Data Corporation (CDC) mainframe for the reference trajectory generation operations became excessive. To alleviate this problem, an interactive, weighted least-squares, single-satellite processing capability called the new system of programs (NSOP)⁸ was developed in 1981. It used the CELEST orbit integrator but did all the editing, normal equation formation, and solutions with new code. It featured graphical displays of data residuals and the use of backward predictions to evaluate the quality of the orbit fits and forward predictions. With this system in place, the error rates were reduced to less than 10 m per day,⁹ and the operations streamlined so that 41-day reference trajectories could be generated every other week. In September 1985, the need for NSWCDD’s prediction role ended as planned. The second-generation GPS control segment, called the Operational Control Segment (OCS), came on-line and performed all tasks related to the broadcast ephemeris generation, as well as all other operations of the satellites. The OCS operates today with its Master Control Station at Schriever AFB near Colorado Springs and with additional tracking stations in Ascension, Diego Garcia, Kwajalein, and Hawaii.

4. PRECISE EPHEMERIS DEVELOPMENT

The fitted portions of the reference trajectories produced by NSWCDD were called “precise” ephemerides and were provided to organizations such as DMA, NRL, and others from 1980 through 1985. These fits were based on processing 1-week

spans of range difference data derived from pseudo-range measurements. In this process, successive 15-minute smoothed pseudorange measurements from each satellite/station pair were differenced before being used in the estimation process. This differencing was done to remove the time offsets, because the GPS clocks are stochastic in nature, and these errors cannot be removed in a batch estimation process like that used in CELEST.

By 1980, DMA had decided to eventually replace Transit with GPS for all of its operational geodesy work. To support this, DMA funded the development and deployment of additional tracking equipment called “Doppler Vans” (see Section 5). In 1981 NSWCDD began experiments to produce more precise ephemerides using data from the four Air Force tracking sites, augmented with data from up to three DMA Doppler Van sites.

A decision was also made in 1980 to develop software implementing a multisatellite Kalman filter/smoothing estimation algorithm and to begin experiments using this approach to generate the precise ephemerides. This algorithm would allow the smoothed pseudorange data to be used directly, since the stochastic nature of the satellite and station clocks could be accommodated as filter states in a sequential processor. Unmodeled accelerations acting on the satellites could also be accommodated in such a processor. The multisatellite capability also would allow better separation of the satellite and station clock variations. An engineering version of this software, based on using CELEST batch reference trajectories, was developed in the early 1980s and experiments were begun using the tracking data from the four Air Force sites and two DMA sites in Australia and Seychelles. The initial capabilities of this software system and its application were presented at the first international symposium dedicated solely to GPS in 1985.⁹

By April 1986, DMA had deployed second-generation TI4100 receivers (see Section 5) to tracking sites in Argentina, England, and Australia. Eight-day fit spans were used for each week with a Kalman measurement update done every hour, even though the smoothed pseudorange data were available every 15 minutes. This mini-batch process-

ing was necessary to reduce computation time on the CDC mainframe computer in use at that time.

A standard set of processing procedures for generation of the precise ephemerides was adopted at the beginning of 1987. During 1987 several changes occurred that affected the generation of the precise ephemerides. Doppler-realized WGS 84 coordinates for all tracking sites were made available by DMA (see Section 6). DMA deployed two additional TI4100 receivers to Ecuador and Bahrain. New preprocessing software for handling the data stream coming from the Air Force was developed and put into operational use, and the engineering

handle these variations. A solid earth tide correction to the station coordinates was also added at this time.¹²

Up until 1989, there were, at most, seven Block I GPS satellites operational at any given time. The first Block II launch occurred on 14 February 1989 and was followed by four others that year. Precise ephemerides for these Block II satellites were generated at NSWCDD using a special version of the OMNIS software that could process more than seven satellites simultaneously. In July 1989, the production of the precise ephemerides for the Block I satellites was transitioned to DMA in

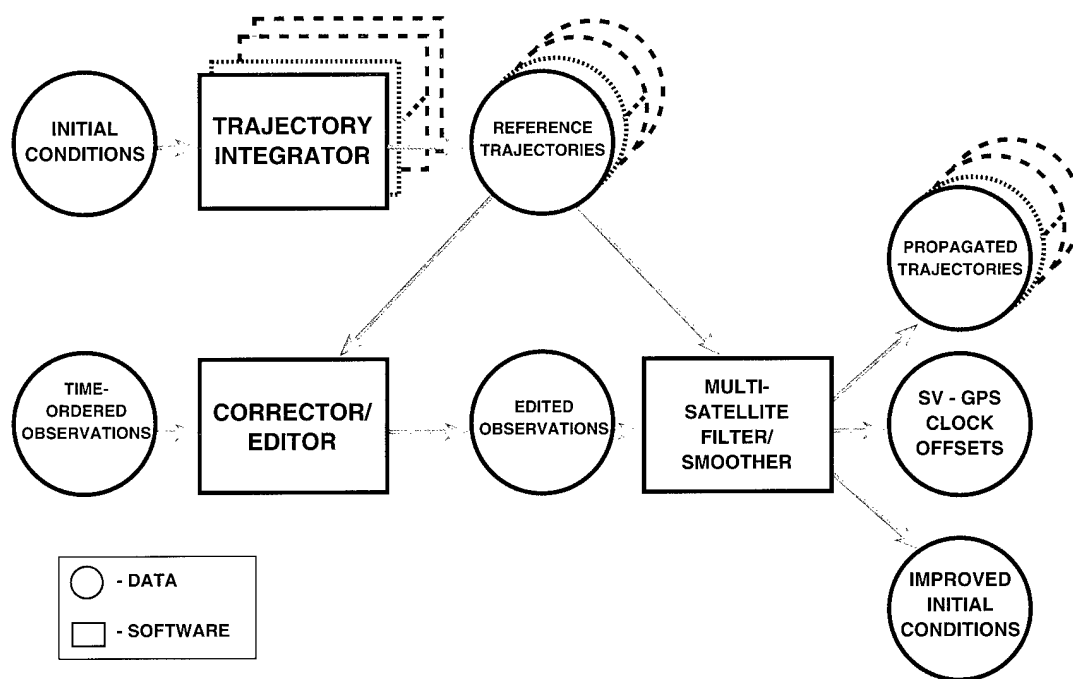


Figure 3—OMNIS GPS Orbit Estimation Software Flowchart

multisatellite filter/smoothing software was replaced with the NSWCDD-developed OMNIS operational software system (see Figure 3).¹⁰ In the analysis area, NSWCDD generated the most compelling evidence that the Block I clocks were undergoing large orbit period variations (up to 50 ns in amplitude for rubidium clocks and 15 ns for cesium clocks). This was believed to be due to thermal cycling on the satellites.¹¹ Changes to the clock estimation procedures were implemented at the beginning of 1988 to

Bethesda, Maryland. The UNIVAC mainframe used there limited the number of satellites that could be processed simultaneously to seven. NSWCDD continued generating precise ephemerides for the Block II satellites until the end of 1989. At the beginning of 1990, DMA began processing all Block I and II satellites using groupings (called partitions) of no more than seven satellites each. NSWCDD developed the methodology for deciding how to best group the satellites for processing.¹³

At about the same time NSWCDD also discovered that the accuracy of the precise ephemeris and clock estimates degraded during eclipse seasons. Additional processing changes related to the radiation pressure scale parameter were implemented at the beginning of 1990 to prevent this degradation.¹⁴ Starting in 1991 plate motion effects on the station coordinates were first incorporated and earth orientation modeling was improved. All of the improvements to the precise ephemeris estimation procedures up until early 1991 were summarized in Reference 15.

The next major change in the precise ephemeris generation occurred in May 1992 when the OMNIS processing was shifted to an IBM RS/6000 workstation at DMA. This additional computing power allowed a single partition containing all satellites to be used beginning in 1993. In June of 1993, production was moved from Bethesda to DMA facilities in St. Louis, Missouri.

At the beginning of 1994, DMA adopted the station coordinates derived by NSWCDD.¹⁶ These were the first GPS-realized WGS 84 coordinates for the tracking sites and had an estimated accuracy better than 10 cm per component. During 1995, DMA deployed additional sites at the U.S. Naval Observatory (USNO) in Washington, D.C., and Beijing, China, bringing the total number of stations to 12. Based on NSWCDD studies and recommendations, DMA began processing data in 3-day overlapping fit spans using a 15-minute Kalman measurement update interval, the same as the data rate. These changes were possible because of upgrades in the IBM RS/6000 workstations and increased experience and efficiency of the DMA ephemeris production staff.

Due to the addition of two DMA stations to the network and two other stations being relocated, NSWCDD rederived the coordinates for all 12 stations in 1996.¹⁷ Studies indicated that further improvement in the precise ephemerides could be obtained by using the carrier phase data in addition to the smoothed pseudorange data, along with different processing techniques.¹⁸ Both of these improvements were adopted by DMA in

September 1996. Further NSWCDD analysis and the addition of better tropospheric refraction modeling resulted in another set of changes being adopted by NIMA in November 1997.¹⁹ The result of all this development is that the user range errors associated with the NIMA precise ephemerides are now less than 10-cm root mean square (RMS), and the satellite clock estimates are believed to be accurate to better than 0.7 ns.²⁰

5. TRACKING STATION RECEIVER DEVELOPMENT

Developing new and improved receivers was a major contributor to improving the accuracy of the precise ephemeris production at NSWCDD and DMA. Personnel at NSWCDD have made major contributions to the development of GPS geodetic receivers in each of the past three decades. The first of these was called the NAVSTAR Geodetic Receiver System (NGRS), and was designed and integrated at Dahlgren in the fall of 1978.²¹ The heart of the NGRS was Stanford Telecommunications, Inc.'s (STI's) 5007 receiver, which was integrated with a microprocessor controller, time interval counters, a Cesium atomic clock, and related ancillary hardware to provide control and input/output. Of particular interest was the Dahlgren-designed and -built full-cycle counter, which greatly enhanced the ability to accurately measure integrated Doppler phase count over long time intervals. A photograph of the components composing the first system is shown in Figure 4.

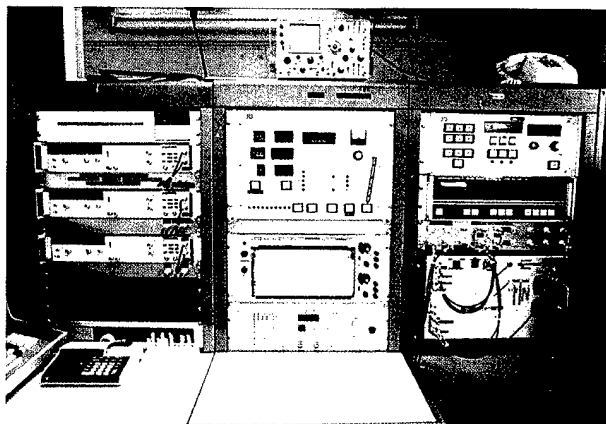


Figure 4—First NAVSTAR Geodetic Receiver System (NGRS)

The first of two systems, mounted in a small truck called the Doppler Van, was deployed to the Yuma Proving Ground (YPG) in January 1979 to participate in early GPS testing. The NGRS demonstrated an overall data accuracy of 3 cm for integrated Doppler and an absolute positioning capability of about 2 m. After YPG, the truck traveled to the Physical Science Laboratory at the New Mexico State University at Las Cruces, the Applied Research Laboratories of the University of Texas at Austin (ARL:UT), and finally, to the U.S. Naval Observatory in Washington, D.C.

Based on the favorable results from the test tour, DMA tasked NSWCCD to build a second NGRS system, incorporating two-frequency pseudorange capability with an upgraded STI 5010 receiver. The second receiver was completed in December 1980. Both of these systems were deployed abroad to Australia and Seychelles to provide supplemental tracking of the GPS satellites.²² In late 1982, another STI 5010 receiver became available and was used to build and deploy a third NGRS. By May 1983, the third system was operating in Argentina. All three NGRSs provided high-quality tracking data until they were replaced in 1986.

Soon after the successful NGRS program, Dahlgren was tasked to develop a man-portable, field-deployable, GPS geodetic receiver. Sponsored jointly by DMA, the U.S. Geological Survey (USGS), and the National Oceanic and Atmospheric Administration (NOAA), the system was initially termed the Tri-Service Receiver.²³ A cooperative effort by NSWCCD and Johns Hopkins University's Applied Physics Laboratory (JHU/APL) resulted in the design of a largely digital receiver that would sequence through the GPS satellites. At the time, efforts in industry were also tending toward digital receivers. Based on an extensive review of industry developments, the decision was made to acquire the receiver competitively from industry. The ARL:UT was tasked by NSWCCD to be the agency for the procurement. In October 1981, a fixed-price contract for up to 100 receivers was let to Texas Instruments (TI) for the TI4100 receiver. The TI4100 was unique in that it had two microprocessors: one termed the digital receiver and the other, the navigation computer. Dahlgren personnel designed and

developed the geodetic positioning software in the navigation computer. The TI4100 proved to be an extremely capable receiver system, and for many years was used as a yardstick for judging less capable receivers. It became the heart of the DMA Monitor Station (designed and integrated by ARL:UT) that was deployed in numerous locations worldwide to support GPS precise ephemeris work at Dahlgren and DMA.²⁴

In 1992, NSWCCD and ARL:UT were tasked by DMA to develop a specification for the third-generation GPS receiver. Following the model for procurement established with the TI4100, ARL:UT released the jointly derived specification for competitive procurement. The contract for the third-generation GPS receiver was awarded to Ashtech Inc., for the Ashtech Z/Y-12. In late 1994 after extensive testing by personnel from DMA, ARL:UT, and Dahlgren, the DMA monitor stations were upgraded with the Ashtech Z/Y-12. These new receivers have proven to be accurate and reliable in tracking the GPS satellites.

6. GPS TRACKING SITE POSITIONING AND WGS 84 COORDINATE FRAME DEVELOPMENT

The coordinates of the satellite tracking stations used in orbit estimation define the reference frame of the estimated satellite orbits. Similarly, the accuracy of the tracking station coordinates strongly influence the accuracy of the estimated orbits. NSWCCD determined the GPS-realized tracking station coordinates used by DMA in their precise orbit and clock estimation, and by the Air Force in their real-time computations on which the broadcast ephemerides are based (see Figure 5).

Prior to 1986, both DMA and the Air Force used WGS 72 coordinates for GPS tracking stations. The preliminary WGS 84 coordinates of the tracking stations were obtained by transformation²⁵ from their WGS 72 coordinates. During 1986 and 1987, the WGS 84 coordinates were directly derived using Doppler Transit point positioning by DMA. This positioning technique used the recently calibrated WGS 84 Transit station coordinates,²⁶ Doppler observations collected from Transit satellites, and

the WGS 84 gravity model. The WGS 84 positions of the GPS stations were defined by transferring WGS 84 positions of nearby collocated Doppler stations using terrestrial survey differences. These Doppler-derived, WGS 84 coordinates for the GPS tracking stations had an estimated accuracy at the meter level.

Uncertainties in the Transit-derived station coordinates were attributed principally to uncompensated ionospheric effects on signal propagation and, to a smaller extent, on the determination of the electrical phase center of the antennas. The

The first derivation of WGS 84 coordinates used GPS data collected in 1992 from the existing ten DMA and Air Force stations and from a set of globally distributed civilian stations defined in the ITRF.¹⁶ Using only carrier phase observations, the OMNIS system of programs was used to compute the new DoD coordinates. A subset of the ITRF stations, called fiducial sites, were held fixed while simultaneously estimating GPS clocks, orbits, and the station coordinates of the DMA, Air Force, and remaining ITRF sites. These WGS 84 coordinates of the DoD stations were improved over the Doppler-realized coordinates due primarily to elimination of

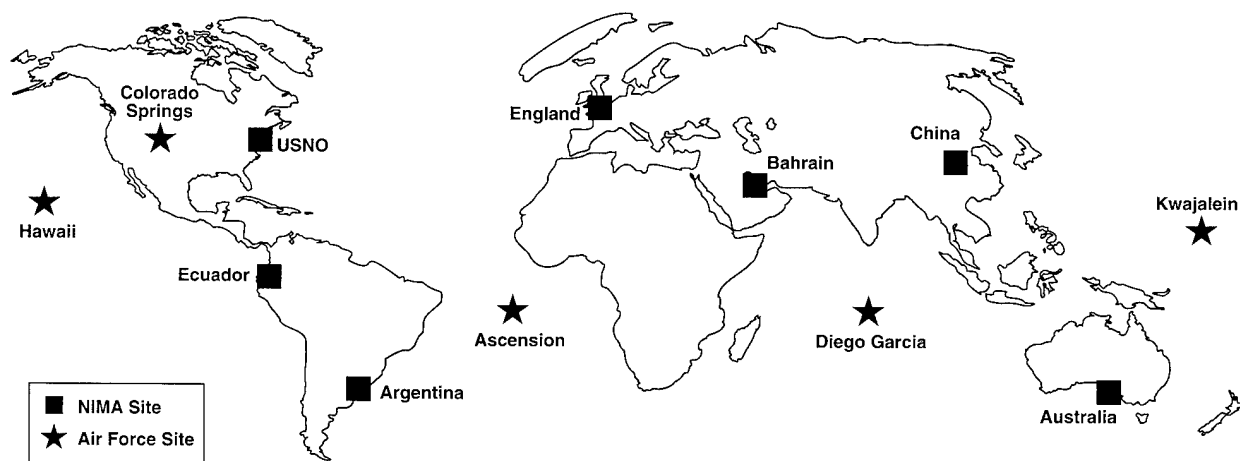


Figure 5—Seven NIMA and Five Air Force Tracking Stations

combination of these and other errors made the initial GPS station coordinates internally inconsistent and biased with respect to the Bureau International de l'Heure Terrestrial System (BTS) reference frame. The largest bias, in the GPS station heights, was estimated to be at the meter level.²⁷⁻³⁰ Over time, the BTS has been refined to become the International Earth Rotation Service Terrestrial Reference Frame (ITRF). To remove the biases and improve consistency, NSWCDD derived WGS 84 GPS station coordinates tied to the ITRF. New coordinates for the operational DMA and Air Force tracking stations have been determined twice.

the height bias (approximately 1.5 m in magnitude) and redefinition of longitude. The estimated accuracy of these GPS-realized WGS 84 coordinates was 10 cm per component, one sigma. This was an order of magnitude better than the accuracy of the Doppler-realized coordinates. DoD adopted these WGS 84 coordinates in 1994.

These coordinates were rederived in 1996 for the purpose of validation and also to improve the coordinates of four DMA stations; sites in Australia and England had been moved and two stations—USNO in Washington, D.C., and Beijing, China—

had been added subsequent to the first GPS-based derivation. In this second GPS-based derivation, the OMNIS system of programs used both pseudorange and carrier phase data collected from the twelve DMA and Air Force stations and ITRF civilian stations. The DoD coordinate solutions were tied to the ITRF by again holding fixed the coordinates of the fiducial stations, while solving simultaneously for GPS clocks, orbits, and the station coordinates.¹⁷ This validation showed that the 10 cm per component sigma that had been estimated for the first GPS-derived coordinates was conservative. The new DoD coordinates were estimated to have an accuracy of better than 5 cm per component, one sigma. These coordinates were adopted by DMA in September 1996 and by the Air Force in January 1997.

7. GEODETIC POSITIONING

Global geodetic positioning based on Doppler observations of the Transit satellite system had been established to the 1-m level by the early 1970s. At DMA, it had been recognized that a future operational geodetic positioning capability would be linked to the use of GPS observations and precise ephemerides. The first paper that addressed the potential geodetic applications of GPS was published the same year the first satellite was launched.³¹ In 1980, a detailed analysis of GPS geodetic positioning was published³² as a dissertation by The Ohio State University. The work that led to this dissertation was performed at NSWCDD between 1977 and 1979. The study examined geodetic positioning using GPS range and Doppler observations. It also examined precise baseline determination from GPS observations, including satellite interferometry. In 1979, previous simulations and analyses of baseline determination were confirmed with one of the first experimental GPS baseline determinations based on Doppler data.³³ Since data collection was accomplished by moving a single antenna between stations, this experiment also demonstrated the possibility of dynamic positioning applications. The geodetic potential of GPS was clearly established. The next step was the development of operational survey capabilities supported by portable satellite tracking equipment and precise GPS ephemerides. In the late 1980s, NSWCDD

completed a research algorithm that performed geodetic positioning with submeter accuracy given 6 or more hours occupation on a site.³⁴⁻³⁸

Because observations corrected for Selective Availability (SA) require a keyed military receiver and are classified, an effort was made at NSWCDD to upgrade to the precise ephemeris using unclassified positions and knowledge of the broadcast ephemerides used by the receiver. This Precise Absolute Navigation (PAN) algorithm has demonstrated navigation position accuracies equivalent to those that would have been obtained by direct processing of the corrected observations.^{39,40}

8. PERFORMANCE EVALUATION

As a quality check of the precise ephemerides and satellite clock corrections generated at NSWCDD for use by DMA, overlap comparisons were instituted in the late 1980s. The precise ephemerides were computed for 8 consecutive days beginning a half day before the beginning of a week and ending a half day after the week's end. The one-day overlap span common to both weeks was used to do the check.^{41,42} Another quality check included collecting and processing observations obtained from a GPS receiver located at Dahlgren.³⁴⁻³⁶ Absolute position solutions were computed and the variation compared day-to-day.⁴² Still another analysis effort involved computing the satellite clock performance by using the satellite clock corrections estimated in the precise ephemeris filter/smoothen. The Allan variance of each satellite clock was computed from many weeks of precise clock estimates.¹¹ All these efforts made important contributions to the improvement of the satellite ephemeris and clock estimation algorithm.

A variety of methods have been developed to compute a figure of merit for the accuracy of the GPS broadcast ephemerides. A definition and range of applicability of several of the most common measures is outlined in Reference 43. The User Range Error (URE) used by NSWCDD is one of those described.⁴⁴ It is defined for pseudorange data collected at sites of known WGS 84 positions that are not part of the GPS monitor station network.

Satellite Laser Ranging (SLR) data are collected by the National Aeronautics and Space Administration (NASA) from a worldwide network of laser tracking stations. These stations primarily track satellites other than GPS satellites. However, since two GPS satellites (SVN35 and SVN36) do have laser retroreflectors attached, NASA collects, on a low priority basis, SLR data from these GPS satellites. Starting in 1995, NSWCDD began analyzing these data by calculating SLR residuals. The residuals are the same as the URE values above, except that there are no satellite or station clock errors involved. By observing the value of these residuals and by calculating the residuals from the GPS ephemerides generated by other organizations, an estimate can be made of the accuracy of the operational ephemerides calculated by the OCS and the precise ephemerides calculated by NIMA.^{45,46}

The primary after-the-fact performance analysis technique employed by OCS consists of a comparison between OCS Kalman filter orbit and clock estimates and the NIMA GPS orbit and clock estimates derived from OMNIS. This performance analysis technique is routinely used to characterize the performance of the Kalman filter and broadcast navigation messages. The orbit and clock differences are usually reported as RMS Signal in Space Range Errors (SISRE) and assume that the NIMA estimates are "truth." The satellite clock differences and the radial, along-track, and cross-track orbit differences at a given epoch are used to generate this quantity for individual satellites or the complete constellation. The UREs for the navigation messages are sometimes given as a function of 'age of data' (AOD), where the Kalman estimates correspond to "zero AOD."⁴⁷ On selected occasions, NSWCDD has also evaluated OCS 3-hourly predictions and associated covariances. Analysis conducted by NSWCDD led to the discovery of an error in the technique used to generate these covariance matrices.

Recently, NSWCDD participated in a study to evaluate expected improvements in the performance of OCS Kalman estimates and predictions. These improvements, collectively known as the GPS Accuracy Improvement Initiative (AII), will be implemented over the next few years. For this study,

NSWCDD emulated the OCS Kalman filter, with the inclusion of pseudorange data from six additional NIMA tracking stations and all satellites in the constellation. Analysis revealed the accuracy of the OCS Kalman estimates will improve by 50 percent, and the accuracy of the OCS 3-hourly predictions will improve by 20 to 35 percent.⁴⁸ These results, along with those from other institutions, clearly indicate that the OCS SISRE performance will exceed the AII performance levels of 75 cm for the OCS Kalman estimates ('zero AOD') and 1.5 m for the OCS navigation messages.

In addition to ephemeris quality assessment, receiver measurement evaluations were also performed. The TI4100 GPS Geodetic Receiver was in operational use by 1984. It was capable of tracking four satellites simultaneously in a time-multiplexing mode. The receiver provided dual-frequency, P-code pseudorange and phase observations in the era before the advent of SA and Antispoofing. The performance of this receiver was thoroughly investigated by NSWCDD and ARL:UT.⁴⁹ The characteristics of the TI4100 were described by tests in the NASA Goddard indoor antenna range.⁵⁰ It was found to be susceptible to multipath under certain conditions.

In 1985, NSWCDD developed a method that used only the receiver measurements to evaluate the level of signal multipath.⁵¹ The method simply used the ionospherically corrected pseudoranges differenced with the ionospherically corrected, biased Doppler ranges, with the bias conveniently set to zero. The standard deviation of this difference provided a good relative indicator of the signal multipath affecting the receiver measurements. This method was important because it demonstrated that multipath was causing severe measurement errors (over 10 m in pseudorange) and even loss of satellite tracking lock. This was mainly due to the high gain at low-elevation angles intentionally designed into the early receiver antennas to track the few satellites then available as long as possible.

Signal multipath was evaluated at many different locations, including the DMA satellite tracking sites.⁵¹ Further analysis determined the multipath error effect on satellite ephemeris determination.⁵²

In order to evaluate the multipath effect, tests were performed for various antenna situations, such as placement of the antenna close to the ground, larger and special ground planes, and the use of absorption material.^{53,54} Further, the effects of multipath were demonstrated to be significantly reduced by combining the ionospherically corrected pseudorange and Doppler change-in-ranges.⁵⁵

9. RELATIVE/DIFFERENTIAL POSITIONING AND ATTITUDE DETERMINATION

The first NSWCDD contributions to the use of GPS carrier phase measurements for precise positioning grew from similar earlier work with the Transit satellite system.⁵⁶ This was possible because the NGRS (Doppler Van) made GPS phase measurements available to the user. The first demonstration of centimeter-level relative positioning capability took place as part of a GPS sensitivity experiment at NSWCDD in April 1980. Individual satellite measurements from two satellites were used to estimate three-dimensional antenna locations relative to their original location for six repeated position changes around a small triangle.⁵³ Additional studies over the next few years used different processing techniques to determine more and more accurate relative positions over longer and longer baselines.⁵⁷⁻⁶⁰

A number of military applications—such as an aircraft landing on a carrier and miss distance determination for missile intercept testing—require precise positioning of one moving platform relative to another. NSWCDD and The XYZ's of GPS, Inc., were the first to develop this capability, which was demonstrated in a series of tests, all with baselines less than 30 km. These tests included a car drive-by, an aircraft fly-by and finally, a rocket sled test at Holloman AFB.⁶¹⁻⁶³ The latter emulated the missile intercept T&E problem. The car drive-by test was the first demonstration of precise, centimeter-level, relative positioning between two moving platforms. This positioning was done on the fly—that is, without static initialization. For this test, videometric truth measurements were obtained to determine the distance between GPS antennas on two vehicles at closest approach. The videometric and GPS miss distances were compared for

15 drive-bys. The largest error was a few centimeters. The aircraft fly-by test demonstrated agreement to within a few decimeters, which was the accuracy of the truth data.

In order to evaluate kinematic positioning and miss distance determination at even higher dynamics and higher precision, a rocket sled test was performed on the test track at Holloman AFB, New Mexico. The test track provided very precise timing and control. Here, a GPS receiver and antenna were on the rocket sled, and a second receiver and antenna were placed about 6 m to the side of the track, as shown in Figure 6. These tests used dual frequency, carrier phase measurements and demonstrated the potential of using GPS data, processed after the fact, to obtain interpolated miss distances to an accuracy of a few centimeters.⁶³ Precise relative positioning has progressed to real time and was recently demonstrated for an NRL robotic helicopter application. Research into precise kinematic positioning for longer baselines is underway.

Wide Area Differential GPS (WADGPS) techniques provide real-time navigation accuracy at the meter-level over vast areas. The predominant navigation error sources removed by WADGPS techniques include broadcast ephemeris and clock error (including the SA effects for civilian receivers), and range errors caused by atmospheric effects. These techniques utilize a widespread network of

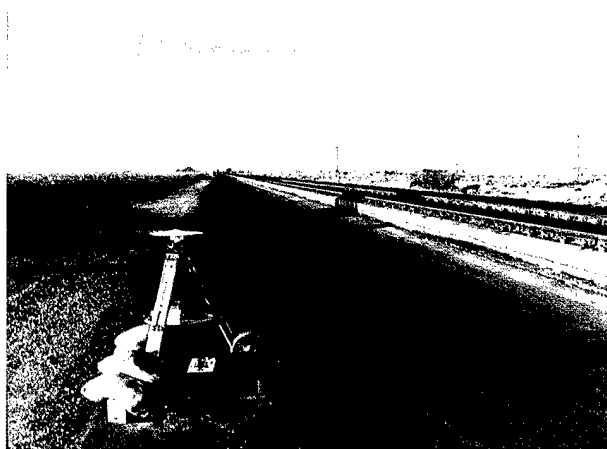


Figure 6—Location of the Track-Side Antenna Next to the Rocket Sled Track at Holloman AFB

reference tracking stations. Error corrections are collected from each of the network stations and optimally combined for the user. The WADGPS technique developed by NSWCDD and The XYZ's of GPS, Inc., computes corrections that eliminate most errors for users located thousands of kilometers away from the reference stations. This has been demonstrated in experiments conducted with data from both static and dynamic users. These tests have shown that real-time navigation solutions with errors less than 2 m can be achieved for users nearly 2000 km from the reference stations.⁶⁴ Furthermore, relative position (miss distance) between two such remote users can be determined to submeter-level accuracy using this technique. Recently the WADGPS technique was successfully applied to a high dynamic (15 G, 450 G/s) missile test flight.⁶⁵

The first demonstration of using GPS to determine the attitude (i.e., roll, pitch, and yaw) of a user platform was completed in November 1982.⁶⁶ Change-in-phase measurement data that had been collected in May 1980 as part of the GPS sensitivity experiment³³ were reprocessed for this demonstration. This method of using change-in-phase measurements to determine attitude was patented by NSWCDD in 1986.⁶⁷ The advent of coherent carrier phase measurement receivers enabled interferometric attitude determination to become a reality. The TI4100 allowed phase measurements on separate receivers to be made at essentially the same GPS instant; i.e., to within a 100-ns synchronization error. Static azimuth and elevation observations were obtained using two of these receivers connected to a single external clock with their antennas separated by 25 m. A standard deviation of 0.1 mrad demonstrated the potential accuracy of GPS for attitude determination.

The first GPS receiver that could be used to determine both position and attitude was developed under an NSWCDD Small Business Innovative Research contract with Trimble Navigation, Ltd., of Sunnyvale, California.⁶⁸ The prototype receiver used three antennas in a right triangular array, as shown in Figure 7 on board USS *Yorktown*, during a test in July 1988.⁶⁹ This receiver became the first commercial GPS attitude receiver. A prototype TI attitude receiver was tested in November 1989 and July 1990

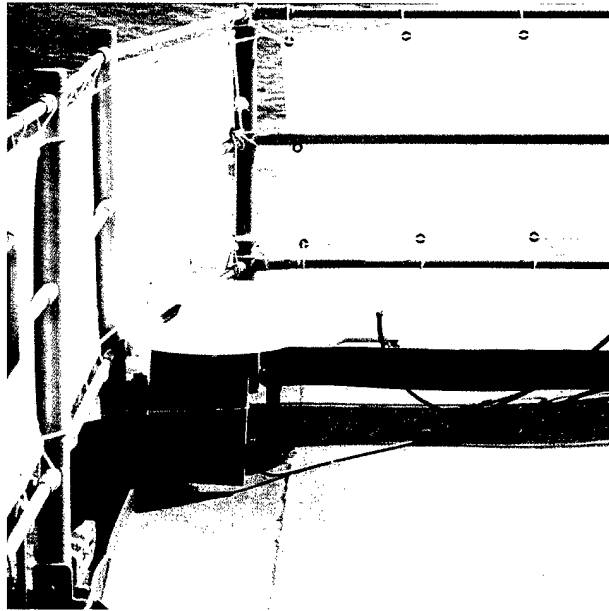


Figure 7—Heading and Attitude Receiver Antenna on USS *Yorktown*. Roll, pitch, and yaw moments are sensed as phase differences by the array. Note that the guardrails are made of nonreflective fiberglass

as part of a NSWCDD Independent Exploratory Development project. Both static and dynamic tests were performed with a 1-m antenna separation. Various antenna and ground plane configurations were used to minimize multipath effects. For the dynamic tests, the antennas were attached to a beam across the back deck of a Light Armored Vehicle (LAV) as shown in Figure 8.⁷⁰

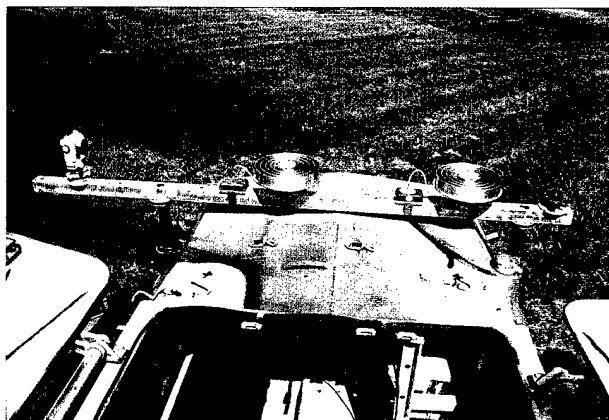


Figure 8—Choke Ring Antennas on the Beam with Optical Survey Equipment on LAV

Precise determination of astronomic azimuth and gravity deflections of the vertical (DOV) is required in support of accurate strategic inertial navigation technology. NSWCDD proposed a method to use GPS to determine astronomic azimuth in 1986.⁷¹ In July 1987, NSWCDD conducted a joint test of this method with NGS and NIMA.⁷² Using about three hours of static GPS data per day from TI4100 receivers, precise relative positions were obtained.⁷³ Results were comparable with conventional astrogeodetic results and required much less time to collect. Gravity DOV, the angular differences between the gravity vectors (normals to the geoid) and vectors normal to the WGS 84 ellipsoid model for the earth also agreed with conventionally determined astronomic estimates. The techniques use precise pseudokinematic GPS positioning and first-order leveling, and demonstrated millimeter-level accuracy.⁷⁴

Gravity DOV are conventionally determined at sea using gravimeter survey techniques. The use of GPS offers a simpler and potentially more accurate approach. The ocean itself performs the leveling; however, measurements made at the surface are corrupted with oceanographic errors and must be corrected to depths well below the surface. A test to demonstrate this procedure was conducted in May 1994.⁷⁵ Conventional estimates of DOV were determined by combining high-frequency ship survey data and low-frequency satellite altimetry data. The conventionally determined values for the centers of the baselines at the test site were in agreement with the experimental values to about 0.2 arcseconds.⁷⁶

10. SYSTEM APPLICATIONS SUPPORT

Over the years, NSWCDD has provided GPS support to a number of system applications. The applications include satellites, missiles, and guided projectiles. The support has included simulation and modeling of navigation errors, jamming, feasibility analyses, and T&E support. The first GPS receiver system to fly onboard a satellite was called the GPS Package (GPSPAC). Work on GPSPAC began in 1976 and was funded jointly by DMA and NASA. JHU/APL was the prime contractor and

system integrator for GPSPAC, with the receiver provided by Magnavox, Inc., and with technical assistance provided by NSWCDD.^{77,78} NSWCDD also provided technical direction for the flight software development, conducted extensive navigation simulations, and postprocessed selected subsets of the collected data. NSWCDD developed a GPSPAC simulator consisting of a program that generated simulated GPSPAC data for all GPS satellites in view, and a program that simulated both the satellite selection and Kalman filter algorithms.⁷⁹ These simulations provided guidance for several design decisions in the areas of constellation review times, acquisition strategy, antenna coverage angles, orbit-adjust thrust handling, and the merits of collecting data from two additional satellites beyond the four needed for navigation. The postprocessing involved troubleshooting receiver problems, evaluation of the onboard receiver and algorithm performance, and computation of precise ephemerides for the host vehicles.

The first GPSPAC unit was launched on LANDSAT 4 in July 1982. Three more units were successfully launched: one on LANDSAT 5 in March 1984 and two on DoD host vehicle satellites in 1983 and 1984. Overall, GPSPAC performed exceptionally well. It was a system well ahead of its time—the GPS system was supposed to be operational by the early 1980s, but because of delays, it actually consisted of only six satellites during most of this period. With this small constellation, four satellites were in view for only a few hours each day. Even with limited data, GPSPAC demonstrated that it could navigate as accurately as it was designed to do.⁸⁰

In 1992, DMA decided to initiate development of a precise orbit estimation capability based on GPS to support their current and future low-altitude satellites (host vehicles). NSWCDD developed this capability. The initial mathematical formulation required to integrate a simultaneous host vehicle/GPS orbit estimation capability into OMNIS was completed in April of 1993.⁸¹ Additional formulation was written over the next few years, and extensive software development and testing have resulted in all GPS orbit estimation capabilities now being part of the operational OMNIS system. These capabilities were applied to data collected by NASA's

TOPEX/POSEIDON satellite, and a 5-cm radial orbit accuracy was demonstrated.⁸² These capabilities have been extensively utilized for evaluating orbit accuracies to be expected for future satellites of interest to NIMA. The current OMNIS version contains a flexible and unique state-of-the-art, GPS-based, host-vehicle orbit estimation capability.

Satellite Tracking (SATRACK) is an instrumentation and analysis system developed by JHU/APL that provides weapon system accuracy evaluations for the Trident FBM developmental and operational flight tests. In support of these SATRACK flight tests, NSWCDD has provided precise GPS orbit, clock, and covariance estimates to JHU/APL. Initial NSWCDD support to JHU/APL began with the SATRACK I program in 1978. SATRACK I provided accuracy evaluations for the Trident I flight tests. Support of the SATRACK II program began with the Trident II flight tests in 1987 and included pad-launched and submarine-launched flight tests.²⁸ In

1997, the SATRACK support was transitioned to NIMA, and NSWCDD now serves as a consultant to both NIMA and JHU/APL for SATRACK support.

NSWCDD has also supported the incorporation of GPS into navigation systems.⁸³ The Standard Missile (SM-3) is the Navy's primary interceptor for theater-wide Tactical Ballistic Missile Defense (TBMD). Effective use of the SM-3 requires the elimination of system alignment errors arising from missile in-canister initialization, ship navigation errors, and ship radar-face misalignments. These errors are removed during flight using a missile inertial navigation system (INS) that processes measurement data from GPS satellites using a tightly-coupled GPS/INS (see Figure 9). NSWCDD has been very active in analyzing SM-3 requirements and defining performance of the inflight alignment algorithms as part of a government-contractor team. A system-level, 6-DOF Navigation Simulation (NAVSIM) has been developed that includes a

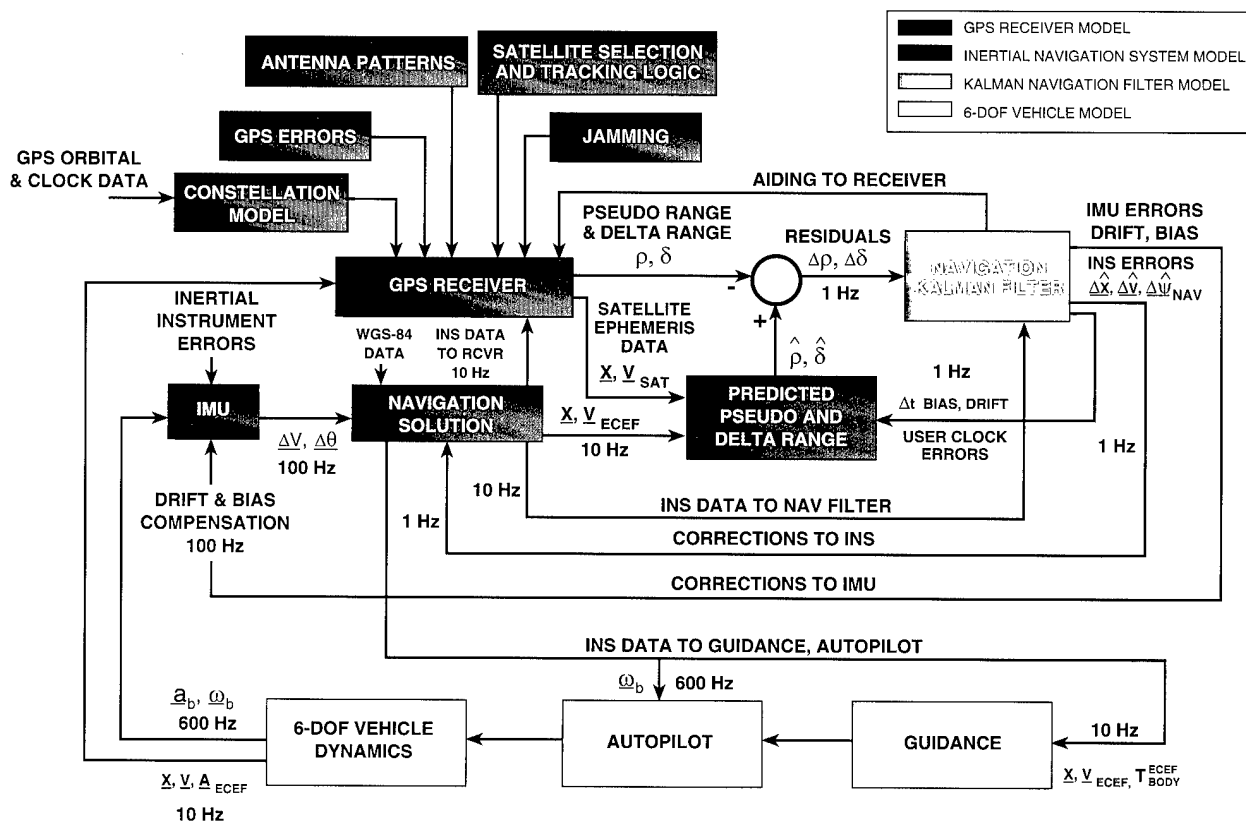


Figure 9—NAVSIM Tightly Coupled GPS/INS System Diagram

detailed GPS receiver model, a GPS and radar-aided INS, and a Kalman filter for implementing the inflight alignment functions. Using NAVSIM, analysis results were generated that showed the SM-3 integrated navigation system met all performance specifications.⁸⁴

NSWCDD has provided long-term support for the Extended Range Guided Munition (ERGM). This effort started in 1987 as a study that concluded that the concept of using a combined GPS and Inertial Measurement Unit (IMU) was feasible.⁸⁵ This study was later updated⁸⁶ to further evaluate the special requirements of a gun-launched projectile. GPS acquisition from a gun-launched projectile was demonstrated at the NSWCDD main range in May 1996.⁸⁷ The ERGM program has progressed to state-of-the-art receiver and IMU developments.⁸⁸ Operational tests and evaluations are scheduled for 2000. Antijam performance has been evaluated via 6-DOF NAVSIM modeling,⁸⁹ and support to the ERGM development program is being provided through ongoing assessment of navigation system algorithms.⁹⁰

In addition to the above major support programs, NSWCDD has provided GPS support for additional system applications. These include UAV targeting,^{91,92} forward-observer targeting,⁹³ counter-mine warfare,⁹⁴ and GPS enhanced Tomahawk cruise missile guidance.⁹⁵

11. SUMMARY

NSWCDD has been one of the principal contributors to GPS for nearly three decades. These contributions have ranged from concept definition and constellation design studies in the earliest days to ongoing precise, dynamic positioning applications. Beginning in 1978, NSWCDD processed Air Force tracking data on a weekly basis to produce long-term, predicted GPS satellite trajectories. These trajectories were updated with near real-time tracking data at the Master Control Station to produce the navigation messages that were uploaded to the satellites about once a day. This NSWCDD ephemeris prediction role ended in 1985 when the second-generation GPS Control Segment came

on-line and took over. Meanwhile, NSWCDD had begun experiments designed to produce more accurate ephemerides. These experiments used data from additional tracking stations, such as the Doppler Vans equipped with NGRS, to augment the Air Force tracking network. At about the same time, DMA had decided (based in part on results obtained using NSWCDD precise weekly-fit ephemerides) to replace Transit with GPS to meet all of its geodetic requirements. The seeds had been sown for GPS to move beyond the real time navigation role for which it was originally conceived, and become a system that would support precise surveying and geodetic requirements.

These precise geodetic positioning requirements, in turn, helped drive requirements to further improve orbit estimation techniques, tracking network performance, and reference frame models. NSWCDD led efforts in all of these areas. Over the years, the software used to produce the GPS orbits evolved from a single satellite batch least-squares process that ran on mainframe computers of the early 1980s to today's sophisticated, multisatellite filter/smoothing that executes very rapidly on a workstation.

NSWCDD built the first geodetic-quality GPS receiver systems (the Doppler Vans), which were deployed by DMA and used for several years to augment the Air Force tracking network. Experience gained in this effort has been brought to bear in the development of two new generations of receivers: development of controlling software for the TI4100 and the NSWCDD- and ARL:UT-developed requirement specifications for the receivers currently deployed by NIMA. Meanwhile, studies were performed to determine the "optimal" distribution of tracking stations and improved methods of data processing. Orbit and clock estimation processes and station positioning accuracies were further enhanced by a GPS-realized WGS 84 reference frame. Tracking station coordinates have been determined by NSWCDD to accuracies better than 5 cm. These station coordinates are used operationally by the GPS Control Segment in generating the broadcast messages used for real-time navigation. Postfit orbits are routinely computed to accuracies better than 10 cm. NSWCDD is supporting the

Accuracy Improvement Initiative program to improve the operational ephemerides and, thus, further enhance GPS performance for navigation applications.

From the GPS user community perspective, NSWCDD has made many pioneering advances. The first spaceborne GPS receivers, GPSPAC, flew on four NASA and DoD satellites. NSWCDD provided technical direction for flight software development and conducted extensive navigation simulation and flight data analysis. Key support to the FBM flight test program through SATRACK has been provided since 1978. NSWCDD has been responsible for numerous breakthroughs in the use of GPS for relative and differential positioning, for attitude estimation, and in geodetic applications. Technological advances are creating exciting new opportunities in precise positioning. Receivers are becoming smaller, more rugged, more accurate, and less expensive. These receivers can be integrated with similarly advanced IMUs and enhanced computing capabilities to produce very small, very robust, real-time navigation systems. Such systems have obvious utility to advanced weapons such as guided projectiles, missiles, and robotic vehicles. These enabling technologies are making new applications to T&E possible.

GPS is now a mature system. It is becoming ever more ubiquitous in DoD applications as well as in the private sector. NSWCDD has made major, often defining, contributions to GPS and expects to continue to do so into the next century.

12. ACKNOWLEDGMENTS

The authors wish to thank the other contributors to this article. The contributors are listed with the group photograph at the end of the article. In addition, the authors would like to recognize the following individuals for their years of work on GPS related efforts: Ms. Treva Burgess, Mr. Bill Birmingham, Mr. Pat Beveridge, Dr. Mike Harkins, Dr. Ralph Gibson, Dr. Bill Stein, Mr. Mike Sims, Mr. Don Clark, Mr. John Ellis, Ms. Ruth Darnell, Mr. Ted Saffos, Mr. Ralph Dickerson, Mr. Glenn Bowen, Mr. Ling Szeto, Ms. Virginia Curtis,

Ms. Evelyn Durling, Mr. John Pekar, and Mr. Jim Sloop. Other former and current NSWCDD personnel, too numerous to name here, are also acknowledged for their contributions to NSWCDD's GPS technology knowledge base.

The single most important sponsor of this body of work has been NIMA. For over two decades, NIMA has provided excellent technical direction, support, and direct contributions to our efforts.

Finally, the authors wish to acknowledge the many contributions of Dr. Charles Cohen and Dr. Richard Anderle. Dr. Cohen's pioneering work in gravity and geoballistics and his critical technical oversight and guidance led to solutions of some of the most difficult problems in geodesy and geophysics. Dr. Anderle authored over 200 papers in the fields of satellite geodesy and orbit estimation and, as research scientist and manager, directed the astronautics and geodesy program at Dahlgren from the late 1950s until he retired in 1984.

REFERENCES

1. Niemann, R.A., *Dahlgren's Participation in the Development of Computer Technology*, Naval Surface Weapons Center, MP 81-416, Dahlgren, VA, Sep 1982.
2. Hughey, R.H. and Hill, R.W., *More Than 25 Years of Space and Geodesy*, NSWC 10th Anniversary Technical Symposium, Dahlgren, VA, 12 Oct 1984.
3. Anderle, R.J., "Keynote Address," *Proceedings of the Third International Geodetic Symposium on Satellite Doppler Positioning*, Vol. 1, pp. 3-7, Las Cruces, NM, Feb 1982.
4. Van Dierendonck, A.J.; Melton, W.C.; Birnbaum, M. and Harkins, M.D., "The Approach to Satellite Ephemeris Determination for the NAVSTAR Global Positioning Systems," *Navigation*, Vol. 23, No. 1, pp. 76-86, Spring 1976.

5. O'Toole, J.W., *CELEST Computer Program for Computing Satellite Orbits*, NSWC/DL TR-3565, Dahlgren, VA, Oct 1976.
6. Hill, R.W., "An Overview of the Global Positioning System and the Navy Navigation Satellite System," *American Astronautical Society, Advances in the Astronautical Sciences*, Vol. 40, Pt. 1, pp. 21-32, Jun 1979.
7. Harkins, M.D., "The Relativistic Doppler Shift in Satellite Tracking," *Radio Science*, Vol. 14, No. 4, Jul-Aug 1979.
8. Carr, J.T. and O'Toole, J.W., "Point Positioning with the NAVSTAR Global Positioning System," *Proceedings of IEEE Plans 82 Position Location and Navigation Symposium*, pp. 166-170, Atlantic City, NJ, Dec 1982.
9. Swift, E.R., "NSWC's GPS Orbit/Clock Determination System," *Proceedings of the First International Symposium on Precise Positioning with the Global Positioning System*, Vol. 1, pp. 51-62, Rockville, MD, 15-19 Apr 1985.
10. Swift, E.R., *Mathematical Description of the GPS Multisatellite Filter/Smoothen*, NSWC TR 87-187, Dahlgren, VA, Oct 1987.
11. Swift, E.R. and Hermann, B.R., "Orbit Period Frequency Variations in the GPS Satellite Clocks," *Proceedings of the 20th Annual Precise Time and Time Interval (PTTI) Applications and Planning Meeting*, Vienna, VA, 29 Nov-1 Dec 1988.
12. Groeger, W.J., *Station Displacement Caused by Solid Earth Tides*, NSWC TN 84-293, Dahlgren, VA, Aug 1984.
13. Gouldman, M.W., "Partitioning of GPS Satellites for Orbit/Clock Determination," *Proceedings of the Second International Symposium on Precise Positioning with the Global Positioning System*, Ottawa, Canada, 3-7 Sep 1990.
14. Swift, E.R., "Reducing the Effects of Eclipsing on the GPS Precise Ephemeris and Clock Quality," *Proceedings of the Second International Symposium on Precise Positioning with the Global Positioning System*, Ottawa, Canada, 3-7 Sep 1990.
15. Swift, E.R., "GPS Orbit/Clock Estimation Based on Smoothed Pseudorange Data from a Ten-Station Global Network," presented at the IUGG General Assembly IAG Symposium G-2, *Permanent Tracking Networks for Geodesy and Geodynamics*, Vienna, Austria, 16 Aug 1991.
16. Swift, E.R., "Improved WGS 84 Coordinates for the DMA and Air Force GPS Tracking Sites," *Proceedings of ION GPS-94*, Salt Lake City, UT, 20-23 Sep 1994.
17. Cunningham, J. and Curtis, V.L., *WGS 84 Coordinate Validation and Improvement for the DMA and Air Force GPS Tracking Stations*, NSWCDD/TR-96/201, Dahlgren, VA, Nov 1996.
18. Cunningham, J.P. and Swift, E.R., *Additional DMA Tracking Sites for Improving GPS Orbit and Clock Estimates*, NSWCDD/TR-95/70, Dahlgren, VA, Jun 1995.
19. Cunningham, J., *Improving the NIMA Precise GPS Orbit and Clock Estimates through OMNIS Filter/Smoothen Retuning*, NSWCDD Study Report, Dahlgren, VA, Jun 1997.
20. Cunningham, J.P., Swift, E.R. and Mueller, F., "Improvement of the NIMA Precise Orbit and Clock Estimates," *Proceedings of ION GPS 98, The 11th International Technical Meeting of the Satellite Division of the Institute of Navigation*, Nashville, TN, Sep 1998.
21. Senus, W.J. and Hill, R.W., "GPS Application to Mapping, Charting, and Geodesy," *Navigation*, Vol. 30, No. 2, pp. 157-170, Apr 1981.
22. Heuerman, H.R., "Global Positioning System Geodetic Tracking Program," *Proceedings of the*

- Third International Geodetic Symposium on Satellite Doppler Positioning*, Vol. 1, pp. 1041-1056, Feb 1982.
23. Hill, R.W. and Senus, W.J., "The Development of a Navstar Geodetic Receiver," *Proceedings of IEEE Plans 82 Position Location and Navigation Symposium*, pp. 339-341, Dec 1982.
24. Roth, B. and Renfro, B., "The DMA GPS Tracking Network," *Proceedings of the 44th Annual Meeting of the Institute of Navigation*, pp. 487-494, Jun 1993.
25. Cunningham, J.P.; Malyevac, C.A.; Whitesell, R. and Malys, S., "Testing of the World Geodetic System 1984 in Precise Orbit Determination and Point Positioning," *Proceedings of the Fourth International Geodetic Symposium on Satellite Positioning*, Vol. 1, pp. 117-131, Austin, TX, Apr-May 1986.
26. Cunningham, J.P., *Determination of TRANET and SMTP Tracking Station Coordinates for Use in the WGS 84*, NSWC TR 87-61, Dahlgren, VA, Jun 1987.
27. Swift, E.R., "Determination of WGS 84 Station Heights for the Combined Air Force and DMA Tracking Network Using GPS Data," *Proceedings of the Fifth International Geodetic Symposium on Satellite Positioning*, Vol. 1, pp. 142-152, Las Cruces, NM, Mar 1989.
28. Cunningham, J.P. and Curtis, V.L., *Estimating GPS Orbits, Clocks, and Covariances in Support of SATRACK II*, NAVSWC TR 91-539, Dahlgren, VA, Aug 1991.
29. Swift, E.R., "Preliminary Comparison of the WGS 84 and the SV5 Reference Frames Using GPS Pseudorange Data," *Proceedings of the Sixth International Geodetic Symposium on Satellite Positioning*, Vol. 1, pp. 69-78, Columbus, OH, Mar 1992.
30. Fell, P.; Swift, E. and Cunningham, J., *Bridging the Gap Between Transit and GPS Point Positioning—Implications of Higher-Order Ionospheric Refraction on the Realization of the WGS 84 Reference Frame*, NSWCDD/TR-92/557, Dahlgren, VA, Oct 1992.
31. Anderle, R.J., "Geodetic Applications of the NAVSTAR Global Positioning System," *Proceedings of the Second International Symposium on Problems Related to the Redefinition of North American Geodetic Networks*, pp. 463-480, Arlington, VA, Apr 1978.
32. Fell, P.J., *Geodetic Positioning Using a Global Positioning System of Satellites*, The Ohio State University, Report No. 299, Columbus, OH, Jun 1980.
33. Evans, A.G., Hermann, B.R. and Fell, P.J., "Global Positioning System Sensitivity Experiment," *Navigation: Journal of the Institute of Navigation*, Vol. 28, No. 2, pp. 77-84, Summer 1981.
34. Hermann, B.R.; Swift, E.R. and Gouldman, M.W., "The Results of More Than Three Years of GPS Absolute Position Solutions From One Site," *Proceedings of ION GPS-90, The Third International Technical Meeting of the Satellite Division of the Institute of Navigation*, Colorado Springs, CO, Sep 1990.
35. Hermann, B., "Five Years of Absolute Positions at the Naval Surface Warfare Center," *The Sixth International Geodetic Symposium on Satellite Positioning*, The Ohio State University, Columbus, OH, Mar 1992.
36. Hermann, B., *Five Years of Absolute Positions at the Naval Surface Warfare Center*, The 48th Annual Meeting of the Institute of Navigation, Washington, DC, 1 Jul 1992.
37. Gibson, L.R., *Some Expansions for an Electromagnetic Wave Propagating Through a Spherically Symmetric Refracting Medium*,

- NSWC Technical Report, NSWC/DL TR-3344, Jun 1975.
38. Gibson, L.R., *A Derivation of Relativistic Effects in Satellite Tracking*, NSWC Technical Report, NSWC TR 83-55, Apr 1983.
39. Hermann, B.R. and Malys, S., "Precise Absolute Navigation: An Evaluation of PPS Position Improvement," *Proceedings of the ION GPS-95*, Palm Springs, CA, 12-15 Sep 1995.
40. Hermann, B. and Risinger, B., *Precise Absolute Navigation: An Evaluation of PPS Position Improvement*, NSWCDD/TR-95/196, Oct 1995.
41. Gouldman, M.W.; Hermann, B.R. and Weedon, D.L., "Evaluation of GPS Production Ephemeris and Clock Quality," American Geophysical Union Fall Meeting, San Francisco, CA, 5-9 Dec 1988.
42. Gouldman, M.W., Hermann, B.R. and Weedon, D.L., "Evaluation of GPS Production Ephemeris and Clock Quality," *Proceedings of the Fifth International Geodetic Symposium on Satellite Positioning*, Las Cruces, NM, 13-17 Mar 1989.
43. Feess, B., Iroz, J., Satin, A. and Winn, B., The Aerospace Corporation, El Segundo, CA; Wiseman, C., General Dynamics Service Company, Yuma, AZ; Hermann, B. and Swift, E., Naval Surface Weapons Center, Dahlgren, VA; Beisner, H., IBM Corporation, Gaithersburg, MD; Allan, D., Davies, D. and Weiss, M., National Bureau of Standards, Boulder, CO; and Klepczynski, W. and Withington, F., U.S. Naval Observatory, Washington, D.C., "GPS Satellite-to-User Range Accuracies: A Calibration Experiment," *NAVIGATION: Journal of The Institute of Navigation*, Vol. 34, No. 3, Fall 1987.
44. Hermann, B.R., Gouldman, M.W. and Swift, E.R., "User Range Error and Frequency Standard Performance For the First Block II Satellite," *Proceedings of ION GPS-89, The Second International Technical Meeting of the Satellite Division of the Institute of Navigation*, Colorado Springs, CO, Sep 1989.
45. O'Toole, J.W. and Merrigan, M., "Evaluation of DoD GPS Satellite Orbits Using NASA Laser Ranging Data," *Proceedings of ION GPS-95*, pp. 45-54, 1995.
46. O'Toole, J.W., "Evaluation of NIMA and Air Force GPS Satellite Ephemerides Using NASA Laser Ranging Data," *Proceedings of the 54th Annual ION Meeting*, Denver, CO, 1-3 Jun 1998.
47. Malys, S., National Imagery and Mapping Agency; Larezos, Capt. M., GPS Joint Program Office; Gottschalk, Capt. S., Air Education and Training Command; Mobbs, Lt. S., Air Force Space Command; Winn, B., Feess, W. and Menn, M., Aerospace Corporation; Swift, E. and Merrigan, M., NSWCDD; Mathon, W., Lockheed Martin Federal Systems, "The GPS Accuracy Improvement Initiative," *Proceedings of ION GPS-97*, 1997.
48. Swift, E. and Merrigan, M., "Expected Improvement in OCS Kalman Filter Estimates and Predictions Due to Adding DMA Stations and Using a Single Partition," GPS Control Segment Performance and Analysis Working Group Meeting, Falcon AFB, Aug 1996.
49. Evans, A.G., Hermann, B.R., Coco, D.S. and Clynch, J.R., "Collocation Tests of an Advanced Geodetic Global Positioning System Receiver," *Proceedings of the First International Symposium on Precise Positioning with the Global Positioning System*, Rockville, MD, Apr 1985.
50. Sims, M.L., "Phase Center Variation in the Geodetic TI4100 GPS Receiver System's Conical Spiral Antenna," *Proceedings of the First International Symposium on Precise Positioning with the Global Positioning System*, Rockville, MD, Apr 1985.

51. Evans, A.G., "Comparison of GPS Pseudorange and Biased Doppler Range Measurements to Demonstrate Signal Multipath Effects," *Proceedings of the Fourth International Geodetic Symposium on Satellite Positioning*, Austin, TX, Apr 1986.
52. Evans, A.G. and Carr, J.T., "Effect of Signal Multipath Errors at DMA Global Positioning Sites on Orbit Accuracy," *Manuscripta Geodaetica*, Vol. 14, pp. 143-148, 1989.
53. Evans, A.G. and Hermann, B.R., "On the Reduction of GPS Multipath," *Eos*, 68-44, 1238, Nov 1987.
54. Evans, A.G. and Hermann, B.R., "A Comparison of Several Techniques to Reduce Global Positioning System Signal Multipath," General Meeting of the International Association of Geodesy, Edinburgh, Scotland, Aug 1989.
55. Meyerhoff, S.L. and Evans, A.G., "Demonstration of the Combined Use of GPS Pseudorange and Doppler Measurements for Improved Dynamic Positioning," *Proceedings of the Fourth International Geodetic Symposium on Satellite Positioning*, Austin, TX, Apr 1986.
56. Anderle, R.J., "Error Model for Geodetic Positions Derived from Doppler Satellite Observations," *Bulletin Geodesique* 50 (1), pp. 43-77, 1976.
57. Evans, A.G.; Anderle, R.J. and Hermann, B.R., "Collocation Test Results from Experimental Global Positioning System Geodetic Receivers," *Proceedings of the Third International Geodetic Symposium on Satellite Doppler Positioning*, Las Cruces, NM, Feb 1982.
58. Anderle, R.J. and Evans, A.G., "Relative Positioning Test Using the Global Positioning System and Doppler Techniques," *Proceedings of the Third International Geodetic Symposium on Satellite Doppler Positioning*, Las Cruces, NM, Feb 1982.
59. Evans, A.G. and Hermann, B.R., "Long Baseline (Transoceanic) Surveying Using the Global Positioning System and Its Broadcast Ephemeris," Third International Symposium on the Use of Artificial Satellites for Geodesy and Geodynamics, Athens, Greece, Sep 1982.
60. Evans, A.G., "Use of GPS Phase Measurements for Dynamic Relative Position and Velocity Estimation: Laboratory Test Results," *Proceedings of the Fourth International Geodetic Symposium on Satellite Positioning*, Austin, TX, Apr 1986.
61. Hermann, B.R.; Evans, A.G.; Law, C.S. and Remondi, B.W., "Kinematic On-The-Fly Positioning Relative to a Moving Reference," *Navigation: Journal of the Institute of Navigation*, Vol. 42, No. 3, Fall 1995.
62. Evans, A.G.; Hermann, B.R.; Law, C.S.; Remondi, B.W.; Briggs, T. and Nelson, T., "An Evaluation of Precise Kinematic On-The-Fly GPS Positioning with Respect to a Moving Aircraft," *Proceedings of the 8th International Technical Meeting of the Satellite Division of the Institute of Navigation*, Palm Springs, CA, Sep 1995.
63. Evans, A.G.; Hermann, B.R.; Simpson, P.B.; Feist, J.L. and Wiles, G.C., "An Evaluation of Precise Kinematic On-the-Fly Relative GPS Positioning for a Rocket Sled Test," *Proceedings of the 52nd Annual Meeting, Institute of Navigation*, Cambridge, MA, Jun 1996.
64. Cunningham, J.P.; Remondi, B.W.; Hermann, B.R. and Evans, A.G., "Evaluation of Wide Area Differential GPS for Missile Testing," *Proceedings of the National Technical Meeting of The Institute of Navigation*, Long Beach, CA, Jan 1998.
65. Cunningham, J.P.; Evans, A.G.; Remondi, B.W. and Hermann, B.R., *Analysis of Vandal WADGPS Navigation*, NSWCD/D/T12 Technical Note, Dahlgren, VA, Apr 1998.

66. Evans, A.G., "Roll, Pitch, and Yaw Determination Using a Global Positioning System Receiver and an Antenna Moving in a Plane," *Journal of Marine Geodesy*, Vol. 10, No. 1, pp. 43-51, 1986.
67. Evans, A.G., "Method to Determine the Orientation of a Moving Platform," U.S. Patent No. 4,599,620, 8 Jul 1986.
68. Kruczynski, L.R.; Pui, C.L.; Evans, A.G. and Hermann, B.R., "Using GPS to Determine Attitude," *Proceedings of the First International Technical Meeting of the Institute of Navigation's Satellite Division: GPS-88*, Colorado Springs, CO, Sep 1988.
69. Kruczynski, L.R.; Pui, C.L.; Evans, A.G. and Hermann, B.R., "Using GPS to Determine Attitude: USS Yorktown Test Results," *Proceedings of the Second International Meeting of the Satellite Division of the Institute of Navigation: GPS-89*, Colorado Springs, CO, Sep 1989.
70. Brown, R.A. and Evans, A.G., "GPS Pointing System Performance," *Proceedings of the Third International Meeting of the Satellite Division of the Institute of Navigation: GPS-90*, Colorado Springs, CO, Sep 1990.
71. Evans, A.G. and Stein, W.L., "Method for Determining Astronomic Azimuth," U.S. Patent No. 4,954,933, 4 Sep 1990.
72. Evans, A.G.; Soler, T.; Hothem, L.D. et al., "Vertical Deflections and Astronomic Azimuth Derived From GPS and Leveling: Joint Test Description and Results," *Proceedings of the Fifth International Geodetic Symposium on Satellite Positioning*, Las Cruces, NM, Mar 1989.
73. Soler, T.; Carlson, Jr., A.E. and Evans, A.G., "Determination of Deflections of the Vertical Using GPS and Geodetic Leveling," *Geophysical Research Letters*, Vol. 16, No. 7, pp. 695-698, Jul 1989.
74. Evans, A.G. and Remondi, B.W., "Gravity Deflections of the Vertical Using Pseudokinematic GPS and Leveling," *Proceedings of the Fourth International Technical Meeting of the Satellite Division of the Institute of Navigation: GPS-91*, Albuquerque, NM, Sep 1991.
75. Hermann, B.R.; Evans, A.G.; Sitzman, G.L. et al., "Off-Shore Differential Sea Height Determination Using Precise Relative GPS Processing," *Proceedings of the 51st Annual Meeting of the Institute of Navigation*, Colorado Springs, CO, 1995.
76. Evans, A.G.; Hermann, B.R.; Sitzman, G.L. et al., "Application of the Global Positioning System to Determine Gravity Deflections of the Vertical at Sea," *Proceedings of the Gravity, Geoid, and Marine Geodesy International Symposium*, Tokyo, Japan, 30 Sep-5 Oct 1996.
77. Miller, B.L., "Kalman Filter Models for Satellite On-Board Navigation Using Global Positioning System Data," *Proceedings of the NASA Flight Mechanics/Estimation Theory Symposium*, Greenbelt, MD, Oct 1977.
78. Hoffman, E.J. and W.P. Birmingham, "GPSPAC: A Spaceborne GPS Navigation Set," *Proceedings of IEEE PLANS'78*, pp. 13-20, Nov 1978.
79. Stein, W., "GPSPAC Space Navigation Simulation Results," *Proceedings of the ION National Aerospace Conference*, Springfield, VA, 6-8 Mar 1979.
80. Birmingham, W.P.; Miller, B.L. and Stein, W.L., "Experimental Results of Using the GPS for Landsat 4 Onboard Navigation," *Navigation*, Vol. 30, No. 3, pp. 244-251, Fall 1983.
81. Swift, E.R., "HV OMNIS Formulation," unpublished notes, Dahlgren, VA, 26 Apr 1993.
82. Swift, E.R.; Merrigan, M.J. and Gouldman, M.W., "Orbit Estimation for

- TOPEX/POSEIDON Based on GPS Tracking Data," *Proceedings of the AAS/AIAA Space Flight Mechanics Meeting*, Austin, TX, 12-15 Feb 1996.
83. Miller, B.L., *Use of the Navstar Global Positioning System to Update the Inertial Navigation System of Carrier-based Aircraft*, NSWC/DL TR-3437, Mar 1976, Dahlgren, VA.
84. Ohlmeyer, E.J. and Pepitone, T.R., "In-Flight Removal of TBMD System Alignment Errors Using GPS and Radar Measurements," *Unclassified Proceedings from the 6th Annual AIAA/BMDO Technology Readiness Conference*, San Diego, CA, Aug 1997.
85. Evans, A.G. and Hermann, B.R., *Feasibility Study: Application of a Miniature GPS Receiver System for Guiding a Gun-Launched Projectile to a Target*, unpublished technical report, NSWCDD, Dahlgren, VA, 1987.
86. Evans, A.G. and Hermann, B.R., "Feasibility of Using a GPS Receiver to Navigate a Naval Gun-Launched Projectile to a Target," *Proceedings of the Institute of Navigation National Technical Meeting*, San Diego, CA, 27-29 Jan 1992, pp. 95-104.
87. Evans, A.G.; Hagan, J.D.; Fraysse, J.W.; DeSimone, L.M.; Doran, T.E. and Wiles, G.C., "Using GPS to Guide a Gun-Launched Projectile for Naval Surface Fire Support," *Proceedings of the 9th International Technical Meeting of the Satellite Division of the Institute of Navigation*, pp. 1535-1543, Kansas City, MO, 17-20 Sep 1996.
88. Hagan, J.D., "Future Gun Weapon System Technology," *Naval Surface Warfare Center, Dahlgren Division Technical Digest 1996 Issue*, NSWCDD/MP-96/96, Dahlgren, VA.
89. Ohlmeyer, E.J.; Pepitone, T.R.; Miller, B.L.; Malyevac, D.S.; Bibel, J.E. and Evans, A.G., "Application of GPS/INS to Extended Range Guided Munitions and Tactical Ballistic Missile Interceptors," *Naval Surface Warfare Center, Dahlgren Division Technical Digest 1996 Issue*, NSWCDD/MP-96/96, Dahlgren, VA. (Also appears in AIAA-97-3683, *Proceedings of AIAA Guidance, Navigation, and Control Conference*, pp. 954-968, New Orleans, LA, Aug 1997.)
90. Ohlmeyer, E.J.; Pepitone, T.R. and Miller, B.L., "Assessment of Integrated GPS/INS for the EX-171 Extended Range Guided Munition," AIAA-98-4416, *Proceedings of AIAA Guidance, Navigation, and Control Conference*, pp. 1374-1389, Boston, MA, Aug 1998.
91. Evans, A.G.; Hermann, B.R.; Law, C.S. and Sitzman, G.L., "Precise GPS Relative Positioning and Near Real-Time Targeting," *Precision Strike Technology Symposium*, Laurel, MD, Aug 1995.
92. Horman, S.R., *Precision Targeting for Naval Fire Support*, NSWCDD White Paper for the Office of Naval Research, Dahlgren, VA, Apr 1998.
93. Melton, C.T., "FO/FAC Brings a Digital Link to the Forward Fire Support Teams," *Naval Surface Warfare Center, Dahlgren Division Technical Digest 1996 Issue*, NSWCDD/MP-96/96, Dahlgren, VA.
94. Evans, A.G.; Hermann, B.R. and Jeroski, J.F., "GPS-Aided Lane Marking and Reporting for Shallow-Water Mine Neutralization," *Navigation: Journal of the Institute of Navigation*, Vol. 43, No. 4, Winter 1996-1997.
95. Creasy, R. and Hewston, B., *Ship/Sub Environment and Missile Simulation (SEMS) Hardware/Software Requirements Specification*, Technical Report T-BSN-0457-01, NSWCDD, Dahlgren, VA, Jun 1997.

THE AUTHORS AND CONTRIBUTORS



Contributors: (Seated l. to r.) Mr. B. Larry Miller,* Dr. Bruce R. Hermann,* and Mr. Everett R. Swift*
(Second row) Ms. M. Wendel Gouldman, Dr. Alan G. Evans* (Paper Coordinator), Dr. Jeffrey N. Blanton* (Paper Editor),
Mr. Robert W. Hill,* and Mr. Joseph M. Futcher, Jr.
(Third row) Mr. Ernest J. Ohlmeyer, Jr., Mr. Michael Merrigan, Mr. James P. Cunningham,* and Mr. Stanley L. Meyerhoff

*denotes lead authors

Other contributors not shown are: Dr. James W. O'Toole, Mr. John T. Carr III, Dr. Patrick J. Fell, Mr. Mark Tanenbaum,
Mr. George C. Wiles IV, Mr. Gary L. Sitzman, and Dr. Richard D. Hartman.

Mr. B. Larry Miller received a B.A. degree from Western Kentucky University in 1967 and an M.A. degree in mathematics from the University of Louisville in 1971. Since 1974, he has worked on numerous aspects of GPS, including satellite constellation design, concept evaluation of ground and space applications, and development of the first spaceborne GPS navigational unit.

Dr. Bruce R. Hermann received his B.S.E.E. from Bradley University in 1965, his M.S. from Colorado State University in 1966, and his Ph.D. in electrical engineering from the University of Illinois in 1972. Dr. Hermann has been employed at NSWCDD since 1972 and has been working on various aspects of GPS since 1978.

Mr. Everett R. Swift has been involved in GPS-related orbit and clock estimation work at NSWCDD for over 18 years. He has a B.S. in mathematics from Kent State University and an M.A. in mathematics from The Pennsylvania State University.

Mr. Robert W. Hill is currently associate for Space Technology and past head of Satellite Geophysics at ARL:UT. He retired after more than 32 years from NSWCDD in 1992. While employed as a space scientist at NSWCDD, he successfully directed the Satellite Systems Branch and the NSWCDD Office of Space Technology.

Dr. Alan G. Evans has been working in GPS applications since 1981. He received a B.S.E.E. degree from Widener University in 1964, and M.S. and Ph.D. degrees in electrical engineering from Drexel University in 1967 and 1972, respectively.

Mr. James P. Cunningham has been involved in GPS research and applications at NSWCDD since 1985. He received a B.S. in geology from Bucknell University in 1981 and an M.S. in geophysics from the Georgia Institute of Technology in 1983.

Dr. Jeffrey N. Blanton has been head of the Space Systems Applications Branch since 1992. He has over 25 years experience in estimation theory and satellite orbital and attitude dynamics. He received his Ph.D. in aerospace engineering from the University of Virginia in 1976. Dr. Blanton has worked at Dahlgren in the Space and Weapons Systems Analysis Division since that time.

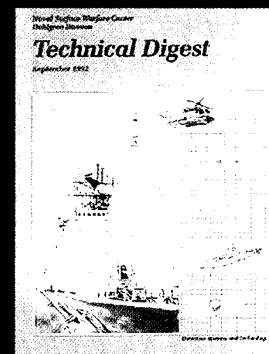


Dr. Thomas A. Clare

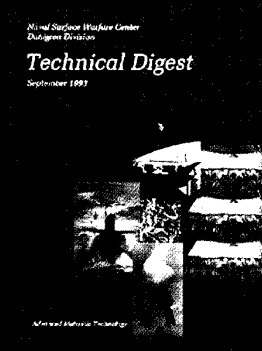
Technology transition and dual-use technology are the topics of this year's *Naval Surface Warfare Center, Dahlgren Division Technical Digest*. Transition takes many forms—personal as well as technological. On a personal note, NSWCDD's Executive Director, Dr. Thomas A. Clare, retired 30 September 1998. We gratefully dedicate this issue of the *Technical Digest* to its founder, Dr. Clare, in appreciation for his exceptional vision and steadfast support of this publication. The Technical Advisory Board and Editorial Staff take this opportunity to thank him and wish him well in his retirement.



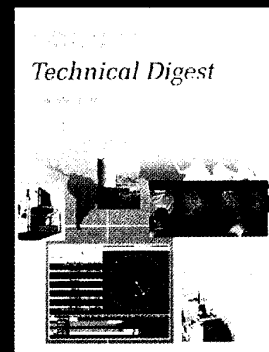
1991



1992



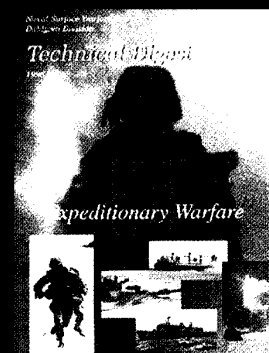
1993



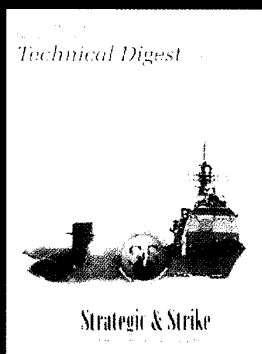
1994



1995



1996



1997



1998

